Modulation of *Candida albicans*-associated Denture Biofilms by Environmental and Microbial Factors

Thesis submitted in the part-fulfilment of the requirements of the degree of Doctor of Philosophy

Megan Rebecca Williams

Oral and Biomedical Sciences

School of Dentistry

Cardiff University

2023

Supervisory team: Prof. David Williams, Dr Melanie Wilson, Prof. Ian Fallis, Dr David Bradshaw, Dr Jonathan Pratten

Acknowledgments

Firstly, I would like to thank my supervisory team Prof. David Williams, Dr Melanie Wilson, Prof. Ian Fallis, Dr David Bradshaw and Dr Jonathan Pratten. I am so grateful for all their support and guidance throughout my PhD and the amazing opportunity and experience this has been. I would also like to express my appreciation to Biotechnology and Biological Sciences Research Council BBSRC and Haleon (formerly GSK consumer healthcare) for funding my PhD and giving me this great opportunity.

I would also like to thank Dr Laurent Bozec who hosted me at the University of Toronto. He and all his lab made me feel so welcome and I learnt so much in my short time there. Thank you to Sophia, Mina, Mehrnoosh and Emelie who made my time there so memorable.

I am extremely grateful to Dr Siôn Edwards for all his help with the chemical analyses and interpretation in Chapter 2. I would also like to thank Ms Wendy Rowe, Dr Wayne Arye and Dr Adam Day for all their help, guidance, and advice. I would also like to thank Dr Angela Marchbank and her colleagues at the Genomics Hub at the School of Biosciences for their guidance and work on the metagenomic sequencing in Chapter 5. Additionally, thank you to Prof. Peter Kille and Dr Ann Smith for their help with the analysis of the metagenomic sequencing.

The experience of my PhD wouldn't have been the same without the people who I shared an office with who were always supportive, and I have many great memories with. Thank you all. Also thank you to everyone who volunteered to donate their saliva, it was greatly appreciated.

Last but not least, I would like to thank all my wonderful friends and family especially my parents and my sisters, who have supported me so much. I love and appreciate you all so much and couldn't have done this without you all.

Contents Page

Table of Figures

List of Tables

Abbreviations

AI	Autoinducer
AIDS	Acquired Immunodeficiency Syndrome
ALS	Agglutinin Like Sequence
ANOVA	Analysis Of Variance
AS	Artificial Saliva
c-di-GMP	Cyclic Diguanylate
CFU	Colony Forming Unit
CHC	Chronic Hyperplastic Candidosis
cis-DA	*cis*-2-Decenoic Acid
CLSM	Confocal Laser Scanning Microscopy
CSC	Cigarette Smoke Condensate
CSP	Competence-Stimulating Peptide
dH_2O	Distilled Water
DNA	Deoxyribonucleic Acid
DS	Denture Stomatitis
DSM	German Collection Of Microorganisms And Cell Cultures Gmbh
DSREC	Dental School Research Ethics Committee At Cardiff University
EAP	Cell Wall Adhesin
eDNA	Extracellular Deoxyribonucleic Acid
eHOMD	Human Oral Microbiome Database
EPA	Epithelial Adhesin
EPS	Extracellular Polymeric Substance
FAM	5-Carboxyfluorescein
FISH	Fluorescence In-Situ Hybridisation
FITC	Fluorescein Isothiocyanate
GFP	Green Fluorescent Protein
GlcNAc	N-Acetyl-D-Glucosamine
GtfB	Beta Glucosyltransferase
h	Hour
HIV	Human Immunodeficiency Virus
HWP	Hyphal Wall Protein
LPS	Lipopolysaccharide

MAPK	Mitogen-Activated Protein Kinases
MIC	Minimum Inhibitory Concentration
MSA	Mitis Salivarius Agar
MSG	Mitis Group *Streptococcus*
NCTC	National Collection of Type Cultures
PBS	Phosphate Buffered Saline
PCA	Principle Component Analysis
PCR	Polymerase Chain Reaction
PKA	Protein Kinase A
PNA	Peptide Nucleic Acid
PTFE	Polytetrafluoroethylene
qPCR	Quantitative Polymerase Chain Reaction
QS	Quorum Sensing
RNA	Ribonucleic Acid
S.E.M	Scanning Electron Microscopy
SAP	Secreted Aspartyl Proteinase
SCC	Squamous Cell Carcinoma
SDA	Sabouraud Dextrose Agar
SDSF	Trans-2- Decenoic Acid
SEM	Standard Error Of The Mean
S.E.M	Scanning Electron Microscopy
sIgA	Secretory Immunoglobulin A
STAMP	Statistical Analysis of Taxonomic and Functional Profiles
TC	Tobacco Condensate
TFs	Transcription Factors
TR	Tandem Repeats
TSA	Trypticase Soy Agar
TSB	Trypticase Soy Broth
UDMA	Urethane Dimethacrylate
v/v	Volume Per Unit Volume
w/v	Weight Per Unit Volume
WC	Water Conditioned Control
WT	Wildtype
YNB	Yeast Nitrogen Base

ΔALS3	*Candida albicans* SC5314 UB1941 Δ*als3* mutant strain

Summary

Candida albicans has been designated as a critical priority in the WHO fungal pathogens list to guide research, development and public health action (World Health Organization 2022). *Candida*-associated denture stomatitis affects approximately 65-75% of denture wearers and is one of the most common forms of candidosis. The predominant species involved is *C. albicans*, an opportunistic pathogen problematic for people who are immunocompromised or have implanted medical devices.

The overall aim of this research was to explore the impact of surface conditioning (Chapter 2), surface topography (Chapter 3) and bacterial presence (Chapters 4 and 5), on the behaviour of *C. albicans* in *in vitro* biofilms. It was evident from the surface conditioning investigations that both the quantity and morphology of *C. albicans* in biofilms could be modulated by these variables in a strain dependent manner. Denture material surfaces with significant differences in surface roughness were created and shown to affect the quantity of *C. albicans* present. *C. albicans* cells were clearly observed in the topological features in the surfaces. Dual species of *C. albicans* and relevant oral *Streptococcus* species resulted in increased *C. albicans* quantity though the same effect was not observed in experiments with spent media from the streptococcal species, suggesting microbial cells were required to be present. Based on studies of bacterial association with *C. albicans* hyphae, physical binding of some bacteria with the ALS3 protein was evident which could promote interactions. More complex saliva-derived biofilms were shown to influence *C. albicans* quantity and morphology, and differences between biofilms from separate individuals were explored using metagenomic sequencing.

If such *in vitro* effects translate to the *in vivo* environment, knowledge of these effects may provide insight into how the usually commensal organism *C. albicans* could become pathogenic and inform future treatment and management strategies for *Candida*-associated denture stomatitis.

CHAPTER 1: Literature Review

1.1. Microbial Biofilms: Introduction and prevalence

A biofilm is described as a community of microbial cells, adhered to a solid surface or at an liquid-air interphase, and embedded in extracellular polymeric substances (EPS) produced by the microorganisms themselves (Nobile and Johnson 2015). Biofilms are frequently encountered in natural environments and on host surfaces and are now generally acknowledged as the most prevalent form in which microorganisms grow (Flemming et al. 2016). Biofilms are the preferred mode of growth for many microorganisms due the benefits and protection that a biofilm provides. These benefits include an innate resistance to host immune defences and increased tolerance to other stressors including nutrient limitations, dehydration, and exposure to antimicrobial substances (Rumbaugh and Sauer 2020). Due to these key features of a biofilm lifestyle, microorganisms in biofilms can colonise competitive niches and survive in environments that would be too stressful for their free-living (planktonic) counterparts (Serra and Hengge 2014). A biofilm may contain a single microbial species, but most frequently, they are polymicrobial. Polymicrobial biofilms can therefore have additional advantageous properties because of exchanges and sharing of functions between different species (Berger et al. 2018).

1.1.1. Biofilm formation and development

Biofilm formation is a cyclical process that can be described in five, though some suggest four, phenotypically distinct, highly regulated stages (Figure 1.1) (Monroe 2007). These stages are evident for all biofilm forming microorganisms, with each developmental stage presenting a distinct pattern in protein production and gene expression (Stoodley et al. 2002; Petrova et al. 2017). Hallmark characteristics of biofilm growth include a decreased expression of flagella-associated genes (when present), production of EPS forming a biofilm matrix, induction of mechanisms for resistance to antimicrobials and increased production of virulence determinants (Rumbaugh and Sauer 2020).

Biofilm formation commences with the initial adherence of planktonic cells to a surface, and this is a reversible process (Monroe 2007; Berger et al. 2018). Planktonic cells attach and adhere to either abiotic or biotic surfaces, reproduce

and attract and adhere with other microorganisms (expansion stage). The biofilm begins to mature as the microorganisms produce EPS, communicate, and respond through quorum sensing (QS) stimuli as the population increases (Stoodley et al. 2002). The microbes in this 'mature' biofilm stage exhibit higher tolerance to host defences and chemical factors such as antibiotics. The last stage of biofilm development is dispersion, where biofilm cells are released, and may then cause infection at distal sites in the body (Kaplan 2010). Cells that are dispersed from biofilms are often virulent and can modulate the local environment to one that is favourable for new biofilm development (Bjarnsholt et al. 2013).

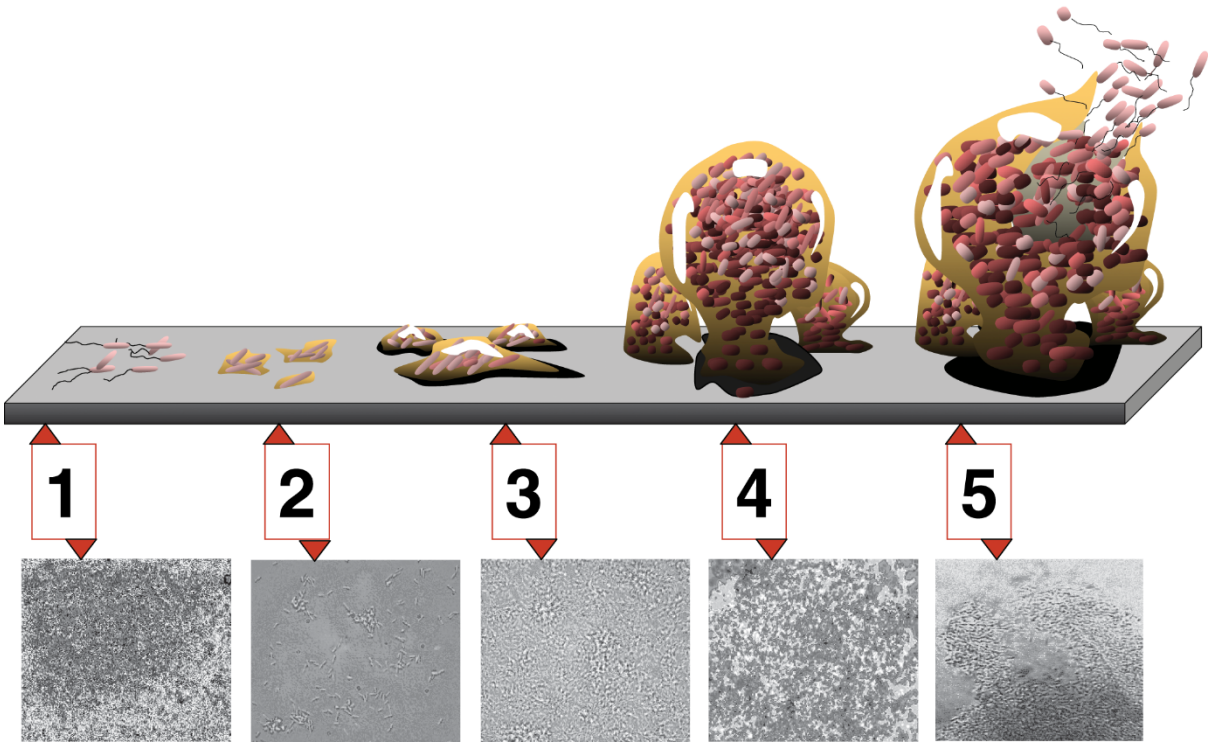

Figure 1.1. The five stages of biofilm formation and development. The five stages of biofilm formation are depicted schematically in the upper section and beneath as corresponding photomicrographs of *Pseudomonas aeruginosa* biofilm development. 1) Initial attachment; 2) adhesion – irreversible; 3) growth of microcolonies and EPS deposition; 4) maturation into a complex biofilm with a climax community; 5) dispersal of planktonic cells. (Image from Monroe, 2007 (Image used under Creative Commons License))

1.1.1.1. Stage 1: Attachment

The first stage of biofilm development on a surface is cell attachment. On dental surfaces, surface preconditioning is a precursor to attachment, and this primarily involves adsorption of glycoproteins on to the surfaces (Kolenbrander et al. 2010; Bowen et al. 2018). In the mouth, the adsorbed conditioning film components is referred to as the acquired pellicle (AP) and is derived from a combination of host and microbial sources (Bowen et al. 2018). The AP primarily consists of salivary components, including saliva-derived proteins, glycoproteins, lipids and glycolipids (Marsh and Bradshaw 1995). The pellicle coats all surfaces in the oral cavity and has an important role in determining the initial attachment of microbes and in maintaining a healthy, balanced oral microbiome (Lynge Pedersen and Belstrøm 2019). Deposition of the AP changes the characteristics of the surface, including its charge, which has a pivotal role in microbial attachment. Initial microbial attachment is mostly driven by non-specific forces such as electrostatic and van der Waals forces interacting between the surface and the microbial cells (Eliades et al. 1995; Sipahi et al. 2001).

The topology of microbial cell surfaces also contributes to how non-specific forces interact with them (Zheng et al. 2021). Such microbial topological features include, but are not limited to, lipopolysaccharides (LPS), flagella, pili and various antigens that increase the surface area of the cells, thus enhancing surface attachment (Harimawan et al. 2011). Many non-microbial factors can influence attachment and retention of microorganisms and one of these relates to the irregularities and roughness of the surface to which microorganisms may attach (Zheng et al. 2021).

1.1.1.2. Stage 2: Adhesion

After initial attachment, microbial cells adhere to the surface. Adherence is a more permanent attachment and considered to be irreversible (Stoodley et al. 2002). Adhesion is an active process, usually through more specific mechanisms including binding and ligand-mediated receptor interactions. The specificity of these interactions means that they are both species- and substrate-dependent. In the oral cavity, attached cells have to resist clearance by salivary flow and so adherence is essential to ensure colonisation and establishment of the biofilm on the oral surface. It is important to highlight that adhesion to the surface also

promotes cell-to-cell adhesion, with some adhesins having a multi-faceted role in binding. For example, *Streptococcus gordonii* surface proteins SspA and SspB can bind to mucosal surface components and to the fungus *Candida albicans* which may then be recruited to the biofilm (Bamford et al. 2009).

1.1.1.3. Stages 3 and 4; Growth and Maturation

After irreversible adherence, microbial motility is lost, and production of biofilm matrix components commences (Monroe 2007). These processes mark the switch from a simple aggregation of cells to the cyclical process of biofilm formation. Resources can be reallocated to the maturation and growth of the biofilm by means of clonal growth and recruitment of other cells (Rickard et al. 2003). The biofilm matrix itself is also able to promote recruitment, as it possesses many molecular components for binding cells (Flemming et al. 2007; Flemming and Wingender 2010).

1.1.1.4. Stage 5: Dispersal

The final stage of biofilm formation is dispersal. This is an active and highly regulated event during which planktonic cells are released from the biofilm and can then colonise new sites (Rumbaugh and Sauer 2020). The dispersal stage is of great interest in terms of human diseases, but this has only recently been recognised. Knowledge of the dispersal stage is derived mostly from *in vitro* studies and therefore extrapolation to *in vivo* and clinical situations should be done with caution (Kaplan 2010; Rumbaugh and Sauer 2020). Dispersion allows biofilm cell dissemination and colonisation of new sites. However, it may render the parental biofilm vulnerable, and the dispersed cells may also be more susceptible if they have switched to planktonic forms.

Biofilms, while greatly advantageous to some of their constituent cells, are not equally beneficial to all members of the community (Hunter 2008). Biofilms are subject to dynamic chemical, oxygen, nutrient and waste product concentration gradients, and these become more extreme as the biofilm develops and grows. While these gradients provide niches within the biofilm structure for a variety of species, they can also leave cells in a disadvantaged zone, with the outcome that subpopulations form. These subpopulations are more susceptible to dispersion

cues and are primed to disperse from the rest of the biofilm. Chemical gradients have therefore been proposed as the driving factors in triggering the stage of biofilm dispersal, with mechanisms not being fully elucidated, but mostly related to alteration of chemical gradients (Serra and Hengge 2014; Rumbaugh and Sauer 2020). Induction of active dispersal has been divided into two types of trigger: native and environmental induction. Native dispersion is initiated by internal biofilm factors, and signalling molecules derived from cells within the biofilm, and are produced as a response to the chemical gradients (Rumbaugh and Sauer 2020). In contrast, environmental induction of dispersion is in response to external environmental factors.

Native dispersion is observed as a coordinated movement of cells from the centre of the biofilm leaving a 'hollow cavity' in the biofilm (Sauer et al. 2002; Purevdorj-Gage et al. 2005). Dispersal has been linked to biofilm thickness, rather than biofilm age. However, there is no set biofilm size that triggers dispersion, rather it is the limitations of transport that have been attributed to whether subpopulations within biofilms disperse, and again, this is thought to be due to steep chemical gradients especially of extracellular signalling molecules, nutrient resources and oxygen (Purevdorj-Gage et al. 2005; Flemming et al. 2016). Findings suggest that there is an inducer responsible for dispersion that accumulates within the biofilm as it matures and grows, until chemical gradients limit the ability to effectively remove the inducer, triggering native dispersal. An example of this is a fatty acid signalling molecule called *cis*-2-decenoic acid (*cis*-DA) which was identified for *P. aeruginosa* (Davies and Marques 2009). Fatty acid signalling can mediate intraspecies, interspecies and cross kingdom communication and may regulate a wide range of biofilm processes including growth, virulence, motility, protein production, biofilm development, dispersal and persistence(Davies and Marques 2009). *cis*-DA is thought to induce low cyclic diguanylate (c-di-GMP) levels in bacterial species including *Escherichia coli, Klebsiella pneumoniae, Proteus mirabilis, Staphylococcus aureus,* as well as in the fungus, *C. albicans* (Davies and Marques 2009). This is important, as low c-di-GMP levels are thought to contribute to phenotypic changes in cells, returning them to a planktonic state and aiding dispersal.

Dispersal is also closely related to increased levels of cell death (Kaplan 2010). While cell lysis provides resources to other cells in the biofilm, the process correlates with development of anaerobic pockets, where denitrification occurs. Denitrification can lead to overproduction of nitric oxide (NO) which can produce peroxynitrite ($ONOO^-$), a cell toxic radical, that when accumulated can induce cellular damage and cell lysis (Barraud et al. 2006; Rumbaugh and Sauer 2020). Cell lysis also releases degrading enzymes that breakdown the biofilm matrix, causing reduction in rigidity of the biofilm structure.

Similar to native dispersal, environmental induced dispersal also rarely involves the whole biofilm, with up to 80% of the biofilm dispersing (Barraud et al. 2006). Environmental cues have been identified including levels of nitric oxide, iron, *cis*-2-decenoic acid (*cis*-DA), influx of nutrients and the induction of starvation promoting conditions. *cis*-DA appears to be both a native and environmental triggering chemical. As *cis*-DA is found to disperse a wide range of microorganisms, it is likely to disperse not only single species biofilms, but also polymicrobial biofilms (Rumbaugh and Sauer 2020).

Dispersed cells are described as phenotypically distinct from both biofilm and planktonic cells (Chua et al. 2014). The dispersed subpopulation can be termed as an intermediate lifestyle between biofilm and planktonic existence, key features of which include increased motility, virulence and adherence with distinct metabolic signatures and altered antimicrobial susceptibility (Sauer et al. 2004; Rollet et al. 2009; Vaysse et al. 2011). Dispersed cells also promote further biofilm dissemination through upregulation of genes associated with breakdown of EPS.

1.1.2. Extracellular polymeric substances

Distinguishing between a simple aggregation of cells and a biofilm is based on the presence of extracellular polymeric substances (EPS) in the biofilm matrix. Typical components of the biofilm are water, microbial cells and EPS (Sutherland 2001). EPS is largely responsible for the physical characteristics of the biofilm, including form, structure, and enhanced adhesion, all of which provides protection to the microbial cells. The composition of EPS is highly dependent on the external environment as well as the microbial species in the biofilm (Flemming et al. 2007).

These compositional changes mean that the chemical and physical properties of EPS are variable (Sutherland 2001).

EPS components often include homo- and heteropolysaccharides, extracellular proteins and proteins from cell lysis, and nucleic acids (Skillman et al. 1999; Xiao et al. 2012). There are also ions present, but the proportion of these in the matrix is unknown. Linkages between polysaccharides determine the rigidity or flexibility of EPS and the polysaccharides have been found to form strands attached to bacterial cell surfaces, forming a complex net-like structure (Flemming and Wingender 2010). The EPS matrix provides physical and chemical protection from changes in the surrounding environment, including reducing the detrimental impact of ultraviolet light, altered temperature and pH (Hall-Stoodley and Stoodley 2002).

Within the EPS, microorganisms interact and exchange resources, and EPS may even be used as a source of nutrients (Flemming and Wingender 2010). EPS have a role in the innate increased tolerance of biofilm cells to antimicrobials (Kim et al. 2018). Whilst EPS offer a physical barrier to movement of antimicrobials, resistance is also increased in the biofilm via exchange of resistance genes by horizontal gene transfer (HGT) and active uptake of extracellular DNA (eDNA) (Flemming et al. 2007; Desmond et al. 2018). In mixed species biofilms, EPS also stabilise other cell types even if those cells do not produce any EPS themselves (Flemming et al. 2007; Flemming and Wingender 2010). The proportions of different EPS are not indicative of the proportion of cells present, and different EPS types do not contribute equally to the structure and properties of the resultant biofilm (Sutherland 2001; Flemming et al. 2016).

1.2. The oral cavity as a site for biofilm formation

1.2.1. Anatomy of the oral cavity

The primary function of the oral cavity is the mastication and intake of food and drink (Sedghi et al. 2021). As such it is open to the environment and provides diverse and dynamic environments for microbial colonisation (Şenel 2021). Distinct sites for colonisation include surfaces of teeth, tongue, gingiva (gums) and the mucosa of the hard and soft palate (Figure 1.2).

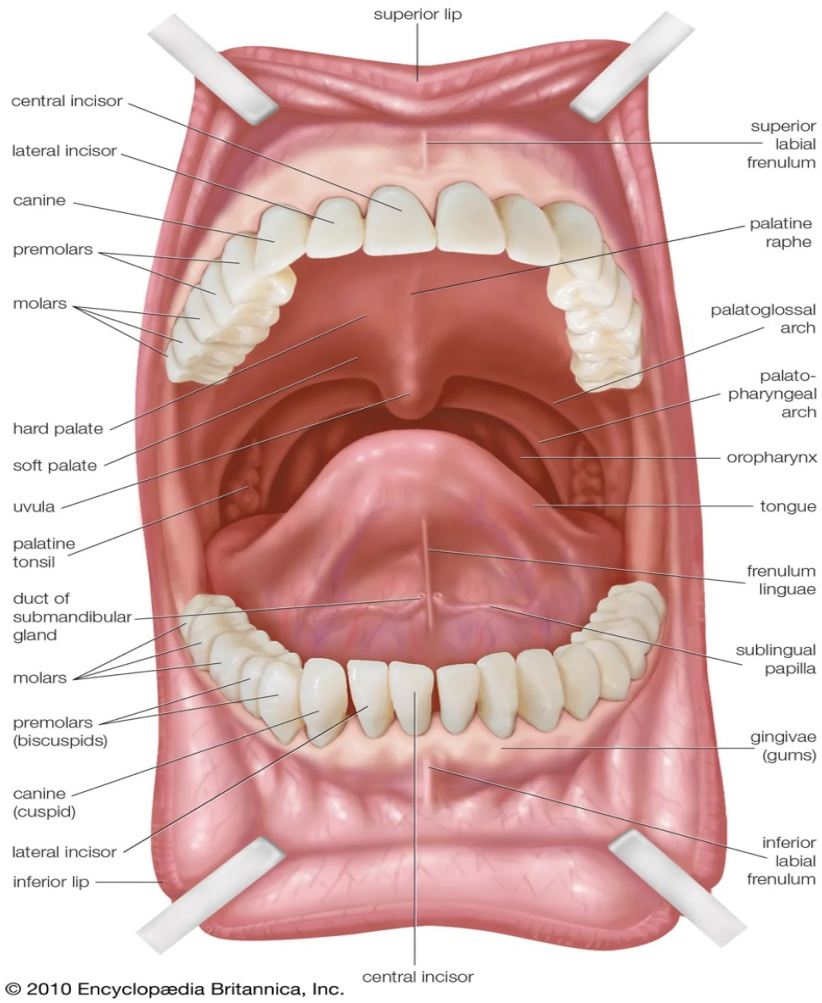

Figure 1.2. Anatomy of the human mouth. Image from the *Encyclopædia Britannica, Inc.* (Britannica 2022) [Accessed: 11th November 2022] (Image used under Creative Commons License).

Salivary glands including the parotid, submandibular and sublingual, secrete salivary components that mix to form whole saliva which has many roles including: maintaining the oral surfaces are moistened, assistance in mastication, digestion and swallowing, and in immunity and microbial regulation (Dawes and Wong 2019; Vila et al. 2019). Mucosal tissue, which encompasses the hard and soft palate, and the gingiva, acts as a barrier to microbial invasion of tissue, much like the skin. The mucosal surface exhibits shedding, which is the constant removal of cells (desquamation) and their replacement by cells from lower layers. Along with epithelial cells, any adhered microorganisms are also removed, and this is an important innate host defence mechanism. The oral mucosa exhibits varying levels of keratinisation depending on its location and function (Şenel 2021). For example,

the hard palate, at the front of the roof of the mouth, is a keratinised mucosal tissue and a barrier to infection. In contrast, surfaces of teeth are hard and non-shedding, and comprised of highly mineralised tissue, of which the outermost layer is enamel. Teeth are readily colonised by microorganisms, which accumulate into the formation of one of the most extensively studied biofilms, dental plaque (Marsh and Bradshaw 1995; Berger et al. 2018). Poor dental hygiene results in the accumulation of dental plaque which can disrupt the integrity of the gingiva, especially at the gingiva sulcus, presenting common oral disease such as gingivitis and periodontal disease (Petersen and Ogawa 2012). It is important to highlight that the oral cavity also supports a community of commensal microorganisms, that is crucial in maintaining a healthy oral environment.

1.2.2. The role and importance of saliva in the oral cavity

The content of whole saliva is primarily water (99%) that contains many electrolytes, immunoglobulins, proteins, enzymes, mucins, and nitrogenous products, such as urea and ammonia (Humphrey and Williamson 2001; de Almeida et al. 2008; Fischer and Aparicio 2021). These components are multifunctional and allow saliva to buffer the pH of enamel surfaces, cleanse the oral cavity, and modulate demineralisation and remineralisation processes (Dodds et al. 2015; Vila et al. 2019). In the oral cavity, biotic and abiotic surfaces are coated with salivary components that result in the salivary pellicle (Dawes et al. 2015). This AP plays an important role in the adhesion of microorganisms to oral surfaces (Kerr and Tribble 2015; Dawes and Wong 2019). The salivary pellicle provides ligands as targets for binding and reduces the charge of the surface which is important for non-specific initial adhesion (Gunaratnam et al. 2021). Many salivary glycoproteins adsorb to oral surfaces and facilitate attachment of commensal organisms such as *Streptococcus* species. The AP acts as a modulator of a healthy oral microbiome, as commensal oral microorganisms typically possess adhesins and lectins that correspond to saliva pellicle components (Kerr and Tribble 2015). For example, *Streptococcus gordonii* is an early coloniser of the oral cavity that adheres to a wide range of AP components including glycoproteins, proline-rich proteins, collagen, parotid salivary agglutinin and submandibular salivary proteins (Dodds et al. 2005; Kerr and Tribble 2015). The presence of the AP increases biofilm

development and produces a more robust *C. albicans* biofilm (da Silva et al. 2015; Cavalcanti et al. 2016b).

In addition, saliva will affect the microbial composition of the mouth through numerous other mechanisms *e.g.,* mechanical removal of loosely adherent microorganisms by salivary flow, provision of ligands and receptors for binding, and through antibacterial action (Humphrey and Williamson 2001; Dodds et al. 2005; Dodds et al. 2015; Kerr and Tribble 2015; Dawes and Wong 2019). Antibacterial components in saliva including secretory IgA (sIgA), lactoferrin, lactoperoxidase, lysozyme, statherin and histatins (Dodds et al. 2005; Dawes and Wong 2019). Mucins in saliva serve to localise antimicrobial components to the oral tissues to act as additional barriers to microbial infection (Humphrey and Williamson 2001). Mechanisms of saliva-mediated modulation of the oral microbiome can therefore be inhibitory or promoting, depending on the microorganism. The binding of microorganisms to receptors in the fluid-phase saliva forms aggregations promoting clearance through agglutination and blocking of surface adhesins, but in contrast can facilitate attachment of aggregates to surfaces, thereby increasing the rate of oral biofilm formation (Vila et al. 2019; Simon-Soro et al. 2022). Individuals with impaired unstimulated salivary flow rate generally have increased likelihood of oral diseases (Dawes and Wong 2019). Saliva production, flow and biochemical composition is highly variable between individuals and is influenced by age, sex, the presence of artificial surface, smoking and diet, to name a few factors (Bhattarai et al. 2018; Dawes and Wong 2019).

1.2.3. The oral microbiome

Colonisation of the mouth is important as endogenous commensal microorganisms play a vital role in regulating the oral environment, with the microbial residents occupying sites that might otherwise be exposed and available to potentially harmful and pathogenic microbial species (Huttenhower et al. 2012; Yamashita and Takeshita 2017; Sedghi et al. 2021). The oral cavity is a dynamic environment as it is an interface between internal body sites and the external environment. As such, many interventions occur in the mouth such as food and drink intake and oral hygiene practices, that cause many physical and chemical fluctuations (Costello et al. 2009; Stegen et al. 2012). The oral cavity is first colonised shortly after birth

when the new-born is exposed to the environment (Nelson-Filho et al. 2013; Xu et al. 2015; Sedghi et al. 2021). During further childhood development, the oral cavity, becomes one of most microbial-rich environments in the human body with temporal oral microbiome changes and ecological shifts (Turnbaugh et al. 2007; Crielaard et al. 2011; Costello et al. 2012; Xu et al. 2015). The early oral microbiome is initially highly influenced by the maternal microbiome, with infants and their mothers sharing approximately 85% of their microbiota (Dzidic et al. 2018; Sedghi et al. 2021). Phylogenetic individualisation occurs later in development when eruption of teeth occurs (Dzidic et al. 2018; Mason et al. 2018). The eruption of teeth alters the microbial community with the introduction of new non-shedding surfaces creating additional habitable sites (Dzidic et al. 2018; Mason et al. 2018).

Characterisation of what is considered a 'normal healthy oral microbiome' has been attempted by several studies focusing on different environmental oral niches including saliva, supragingival plaque, subgingival plaque and oral mucosa (Keijser et al. 2008; Nasidze et al. 2009; Zaura et al. 2009; Bik et al. 2010; Huttenhower et al. 2012; Zaura et al. 2014). However, there are many extraneous factors, for example, the fact that the oral microbiome diversity and abundance is altered throughout the human lifespan that affects findings (Crielaard et al. 2011; Xu et al. 2015). Ageing leads to a notable change in the oral microbiome, this is often attributed to declining host immune responses, the loss of teeth and the introduction of abiotic artificial surfaces such as implants and dentures (Xu et al. 2015).

The dentate state is highly important to the composition of the oral microbiome as seen by changes following eruption of teeth during childhood (Mason et al. 2018), and if an individual later becomes edentulous (De Waal et al. 2014; Gazdeck et al. 2019). Edentulous people exhibit a reduction in the numbers of *Streptococcus* species such as *S. sanguinis* and *S. mutans* (Gazdeck et al. 2019). Losing such species alters the composition of the microbial community network and associated interactions. Being partially or fully edentulous may lead to interventions including the introduction of dental prostheses. The presence of such abiotic surfaces also influences the composition and structure of the oral microbiome.

The oral microbiome can be divided into different individualised microbiomes including those of the tongue, mucosal tissue, gingiva, teeth and saliva (Simon-Soro et al. 2013; Sedghi et al. 2021). Keratinised epithelium of the dorsal tongue has microscopic invaginations in between specialised papillae (taste buds) making the surface highly heterogenous and providing micro-niches that offer protection for the microorganisms from clearance by salivary flow and potentially from oral hygiene/cleansing methods. Despite constant desquamation/shedding, the tongue microbiome is described as the largest and most diverse oral microbiome, which could reflect the diversity of the site (Simon-Soro et al. 2013).

Xu *et al.* (2015) described the oral cavity as being heterogenous with distinct niches with their own unique microbial community. These researchers aimed to define the 'normal' healthy oral microbiome throughout life. Focusing on saliva, mucosal and dental plaque communities they sampled individuals at different ages and dentate states and found that each site had a distinct biofilm composition and speculated that differences were dependent on the receptors for bacterial adhesion, microbial interactions within the biofilms and mucosal shedding (Besemer et al. 2012; Xu et al. 2015). Dental plaque has the highest species richness and diversity in comparison to saliva, and mucosal surfaces have the lowest observed bacterial diversity likely due to shedding and proximity to host immune response triggers (Xu et al. 2015). This study reinforced the complexity of the oral microbiome and concluded that the concept of a core oral microbiome should be related to age and oral site. Studies have reported different levels of average microbial diversity at oral environmental sites depending on techniques and sampling methods used. For example, on average 266 species level bacterial phylotypes were found at each oral site (Zaura et al. 2009; Bik et al. 2010) and saliva is said to usually contain 175 bacterial species (Hasan et al. 2014). Bostanci *et al.* (2021) suggested that previous studies potentially overestimated the diversity of the salivary microbiome through use of 16S rDNA sequencing, whereas whole genome sequencing showed lower diversity identifying 50 bacterial genera belonging to eight phyla, all of which are known to be present in the salivary microbiome (Dewhirst et al. 2010; Segata et al. 2012; Hasan et al. 2014). The Human Oral Microbiome Database V3 (eHOMD) database (v9.15) is an online database that has been curated to make this data web accessible. eHOMD currently (March 2023) has sequences of 774

oral bacterial species, 58% of which are officially named, 16% are cultivated but unnamed, and 26% that are known only as uncultivated phylotypes (Dewhirst et al. 2010; Human Oral Microbiome Database: HOMD. Accessed [02/03/2023]).

In addition to age, dentate state and the addition of abiotic surfaces, the oral microbiome is also known to be influenced by other factors including genetics, socioeconomic variables, hormones, smoking, intake of medical and recreational drugs, diet and the menstrual cycle (Adler et al. 2013; Paropkari et al. 2016; Bostanci et al. 2021; Suzuki et al. 2022). Diet, and especially sugar intake, is an important modulator of the oral microbiome, which has led to the observation that increased sugar consumption can select for more acidogenic bacteria such as streptococci, lactobacilli or bifidobacteria*,* all of which are associated with dental caries (Loesche 1986; Bostanci et al. 2021).

Bostanci *et al.* (2021) employed whole genome (shotgun) sequencing to analyse the salivary microbiome of a large cohort of women over the full course of the menstrual cycle to evaluate fluctuations and potential dysbiosis. The research also examined changes caused by use of oral contraceptives, smoking and sugar consumption. While oral contraceptives were not found to influence the salivary microbiome, the menstrual cycle, smoking and increased sugar intake did have impact. Four genera, namely *Campylobacter, Haemophilus, Prevotella* and *Oribacterium,* were shown to fluctuate in abundance over the menstrual cycle. Higher abundance of *Prevotella* in saliva, likely caused by bacterial growth affected by progesterone and oestradiol hormone levels, may alter the oral environment by increasing pH and altering gingival crevicular fluid (Bostanci et al. 2021). This is important as environmental changes such as in pH can have a significant effect on microbial composition and serve as a modulator of pathogenicity of some species such as *C. albicans.* This would suggest that women could be at higher risk of dysbiosis and from opportunistic pathogens at specific times in their menstrual cycle. In addition, the abundance of Gram positive bacterial pathogenic species such as *S. mitis* and *S. oralis* was reduced during the luteal phase of the menstrual cycle, further supporting oral microbiome regulation by the menstrual cycle and hormones.

1.3. Denture appliances and biofilms

Removable dentures are of particular research interest as interaction between denture surfaces, the oral environment and with microorganisms is important in both the management of oral health and understanding of denture related diseases. Full or partial removable dentures are worn by an estimated 19% of the UK population (Adult Dental Health Survey 2009, 2011). With global population increasing and longer life expectancy, it is predicted that elderly people will become a larger proportion of society, with the number of people over 65 years old expected to double by the year 2050 (United Nations 2019). The risk of becoming edentulous and requiring full or partial dentures increases with age and the impact and effects of long-term denture wearing are not entirely understood.

Dentures are most commonly made from polymethylmethacrylate (PMMA) and with chrome cobalt metal alloy fixtures in partial dentures; both material types will be in contact with the oral mucosa. This interface is important as it creates shielded areas where microorganisms accumulate. The fact that biofilms adhere to, and form on denture acrylic is well recognised, especially in cases of poor denture hygiene (Radford et al. 1999). The presence of a denture will alter normal salivary flow, which as mentioned previously is important for effective microbial clearance (Niedermeier et al. 2000). Reduced salivary flow over a denture is detrimental to both physical and chemical removal of microorganisms and thus promotes maturation and persistence of biofilms on denture surfaces (Vila et al. 2020). Due to the 'non-self' denture material being present in the oral cavity, exogenous bacteria that lack evolved mechanisms to colonise the mouth may now be presented with a surface upon which they can competitively adhere and colonise (Berger *et al.* 2018). Denture-associated biofilm studies frequently focus on the genus *Candida* as these fungal microorganisms, while not the most abundant, are efficient at adhering to acrylic surfaces and are involved in associated infections such as *Candida*-associated denture stomatitis (Berger et al. 2018; Lohse et al. 2018).

1.3.1.1. Denture plaque development and composition

Denture surfaces accumulate plaque in a similar manner to natural teeth (Nikawa et al. 1998; Sumi et al. 2007). As with all oral surfaces, when a denture is

introduced to the oral cavity it becomes coated with saliva and obtains an AP, which differs to that on teeth. The denture pellicle lacks mucin 7, cystatins and proline-rich-proteins, which will change the colonisation pattern of the surface (Edgerton and Levine 1992; Dawes et al. 2015; Fischer and Aparicio 2021). On denture surfaces, the AP usually consists of lysozyme and histatins, whilst natural dental surfaces also have adsorbed carbonic anhydrase, carbonate dehydratase and cystatins (Svendsen and Lindh 2009; Redfern et al. 2022). As mentioned previously, saliva provides adhesion receptors for various bacteria (Mukai et al. 2020). For example, certain *Streptococcus* species adhere to proline-rich-proteins and alpha-amylase. However, whilst changes have been observed in the AP content on different dental materials (Sang et al. 2020; Fischer and Aparicio 2021), Mukai *et al.* (2020) reported that primary colonisers did not change significantly *in vivo*.

The most commonly reported primary colonisers on denture materials are streptococci including *S. mutans, S. gordonii, S. sanguinis, S. mitis, S. oralis,* and *S. parasanguinis* (Redfern et al. 2022). Other primary colonisers include species of *Veillonella, Neisseria, Rothia, Abiotrophia, Gamella* and *Granullicatella* (Theilade et al. 1983; Aas et al. 2005; Diaz-Torres et al. 2006; Jenkinson 2011; Yitzhaki et al. 2018; Redfern et al. 2022). Adherence of these species provides the foundation for subsequent attachment of secondary colonisers such as *Fusobacterium nucleatum, Tannerella forsythia, Treponema denticola* and *Porphyromonas gingivalis* (Wright et al. 2013), leading to complex community networks (Marsh and Bradshaw 1995; Redfern et al. 2022). Co-adherence between microorganisms as opposed to direct binding to surface or pellicle components increases microbial diversity (Jenkinson 2011). Recently, Simon-Soro *et al.* (2022) reported that saliva contained preformed microbial aggregates in the fluid-phase. Therefore, colonisation of a surface and the formation of complex oral biofilms may occur by adherence of ‘colonising units’ rather than linearly by succession. The model presented by these researchers was one that operated in parallel to the accepted linear succession model of biofilm development. In this model, later colonisers are already adhered to primary colonisers, which in turn bind directly to oral surfaces. The authors also suggest that these preformed

attaching consortia are a mechanism of immune evasion promoting retention and persistence of undesirable microbes in oral biofilms.

As previously discussed, denture plaque shares many similarities with dental plaque, but does differ as it is usually has elevated levels of *Candida* (Nikawa et al. 1998; Nikawa et al. 2003; Mukai et al. 2020). *Candida* species are frequent secondary colonisers of denture surfaces and can adhere through interactions with *Streptococcus* species and *Actinomyces* species (Bamford et al. 2009). Though bacteria are more abundant in dental and denture plaque, *C. albicans* is often the focus of denture microbial research (Ramage et al. 2004; Verran et al. 2014; Ohshima et al. 2018), due to its relationship with *Candida*-associated denture stomatitis.

As a denture is a removable surface, contact with other environments outside the oral cavity occurs. This external contact may account for colonisation by microorganisms such as *Staphylococcus* and *Micrococcus* species that are not normally associated with the oral microbiome (Webb et al. 1998; Redfern et al. 2022). Respiratory pathogens can be detected in denture and dental plaque when there is poor oral hygiene (Hannah et al. 2017). It has been found that individuals that do not remove their dentures at night double their risk of contracting pneumoniae due to opportunistic respiratory pathogens from the denture being aspirated into the lungs (Iinuma et al. 2015), which is in addition to increased tongue and denture plaque, gum inflammation, and the presence of *C. albicans*, further highlighting the importance of improving oral hygiene and denture practice.

1.4. *Candida*

Fewer than 0.001% of the estimated number of fungal species are classed as human pathogens, and many of these only cause innocuous infections (Köhler et al. 2015). There are four basic requirements of a fungus to facilitate human infection. These include an ability to invade the human host, tolerate a higher temperature than the external environment, facilitate lysis of human tissue and nutrient absorption, and be able to evade the host's immune system (Köhler et al. 2015; Lohse et al. 2018).

Candida is a highly diverse fungal genus containing over 350 species which were originally defined as 'yeast-like fungi', with only a minority of species associated with diseases (Williams et al. 2011). *Candida* are usually harmless commensals, co-existing in many niches at various sites of the body of animals and humans (Lohse et al. 2018). However, *Candida* can cause systemic infections with high fatality rates of up to 50%, and is the fourth most common cause of nosocomial infection in the US (Pfaller and Diekema 2010). *Candida* is also the most predominant fungal genus isolated from medical devices and accounts for >40% of sepsis cases (Gow and Yadav 2017; Lohse et al. 2018). Many *Candida* species are opportunistic pathogens including *C. albicans, C. tropicalis, C. parapsilosis, C. glabrata, C. dubliniensis* and *C. auris* (Ramage et al. 2006; Tsui et al. 2016; Ponde et al. 2021). *C. auris* is associated with invasive candidosis, intrinsically resistant to most antifungal drugs and therefore, becoming a concern in clinical settings (Ponde et al. 2021; World Health Organization 2022). *Candida albicans* is considered the most pathogenic species, which is supported by the fact that it is the most commonly identified *Candida* in clinical settings (Williams *et al.* 2000).

1.4.1. Candida albicans

The World Health Organisation has recently published the "WHO fungal priority pathogens list to guide research, development and public health action" and listed *C. albicans* as one of four microbial species in the critical priority group (World Health Organization 2022). *Candida albicans* is a highly diverse species exhibiting metabolic flexibility that allows it to exploit a wide range of nutrient sources simultaneously through post-transcriptional changes and alternative metabolic pathways (Brown et al. 2014). The species is also highly polymorphic and switches between morphological forms including spherical yeast, pseudohyphae and true hyphae (Nobile and Johnson 2015; Gow and Yadav 2017). However, *C. albicans* is also an opportunistic pathogen, which is especially problematic for individuals who are immunocompromised, as well as those who have implanted medical devices. Dysbiosis caused by a range of factors such as changes in pH, nutritional changes, O_2 levels, antibiotics or suppression of the immune system can trigger increased pathogenicity and over-proliferation of *C. albicans* (Lohse et al. 2018).

Candida albicans infections range from superficial dermal infections, usually of moist mucosal tissues, to bloodstream systemic infections which are associated with high mortality (>40%) (Cannon et al. 1995; Lohse et al. 2018). The latter typically only occurs in individuals who are severely immunocompromised. Infections caused by *C. albicans* are referred to as candidosis (or candidiasis) and are the most prevalent fungal infections of humans (Lewis and Williams 2017). Invasive candidosis (candidaemia) despite the availability of antifungals and resistance being uncommon has an overall mortality of 20% to 50% (World Health Organization 2022). The main routes to prevent invasive candidosis is surveillance and prevention of colonisation, but preventability is deemed to be low (World Health Organization 2022).

Poor dental hygiene is linked to oral candidoses, and several other factors including smoking and diet, lead to some individuals being more susceptible. Denture wearers commonly present with candidosis (*Candida*-associated denture stomatitis) of varying severity, with the proportion affected ranging from 35-75% of the population, depending on the cohort studied (Webb et al. 1998; Barbeau et al. 2003; Shulman et al. 2005; Zomorodian et al. 2011; Vila et al. 2020). It has also been suggested that *C. albicans* may be involved in other oral diseases including oral cancers, burning mouth syndrome, taste disorders and endodontic disease (Lewis and Williams 2017). *Candida* are not implicated in causing periodontal disease, however, there is a strong association between the presence of *Candida* and such diseases (Unniachan et al. 2020).

1.4.2. Virulence factors

In vitro studies show that *C. albicans* expresses higher levels of virulence factors compared with other *Candida* species (Moran et al. 2012; Tsui et al. 2016). *Candida albicans* virulence factors can be categorised into those contributing to polymorphism, adhesion, secreted hydrolytic enzymes and host immune evasion mechanisms, and these are detailed below.

1.4.2.1. Polymorphism

The highly polymorphic nature of *C. albicans* is thought to be a significant virulence factor (Dadar et al. 2018). *Candida albicans* can alter its morphology as a response

to changing environmental conditions (Gow and Yadav 2017; Kadosh 2019). As mentioned earlier, *C. albicans* can grow as a spherical cell referred to as a yeast, and also as filamentous forms including pseudohyphae and true hyphal forms. *In vitro*, spherical 'spore like' structures which are referred to as chlamydospores can also be generated when cultured on nutrient poor solid agar media (Gow and Yadav 2017). The ability of *C. albicans* to alter its morphology in response to environmental conditions is recognised as an important virulence factor as it contributes to invasion of host tissues, dispersal within the host and enhanced evasion of host immune responses.

1.4.2.1.1. Hyphal transition of *Candida albicans*

Transition from yeast to hyphal morphology is a highly controlled and regulated process that can be initiated by multiple environmental stimuli triggering signalling cascades which results in hyphal development (Sudbery 2011). Hyphae are induced by elevated temperatures, pH changes, low nitrogen, high CO_2, the presence of serum and N-acetylglucosamine (GlcNAc) (Desai 2018). Alkaline pH promotes hyphal forms, whilst pH ≤ 6 is more favourable to budding yeast forms (Mayer et al. 2013).

Quorum sensing (QS) molecules are a mechanism of extracellular microbial communication. QS is density dependent, relying on a threshold of QS molecules being achieved to trigger effects through altering gene expression in the microbial community. Farnesol is a QS molecule of *C. albicans* which inhibits hyphal production (Hornby et al. 2001; Shchepin et al. 2003). Cell density is a regulator of morphology and $>10^6$ cells/mL promotes yeast through farnesol production and hyphal inhibition (Hornby et al. 2001).

Signalling pathways involved in hyphal morphogenesis include mitogen-activated protein kinase (MAPK) signalling and cyclic adenosine monophosphate (cAMP)-dependent Protein Kinase A (PKA) pathways, resulting in increased expression of a large number of genes, and many transcription factors (TFs) (Sudbery 2011; Desai 2018). An example of a transcription factor involved in this process is Nrg1, which inhibits hyphal development until Nrg1 is downregulated through activation of the cAMP-PKA pathway (Su et al. 2018; Kadosh 2019). Activation of these signalling pathways not only results in hyphal production, but also upregulation of

hyphal specific genes such as those encoding secreted aspartic proteases (SAP) *e.g. SAP4* and hyphal specific adhesins like agglutinin-like sequence proteins (ALS) *e.g.* Als3 (Kumamoto and Vinces 2005b).

1.4.2.2. Adherence of *Candida albicans*

Adherence of *C. albicans* to biotic and abiotic surfaces is important for colonisation and biofilm formation (Gulati and Nobile 2016). *Candida* adheres to many different host surfaces including epithelium, endothelium, phagocytic cells and dental protheses (Williams and Lewis 2011). *Candida albicans* adhesion is facilitated through expression of surface adhesins including the Als family (Als1-7 and Als9), Hyphal Wall Protein 1 (Hwp1) and epithelial adhesin 1 (Epa1) (Zhao et al. 2004; Kumamoto and Vinces 2005b; Alves et al. 2014; Hoyer and Cota 2016). These adhesins are also associated with virulence and pathogenicity (Williams and Lewis 2011)

The hyphal specific Als3 adhesin is multifunctional and mediates attachment to epithelial cells, endothelial cells, and extracellular matrix proteins as well as biofilm formation on dental protheses (Liu and Filler 2011; Deng et al. 2021). Loss of Als3 affects adhesion more than loss of Als1, suggesting a greater dependence on Als3 for adhesive roles (Zhao et al. 2004). Clinical strains of *C. albicans* have varying levels of Als3 expression (Bruder-Nascimento et al. 2014) and higher expression of Als3 has been suggested as a predictor of biofilm formation (Deng et al. 2021). Additionally, Als3 is also categorised as an invasin with the ability to bind E-cadherin and N-cadherin, triggering clathrin-dependent endocytosis by host cells and assisting *C. albicans* invasion into cells and tissues resulting in an important role in pathogenicity (Liu and Filler 2011). Als3 is also known to mediate adherence and interactions with other microorganisms (Silverman et al. 2010; Bamford et al. 2015; Pidwill et al. 2018).

1.4.2.2.1. Relationship between surface conditioning and *Candida albicans* adherence

Properties of the surfaces on which biofilms adhere and develop can impact adherence and colonisation and biofilm characteristics. For example, the roughness and surface charge following conditioning of the surface likely alters the original properties of the substrate for biofilm development. Sterile medical devices

are quickly covered with a conditioning film after implantation. Conditioning films vary depending on body site, but invariably comprise of host proteins and cells derived from surrounding body fluids (Frade and Arthington-Skaggs 2010).

Conditioning pellicles are key for the adhesion stage of biofilm development as they provide receptor binding sites for planktonic microorganisms, such as *C. albicans* to attach (Ramage et al. 2004; Frade and Arthington-Skaggs 2010). Components of the AP, such as mucins, are thought to interact with *C. albicans* initiating and promoting biofilm formation and maturation (Nikawa et al. 2000).

In the oral cavity, biotic and abiotic surfaces are rapidly coated with an AP, which as has been previously discussed, increases biofilm development and robustness of the *C. albicans* biofilm (da Silva et al. 2015; Cavalcanti et al. 2016b). The virulence of *C. albicans* biofilms on surfaces with an AP has not been extensively researched, although an AP has been found to increase metabolic activity and up-regulated genes associated with virulence such as *ALS1, ALS3* and *HWP1* (Cavalcanti et al. 2016b).

1.4.2.2.2. Relationship between surface topology and *Candida albicans* adherence

Surface roughness and topological features are variable especially on a microscopic scale. The soft acrylic surfaces of dentures can develop irregularities from brushing with abrasive/unsuitable cleansers, or through damage from consumption of hard foods (MacHado et al. 2012; Onwubu and Mdluli 2021). Resulting abrasions increase adherence and retention of microorganisms including *C. albicans* (Zamperini et al. 2010; Verran et al. 2014). Increased roughness results in a higher surface area, which affords greater binding opportunities to microorganisms. When the contact area between microbial cells and the surface is increased and when surface features are of similar dimensions to those of the attaching cell, there are a higher number of contact points for bonds to form (Medilanski et al. 2002; Whitehead et al. 2004; Whitehead et al. 2005; Whitehead and Verran 2006; Verran et al. 2010).

1.4.2.3. Hydrolytic enzymes

Candida albicans virulence is associated with secretion of several hydrolytic enzymes including proteinases and lipases. The production of secreted aspartyl proteinases (SAPs) is considered important in the development of *Candida* infections (Kumamoto and Vinces 2005b). SAPs are optimally active in more acidic conditions (~ pH 3 – 5) (Naglik et al. 2003), which is significant in oral infections since salivary pH is acidic (Abuhajar et al. 2023). However, not all *Candida* species produce SAPs.

Candida albicans secretes ten SAPs and these are usually expressed at higher levels compared with other *Candida* species (Kumamoto and Vinces 2005b). It has also been found that *Candida* from clinically evident candidoses produce higher levels of SAPs compared with strains from healthy mucosa (Williams and Lewis 2011; Lewis and Williams 2017). These observations indicate that *C. albicans* with active roles in infection are potentially more inherently virulent than 'commensal' strains, possibly through upregulated SAP expression. Despite these observations, there is no conclusive evidence that SAP activity has a role in infection, and it is possibly a lifestyle feature of *C. albicans* (Kumamoto and Vinces 2005a; Williams and Lewis 2011).

1.4.2.3.1. Phospholipases

Phospholipase activity has been reported for many fungal pathogens including *Candida* species and these enzymes contribute to virulence (Williams and Lewis 2011). Phospholipases hydrolytically cleave the ester bonds of glycerophospholipids, and this process is enhanced when hyphae are in contact with host tissues (Ghannoum 2000). The hyphal forms of *C. albicans* exhibit localised production and secretion of phospholipases around hyphal tips. These facilitate breakdown of phospholipid membranes of host cells and aids hyphal invasion into epithelial tissues and cell damage (Tsui et al. 2016). Phospholipases also promote exposure of receptors that have a role in adherence (Williams et al. 2011).

1.4.2.4. Evasion of host immune responses

Candida albicans can evade host immune responses by altering its cell wall components, changing its morphology and by secretion of hydrolytic enzymes (Lewis and Williams 2017). The *Candida* cell wall has a bilaminate structure with ß-glucans and chitin in between the outer fibrillar mannoproteins (Shibata et al. 2007; Gow and Hube 2012). Changes in the microenvironment around cells and the presence of antifungal drugs can alter cell wall composition and structure, thus interfering with phagocytosis, while also inhibiting inflammasome immune responses, as well as T cell-mediated responses such as Th1 and Th17 responses, whilst Th2 are promoted leading to host tolerance towards *Candida* (Netea et al. 2015). In addition to interfering with phagocytoses, *C. albicans* can also escape phagocytosis (Netea et al. 2015). Yeast cells that have been phagocytosed can form hyphae and induce host cell apoptosis through NLRP3 inflammasome activation (Netea et al. 2015). *Candida albicans* has its own mechanism of non-lytic expulsion from the phagocyte through inhibition of phagolysosome acidification and maturation, as well as expressing detoxifying enzymes to counteract damage from free radicals (Gow and Yadav 2017).

Invasins and candidalysin, the latter being a pore forming toxin, encourage *C. albicans* uptake into epithelial cells, resulting in tissue invasion and damage to host epithelia leading to triggering of host immune responses (Liu and Filler 2011; Sztukowska et al. 2018). *Candida albicans* can also inhibit host complement activation, inactivate antimicrobial peptides and inhibit other immune cell functions (Lee et al. 2012; Gow and Yadav 2017).

1.4.3. Interactions between *Candida* and other oral microorganisms

It is recognised that the behaviour of microorganisms can be markedly different between *in vitro* and *in vivo* environments for a wide range of reasons, including the types of other microorganisms present. Our knowledge of microbiomes, whole community effects and the importance of interspecies interactions is increasing following advancements in molecular techniques which allow for exploration of species that may not be culturable or not isolated due to the culture conditions required (Malla et al. 2019; Gurbich et al. 2023).

Candida albicans exhibits interactions with other microorganisms with candidaemia nosocomial infections being polymicrobial in approximately 27-56% of cases (Harriott and Noverr 2011). Recent research indicates modulation of *C. albicans* virulence by oral bacteria such as *Streptococcus sanguinis, Streptococcus gordonii, Actinomyces odontolyticus* and *Actinomyces viscosus* by promoting hyphal production and increased expression of virulence associated genes such as agglutinin-like sequence 3 (Als3) and hyphal-wall protein 1 (Hwp1) (Morse et al. 2019). However, the underlying mechanisms of this modulation remain unknown and whether all four of these oral bacterial species are required for this response or whether they also exhibit this influence on *C. albicans* individually. Denture-associated biofilm specific bacteria, *Streptococcus* and *Actinomyces* species can all promote hyphal development, increase epithelial tissue invasion and upregulate virulence genes, resulting in *Candida* that is potentially more pathogenic (Cavalcanti et al. 2016a)

Mutualism between *Candida* and *Streptococcus* species has frequently been reported and can affect biofilm formation and morphology and virulence of *Candida* (Bamford et al. 2009; Diaz et al. 2014; Bamford et al. 2015; Xu et al. 2016; Pidwill et al. 2018). *Streptococcus* species are found throughout the human body and are the most prevalent species in the oral cavity (Abranches et al. 2018). Oral streptococci are primary colonisers of the oral cavity and possess adhesins that facilitate binding to oral surfaces and AP components (Abranches et al. 2018; Simon-Soro et al. 2022). This is important for *C. albicans* as it can bind either to the surface via already adhered species like *Streptococcus* or co-aggregate and bind to surfaces as an aggregation (Simon-Soro et al. 2022). Mitis Group Streptococcus which include *S. gordonii and S. sanguinis* form robust mixed biofilms with *C. albicans* on titanium and increase tissue damage (but not an increased immune response) compared to single species *C. albicans* biofilms (Souza et al. 2020). *Streptococcus gordonii* interactions with *C. albicans* promotes *C. albicans* hyphal production and biofilm formation (Bamford et al. 2009), and enhance the efficacy of binding to host epithelial tissues (Pidwill et al. 2018). There is evidence that QS molecules from both species are involved in interactions, with the autoinducer-2 *S. gordonii* QS molecule being implicated in promoting *C. albicans* hyphal morphology and biofilm formation through suppressing the effects

of the *C. albicans* QS molecule farnesol which usually inhibits hyphal morphogenesis (Bamford et al. 2009; Salvatori et al. 2016; Ponde et al. 2021). *Candida albicans* also lowers oxygen in the environment which is beneficial for *Streptococcus* species that are facultative anaerobes (Janus et al. 2017). Antagonism between *Streptococcus* species such as *S. mutans, S. gordonii* and *S. sanguinis* often results in elevated levels of hydrogen peroxide, especially in more aerobic conditions, and this has been shown to induce *C. albicans* hyphal development (Kreth et al. 2005; Nasution et al. 2008).

The mechanisms of interaction between *S. gordonii* and *C. albicans* has been studied and highlights the importance of the hyphal specific Als3 protein (Nobbs et al. 2010; Hoyer et al. 2014; Pidwill et al. 2018). Als3 binds to the SspA and SspB proteins of *S. gordonii* and has been proven through use of Als3 deleted mutant strains (Bamford et al. 2009; Silverman et al. 2010; Bamford et al. 2015). This was further supported through expression of the *C. albicans* Als3 protein in *Saccharomyces cerevisiae*, which resulted in *S. gordonii* binding to Als3-expressing *Saccharomyces cerevisiae* which does not normally occur (Silverman et al. 2010).

Streptococcus salivarius inhibits *C. albicans* aggregation, biofilm formation and hyphal transformation (Ishijima et al. 2012; Mokhtar et al. 2021). *Streptococcus salivarius* also had a protective effect in an oral candidiasis mouse model through binding to *C. albicans* hyphae cells and preventing their adherence to mucosal surfaces, which was shown to reduce inflammation and severity of candidosis (Ishijima et al. 2012). Anti-inflammatory properties of *S. salivarius* require it to be metabolically active (Kaci et al. 2014). In a human clinical trial, Passariello *et al.* (2020) reported that *S. salivarius* reduced oral *C. albicans* colonisation and symptoms of *Candida*-associated denture stomatitis.

Streptococcus mutans forms biofilms with *C. albicans* with interactions proposed to be through a bacterial-fungal-EPS complex between *C. albicans* mannans and glucosyltransferases B of *S. mutans* (Gregoire et al. 2011; Hwang et al. 2017). Mannans are present on all *C. albicans* morphological forms mediating their interaction with *S. mutans*. *Streptococcus mutans* inhibits hyphal transition through

the QS molecule, competence-stimulating peptide (CSP) that is produced during the exponential phase of growth (Jarosz et al. 2009).

Candida albicans and *Pseudomonas aeruginosa,* though they are commonly co-isolated from infection and disease of the skin and lung, frequently exhibit antagonism towards each other *in vitro*, which is thought to be due to QS molecules from both species which can cause oxidative damage to each other (Hogan 2002; Hogan et al. 2004; Fourie et al. 2016; Lohse et al. 2018). *Candida albicans-P. aeruginosa* interaction involves both physical and secreted factors and their chemical antagonism causes substantial damage to the host. Understanding the mechanisms of such interactions therefore has implications for disease and infection treatment and management (Fourie et al. 2016).

1.4.4. Oral Candidosis

Oral candidosis is mainly caused by *C. albicans* and is colloquially referred to as 'thrush' and is identifiable through white lesions in the oral cavity (Vila et al. 2020). Oral candidosis had increased prevalence in the 1980s due to the acquired immune deficiency syndrome (AIDS) epidemic (Vila et al. 2020). As an opportunistic pathogen *C. albicans* is more problematic for immunocompromised individuals and remains the most common oral opportunistic infection in human immunodeficiency virus (HIV)-positive individuals (Fidel Jr 2006; Vila et al. 2020).

There are four distinct forms of primary oral candidosis that are categorised by clinical presentation (Table 1.1). These include pseudomembranous candidosis (Figure 1.3A), chronic hyperplastic candidosis (Figure 1.3B), chronic erythematous candidosis (Figure 1.3C), and acute erythematous candidosis (Figure 1.3D) (Marsh et al. 2016a). In addition, there are secondary forms of oral candidosis that cause *Candida*-associated lesions, including angular cheilitis, median rhomboid glossitis and chronic mucocutaneous candidosis (Marsh et al. 2016a). Poor dental hygiene is linked to oral candidoses, and several other factors lead to some individuals being more susceptible to candidosis such as tobacco smoking, antibiotic use and having a compromised immune system (Williams and Lewis 2011).

Table 1.1. Summary of the four primary types of oral candidosis. (Marsh et al. 2016a; Vila et al. 2020)

Types of oral candidosis	Summary of infection
Pseudomembranous candidosis (oral thrush) Figure 1.3A	• Presents as white plaque-like lesions. • Most frequent in neonates and elderly individuals. • Usually, an acute infection but can become chronic for immunocompromised individuals. • Associated with weakened immune systems, age-related factors and the use of steroid inhalers.
Chronic hyperplastic candidosis Figure 1.3B	• Comparatively rare form of oral candidosis. • Most commonly found in middle-aged men who are smokers and have high alcohol consumption. • Often asymptomatic • Can lead to dysplasia and development of oral cancer. • Characterised by hyphal invasion of the *Candida* into oral epithelium.
Chronic erythematous candidosis (*Candida*-associated denture stomatitis) Figure 1.3C	• Most common form of oral candidosis seen in up to 75% of denture wearers (Vila et al. 2020). • Reddening of the mucosa in contact with the denture fitting surface. • Associated with poor oral hygiene and ill-fitting dentures. • Hyphal invasion of the mucosa is not observed.
Acute erythematous candidosis (antibiotic sore mouth) Figure 1.3D	• Presents as painful, reddened patches on the oral mucosa. • Associated with use of broad-spectrum antibiotics. • Loss of bacterial microorganisms allow over proliferation of *Candida.*

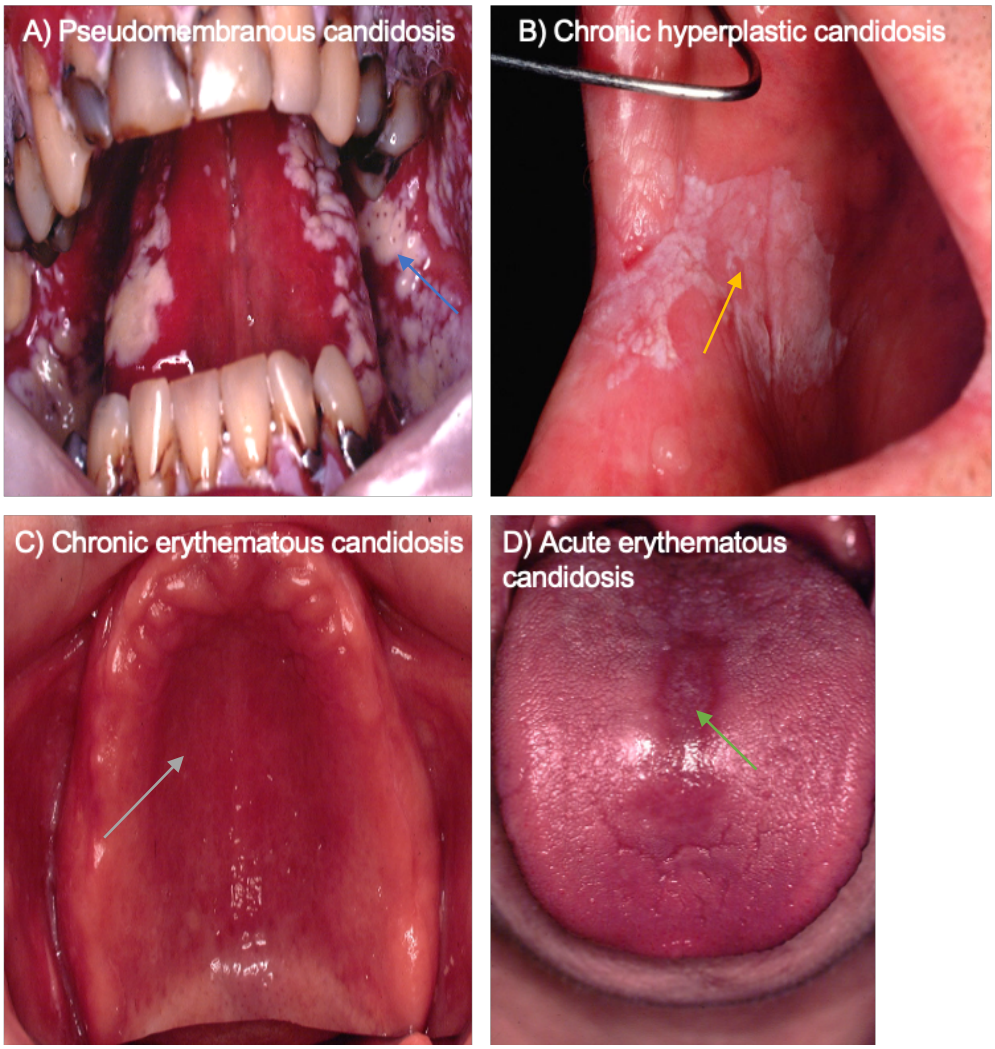

Figure 1.3. Clinical presentation of the four primary forms of oral candidosis. A) pseudomembranous candidosis (oral thrush), blue arrow indicates characteristic white plaque-like mucosal lesions, B) chronic hyperplastic candidosis, yellow arrow indicating mucosal lesion C) chronic erythematous candidosis (*Candida*-associated denture stomatitis), grey arrow to the inflammation of the hard palate which presents as reddening of the hard palate and D) acute erythematous candidosis green arrow pointing to the red lesion on the tongue these red patches are often painful.

1.4.4.1. *Candida*-associated denture stomatitis

Denture wearers commonly present with *Candida*-associated denture stomatitis (chronic erythematous candidosis) (Figure 1.3 and Table 1.1) of varying severity with an estimated 35-75% of wearers being affected depending on the cohort studied (Webb et al. 1998; Barbeau et al. 2003; Shulman et al. 2005; Zomorodian et al. 2011; Vila et al. 2020). In addition to the risk factors for all oral candidoses, additional risk factors for *Candida*-associated denture stomatitis are inadequate oral and denture hygiene, ill-fitting dentures, continuous denture wear including overnight, and development of a microenvironment that promotes *Candida* growth and suppresses bacterial species.

Denture biofilms (section 1.3.1.1) act as a microbial reservoir which continuously seeds *Candida* onto the palatal mucosa (Vila et al. 2020). Poorly-fitting dentures increase the risk of *Candida*-associated denture stomatitis through frictional damage to the mucosal surfaces, allowing infiltration of *Candida* (de Senna et al. 2018; Vila et al. 2020). *Candida* colonising the denture surface is significantly increased in *Candida*-associated denture stomatitis compared to healthy denture wearing individuals (O'Donnell et al. 2017). The denture fitting surface experiences reduced salivary flow, creating an area that is stagnant and develops its own microenvironment which becomes preferential to *Candida* through a more alkaline pH, elevated temperature, increased carbohydrate availability and nitrogen starvation which also suppresses oral bacterial species (Abuhajar et al. 2023).

1.4.4.1.1. Association between tobacco use and *Candida*-associated denture stomatitis.

Candida-associated denture stomatitis has a higher prevalence in people who smoke cigarettes, and this is also considered a major risk factor for the other forms of oral candidosis (Shulman et al. 2005; Soysa and Ellepola 2005; Akram et al. 2018). It is currently unclear why cigarette smoke is associated with increased risk of oral candidosis, but components of tobacco have been shown to disrupt innate immune responses, induce biofilm formation and upregulate expression of genes associated with *Candida* virulence (Mehta et al. 2008; Semlali et al. 2014). Semlali et al. (2014), found that cigarette smoke condensate increased *C. albicans* adhesion, growth, biofilm formation and expression of the virulence genes *EAP1,*

HWP1 and *SAP2* and the effects were concentration dependent. There is also evidence that tobacco extracts induce the yeast to hyphal transition (Awad and Karuppayil 2018), suggesting that *C. albicans* might be more pathogenic in the mouths of smokers than non-smokers. Waterpipe smoking, a term encompassing goza, hookah, narghile, and shisha, which is commonly misconceived as being 'safer' or 'healthier' than smoking cigarettes, has also been found to lead to the same levels of *C. albicans* carriage as in cigarette smokers, which is significantly higher than in non-smokers (Akram et al. 2018). The emergence and increasing popularity of e-cigarettes and vaping has directed research to be conducted on these products and it was found that e-cigarettes promote *C. albicans* growth but less than conventional cigarette smoke (Alanazi et al. 2019). Enhanced oral *C. albicans* adherence and biofilm thickness has also been attributed to nicotine, which increases cell number and abundance of EPS, as well as upregulation of *HWP1* and *ALS3* hyphal specific virulence genes, in a dose-dependent manner (Gunasegar and Himratul-aznita 2019). Research suggests that cigarette smoke can also affect the surface roughness of denture materials (Mahross et al. 2015; Singh et al. 2019), which would have relevance in adherence and retention of *C. albicans* in *Candida*-associated denture stomatitis.

1.4.4.2. Treatment and management of *Candida*-associated denture stomatitis

Management strategies for *Candida*-associated denture stomatitis is primarily through reducing risk factors and the level of *Candida* (Abuhajar et al. 2023). It is of utmost importance to inform patients of the risk factors and how to limit them to reduce recurrence of infection. Any issues with oral or denture hygiene should be addressed by explaining suitable cleansing protocols and products, particularly recommending the use of denture cleansers that include anti-*Candida* properties such as 1% sodium hypochlorite or 0.2% chlorhexidine (Williams and Lewis 2011). However, research has shown that denture cleansers do not fully eradicate all *C. albicans* and, therefore, should be used in combination with other interventions (O'Donnell et al. 2017). Ideally the patient should also stop smoking, if applicable, and ensure removal of their dentures during the night, ideally removing dentures for eight hours a day (Abuhajar et al. 2023). The denture should be assessed to

ensure it fits well and that there is no damage or wear that may increase adherence and retention of microorganisms.

Antifungals, whilst more limited than antibiotics, are available for the treatment of infections and can be topical or systemic, the choice of which would depend on the severity of the infection (Pappas et al. 2015; Abuhajar et al. 2023). Current reports state that antifungal resistance in *C. albicans* remains low (World Health Organization 2022). Azoles are the most frequently used antifungal class to treat candidosis (Santos et al. 2018). Azoles are fungistatic through the inhibition of the enzyme lanosterol demethylase which is involved in ergosterol production (Andes 2003; Williams and Lewis 2011). The most commonly used azole is fluconazole which has a relatively low cost and low toxicity and can be administered systemically and is then secreted in high levels in saliva which is ideal for the treatment of oral infections (Force and Nahata 1995; Kim et al. 2020). However, fluconazole resistance has been detected and can develop from prolonged use and so a synergistic approach with other drugs is advised but not yet clinically available (Lu et al. 2021). Alternative antifungals include polyenes, which are fungicidal and include the drugs amphotericin B and nystatin which bind to ergosterol in fungal cell membranes, causing leakage of cytoplasm leading to fungal cell death (Williams and Lewis 2011; Santos et al. 2018). However, these need to be used at lower doses due to a degree of toxicity in humans and must be topical as they are not adsorbed well in the gut.

A new approach to reducing *Candida*-associated denture stomatitis is to incorporate antifungals and nanoparticles into the denture resin (Abuhajar et al. 2023). Sliver nanoparticles exhibit antimicrobial properties and could be added to PMMA denture material to decrease colonisation by *C. albicans* (Benoit et al. 2019; De Matteis et al. 2019). A systematic review by An *et al.* (2021), states that while incorporation of nanoparticles and antimicrobials into denture material has been shown to be effective in reducing *Candida*-associated denture stomatitis there are still many disadvantages that need to be addressed, including development of microbial resistance to antifungals and diffusion of nanoparticles to cells and tissues.

1.5. Research aims and objectives.

Current understanding of the modulators of *C. albicans* adhesion, biofilm formation and morphological changes in the oral cavity is limited and are areas that require more research. There is a complex network of interactions occurring in the oral cavity that has yet to be understood and this would give better insight as to why certain individuals may be predisposed to candidoses. Defining risk factors in more detail and how these are influenced by the local environment and microbial community could facilitate interventions in the management of oral candidosis. Elucidating the role of bacteria in denture biofilms is also important as it may have implications in the treatment and prevention of *Candida*-associated denture stomatitis among other oral *Candida*-associated infections and diseases. The findings of this research may be further extrapolated to the behaviour of biofilms containing *C. albicans* that colonise other niches in the human body.

The underlying hypothesis of the research was that key properties of *C. albicans* in biofilms are modulated by specific local environment factors. Such properties would include *C. albicans*' biofilm forming ability and morphological transformation to filamentous forms. Changes in the local environment that could affect these properties were examined and these included:

- Altering surfaces for biofilm attachment through specific conditioning using artificial saliva, water and tobacco condensate (Chapter 2)
- Changing surface roughness (Chapter 3)
- Inclusion of certain oral bacterial species in the biofilms (Chapter 4 and 5).

CHAPTER 2: The Effect of Acrylic Surface Conditioning on *Candida albicans* Adherence and Biofilm Development

2.1. Introduction

The majority of microorganisms naturally grow within biofilms, which are prevalent on environmental surfaces and on, or within hosts (Lohse et al. 2018). Biofilms are responsible for ~80% of microbial infections in humans. However, studying biofilms rather than planktonic microorganisms is a relatively new concept (Lohse et al. 2018) and many of the interactions that occur between biofilms and local environmental factors have yet to be fully explored.

One of the most widely studied biofilms is dental plaque, which is present on the enamel surface of teeth (Berger et al. 2018). However, there are also biofilms that develop on other oral surfaces, including the mucosa and abiotic surfaces of dental protheses (*e.g.,* dentures, dental implants). The fact that biofilms adhere to, and form on denture acrylic is well recognised, and these biofilms are particularly prevalent in instances of poor denture hygiene (Webb et al. 1998).

Whilst natural oral surfaces have mechanisms to remove microorganisms, such as surface renewal or the sloughing off of cells, the abiotic acrylic surface of a denture is unable to do this. There is also reduced salivary flow over the upper fitting surface of a denture which limits physical and chemical removal of biofilm microorganisms (Monsenego 2000; Hannah et al. 2017). These factors promote the development of mature and persistent biofilms on denture surfaces.

Due to the 'non-self' nature of denture material in the oral cavity, exogenous bacteria that are not usually associated with the mouth may better compete with endogenous microorganisms to adhere and colonise (Berger et al. 2018). Denture-associated biofilm studies have often focussed on the genus *Candida* as these fungi are efficient at adhering to acrylic surfaces and are involved with infection, most notably, *Candida*-associated denture stomatitis (Berger et al. 2018; Lohse et al. 2018).

The *Candida* genus contains over 350 species of 'yeast-like' fungi, but only a minority are associated with human infection (Williams et al. 2011). The most prevalent *Candida* species in human health and disease is *C. albicans,* which is frequently encountered as a commensal microorganism in ~50% of individuals (Williams et al. 2011). *Candida albicans* is polymorphic and can grow as yeast,

pseudohyphae and true hyphae. The species is also an opportunistic pathogen and may progress from being a harmless commensal microorganism to one able to cause disease in individuals who are immunocompromised, or where there is an underlying debilitation or risk factor (Lewis and Williams 2017).

The physical and chemical properties of surfaces on which biofilms form can potentially impact adherence and subsequent growth of microorganisms and thus influence biofilm characteristics. For example, surface topography, hydrophobicity, and charge (often associated with surface conditioning) can affect physical retention and adherence of microorganisms (Whitehead et al. 2004; Zamperini et al. 2010). Sterile medical devices rapidly acquire a conditioning film after introduction into the body. The type of conditioning film varies with body location, but invariably comprises of host proteins and cells from surrounding body fluids (Frade and Arthington-Skaggs 2010).

Conditioning films or pellicles are important in the adhesion stage of biofilm development as they may offer receptor binding sites for planktonic microorganisms to attach (Ramage et al. 2004; Frade and Arthington-Skaggs 2010), or indeed molecules that repel or inhibit attachment of microorganisms. In the case of the mouth, saliva is the main contributor to conditioning films. Components of the salivary pellicle, such as mucins, are known to interact with *C. albicans* leading to initiation and promotion of biofilm formation (Nikawa et al. 2000). The salivary pellicle has been found to increase biofilm development and lead to more robust *C. albicans* biofilms (da Silva et al. 2015; Cavalcanti et al. 2016b). The virulence of *C. albicans* biofilms on surfaces with a salivary pellicle has not been extensively studied, although the pellicle has been found to increase metabolic activity and up-regulate genes associated with virulence such as Agglutinin-like protein 1 (*ALS1*), Agglutinin-like protein 3 (*ALS3*) and Hyphal Wall Protein 1 (*HWP1*) (Cavalcanti et al. 2016b). ALS1, ALS3 and HWP1 are hyphal-specific, cell wall adhesins that have many functions including promoting adherence to biotic and abiotic surfaces, adherence to other microorganisms and facilitating invasion of host cells and epithelial layers (Cavalcanti et al. 2014; Bamford et al. 2015; Gulati and Nobile 2016; Pidwill et al. 2018)

Candida-associated denture stomatitis has an increased prevalence in people who smoke cigarettes, which is also considered a major risk factor for other forms of candidosis (Shulman et al. 2005; Soysa and Ellepola 2005; Akram et al. 2018). It is currently not fully understood why cigarette smoke is associated with increased rates of candidosis, but components of tobacco have been shown to disrupt the innate immune response, induce biofilm formation and upregulate expression of *Candida* genes associated with virulence (Mehta et al. 2008; Semlali et al. 2014). Semlali *et al.* (2014), reported that cigarette smoke condensate increased adhesion, growth, biofilm formation and expression of the *C. albicans* virulence-associated genes *EAP1, HWP1* and *SAP2*. There is also supporting evidence that tobacco extracts induce yeast to hyphal transition (Awad and Karuppayil 2018), suggesting that *C. albicans* is likely to be more pathogenic in the mouths of cigarette smokers than non-smokers. Waterpipe smoking, which encompasses goza, hookah, narghile, and shisha, are frequently and incorrectly considered to be 'safer' or 'healthier' than smoking cigarettes (Chaouachi 2007; Awad and Karuppayil 2018). However, waterpipe smoking has also been found to lead to the same levels of *C. albicans* carriage as in cigarette smokers, which is significantly higher than in non-smokers (Akram et al. 2018). Enhanced oral *C. albicans* adherence and biofilm thickness has also been attributed to the presence of nicotine, which increases cell number and the abundance of extracellular polymeric substances (EPS). In addition, upregulation of *HWP1, ALS3* and hyphal specific virulence genes occurs in a nicotine dose-dependent manner, suggesting an increase in virulence might be expected (Gunasegar and Himratul-aznita 2019).

The underlying hypothesis of this research was that different surface conditioning treatments applied to acrylic would affect subsequent adhesion, biofilm formation and expression of virulence attributes of *C. albicans*.

2.1.1. Aims and Objectives

The primary aims of this chapter were to:

1. Assess whether *C. albicans* on denture acrylic is influenced by surface conditioning using water, artificial saliva, or a condensate from cigarette smoke. Measured parameters included initial adherence, morphological transformation, and biofilm surface coverage.

2. Chemical and surface properties of the acrylic before and after conditioning were also determined and associated with any observed changes.

2.2. Materials and Methods

2.2.1. Overview of microorganisms used in this research.

Candida albicans SC5314 was used in this research. The strain was originally a clinical isolate from human infection and along with having an available genome sequence, is known to be susceptible to anidulafungin, micafungin, caspofungin, 5-flucytosin, voriconazole, itraconazole and fluconazole. *Candida albicans* SC5314 is not a designated type strain, but has been widely used in research. Four clinical isolates of *C. albicans* were also included in the research (Table 2.1.; Malic *et al.* 2007). The clinical isolates were selected as they had been isolated from a range of oral conditions and demonstrated variation in tissue colonisation and invasion (Malic et al. 2007).

Table 2.1. *Candida albicans* clinical isolates, including source of isolation, and their efficacy at surface colonisation and invasion of tissues. CHC, chronic hyperplastic candidosis; SCC, squamous cell carcinoma. Adapted from Malic et al. (2007).

Strain	Isolate source	Level of surface colonisation*	Invasion*
PB1/93	Normal oral mucosa	++	Low
480/00	SCC oral mucosa	++	Low
PTR/94	CHC buccal mucosa	+++	High
705/93	CHC buccal mucosa	+++	High
*, based on study in a reconstituted human oral epithelium (Malic et al. 2007) SCC, squamous cell carcinoma CHC, chronic hyperplastic candidosis			

2.2.1.1. Culture conditions

Candida albicans was cultured on Sabouraud Dextrose Agar (SDA, Lab M, Heywood, UK) for 48 h at 37°C. Stocks of each strain were stored at -80°C on microbank™ beads from which, SDA streak plates were prepared and retained at 4°C for up to 4 weeks. Liquid cultures were prepared in 10 mL of Yeast Nitrogen Base (YNB; BD Difco™, Oxford, UK) medium supplemented with 0.5 g D-glucose (Fisher Scientific, Waltham, Massachusetts, United States), 0.1 mg L-histidine (Sigma-Aldrich, Burlington, Massachusetts, United States), 0.2 mg L-methionine (Sigma-Aldrich) and 0.2 mg L-tryptophan (Sigma-Aldrich) per L. YNB was filter sterilised using a Minisart™ NML Syringe Filter (Sartorius, Göttingen, Germany) and 10 mL (x10 concentration) aliquots stored at 4°C and then diluted 10-fold with sterile distilled H_2O (dH_2O) at the time of use. For experiments, YNB was inoculated with 1-2 colonies from SDA and incubated at 37°C for 16-18 h.

2.2.1.2. Standardisation of inocula

Prior to inoculation for experimental procedures, YNB cultures were adjusted to a standardised optical density of 1.0 OD_{600nm} (± 0.01) (equivalent to approximately 1 x 10^7 cells/mL) using a spectrophotometer (DiluPhotometer™, Implen, Westlake Village, CA, USA). In all cases, the spectrophotometer was initially calibrated to a zero-baseline using sterile YNB. Sterile YNB was used to dilute cultures as required.

2.2.2. Preparation of denture acrylic materials

2.2.2.1. Production of polymethyl methacrylate (PMMA) coupons

Polymethyl methacrylate (PMMA) is a thermoplastic used to construct denture prostheses and orthodontic retainers. PMMA was used as the solid substratum to grow mono- and polymicrobial biofilms.

Oracryl Cold Cure polymer SW9053 powder (Bracon Dental Laboratory Products, Etchingham, UK) was added to Oracryl Cold Cure Liquid monomer at a 2:1 (w/v) ratio and thoroughly mixed manually until homogenous and devoid of air bubbles. The resultant mixture was poured into a polytetrafluoroethylene (PTFE) mould to generate 24 round PMMA coupons that were 8 mm in diameter and 2 mm in depth.

The mould was compressed between two glass panels to reduce surface irregularities and provide a smooth, polished finish on the coupon. The material was cured at room temperature for at least 1 h. The underside of each coupon was levelled, and any irregularities or sharp protrusions were removed from the edges using a polisher (Kemet International Ltd, Maidstone, UK) with P120 grade silicon carbide paper (Agar Scientific, Stansted, UK). Coupons were marked on the rough underside to indicate the correct orientation to ensure the biofilms formed on the polished face during experimentation. Coupons were then placed in water for a minimum of 5 days to allow excess and uncured monomer to leach from the material. Sterilisation prior to use was achieved by autoclaving the coupons in distilled water at 121°C for 15 min. Coupons were all single use only and were discarded after experimentation.

2.2.2.2. Preconditioning of PMMA coupons

2.2.2.2.1. Artificial saliva and water preconditioning

Artificial saliva (AS) was prepared based on a previously reported composition (Table 2.2) (Cavalcanti et al. 2014; Morse et al. 2019)). Once homogenous, aliquots of 250 mL were placed in Duran® bottles (Sigma-Aldrich) and autoclaved at 121°C for 15 min. Following sterilisation and immediately prior to use, 1.25 mL/L of 40% (w/v) filter sterilised (Minisart™ NML Syringe Filter, Sartorius) urea solution was added to the AS.

Sterile PMMA coupons were randomly selected and aseptically transferred into either 10 mL of AS or sterile distilled H_2O for 16-20 h at 37°C. Water conditioned (WC) PMMA coupons served as controls. Prior to experiments, all coupons were briefly immersed in sterile dH_2O to remove excess conditioning medium.

Table 2.2. Composition of artificial saliva (Cavalcanti et al. 2014; Morse et al. 2019)**.** Components listed in the table were combined and autoclaved. Post sterilisation, 1.25 mL/L of filter sterilised 40% (w/v) urea solution was added.

Chemical Component	g/L
Porcine Stomach Mucin (Oxoid, Basingstoke, UK)	2.5
Sodium Chloride (Fisher Scientific)	0.35
Potassium Chloride (Fisher Scientific)	0.2
Calcium Chloride Dihydrate (Fisher Scientific)	0.2
Yeast Extract (Oxoid)	0.2
Lab Lemco Powder (Oxoid)	1.0
Protease Peptone (Oxoid)	5.0

2.2.2.2.2. Tobacco condensate (TC) preconditioning

A tobacco condensate was produced using the apparatus illustrated in Figure 2.1A. Cigarettes (Mayfair Original Blue, serial; batch number: 84S GQD AZ6 RVU; FJH16C18) had their filters removed before being inserted singly into the apparatus. A vacuum pump (800 mbar) pulled air through the apparatus, allowing the cigarette to be burnt. The generated smoke was drawn through the tubing and into a vessel holding 50 mL of AS and sterilised PMMA coupons. A Dreschel head, without a frit, allowed the smoke to diffuse through the liquid as large bubbles. The smoke was then pulled through two extra vessels containing distilled H_2O that had Dreschel heads with filters, before the airflow was returned into the vacuum pump to prevent smoke components going through the pump and reduce release into the fume hood. Twenty cigarettes were ‘smoked’ over ~ 30 min. After smoking, there was an obvious discolouration to the AS, (which was subsequently referred to as tobacco condensate, TC), and to the PMMA coupons as well as the water vessels (Figure 2.1 B and C). These coupons were stored in the TC at 2 - 4°C until use.

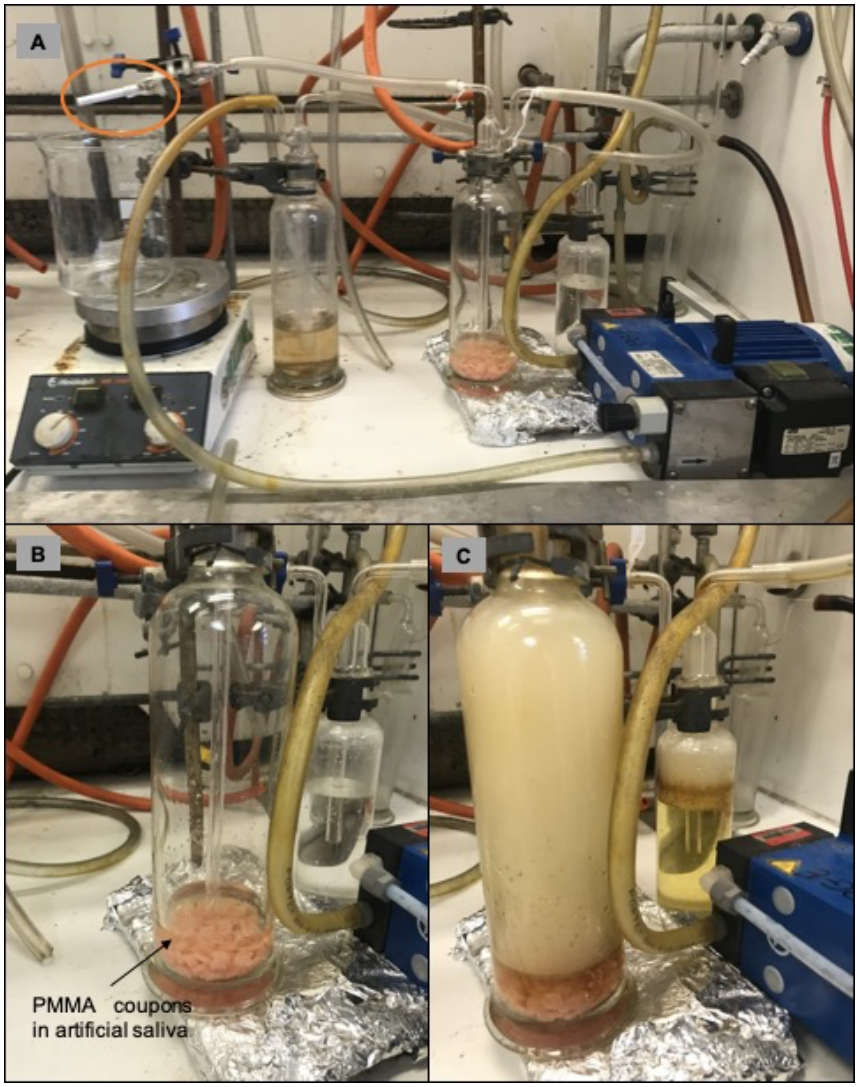

Figure 2.1. Apparatus used to produce tobacco condensate and preconditioning of the poly methyl methacrylate (PMMA) coupons. A) Image of the smoking apparatus. A cigarette devoid of its filter was placed into the holder indicated by the orange circle and lit. The vacuum pump pulled the cigarette smoke through the tubing and through the Dreschel head that did not have a filter which was placed in artificial saliva (AS) containing the PMMA coupons. After this chamber, the cigarette smoke was pulled through two additional vessels containing Dreschel heads with filters that were immersed in water to minimise the amount of smoke going through the vacuum pump and collect any excess components. B) Container with the PMMA coupons and AS before smoking occurred. The water container for filtration can be seen in the background. C) The apparatus after smoking. The container holding the PMMA coupons and AS was filled with smoke. Discolouration of the AS and coupons was evident.

2.2.3. Chemical characterisation of conditioned PMMA coupons

2.2.3.1. Sample preparation

PMMA coupons and samples of the solutions from the different types of preconditioning were prepared for analysis through solvent and water extraction. PMMA coupons preconditioned with TC, AS or water were all subjected to extraction with 5 mL dichloromethane, and 5 mL dH_2O, and ultrasonicated for 1 min to aid dissolution and dispersion of analytes. Samples of the solution in which the PMMA coupons had been conditioned were also analysed. Twenty µL of each extract was diluted to 20 mL in distilled water. For the dichloromethane solvent extraction samples, the suspension was allowed to separate into its two constituent layers, and the dichloromethane layer was collected. Dichloromethane was then removed under reduced pressure, and the residual oil transferred into an amber glass autosampler vial (Thermofisher). Dichloromethane extracts prepared for analysis are listed in Table 2.3.

Table 2.3. Dichloromethane extracts prepared for analysis.

1.	Artificial saliva (AS)
2.	AS preconditioned polymethyl methacrylate (PMMA)
3.	PMMA denture acrylic,
4.	PMMA treated with AS and *C. albicans*,
5.	PMMA treated with tobacco condensate (TC)
6.	PMMA with tobacco condensate and *C. albicans*
7.	The viscous oil that had gathered in the joints of the Drechsel heads

2.2.3.2. Gas Chromatography – Mass Spectrometry (GC-MS)

Extracts (Table 2.3) were analysed using a Waters GCT Time of flight (TOF) mass spectrometer with an Agilent 6980 GC interface. Five µL of the extract was injected

using a split/split-less inlet with 20% split at 190˚C inlet temperature. The temperature was initially programmed to 40˚C, which was held for 5 min. The temperature was then increased at a rate of 5˚C/min to 300˚C, and then held at 300˚C for a further 5 min. The column used was a 30 m, 35% phenyl 65% methyl polysiloxane capillary column. The system was calibrated with heptacosafluorotributylamine. The limit of detection of the apparatus was determined using EPA Volatile Organic Compounds Mix 2, and found to be between 1 to 5 µg/ml.

2.2.3.3. Liquid Chromatography – Mass Spectrometry (LC-MS)

LC-MS analysis was performed using a Waters Synapt G2-Si time-of-flight mass spectrometer coupled to a Waters Acquity UPLC system with an Acquity C18 reverse phase column to ascertain the water-soluble components present. One µL of each sample was injected into the system. The method used a solvent linear gradient aqueous acetonitrile from 5 - 95% (including 0.1% formic acid as a ionisation source). The instrument was held at 40°C throughout the run with a flow rate of 0.3 mL/min.

2.2.4. Surface roughness measurements of PMMA pre- and post-tobacco condensate conditioning

A profilometer (Surftech) was used to determine the mean surface roughness (Ra) measurements before and after conditioning. Post-autoclaving, 16 coupons were randomly selected and each labelled to ensure the measurements were ‘before and after’ of the same coupon. Three transects of 5 mm were measured on each coupon then averaged to give the mean Ra and the standard error of the mean (SEM) was calculated pre- and post-tobacco conditioning. The ‘before conditioning PMMA’ was a WC PMMA that had not been preconditioned in AS.

2.2.5. Contact angle measurements of PMMA surfaces with three different types of preconditioning.

Preconditioning PMMA could change the hydrophobicity of a surface and therefore the interactions between the surface and its environment. Contact angle measurements were used to assess surface hydrophobicity using the sessile drop

method for coupons of each of the three conditioning methods, namely WC, AS and TC. Coupons were preconditioned as previously described and then placed in a sterile petri dish to dry completely for at least 24 h. An Attension Theta Lite (Biolin Scientific) contact angle goniometer was used with OneAttension software (version 3.2, Biolin Scientific). Prior to measurements, the machine was calibrated using a calibration kit as per the manufacturer's instructions. A 4 µL droplet of water was then lowered on to the surface. As soon as the liquid contacted the surface, the software tracked the dispersion of the droplet recording the contact angle measurements on the left and right of the droplet for 10 s using a manually set baseline resulting in 205 timepoints within the 10s. The mean contact angle of the two points was calculated by the software for each timepoint. The mean contact angle was then averaged across the 205 timepoints giving an overall contact angle measurement for each coupon from the 10 s time period. Coupons (n = 4 - 7) were analysed per conditioning type, the mean contact angle measurements for each coupon was input into Prism 9 for MacOS (GraphPad Prism 9.4.0 (453) GraphPad Software, San Diego, California USA, www.graphpad.com) software for analysis and construction of graphs. Statistical significance was determined using One-way ANOVA with Tukey post-hoc test.

2.2.6. *Candida albicans* adherence and biofilm formation on PMMA coupons

All *C. albicans* strains, type of preconditioning and control PMMA coupons were tested in triplicate and imaged using confocal laser scanning microscopy (CLSM). To each well of a 24-well plate, 1900 µL of YNB was added before addition of the PMMA coupon (previously washed in PBS) with the smooth side facing upwards. *Candida albicans* was cultured and standardised as previously described (2.2.1). A 100-µL volume of the standardised culture was added to each well and statically incubated at 37°C to facilitate adhesion. *Candida albicans* adherence to PMMA was assessed after 90 min and biofilm formation was measured after 24 h.

2.2.7. Assessment of *Candida albicans* adherence and biofilm formation by confocal laser scanning microscopy (CLSM)

An inverted Leica TCS SP5 confocal system controlled by Leica confocal software was used for CLSM analysis. PMMA coupons were washed in dH_2O before attached *C. albicans* were stained with a 5% (v/v) solution of calcofluor white (Sigma). PMMA coupons were inverted so that the smooth surface was on the base of a 6-well plate, and these were then imaged using a x10, and x40 objective lens. Five fields of view were imaged from each coupon, and z-stacks and or images were generated. Parameters such as step size, z depth and gain were adjusted to allow for optimum image acquisition.

2.2.8. Image analysis of CLSM Images

CLSM Z-stacks were converted into maximum intensity projection TIFF files using the Leica Application Suite X (LAS X) software (Leica Microsystems). The software processed the Z-stacks slices into a single 2D image, that reflected a top-down view of the surface which was then used for analysis.

2.2.8.1. Surface coverage analysis of PMMA surfaces

FIJI ImageJ Software (Version:2.0.0-rc-69/1.52p Build: 269a0ad53f) was used to analyse the percentage area coverage by *C. albicans* on the coupon surface (x10 objective lens, maximum intensity projection files). A macro was used to convert the files to 8-bit, a threshold was set and the percentage coverage of the field of view determined using the set measurements area. The mean percentage area coverage was determined by combining the output for five fields of view from each of the three replicates (n=15).

2.2.8.2. Quantification of *C. albicans* hyphae on PMMA surfaces

To determine the relative proportions of *C. albicans* hyphae on the surfaces of PMMA coupons, the x40 objective lens maximum intensity projection files were uploaded into FIJI ImageJ Software (Version:2.0.0-rc-69/1.52p Build: 269a0ad53f). A macro was optimised to analyse the files. Files were converted into 8-bit and the threshold adjusted using “Auto Threshold” with the method “moments” with a dark background specified. The “Watershed” action was also used to split

clusters and over-lapping cells so they would be counted separately and not as one. The “Analyze Particles” tool was used with the size restriction “0.005-Infinity” and circularity “0.10-1.00”. This resulted in a total count of the cells present. The output was averaged across the replicates of the same condition (n=15) to obtain the mean total count for each condition.

Using the LAS X software (Leica Microsystems), the counter tool was used to manually enumerate the number of hyphae present in the same maximum intensity projection TIFF files. The hyphal counts were averaged across the replicates of the same condition (n=15) to obtain a total count for each condition. The mean hyphal count was subtracted from the mean total count and divided by 100 to obtain the percentage of hyphal forms which included true hyphae and pseudohyphae present for each preconditioning type and strain.

2.2.9. Statistical analysis of CLSM Images

The significance of the results from the CLSM images for percentage area coverage and the proportion of adhered hyphal forms was determined by Kruskal-Wallis with Dunn’s post-hoc test to compare means between groups. Prism 9 for macOS (GraphPad Prism 9.4.0 (453) GraphPad Software, San Diego, California USA, www.graphpad.com) software was used for statistical analysis and the construction of graphs.

2.3. Results

2.3.1. Chemical characterisation of tobacco condensate (TC), Artificial saliva (AS) and dH2O adsorbed PMMA by Gas Chromatography – Mass Spectrometry (GC-MS) and Liquid Chromatography – Mass Spectrometry (LC-MS)

2.3.1.1. Gas Chromatography – Mass Spectrometry (GC-MS)

Assistance in chemical analyses and data interpretation was provided by Dr Siôn Edwards and Prof Ian Fallis (School of Chemistry, Cardiff University). Numerous peaks at a range of elution times were detected as shown in the GC chromatograms of AS treated with TC (Figure 2.2) This indicated that each extract contained many different compounds with different column binding affinities. The mass spectra of the principal components were analysed (Figure 2.3). Similar principal elution times were present in many of the chromatograms. The principal component, with an elution time of 20.02 min, was present in all seven analysed extracts including the blank control. This was likely an impurity in the GC column given its ubiquitous presence, and therefore unlikely to be a component responsible for any changes occurring during the experiments. The same peak (though as a smaller component) was also present in the sample of oil taken from the Drechsel head. Elution times common to more than one extract, along with the molecular weight of the principal component of the mass spectrum recorded at that respective time were collated for comparison between conditions (Table 2.4)

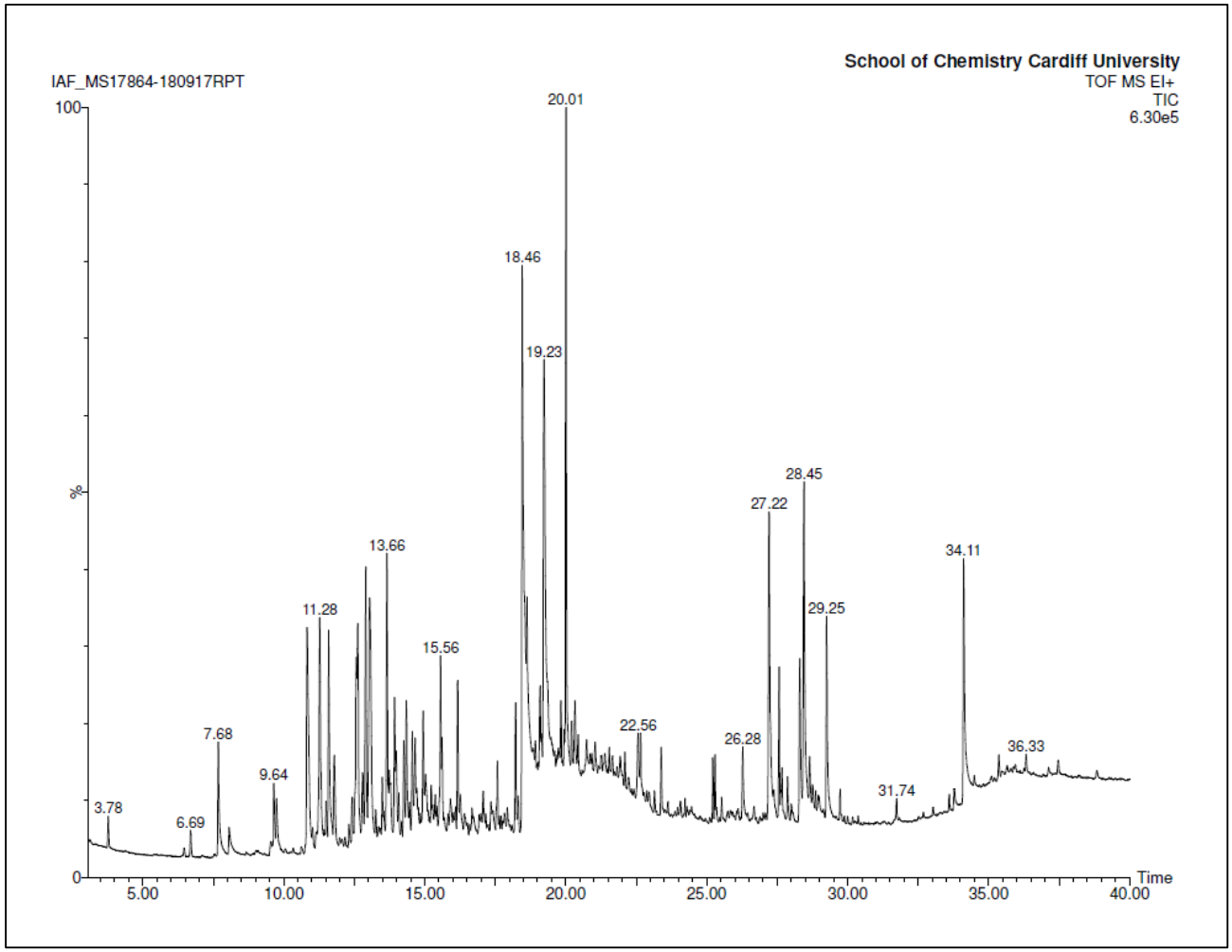

Figure 2.2. GC Chromatogram of the dichloromethane extract of artificial saliva treated with tobacco smoke *i.e.,* tobacco condensate. Recorded using a 30 m, 35:65 (Ph:Me polysiloxane) capillary column. The elution time is given in min.

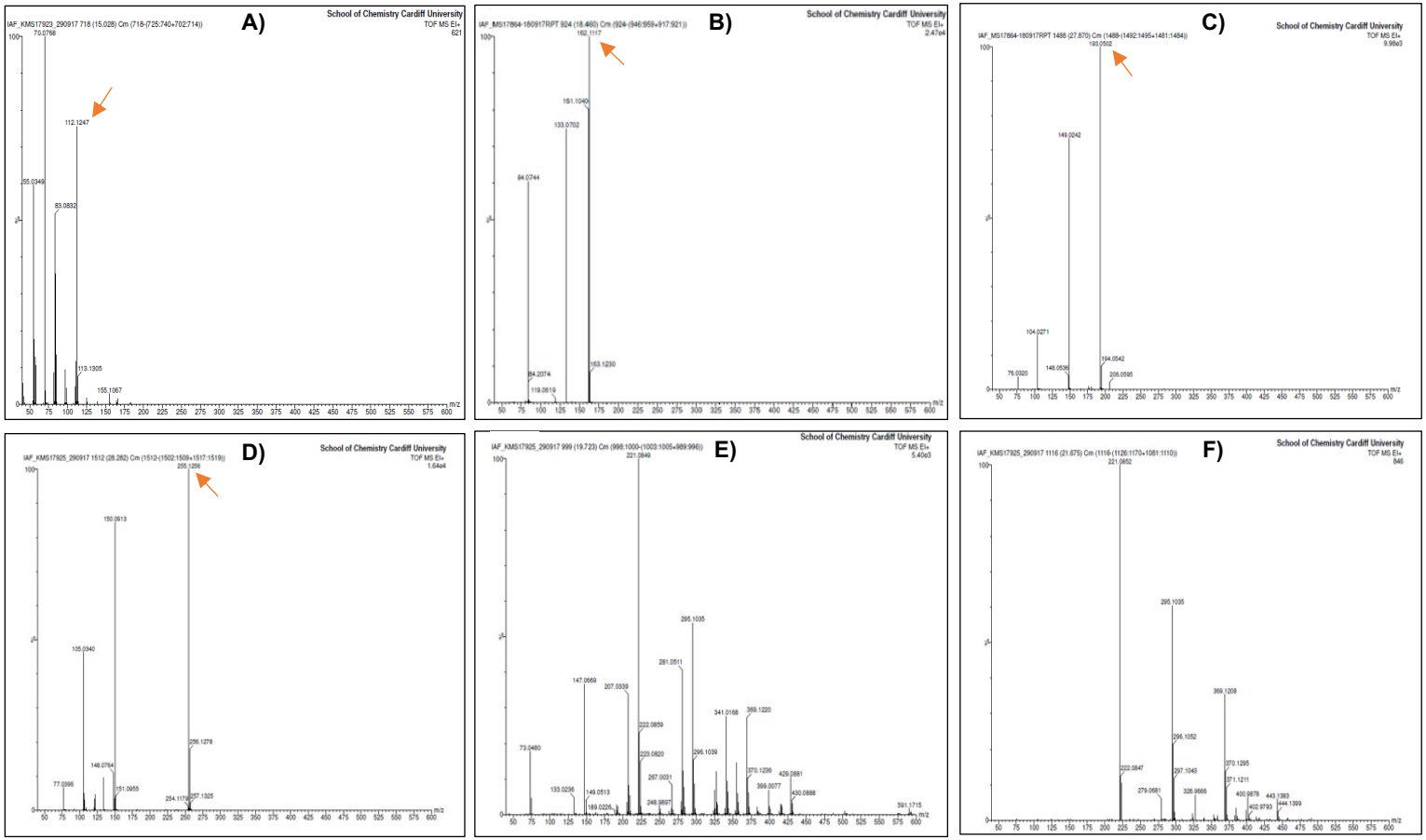

Figure 2.3. Mass spectrum chromatograms of the dichloromethane extract of dental acrylic treated with tobacco smoke. A) Elution at 15.028 min. B) Elution at 18.460 min. C) Elution at 27.870 min. D) Elution at 28.282 min. E) Elution at 19.723 min. F) Elution at 21.675 min. E and F are examples of peaks that were found in all acrylic conditions. The orange arrows indicate the peak displaying the observed mass (m/z) used in further analysis..

Table 2.4. GC-MS elution times and molecular mass of peaks of interest that occurred in the analysed dichloromethane extracts.

Elution Time (min)	Present in dichloromethane extracts	Observed Mass (m/z)	Calculated Mass (m/z)
15.028	Acrylic treated with tobacco condensate	112.1247	112.1252 for C_8H_{16}
15.076	All acrylic conditions	150.0675	150.0681 for $C_9H_{10}O_2$
18.31	All acrylic conditions	185.0817	185.0841 for $C_{12}H_{11}NO$
18.46	Artificial saliva treated with tobacco smoke, residual oil in Drechsel head	162.1117	162.1157 for $C_{10}H_{14}N_2$
19.144	All acrylic conditions	154.0783	154.0783 for $C_{12}H_{10}$
19.723	All acrylic conditions	-	-
20.02	All extracts	-	-
21.675	All acrylic conditions	-	-
23.437	All extracts	-	-
23.782	All acrylic conditions	198.0678	198.0681 for $C_{13}H_{10}N_2$
27.870	Acrylic treated with tobacco condensate; artificial saliva treated with tobacco condensate	193.0491	193.0739 For $C_{10}H_{11}NO_3$
28.282	Acrylic treated with tobacco condensate; artificial saliva treated with tobacco condensate	255.1256	255.1259 for $C_{16}H_{17}NO_2$

There were four elution times of interest with regards to changes to the denture acrylic that may affect interaction with *C. albicans.* These peaks occurred at 15.028, 18.46, 27.870 and 28.282 min (Table 2.4). An elution was observed at 15.028 min in dichloromethane extracts of acrylic treated with tobacco smoke (Figure 2.3). The mass spectrum of the peak at 15.028 min had an observed mass of 112.1247 m/z (mass-to-charge ratio; Figure 2.3A). This suggested the presence of a molecule with the formula C_8H_{16}, which had a calculated mass of 112.1251 m/z. This would correspond to alicyclic hydrocarbon cyclooctane (or related saturated monocyclic hydrocarbons such as ethyl cyclohexane) or monounsaturated C_8 alkenes such as octenes.

A component present in both the TC and the Drechsel head residual oil eluted at 18.46 min (Figure 2.3B). The mass of the principal component was determined to be 162.1117 m/z, which was similar to the calculated mass for a molecule with the formula $C_{14}H_{10}N_2$ which has potential to be nicotine or the structural isomer anabasine. The next fraction at 133.0702 m/z exhibited a mass reduction of 29 m/z which indicated the possible loss of an ethyl or CHO group or more likely indicate the cleavage of a CH_3N group which was only possible from nicotine. There was also a loss of 78 m/z resulting in an 84.0744 m/z peak corresponding to the mass of a pyridyl radical (exact mass = 78.0344). The presence of which indicated dissociation of pyridine from the molecule. Thirdly, there was an elution after 27.870 min with a mass of 193.0502 m/z closely resembling the mass of N-(phenylacetyl)glycine that has a predicted mass of 193.0739 m/z (Figure 2.3C). A loss of CO_2 was suggested by the mass loss of 44 to 149.0421 m/z which was consistent with a carboxylic acid group being present.

Analysis of the final elution peak of interest, which eluted at 28.282 min was found in the extract of acrylic treated with TC (Figure 2.3D). The principal peak had a mass of 255.1256 m/z which matched $C_{16}H_{17}NO_2$, tentatively assigned as the benzyl ester of phenyl alanine. A loss of 105 m/z resulted in the 150.0913 peak indicating the loss of a phenylethyl radical or a C_6H_5-CO radical. The 105 m/z lost was evident in the next fragment, which had a more accurate mass of 105.0340 m/z which is the calculated mass of a C_6H_5CO radical. The last fragment of interest was the 77.0396 m/z peak which equates to the mass of a phenyl radical. There were also peaks in the GC chromatograms present only in the samples that

contained the acrylic. Analysis of two of these acrylic specific peaks that eluted at 19.723 min (Figure 2.3E) and 21.675 min (Figure 2.3F) were presented as an example of acrylic components detected but not extensively analysed.

2.3.1.2. Liquid Chromatography – Mass Spectrometry (LC-MS)

Elution peaks present in both the control and TC treated conditions were considered baseline, and only novel peaks or peaks that were significantly larger in the tobacco treated samples were analysed (Figure 2.4A). The first of these peaks occurred at 0.70 min (Figure 2.4B) and had a principal peak of 163.1225 m/z. This value was essentially identical to the mass of a protonated nicotine, the mass of which is 163.1230 (calculated for $C_{10}H_{15}N_2 + H^+$, 163.1230). At 2.649 min on the chromatogram of the washed tobacco treated acrylic (Figure 2.4C), a mass of 120.0806 m/z was by far the largest signal. The mass correlated to and was likely to be $C_8H_{10}N^+$, which was tentatively assigned as protonated indoline (calculated for $C_8H_9N + H^+$, 120.0808). The remainder of the chromatogram, although complex, presented a similar profile to that of the AS control. Samples of the liquid in which the acrylics were stored, closely resembled each other (Figure 2.5). The exception to this was a broad elution in the TC which peaked at 5.25 min and was not present in the other two conditions *i.e.,* AS and dH_2O. The mass spectrum of the 5.25 mins elution peak (Figure 2.5C) was quite simple showing a main component at 300.1484 m/z and a lack of significant fragmentation of the parent ion to assist the characterisation of the species responsible. This mass corresponds to a protonated species with the formula $C_{17}H_{17}N_2O_3$ (calculated for $C_{17}H_{17}N_2O_3 + H+ = 300.1468$), corresponding to the dipeptide phe-phe. However, the accuracy here is insufficient to state this with confidence.

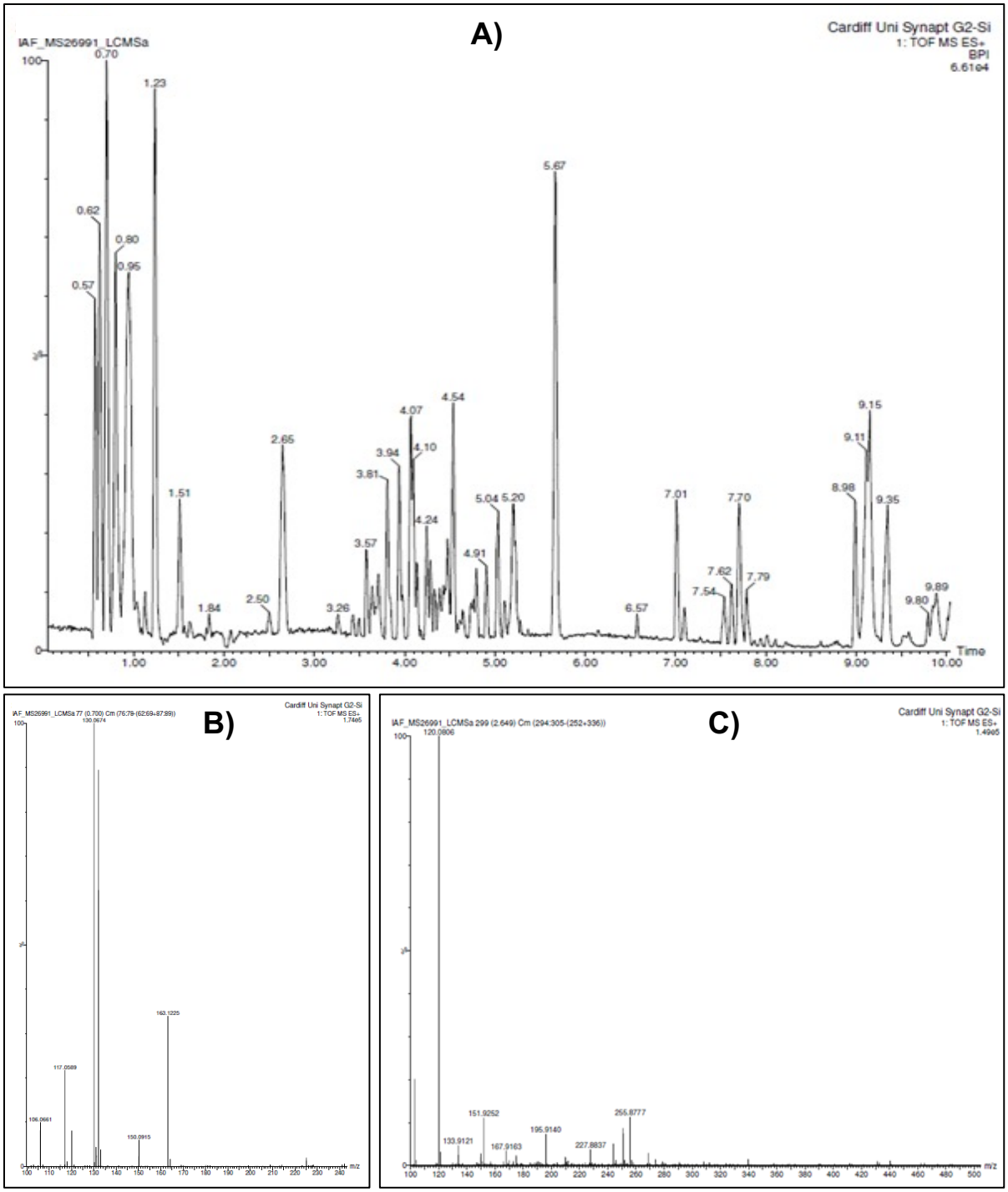

Figure 2.4. LC-MS chromatograms of the water extraction of denture acrylic treated with tobacco condensate. A) LC-MS chromatogram of the water extraction. B-C) LC-MS mass spectra of the fractions from A; B) Elution at 0.700 min. C) Elution at 2.649 min. The elution time was in min.

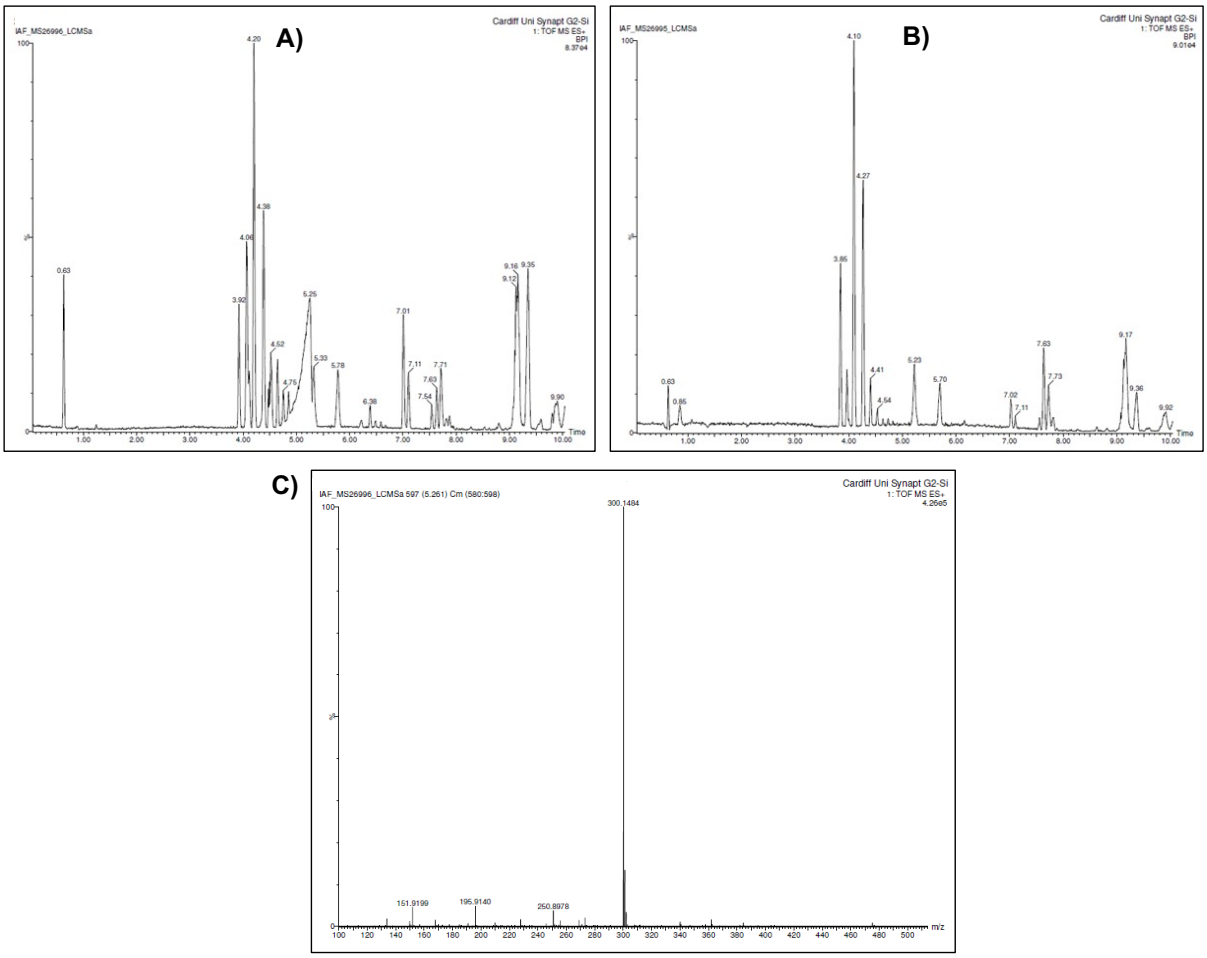

Figure 2.5. LC-MS analysis of the tobacco condensate and artificial saliva and the mass spectrum of the peak of interest identified in the tobacco condensate LC-MS. LC-MS chromatogram of the supernatant of the tobacco condensate (A) and the supernatant artificial saliva (B). The mass spectrum of the broad elution that peaks at 5.25 min was a distinctive feature of the tobacco condensate-treated condition (C). The elution time was in min.

2.3.2. Assessing whether tobacco conditioning altered surface roughness.

Roughness measurements of the PMMA surface before and after tobacco treatment were obtained with assistance from Mrs Wendy Rowe (School of Dentistry, Cardiff University (Table 2.5). Overall, the mean change in Ra values was -0.41 Ra. The coupons before treatment had an mean Ra value of 3.06 which decreased to 2.65 after treatment. The measurements were consistent as evident by the standard error of the mean (SEM); 0.29 for before treatment and 0.21 post treatment.

2.3.3. Assessing whether the types of pre-conditioning altered surface hydrophobicity.

Contact angle measurements are indicative of the hydrophobicity of a surface. Generally, a surface is considered hydrophobic when the contact angle measurement is > 90° and is hydrophilic when the contact angle is < 90°. Conditioning the PMMA with TC (73.86°) resulted in the surface being significantly ($P \leq 0.0001$) more hydrophobic than the AS (23.93°) PMMA surfaces (Figure 2.6). The AS PMMA surface was significantly ($P \leq 0.0001$) more hydrophilic than not just the TC but also the WC (66.24°) PMMA.

Table 2.5. Roughness measurements of the polymethyl methacrylate (PMMA) surface before and after tobacco conditioning. Each coupon was measured across three 5 mm transects before and after TC treatment. The mean Ra value, the unit used to denote average roughness, was used to indicate changes in surface roughness. The standard error of the mean (SEM) is given for each coupon before and after tobacco treatment. Wilcoxon matched pairs signed rank test determined there was no significant difference between the measurements before and after tobacco pre-conditioning ($P \leq 0.1703$).

	Before treatment		After treatment		
Coupon Number	**Mean Ra (µm)**	**SEM**	**Mean Ra (µm)**	**SEM**	**Change**
1	2.74	0.22	3.23	0.18	0.49
2	3.96	0.31	3.37	0.75	-0.59
3	2.05	0.10	2.35	0.07	0.30
4	9.20	1.76	3.80	0.30	-5.40
5	3.40	0.08	3.02	0.15	-0.38
6	3.64	0.37	3.32	0.22	-0.32
7	2.49	0.14	2.25	0.10	-0.24
8	1.87	0.05	2.03	0.05	0.16
9	2.89	0.24	2.29	0.13	-0.60
10	2.87	0.26	2.26	0.17	-0.61
11	1.65	0.16	1.74	0.24	0.10
12	2.17	0.07	2.52	0.36	0.36
13	2.76	0.20	2.59	0.14	-0.17
14	2.90	0.39	2.81	0.19	-0.09
15	2.34	0.03	2.51	0.08	0.17
16	1.96	0.22	2.24	0.25	0.28
Total Mean	**3.06**	**0.29**	**2.65**	**0.21**	**-0.41**

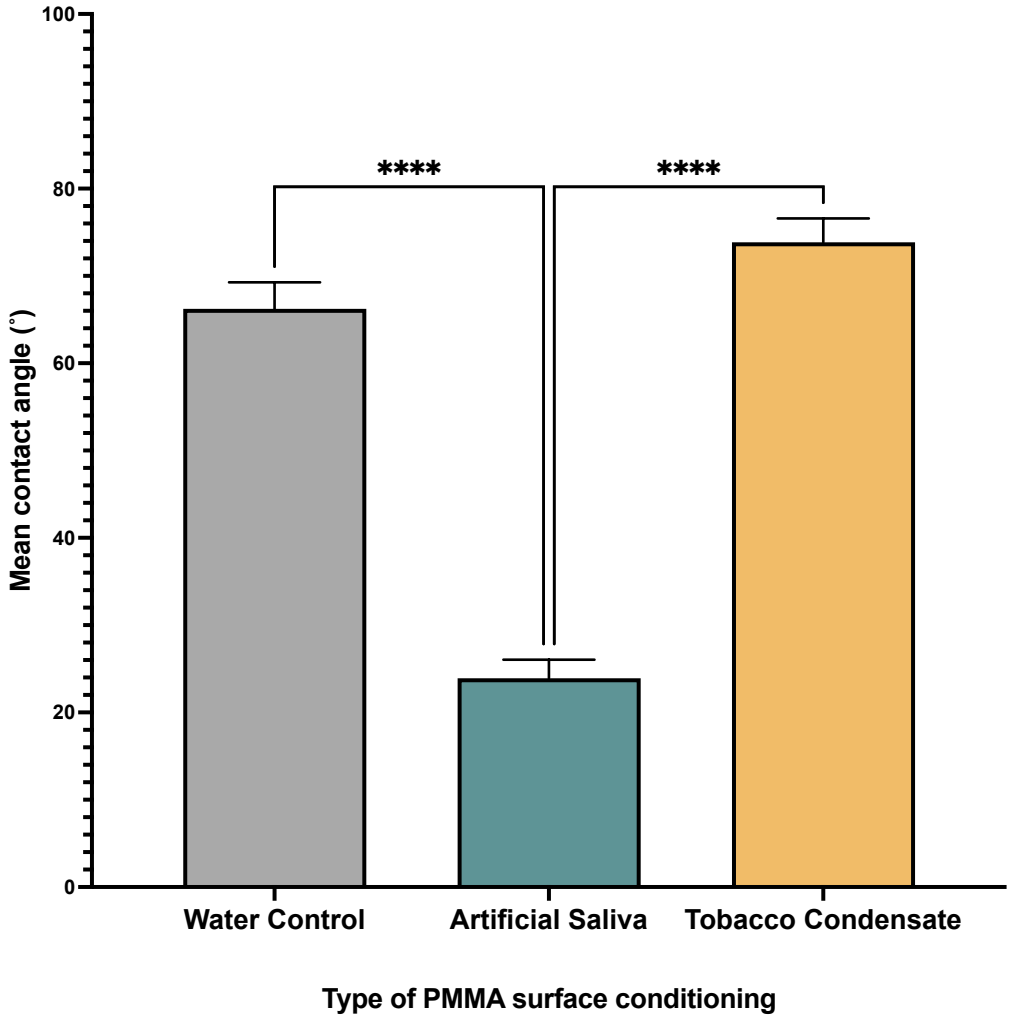

Figure 2.6. Hydrophobicity of polymethyl methacrylate (PMMA) surfaces preconditioned with tobacco condensate, artificial saliva, and the water conditioned control measured as mean contact angle (°). PMMA coupons were preconditioned in artificial saliva, tobacco condensate and water (dH_2O) and a contact angle goniometer was used to measure the mean contact angle using the sessile drop method which was indicative of hydrophobicity. Data presented as mean ± standard error of the mean. *n*(WC) = 4, *n*(AS) = 6, *n*(TC) = 7. Significance determined through One-way ANOVA (*F* (2, 14) = 110.1, *P* ≤ 0.0001) with Tukey Post-Hoc test **** *P* ≤ 0.0001.

2.3.4. *Candida albicans* adherence, biofilm development and proportion of hyphal forms on tobacco condensate, artificial saliva, and water preconditioned PMMA surfaces.

2.3.4.1. Adherence of *C. albicans* to PMMA coupons with three different types of surface conditioning

Candida albicans adherence to the differently conditioned PMMA coupons after 90 min was strain dependent (Figure 2.7). Representative images for each of the *C. albicans* strains for all three conditions at 90 min and 24 h incubations are shown in Figure 2.8 - 2.12. *Candida albicans* SC5314 had similar levels of coverage 8.2%, 7.6% and 7.7% on WC, AS and TC coupons, respectively (Figure 2.7 and Figure 2.8). *Candida albicans* PB1/93 exhibited higher adherence to the AS conditioned surfaces (11.8%) compared with WC or TC (7.2% and 2.9%, respectively) conditioned surfaces (Figure 2.8 – 2.12). Highest adherence of *C. albicans* 480/00 was to the TC surface (18.1% coverage) and lowest adherence was to the AS surfaces (7.9%). *Candida albicans* 705/93 and *Candida albicans* PTR/94 had similar adherence profiles, with adherence increasing from TC to AS and WC surfaces (Figure 2.7). Adherence to the differently preconditioned surfaces was not found to be statistically significant for any of the *C. albicans* strains after 90 min incubation.

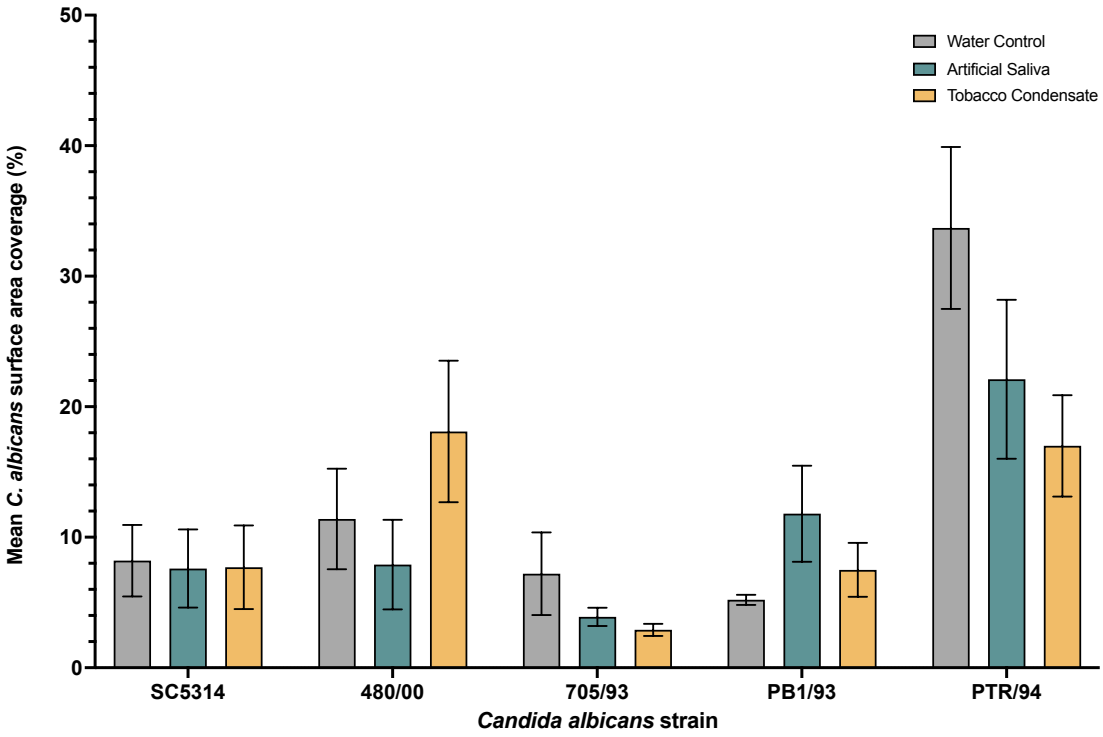

Figure 2.7. Mean surface coverage (%) after 90 min incubation for *Candida albicans* isolates on PMMA coupons preconditioned with either tobacco condensate, artificial saliva, or the water conditioned control (dH_2O). CLSM (x10 objective lens) images were taken after 90 min incubation of *C. albicans* on the surfaces at 37°C and analysed to determine the percentage coverage. *Candida albicans* cells were stained with Calcofluor White. *n* = 15 for each condition. Error bars present the standard error of the mean. None of the results were statistically significant using a Kruskal Wallis Dunn's post-hoc test.

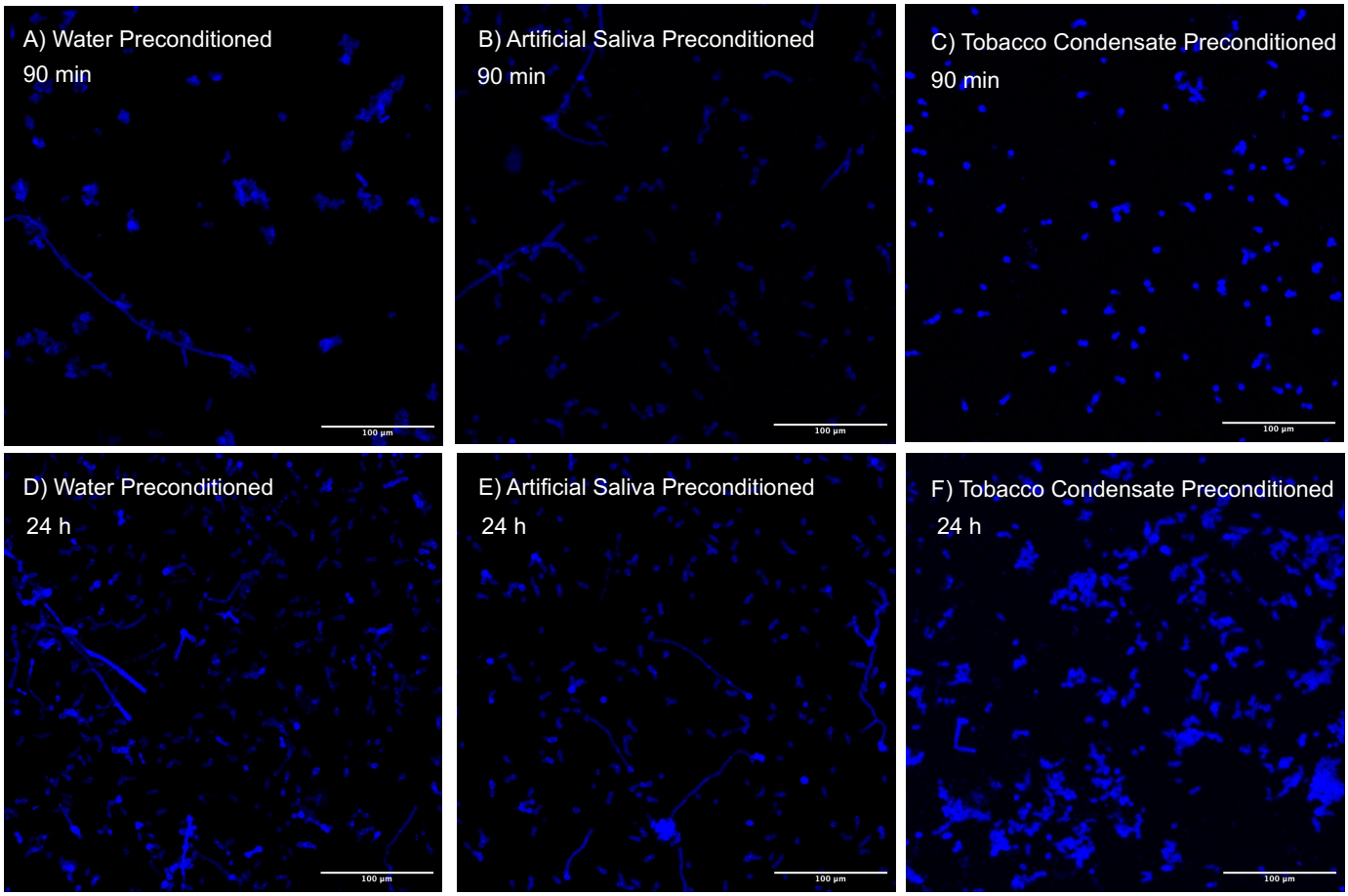

Figure 2.8. *Candida albicans* SC5314 on polymethyl methacrylate (PMMA) coupon surfaces. *Candida albicans* was grown on polymethyl methacrylate PMMA coupon surfaces preconditioned with A and D) water (dH_2O), B and E) artificial saliva, and C and F) were the surfaces preconditioned with tobacco condensate. A-C) were taken from coupons incubated with *C. albicans* for 90 min and D-F) were incubated with *C. albicans* for 24 h. *Candida albicans* was stained with calcofluor white resulting in blue fluorescence. Images were taken using the x40 objective lens on a confocal microscope. Scale bars are 100 µm.

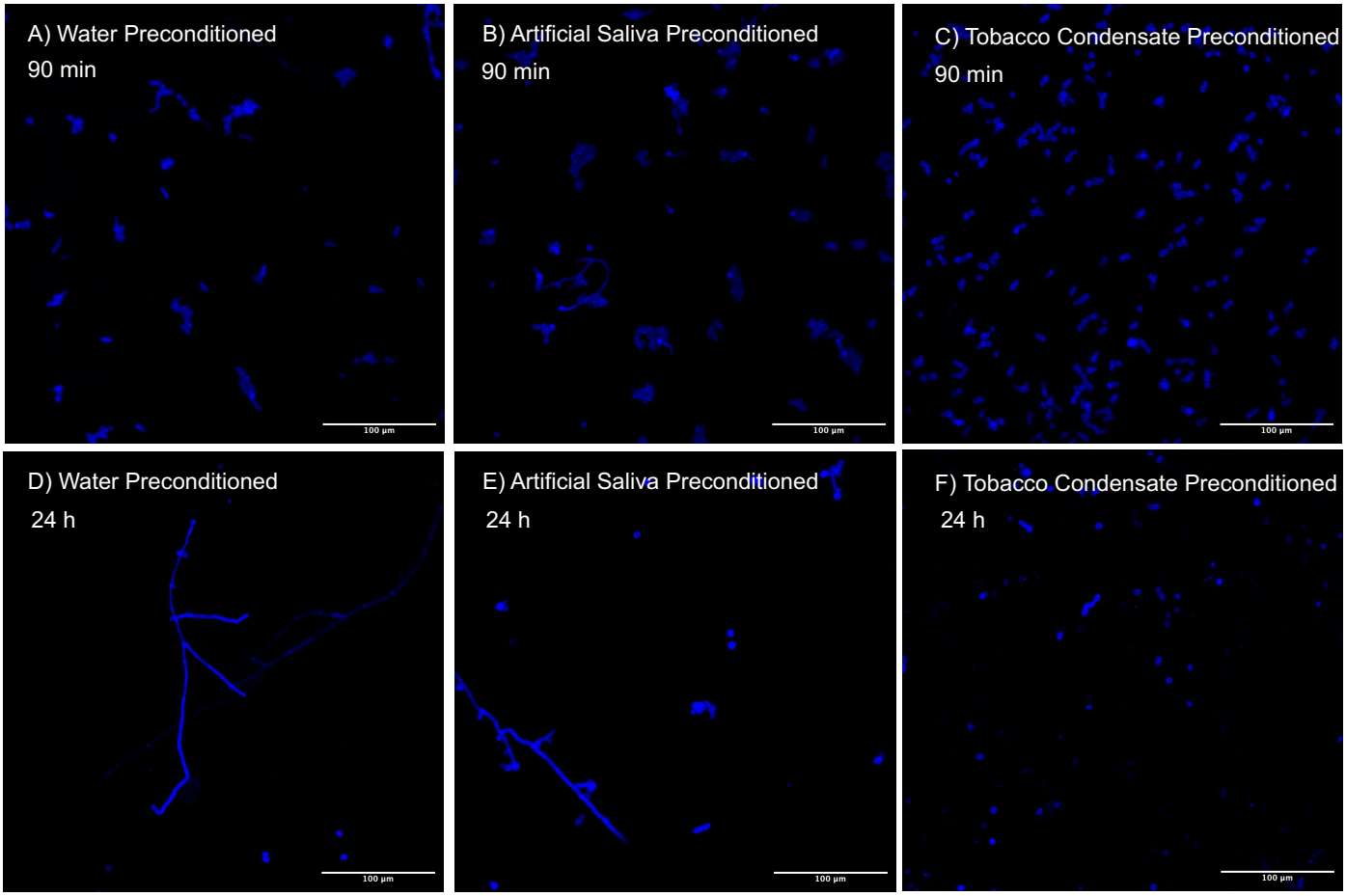

Figure 2.9. *Candida albicans* 480/00 on polymethyl methacrylate (PMMA) coupon surfaces. *Candida albicans* was grown on polymethyl methacrylate PMMA coupon surfaces preconditioned with A and D) water (dH_2O), B and E) artificial saliva, and C and F) were the surfaces preconditioned with tobacco condensate. A-C) were taken from coupons incubated with *C. albicans* for 90 min and D-F) were incubated with *C. albicans* for 24 h. *Candida albicans* was stained with calcofluor white, resulting in blue fluorescence. Images were taken using the x40 objective lens on a confocal microscope. Scale bars are 100 µm.

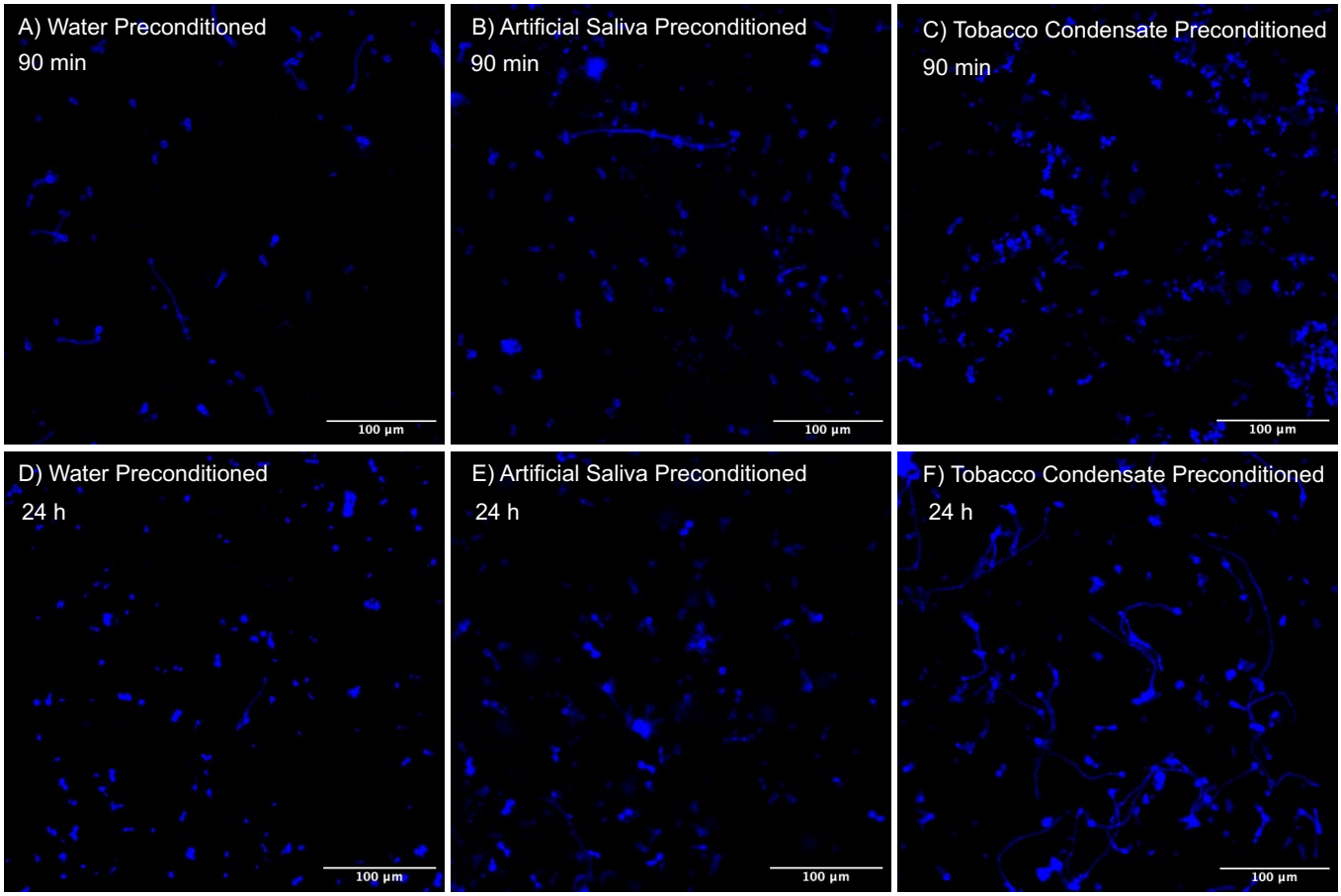

Figure 2.10. *Candida albicans* 705/93 on polymethyl methacrylate (PMMA) coupon surfaces. *Candida albicans* was grown on polymethyl methacrylate PMMA coupon surfaces preconditioned with A and D) water (dH_2O), B and E) artificial saliva, and C and F) were the surfaces preconditioned with tobacco condensate. A-C) were taken from coupons incubated with *C. albicans* for 90 min and D-F) were incubated with *C. albicans* for 24 h. *Candida albicans* was stained with calcofluor white, resulting in blue fluorescence. Images were taken using the x40 objective lens on a confocal microscope. Scale bars are 100 µm.

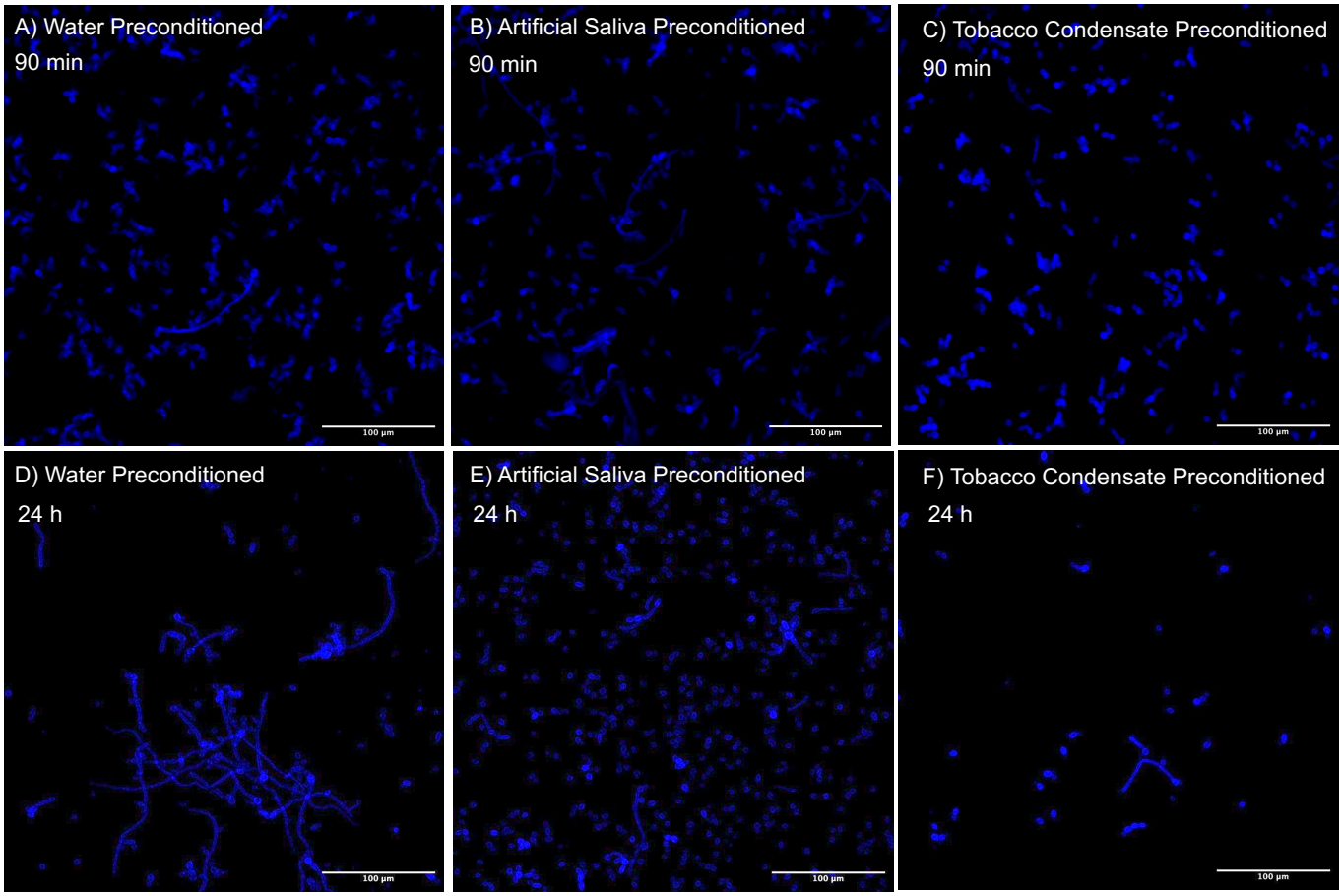

Figure 2.11. *Candida albicans* PB1/93 on polymethyl methacrylate (PMMA) coupon surfaces. *Candida albicans* was grown on polymethyl methacrylate PMMA coupon surfaces preconditioned with A and D) water (dH_2O), B and E) artificial saliva, and C and F) were the surfaces preconditioned with tobacco condensate. A-C) were taken from coupons incubated with *C. albicans* for 90 min and D-F) were incubated with *C. albicans* for 24 h. *Candida albicans* was stained with calcofluor white resulting in blue fluorescence. Images were taken using the x40 objective lens on a confocal microscope. Scale bars are 100 µm.

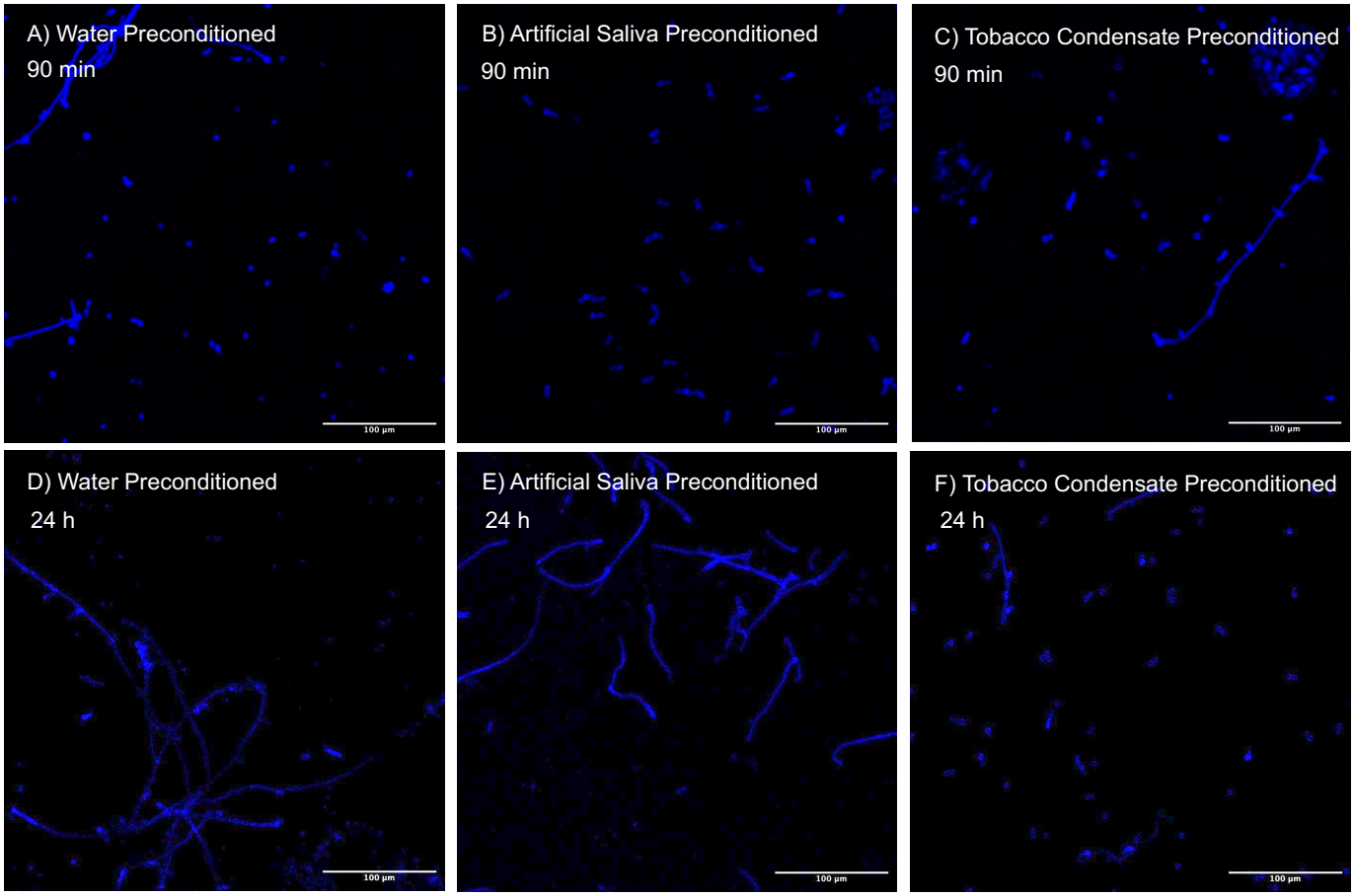

Figure 2.12. *Candida albicans* PTR/94 on polymethyl methacrylate (PMMA) coupon surfaces. *Candida albicans* was grown on polymethyl methacrylate PMMA coupon surfaces preconditioned with A and D) water (dH_2O), B and E) artificial saliva, and C and F) were the surfaces preconditioned with tobacco condensate. A-C) were taken from coupons incubated with *C. albicans* for 90 min and D-F) were incubated with *C. albicans* for 24 h. *Candida albicans* was stained with calcofluor white resulting in blue fluorescence. Images were taken using the x40 objective lens on a confocal microscope. Scale bars are 100 µm.

2.3.4.2. Proportion of *Candida albicans* hyphae adhered to the PMMA surfaces after a 90 min incubation.

Candida albicans 705/93 was the only strain tested that showed a significant difference in the proportion of hyphal forms on the different types of preconditioned surfaces (Figure 2.13). *Candida albicans* 705/93 had a significantly higher proportion of hyphal forms on the WC surfaces where 19.05% of the fungal units present were hyphal compared to only 5.43% on AS ($P \leq 0.0002$) and 0.09% on TC ($P \leq 0.0001$) surfaces (Figure 2.10 and Figure 2.13). *Candida albicans* SC5314 had a lower proportion of hyphae on the TC surfaces (0.38%) than the WC (3.18%) and AS surfaces (2%). 480/00 showed highest level of consistency between the proportion of hyphae between all three preconditioned (1.27% to 2.26%). *Candida albicans* PB1/93 exhibited a higher proportion of hyphae on the AS surfaces (5.60%) compared to both the TC (1.74%) and WC surfaces (1.34%). *Candida albicans* PTR/94 had a lower proportion of hyphae on AS surfaces (0.19%) compared with WC (5.03%) and TC (2.11%) preconditioned surfaces.

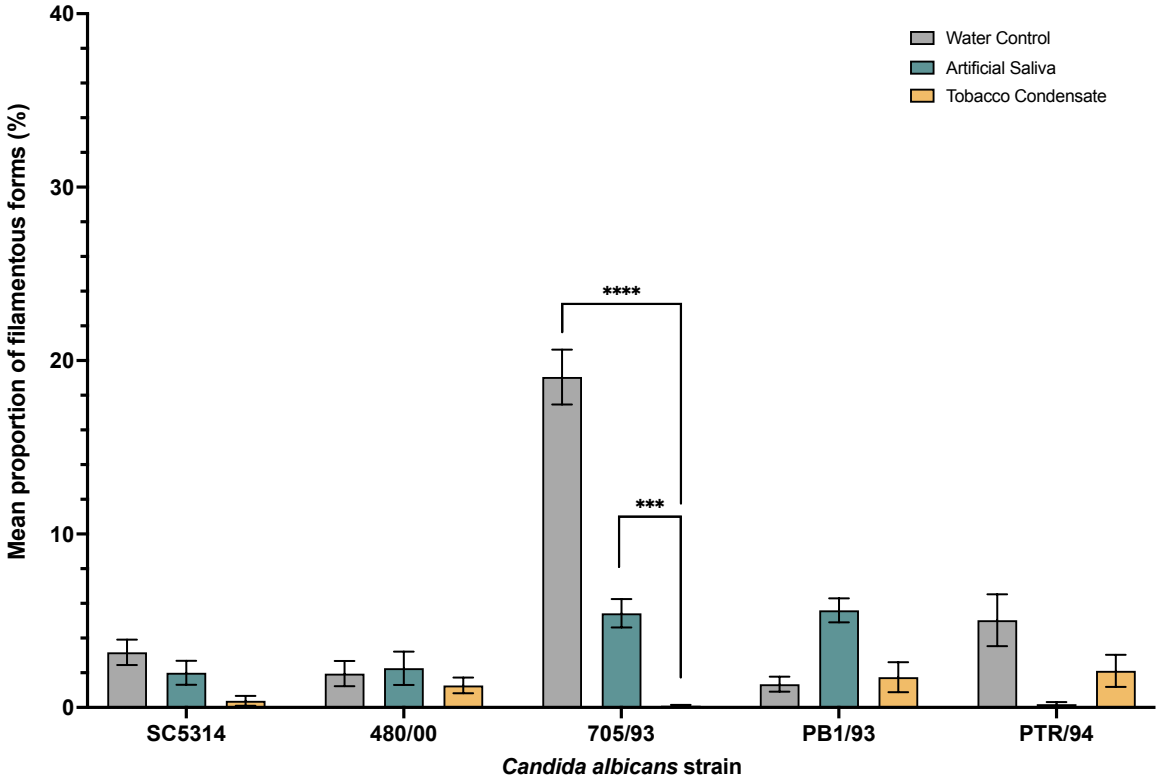

Figure 2.13. Proportion of hyphal forms (%) for five *Candida albicans* strains on PMMA coupons preconditioned with either water, artificial saliva, or tobacco condensate present after a 90 min incubation. After a 90 min incubation at 37°C, x40 objective lens CLSM images were used to determine the proportion of hyphal forms for each strain on each condition. *Candida* cells were stained with Calcofluor White. n = 15 for each condition. Error bars display the standard error of the mean. Statistical significance was determined using Kruskal-Wallis with Dunn's post-hoc test. *** $P \leq 0.001$. **** $P \leq 0.0001$.

2.3.4.3. Biofilm development on the PMMA coupon surface after 24 h incubation

Mean biofilm coverage after 24 h was isolate dependent (Figure 2.14). *Candida albicans* PTR/94 surface coverage on the AS surface (27.9%) was significantly higher than on both WC (3.9%, $P \leq 0.0034$) or TC surfaces (1%, $P \leq 0.0001$). *Candida albicans* SC5314, 480/00 and PB1/93 exhibited consistency in coverage for all three surface conditioning types. *Candida albicans* SC5314 differed by only 1.2% and PB1/93 differed by 0.8% and *C. albicans* 480/00 coverage of WC surfaces was 1.5% higher than the other two conditions suggesting that the different types of preconditioning had no effect on biofilm development of these strains. *Candida albicans* 705/93 exhibited higher biofilm development on the AS conditioned surfaces (11.5%) compared to the WC (2.7%) surfaces and the TC surfaces (4.9%).

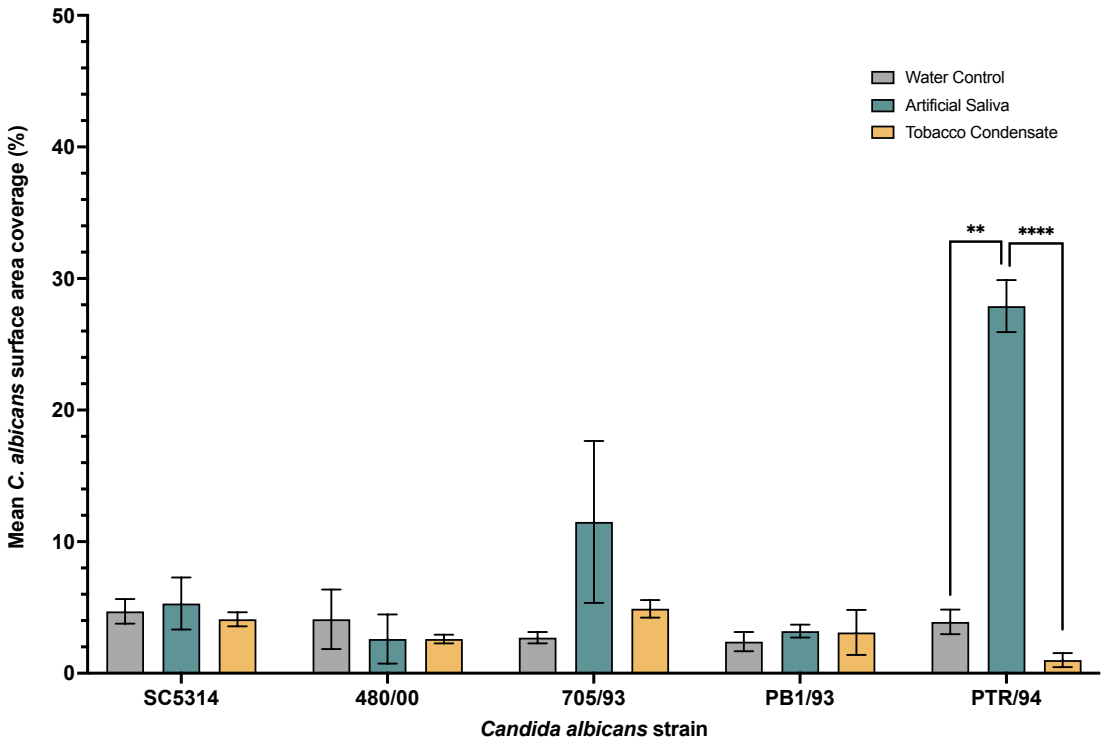

Figure 2.14. Mean surface coverage (%) after 24 h incubation of different *Candida albicans* strains on polymethyl methacrylate (PMMA) coupons preconditioned with either tobacco condensate, artificial saliva, or the water conditioned control (dH_2O). CLSM images (x10 objective lens) were taken after a 24 h incubation of *C. albicans* on the surfaces and analysed to determine the mean percentage area coverage. *Candida albicans* cells were stained with Calcofluor White. n = 15 for each condition. Error bars present the standard error of the mean. Statistical significance was determined by Kruskal-Wallis with Dunn's post-hoc test. ** $P \leq 0.01$. **** $P \leq 0.0001$.

2.3.4.4. Proportion of *Candida albicans* hyphal forms present on surfaces after 24 h

After 24 h incubation, the proportion of *C. albicans* 705/93 hyphal forms on the TC surfaces (28.39%) was higher than for both AS (14.79%) and WC surfaces (2.79% (Figure 2.15)). This difference was extremely significant between the TC and WC surfaces ($P \leq 0.0002$). None of the other isolates demonstrated differences in the proportion of filamentous forms between the three different types of preconditioning. *Candida albicans* SC5314, *C. albicans* 480/00 and *C. albicans* PTR/94 all exhibited the same pattern with the highest proportion of hyphae on the WC surfaces (13.33%, 8.50% and 13.54%, respectively) and the lowest proportion of hyphae on the TC surfaces (6.2%, 2.5% and 6.4%, respectively). *Candida albicans* PB1/93 had the lowest proportion of hyphal forms observed on the AS surfaces (1.85%), the second highest on the TC surfaces (5.11%), and the highest proportion of hyphae on the WC surfaces (7.03%).

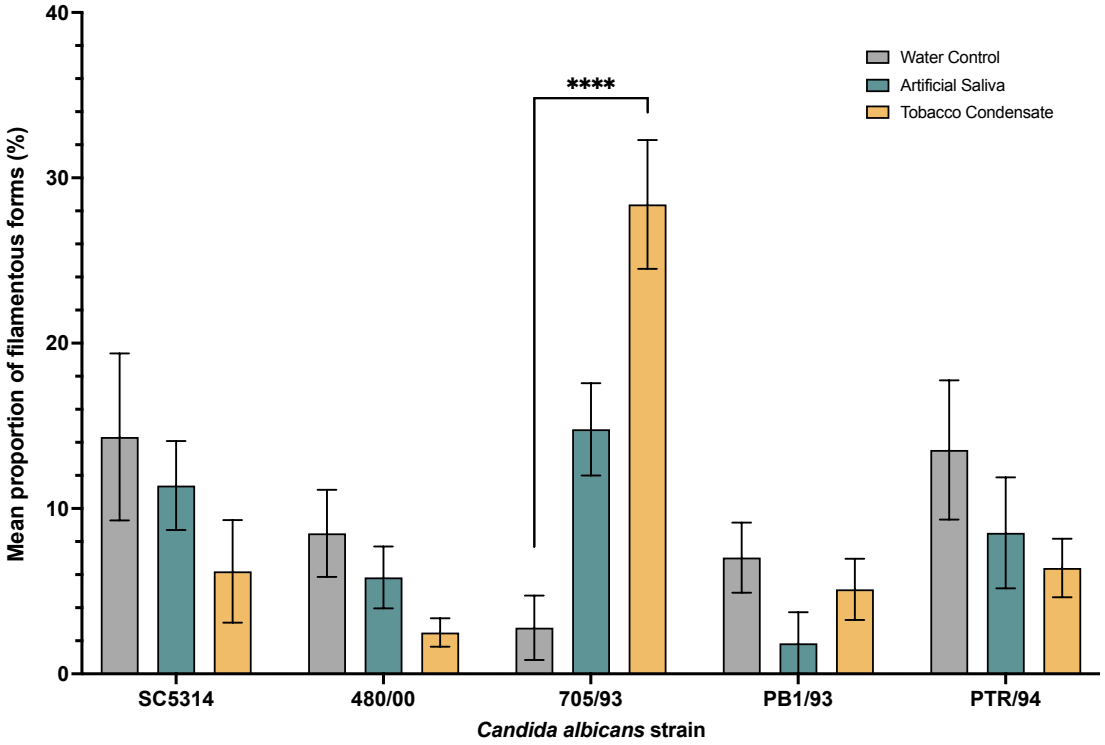

Figure 2.15. Proportion of hyphal forms (%) of five *Candida albicans* strains on polymethyl methacrylate (PMMA) coupons preconditioned with either water (dH_2O), artificial saliva, or tobacco condensate present after a 24 h incubation. After a 24 h incubation at 37°C, x40 objective lens, CLSM images were used to determine the proportion of hyphal forms for each strain on each condition. *Candida albicans* were stained with calcofluor white. Each condition n=15. Error bars display the standard error of the mean. Statistical significance determined by Kruskal-Wallis with Dunn's post-hoc test. **** $P \leq 0.0001$.

2.4. Discussion

Smoking fifteen or more cigarettes per day has been implicated with an increased prevalence of *Candida*-associated denture stomatitis (Shulman et al. 2005). *Candida*-associated denture stomatitis is primarily caused by the opportunistic pathogen *C. albicans*, but the reason why some individuals are more susceptible than others remains unknown. The overarching aim of this research was to ascertain whether different conditioning films on denture acrylic surfaces impacted on adherence, biofilm development, and morphological changes indicative of increased virulence of *C. albicans* in biofilms that could alter pathogenicity.

The effects of preconditioning of PMMA coupons with water, AS and TC was assessed. The water represented a PMMA control, whilst the AS and TC were respectively used to represent a salivary pellicle and the salivary pellicle of a person who smoked cigarettes. AS conditioning partially represented the salivary pellicle, which has previously been shown to 'equalise surface' charge on surfaces, which in turn can influence the binding of microorganisms to acrylic surfaces (Cavalcanti et al. 2016b). Cavalcanti et al. (2016a) also found that saliva and plasma pellicles on acrylic surfaces increased the metabolic activity and expression of virulence associated genes in *C. albicans* that were mostly hyphal specific. The AS formulation used in this current research was an established formulation, which has been used in previous research (Cavalcanti et al. 2016a).

The *C. albicans* properties that were subsequently analysed included the levels of initial adherence to the surfaces after 90 min. The level of *C. albicans* surface coverage after 24 h was measured to assess whether different substances on the surfaces would influence the development and growth of *C. albicans* biofilms. Thirdly, an assessment of changes in *C. albicans* morphology was conducted.

Oncul et al. (2015) reported that two commercially available forms of AS increased adherence of *C. albicans* ATCC 90028 after 3 h on PMMA surfaces compared to a water control conditioned PMMA surface. Preliminary work by Siôn Edwards (unpublished data; Cardiff University, School of Chemistry) also found increased adherence for *C. albicans* ATCC 90028 on PMMA preconditioned with tobacco condensate. This current research employed five different strains of *C. albicans.*

Only one of these strains, *C. albicans* 480/00, exhibited increased adherence to TC surfaces, but this was not deemed significant. None of the results for adherence at 90 min were statistically significant. These results were contradictory to previous research, where cigarette smoke condensate was shown to increase adherence of *C. albicans* SC5314 to glass surfaces (Semlali et al. 2014). However, Semlali *et al.* (2014) measured adherence at 1, 3 and 6 h, and the increase in adherence was concluded from the 3 h and 6 h data. In terms of the 1 h time point, they stated that adherence was low, but was significantly higher ($P < 0.05$) than the 0% 'cigarette smoke condensate' (CSC) and this was the most comparable time point to the 90 min incubation used to assess adherence in this present research. However, the results of the two studies were not comparable as one examined preconditioning a surface and the effects of the components that attach to denture material, while the other involved culture of *C. albicans* in varying concentrations of CSC. Human saliva with the microbial cells removed through centrifugation was used to coat enamel surfaces and enhanced adherence by *C. albicans* yeast cells which was assessed through single-cell force spectroscopy and visualised with scanning electron microscopy compared to uncoated enamel surfaces (Gunaratnam et al. 2021). Strong initial attachment measured at 0-5 secs was found between yeast cell wall associated adhesins and the salivary pellicle (Gunaratnam et al. 2021).

Semlali *et al.* (2014), also investigated differences in biofilm formation with varying levels of CSC after 48 and 72 h. The research reported that *C. albicans* SC5314 biofilm formation was promoted by CSC most significantly after 72 h, but there was also a significant increase at 48 h for the concentration of 20% and higher up to 50%. In comparison, a significant difference in biofilm coverage for *C. albicans* SC5314 was not found between the three conditions in this present study. However, this may be due to the shorter incubation time of 24 h. *C. albicans* PTR/94 had higher coverage on the AS surfaces than the TC surfaces after 24 h. It was possible that if experiments had been extended to 72 h there may have been a greater impact of the TC and therefore, future work could incorporate experiments that include a longer (72 h) time point for assessment.

Conditioning coupons with AS did not influence levels of *C. albicans* adherence as was originally anticipated, with no significant increase in adherence on the AS compared to the WC or TC surfaces. However, *C. albicans* PB1/93 exhibited higher

adherence in terms of surface coverage on the TC and WC surfaces, but not significantly so. Initial adherence is primarily due to charge and attraction through van der Waals forces, and in the oral cavity surfaces and microbes are likely to be of a similar charge (Radford et al. 1999). The salivary pellicle is hypothesised to normalise the effects of surface charge of the denture material (Cavalcanti et al. 2016b). *In vivo,* the salivary pellicle is known to increase adherence (Radford et al. 1999). However, *in vitro* saliva pellicles increase surface free energy and lead to a decrease in adherence of microorganisms which could explain why increased adherence to the AS surfaces was not observed in these experiments (Zamperini et al. 2010; Cavalcanti et al. 2016b).

Studies have shown that nicotine below the minimum inhibitory concentration (MIC), which is given as 4 mg/mL, significantly increases planktonic and biofilm growth of *C. albicans* ATCC 14053 (Gunasegar and Himratul-Aznita 2017). Gunasegar and Himratul-Aznita (2017) categorised *C. albicans* as highly hydrophobic and stated that 1-2 mg/L of nicotine increased cell surface hydrophobicity, which would enhance the cell's ability to adhere to surfaces. TC preconditioned PMMA was found to be significantly more hydrophobic than AS PMMA but not more than WC PMMA. Therefore, while hydrophobicity may account for some changes in adherence seen between AS and TC it does not account for differences between WC and TC as they were very similar in hydrophobicity. The effects of hydrophobicity on *C. albicans* adherence are discussed more thoroughly in Section 3. Nicotine was identified as being present in the tobacco condensate. Nicotine is the primary alkaloid in tobacco, accounting for 96-98% of its alkaloid content (Clemens et al. 2009). The structural isomer anabasine is a nicotinic acetylcholine receptor present in trace amounts in tobacco smoke and can be used to detect a person's exposure to smoking (Jacob et al. 1999). The component detected in the AS treated with TC, and the residual oil found in the Drechsel head samples could plausibly be nicotine or anabasine. The loss in mass observed through the fragmentation pattern was likely to correspond to the cleavage of a CH_3N group, which is possible from nicotine. The loss of a pyridyl radical equivalent mass, which results from the dissociation of pyridine from the molecule suggests that this was in fact nicotine that had been detected. In addition to nicotine, there

was also N-(phenylacetyl)glycine and a molecule that could be one of a number of aromatic carbonyl-based compounds with the formula $C_{16}H_{17}NO_2$.

Protonated nicotine was also detected in the water extractions of the samples containing tobacco condensate. The water-soluble components analysed from the tobacco surfaces also contained a large novel peak that was likely to be protonated $C_8H_9N^+$, with a predicted molecular mass of 120.0808 m/z. A potential source of this fragment is some form of unsaturated alkenated pyridinium salt. A variety of substituted pyridine species are known components of tobacco smoke that can affect biological systems (Ji et al. 2002).

Analysing the components of the TC that adsorbed onto the acrylic surface was important to allow understanding of the potential factors that may affect *C. albicans* within denture biofilms and to identify whether carcinogenic components were being retained on the denture as this would potentially result in longer exposure to the components in the oral cavity than if denture material is not present. Any of the components found could be responsible for the preference or changes displayed by *C. albicans* to the differently conditioned surfaces of denture acrylic. Identifying them could allow for future work to be carried looking into the effects of each component and whether there was a way to prevent their retention on the denture.

An interesting outcome to highlight was the comparative proportion of hyphal forms of *C. albicans* 705/93. During adherence (90 min incubation), there was a significantly lower proportion of hyphae to yeast forms present ($P \leq 0.0002$), with the proportion of hyphae being less than 0.1% of fungal units on average. However, after 24 h there was a dramatic change, that resulted in a significantly higher ($P \leq 0.0002$) proportion of hyphae present on the TC surfaces compared to the WC surfaces. After 24 h, it appeared that hyphal forms were subsequently induced on the TC surfaces as it was shown that that the initial proportion of hyphae adhering to the TC surface was extremely low. The proportion of hyphal forms of all the *C. albicans* strains adhering to the TC surfaces was extremely low initially. This suggests that the TC surfaces could preferentially bind yeast forms rather than hyphal forms or possibly, that the change caused by the conditioning with TC resulted in the surfaces repelling hyphal forms as the proportion of hyphae to yeast in the inoculum was assumed to be the same for any given strain. Alanazi *et al.*

(2019) found that cigarette and e-cigarette smoke increased the length of hyphae. These researchers stated that this may be due to the presence of smoke components eliciting a stress response that promoted hyphal elongation. Hyphae are considered more virulent and pathogenic than yeast and responsible for *C. albicans*' ability to invade host tissue (Mio et al. 1996). Therefore, this suggests that individuals who are colonised by an 'equivalent' strain to *C. albicans* 705/93 in their mouths and smoke, might be at increased risk of denture-associated stomatitis, candidosis and other *C. albicans* related oral health issues.

Alanazi *et al.* (2019), found that the presence of cigarette smoke increased the level of chitin in the *Candida* cell wall, which is also a stress response more commonly seen when *C. albicans* encounters antifungals (Alanazi et al. 2019). Higher levels of chitin in the cell wall has been found to increase tolerance to caspofungin and echinocandins (Lee et al. 2012). This suggests that *C. albicans* recognises components of the TC as possibly damaging and increases production of chitin as a mechanism to maintain cell wall integrity (Munro et al. 2007). Though hyphal production is considered a stress response, there are many factors that contribute to the upregulation of hyphae. Environmental factors play an important part, especially changes in pH. Neutral pH induces hyphal growth in log phase cells through Brg1-mediated removal of Nrg1 inhibition (Su et al. 2018). Efg1 is pivotal in hyphal formation in response to serum, as is CO_2 concentration and the presence of N-acetyl-d-glucosamine (GlcNAc) (Sudbery 2011). Tobacco conditioning could possibly have changed any of these factors to induce a stress response. There is evidence that GlcNAc levels are elevated by the presence of nicotine, which could be an impacting factor *in vivo* (Zhang et al. 2019). Future work could involve the addition of GlcNAc into experiments with and without tobacco condensate to test whether there is synergy resulting in an increased upregulation of hyphal production. An adapted checkerboard assay could be used with the output being proportion of hyphal forms rather than survival (Garcia 2014).

There is some debate as to whether smoking changes denture surface topology. Some papers allude to the fact that smoking/cigarette smoke may change the roughness of the denture surface. Mahross *et al.* (2015), found that there was a significant increase in surface roughness before and after smoking, but only for dentures made from heat cured PMMA acrylic resin and not for visible light cured

urethane dimethacrylate (UDMA) resins. However, while there was a difference in the surface roughness of the PMMA coupons in this chapter after they were conditioned in the tobacco condensate, the change was overall a decrease in the mean roughness and this difference was not statistically significant. Another *in vitro* study concluded that flexible denture base material (VALPLAST) had a greater surface roughness than heat cured PMMA denture samples after exposure to cigarette smoke (Singh et al. 2019). The significant changes in adherence, retention and the proportion of hyphae found in this research could arise due to changes in surface roughness resulting from smoking. This is important as there is evidence in the literature that supports altered surface roughness being associated with modulated adherence of *C. albicans* and oral bacterial species (Verran et al. 2014). The changes in mean roughness of the PMMA denture material surfaces were not large, but it would be important to investigate in future work how changes in the surface impact factors such as adherence, morphology, and biofilm growth. It is also not known what degree of change to the surface roughness would be significant enough to impact microbial retention on the surfaces and how that may affect the development of the biofilm, or the composition of the microbes retained. The effect of surface roughness on *C. albicans* adherence and biofilm development is further explored in Chapter 3.

To conclude, *C. albicans* strains do not all have a uniform profile in terms of adherence, biofilm development or hyphal proportion and instead exhibit strain dependent responses. TC preconditioned PMMA was significantly more hydrophobic than AS preconditioned PMMA. AS preconditioned PMMA was also more hydrophilic than WC PMMA. Chemical characterisation identified several main components within the tobacco condensate including nicotine and anabasine, confirming that they were present in TC PMMA.

CHAPTER 3: Effect of Acrylic Surface Roughness on *Candida albicans* Adherence and Biofilm Development

3.1. Introduction

Adhesion and retention of microorganisms on dentures surfaces is an important area of research as dentures have been shown to accumulate plaque in the same way as the natural oral surfaces (Abelson 1981). Dentures have hard non-shedding surfaces including the smooth polished regions of 'teeth' and the denture base material, which sits in close proximity to the oral mucosa. The fitted denture surface is known to shelter microorganisms, encouraging growth and biofilm formation (Monsenego 2000). The denture biofilm develops its own microenvironment where microorganisms can adjust environmental factors such as pH to generate more conducive conditions for their growth (Allison and Douglas 1973; Kikuchi et al. 1999; Kuhar and Funduk 2005). The denture is exposed to many oral cavity conditions that are present to regulate oral microorganisms. However, in contrast to the natural mucosa it is unable to shed its surface, and this serves to promote retention of attached microorganisms.

Numerous factors contribute to adherence of microorganisms, but surface roughness and topology are essential variables when considering infection risk and also optimising denture hygiene regimes to reduce risk. Increased surface roughness has been shown to increase hydrophobicity, surface area and effects of shear forces (Nikawa et al. 2003; Zamperini et al. 2010; Karakis et al. 2016). Each of these factors will in turn impact upon microbial attachment, adherence and retention.

Initial attachment of *C. albicans* to a surface is primarily attributed to non-specific interactions, including cell and surface hydrophobicity, which some studies have shown has a strong correlation with *C. albicans* adhesion (Minagi et al. 1985; Panagoda and Samaranayake 1998; Danchik and Casadevall 2021). In contrast, other studies have reported no correlation between surface hydrophobicity and *C. albicans* adherence (Zamperini et al. 2010; Ohshima et al. 2018). Microbial attachment is more likely to occur in surface regions which are protected from shear forces, thereby allowing time for colonised cells to progress to an irreversible attachment stage (Verran et al. 1997; Kang et al. 2013). Increased surface area and the heightened difficulties of effectively cleaning the rougher surface, creates

a reservoir of cells which after cleansing can regrow, negating the need for microorganisms having to recolonise the surfaces.

Denture surfaces will naturally incur ‘wear and tear’ over time from physical and chemical abrasion, leading to surface imperfections. Furthermore, other factors and lifestyle choices can alter the roughness of the denture surface, such as smoking of tobacco products (Mahross et al. 2015) and certain methods used to maintain denture hygiene (Sorgini et al. 2015). Exposure to cigarette smoke has been found to increase the roughness of polymethyl methacrylate (PMMA) denture material (Mahross et al. 2015), a finding that was observed in the work of the previous chapter (Section 2). In these previous studies PMMA coupons that were preconditioned with tobacco condensate had increased surface roughness (Mahross et al. 2015). However, the most common reason for increased denture ‘wear and tear’ appears to be from using inappropriate denture cleansing methods with abrasive products (Nikawa et al. 2003; Singh et al. 2019). Abrasive toothpastes and toothbrushes are often incorrectly used by denture wearers, with the misconception that abrasion improves denture hygiene, but instead enhances surface roughness (MacHado et al. 2012; Alanazi et al. 2014; Axe et al. 2016; Zakaria et al. 2018; Chang et al. 2021). Application of abrasive cleansing agents may also be detrimental to longer-term cleanability of the denture, cause dehydration of the material with an associated increased brittleness and heightened susceptibility to mechanical forces (Neppelenbroek et al. 2005; Campanha et al. 2012). Microscopic ‘scratches’ and flaws can offer areas of refuge for microorganisms and reduce accessibility of cleansing to these organisms.

Several approaches that can generate experimental acrylic surfaces of differing roughness are available and these have subsequently been used to investigate the adherence and retention of *C. albicans* and other microorganisms (Panagoda et al. 1998; Radford et al. 1998; Taylor et al. 1998; Radford et al. 1999; Nevzatoğlu et al. 2007). Acrylic surfaces produced by a range of approaches including standard processing machinery for dental protheses, curing materials against smooth glass or dental plaster, or applying a tungsten carbide bur and abrading with different grit size abrasive papers have shown higher levels of *Candida* attachment to rougher surfaces. Verran *et al.* (2014), found that even small surface abrasions enhanced retention of *Candida* and oral bacteria to denture surfaces

and produced surfaces that were harder to clean. Bacteria of the genus *Streptococcus*, were retained at higher levels on low-abraded surfaces, whilst *Candida* were attached at higher levels to highly-abraded surfaces (Verran et al. 2014). Verran *et al.* (2014) did however suggest that the attachment strength, rather than the level of attachment might be more clinically relevant. It was evident that an increased strength of attachment by *Streptococcus oralis* and *C. albicans* to roughened denture surfaces with small abrasions (Ra 50 – 150 nm) enhanced retention and reduced 'cleanability' (Verran *et al.* 2014).

Surface roughness facilitates biofilm formation as shown by the findings of the systematic review of Teughels *et al.* (2006) and supports that the increase in surface roughness above the Ra threshold of 0.2 μm and surface-free energy, to a lesser extent, facilitates biofilm formation on restorative materials. Bollen *et al.* (1996) stated that there was a 'threshold Ra' of 0.2 μm which was the minimum level of roughness required for bacterial adherence from plaque samples to occur on a surface (Zissis et al. 2000). However, adherence and retention of microbes appears to be related to the size and shape of cells in comparison to surface topological features (Minagi et al. 1985; Panagoda and Samaranayake 1998). This was strongly supported by the study of Whitehead et al. (2005) who tested silicon and titanium-coated stainless steel surfaces with clearly defined pore sizes (0.2, 0.5, 1 and 2 μm) using microorganisms of different shapes and sizes. *Staphylococcus aureus, Pseudomonas aeruginosa* and *C. albicans* were used and it was reported that retention was preferential to surfaces of pore size most similar to the cell size of the organism being tested. The contact area between microbial cell and the surface is increased when surface features are of similar dimensions to those of the attaching cell as there would be a higher number of contact points for bonds to form them (Medilanski et al. 2002; Whitehead et al. 2004; Whitehead et al. 2005; Whitehead and Verran 2006; Verran et al. 2010). However, *C. albicans* was observed to have a similar level of adherence to all the different surfaces and pore sizes (Whitehead et al. 2005). As *C. albicans* is highly polymorphic it is more difficult to specify an optimum roughness and size of topological features for its adherence and retention. Larger topological features may harbour filamentous forms of *C. albicans* that can subsequently grow along these features via thigmotropism (Davies et al. 1999; Kumamoto and Vinces 2005a). This in turn

provides a protected area where retained organisms can potentially re-establish a denture biofilm post cleansing.

In terms of denture cleaning, Karakis *et al.* (2016) found that while polished and roughened denture base resin surfaces had significantly different Ra values and hydrophobicity (contact angle), no differences in cleanability (for 4 out 5 disinfectants) were found between polished and roughened surfaces. Zamperini *et al.* (2010) found a significant difference in *C. albicans* adherence using surfaces of different roughness and also with incorporation of saliva. However, these differences were not evident on surfaces that were plasma treated, which was considered to have negated any hydrophobicity differences that might have previously been generated on the surfaces.

3.1.1. Aims and Objectives

The primary aims of the research in this chapter were to:

1. Produce denture acrylic surfaces with different levels of surface roughness.
2. Characterise acrylic surface roughness and assess whether differences in hydrophobicity associate with surface roughness.
3. Investigate whether changes in surface roughness impact upon adherence and biofilm development of *C. albicans* and whether there was a critical threshold of roughness that was preferential to retention of the microorganisms.
4. Measure the adherence and biofilm development of a *Candida albicans* mutant strain that lacked ALS3 compared to the wildtype strain on denture acrylic surfaces of different roughness.

3.2. Materials and Methods

3.2.1. Selection and culture conditions of microbial strains

For this research, wildtype *Candida albicans* SC5314 and the mutant strain *Candida albicans* SC5314 UB1941 Δ*als3* (ΔALS3) were used. The *C. albicans* ΔALS3 strain was gifted from Dr Angela Nobbs at Bristol University (Zhao et al. 2004; Pidwill et al. 2018). *Candida albicans* ΔALS3 is a homozygous mutant strain in which the agglutinin-like protein 3 (*ALS3)* gene has been deleted (Zhao et al. 2004; Pidwill et al. 2018). *ALS3* encodes a hyphal-specific adhesin which has previously been described (section 1.4.2.2.). Culture conditions and standardisation of the inocula for both *C. albicans* strains are the same as previously described in section 2.2.1.

3.2.2. Creating categories of polymethyl methacrylate (PMMA) with different levels of surface roughness

PMMA coupons were constructed as previously described in section 2.2.2 The underside of the coupons was abraded using a polisher (Kemet) for 10-20 s with contact at 500 rev/min and in conjunction with the following grades of silicon carbide paper: P120, P600, P1200, P2500 (Agar ; Table 3.1)). A fifth category of roughness, termed Pn was included, and this was the same coupon type as previously used in section 2, with a ‘smooth surface’ obtained from contact with glass under pressure while curing. After preparation, coupons were rinsed in dH_2O before being autoclaved at 121ºC in dH_2O. All coupons were labelled on the underside to ensure correct orientation and category identification during experimentation and analyses.

Table 3.1. Diameter of the grit of the silicon carbide paper used to abrade the surfaces of the PMMA.

Grade of silicon carbide paper	Diameter of grit (μm)
P120	115
P600	25.8
P1200	15.3
P2500	8.4

3.2.2.1. Roughness measurements

To define categories of surface roughness, the mean surface roughness (Ra) was measured using a profilometer (Surftech). Post-autoclaving, 6 coupons from each category were randomly selected, and five transects of 5 mm were measured in different orientations on each coupon. The mean for each category was calculated to give the average the level of surface roughness of each category. Ra was chosen to represent the surface roughness as it is widely accepted and used as a universal surface roughness parameter.

3.2.2.2. Atomic Force Microscopy (AFM) imaging of PMMA surfaces of varying roughness and roughness measurements

AFM work was carried out at the University of Toronto, Faculty of Dentistry with Dr Laurent Bozec after being awarded a three-month placement from the UK-Canada Globalink Doctoral Exchange Scheme grant from the UKRI and Mitacs. AFM imaging of the PMMA surfaces was performed using a Bruker JPK Nanowizard 4 system. Prior to AFM, PMMA coupons were sonicated in dH_2O for 10 min to ensure there was no debris on the surface. Images were obtained using MSNL-10 cantilevers (Bruker) with a spring constant of 0.1 N/m. Gain parameters were adjusted during imaging to allow for optimum image acquisition. The error signal of the image is presented as a visual representation of a 10,000 μm^2 area of the surface. JPK Data Processing Software v.5.1.8 (JPK Instruments) was used to

render the images of 100 μm^2 and 10,000 μm^2 areas and obtain the mean Ra of 100 μm^2 areas.

3.2.2.3. Hydrophobicity measurements

An Attension Theta Lite (Biolin Scientific, Manchester, UK) contact angle goniometer was used with OneAttension software (version 3.2, Biolin Scientific) to obtain contact angle measurements using the sessile drop method as described in section 2.2.5 (Figure 3.1). Contact angle measurements were indicative of the hydrophobicity of a surface where a contact angle measurement > 90° was typically considered hydrophobic and < 90° hydrophilic. Prior to measurement, the instrument was calibrated using a calibration kit as per the manufacturer's instructions. PMMA coupons of each roughness category were tested with, and without, artificial saliva (AS) preconditioning. Details of the AS composition and the method of preconditioning are described in section 2.2.2.2. All coupons were allowed to dry completely in sterile petri dishes before a 4 µL droplet of water was lowered on to the surface. As soon as the liquid contacted the surface, the software tracked the dispersion of the droplet, recording the contact angle measurements on the left and right of the droplet for 10 s using a manually set baseline. These angles were then averaged to give an overall reading from the 10 s time period.

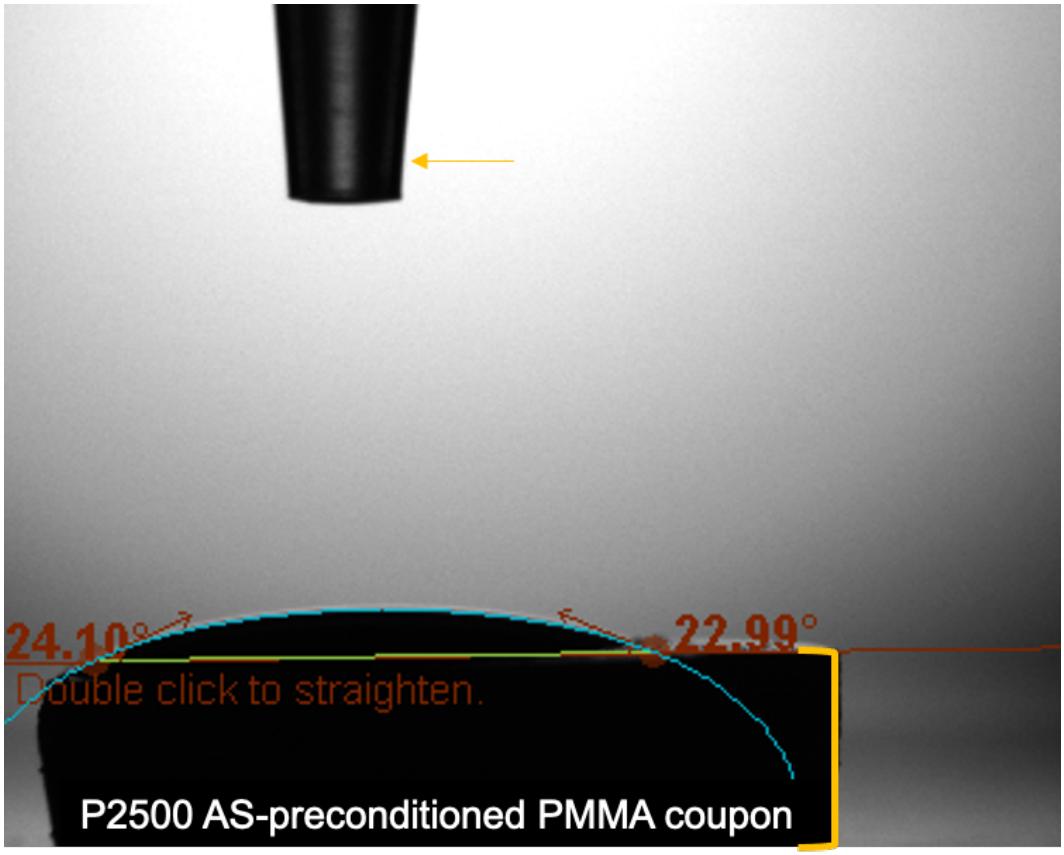

Figure 3.1. An image of the contact angle measurements being taken for the surface of a polymethyl methacrylate (PMMA) coupon. Contact angle measurements were obtained using a goniometer and the sessile drop method. The example image is of a AS-preconditioned PMMA coupon from the P2500 surface roughness category. The yellow shape at the base of the image indicates the PMMA coupon position. The green line indicates the set baseline which tells the software that this is the surface of the PMMA coupon. The baseline was set manually prior to the water droplet being lowered onto the surface. The pipette tip at the top of the image indicated with a yellow arrow was where the 4 µL droplet was expelled and lowered to the surface. The blue curved line indicates the detected boundary of the water droplet, and the red angles and numbers indicate the contact angle measurement on both the right and left side of the droplet these two readings are averaged to determine the mean contact angle (°) reading and multiple readings are taken within a 10 s timeframe that are then averaged to give the overall mean contact angle measurement (°) for each coupon. Six coupons were measured for each surface roughness category.

3.2.3. Adherence of *Candida albicans* to different levels of PMMA surface roughness and subsequent biofilm development

Three PMMA coupons from each roughness category were preconditioned with AS, as described in section 2.2.2.2, washed with dH_2O, and aseptically added to the wells of 6-well plates. Fifty µl of a standardised (OD_{600} 1 ± 0.1) *C. albicans* inoculum was added to the surface of each coupon. Incubation was for 90 min at 37ºC in 5% (v/v) CO_2. The coupons were then rinsed with PBS to remove non-adherent cells. The coupons were then immersed in 1 mL of 10% (v/v) neutral buffered formalin to fix cells prior to staining with 10% (w/v) calcofluor white (Sigma) and imaging using fluorescence microscopy. Initially, *C. albicans* was stained with Live/Dead BacLight Bacterial Viability kit (Thermofisher), but there was too much background fluorescence from the PMMA coupons, especially when the surfaces were more textured. Therefore, calcofluor white was used instead and gave a much clearer image.

To assess biofilm development, the protocol was followed as above, but instead of fixing samples at 90 min the coupons were added to 2 mL of YNB in 24-well plates and returned to the incubator for 24 h. After incubation, processing steps were followed as described for the 90 min samples. Immediately before fluorescence microscopy imaging, 50 µL of 10% (v/v) calcofluor white solution was added to the surface of the coupon for 10 min.

3.2.4. Fluorescence microscopy to determine adherence and biofilm development of *C. albicans*.

Fluorescence micrographs were obtained at a total magnification of x400 using an Olympus Ax70 upright fluorescence microscope and PAX-it imaging software (PAX cam). A DAPI/Hoechst filter cube was used to image cells stained with calcofluor white.

FIJI ImageJ Software (Version:2.0) was used to measure the percentage coverage of *C. albicans* on PMMA surfaces (x400 magnification images). A macro was created and used to convert the files to 8-bit, threshold the images using the 'MaxEntropy' auto threshold method with the specification of a black background and the percentage coverage of *C. albicans* in each field of view determined using

the measure function selecting both area and percentage area. The mean percentage area coverage of *C. albicans* on the surface was determined by combining the output for five fields of view from each of the nine coupons (n = 45).

3.2.5. Statistical analysis

GraphPad Prism 9 (Version 9.3.1 (350)) software was used to construct graphs and for statistical analyses. Data was tested for normal (Gaussian) distribution using the Shapiro-Wilk test and Q-Q plots of residuals.

To compare differences between surface profilometer measured Ra for the coupon categories, the Kruskal-Wallis test with Dunn's post-hoc test of multiple comparisons was used. For the AFM measured Ra values, statistical differences between the groups was evaluated using a One-Way ANOVA with Tukey's post-hoc test for multiple comparisons. Contact angle measurement changes between the roughness categories was assessed by One-Way ANOVA with Tukey's post-hoc tests.

To measure significant differences in percentage surface area coverage of *C. albicans* on the PMMA surface roughness categories, the Kruskal-Wallis test with Dunn's post-hoc test was used. The Kruskal-Wallis test with Dunn's post-hoc test for multiple comparisons was also used to compare *C. albicans* SC5314 and *C. albicans* ΔALS3 adherence and biofilm development on the PMMA roughness categories.

3.3. Results

3.3.1. Defining the surface roughness and hydrophobicity of each surface roughness category.

Initially, it was important to determine the level of surface roughness and hydrophobicity of the PMMA surfaces in each roughness category. A summary of these results is presented in Table 3.2. Profilometer measurements reported a mean Ra value for each category (Figure 3.2). There was an overall significant difference found using the Kruskal-Wallis test (H (4) = 95.25, $P \leq 0.0001$) and Dunn's post-hoc test of multiple comparisons between the groups, as shown in Figure 3.2. All five categories of roughness were therefore used in subsequent experiments.

In addition, Ra measurements were also obtained using atomic force microscopy (AFM), where each reading calculated the Ra value from a 10 μm^2 area rather than transects along the full length of the coupon. In terms of the AFM measurements (Table 3.2 and Figure 3.3), the surface of the P600 coupons on a microscale (100 μm^2 area) had the highest mean Ra value (Ra 6.34 µm) indicating that it was the roughest surface category and this was significantly higher than the other categories; Pn, P120, P1200 and P2500 ($P \leq 0.0001$, $P \leq 0.0007$, $P \leq 0.0001$, and $P \leq 0.0002$, respectively). However, there were no other significant differences between any of the other groups. Representative AFM images depicting the error signal reading allowed for visualisation of the surface of the PMMA in each category (Figure 3.4). Scratches on the PMMA surfaces can be seen in these images from the abrasive technique used to create surfaces of different roughness.

Contact angle measurements were used to determine the hydrophobicity of the PMMA surfaces and whether surface abrasion affected hydrophobicity (Table 3.2). A surface with a contact angle measurement > 90° was considered hydrophobic and < 90° hydrophilic. Therefore, the surfaces of all the PMMA roughness categories were hydrophilic (Table 3.2). Changing the surface roughness of the PMMA did not affect the hydrophobicity of the surface significantly for either AS (F (4, 20) = 0.2061, P ≤ 0.9320) or dH_2O (F (4, 18) = 1.331, P ≤ 0.2967) preconditioned PMMA coupons (Table 3.2 and Figure 3.5). As previously

discussed in section 2.3.3, preconditioning with AS created a significantly more hydrophilic surface than preconditioning with dH_2O. AS-preconditioning was included in subsequent experiments as this is more representative of the conditions in the oral cavity.

Table 3.2. Summary of the polymethyl methacrylate (PMMA) surface roughness for each category, the method of abrasion and surface hydrophobicity. The method used to abrade the surface to create categories of different levels of roughness and the diameter of the grit of the abrasive paper used is presented. For each category, surface roughness was evaluated using the mean Ra value which was measured by profilometer (5 mm transects) and atomic force microscopy (100 μm^2 area). The lower the Ra value the smoother the surface. The mean contact angle (°) was measured after dH_2O or AS preconditioning for each category and indicated the hydrophobicity of the surface (hydrophilic > 90°, hydrophobic < 90°).

			Mean surface roughness Ra (µm)		Mean contact angle (°)	
Roughness category	**Method of abrasion**	**Diameter of grit (µm)**	**Profilometer measurements**	**AFM measurements**	**dH_2O preconditioned**	**AS preconditioned**
Pn	PMMA cured against smooth glass surface under pressure	N/A	3.97	1.16	66.24	23.93
P120	Abraded with silicone carbide paper (grit size P120)	115	5.37	2.85	66.09	24.85
P600	Abraded with silicone carbide paper (grit size P600)	25.8	2.10	6.34	60.56	22.69
P1200	Abraded with silicone carbide paper (grit size P1200)	15.3	1.37	2.17	52.58	25.51
P2500	Abraded with silicone carbide paper (grit size P2500)	8.4	9.75	1.32	55.32	26.23

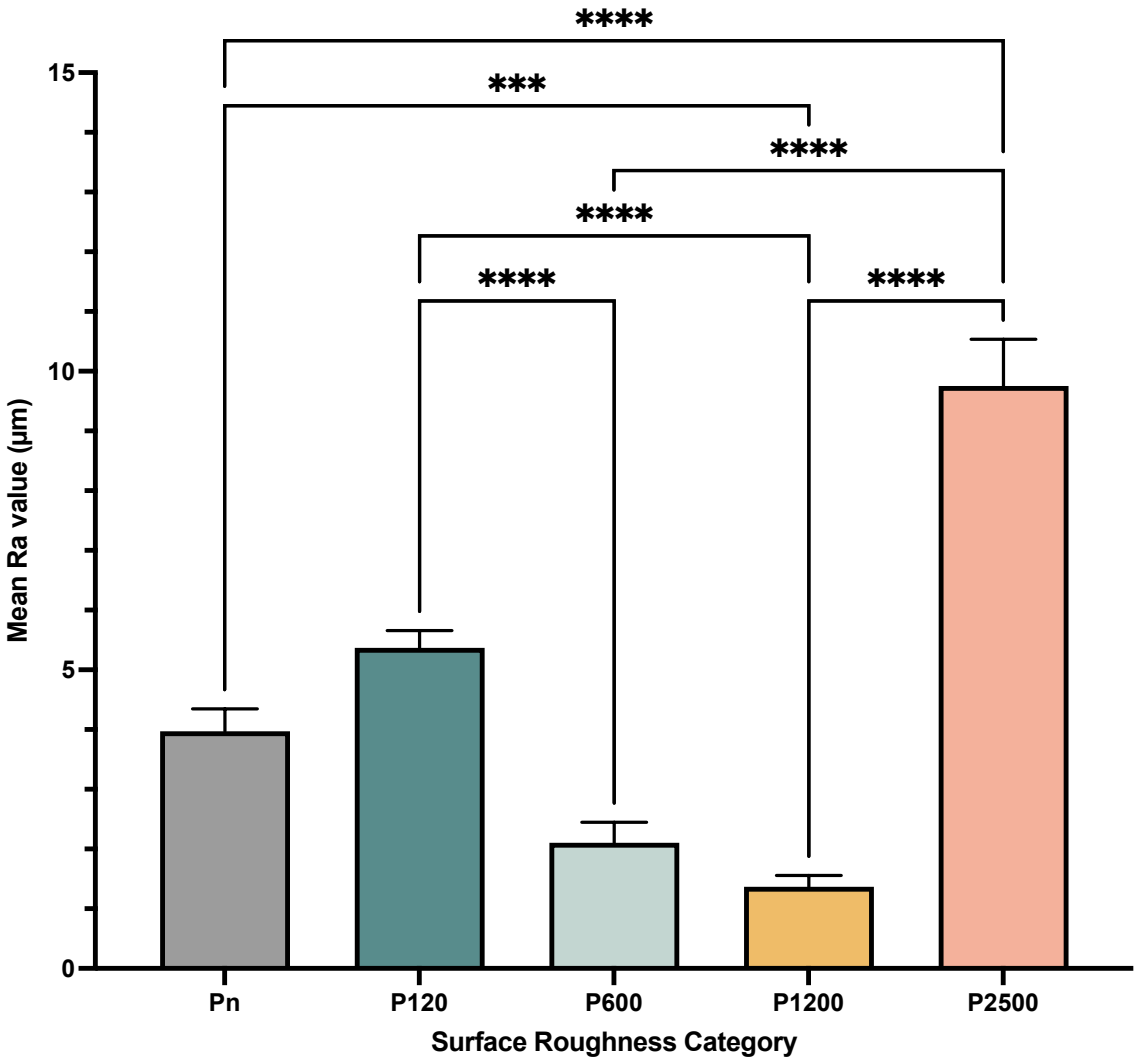

Figure 3.2. Mean surface roughness measurements for each polymethyl methacrylate (PMMA) surface roughness category. The surface of PMMA coupons were polished to create different categories of surface roughness. A profilometer was used to measure 5 mm transects across the surface and averaged to obtain a mean Ra value (µm) for each surface roughness category. Data presented as mean ± standard error of the mean. Each category n = 30. Statistical significance was determined using the non-parametric Kruskal-Wallis test (H (4) = 95.25, $P \leq 0.0001$) with Dunn's post-hoc test of multiple comparisons which determined the P values labelling in the graph. *** indicates $P \leq 0.001$ and **** indicates $P \leq 0.0001$.

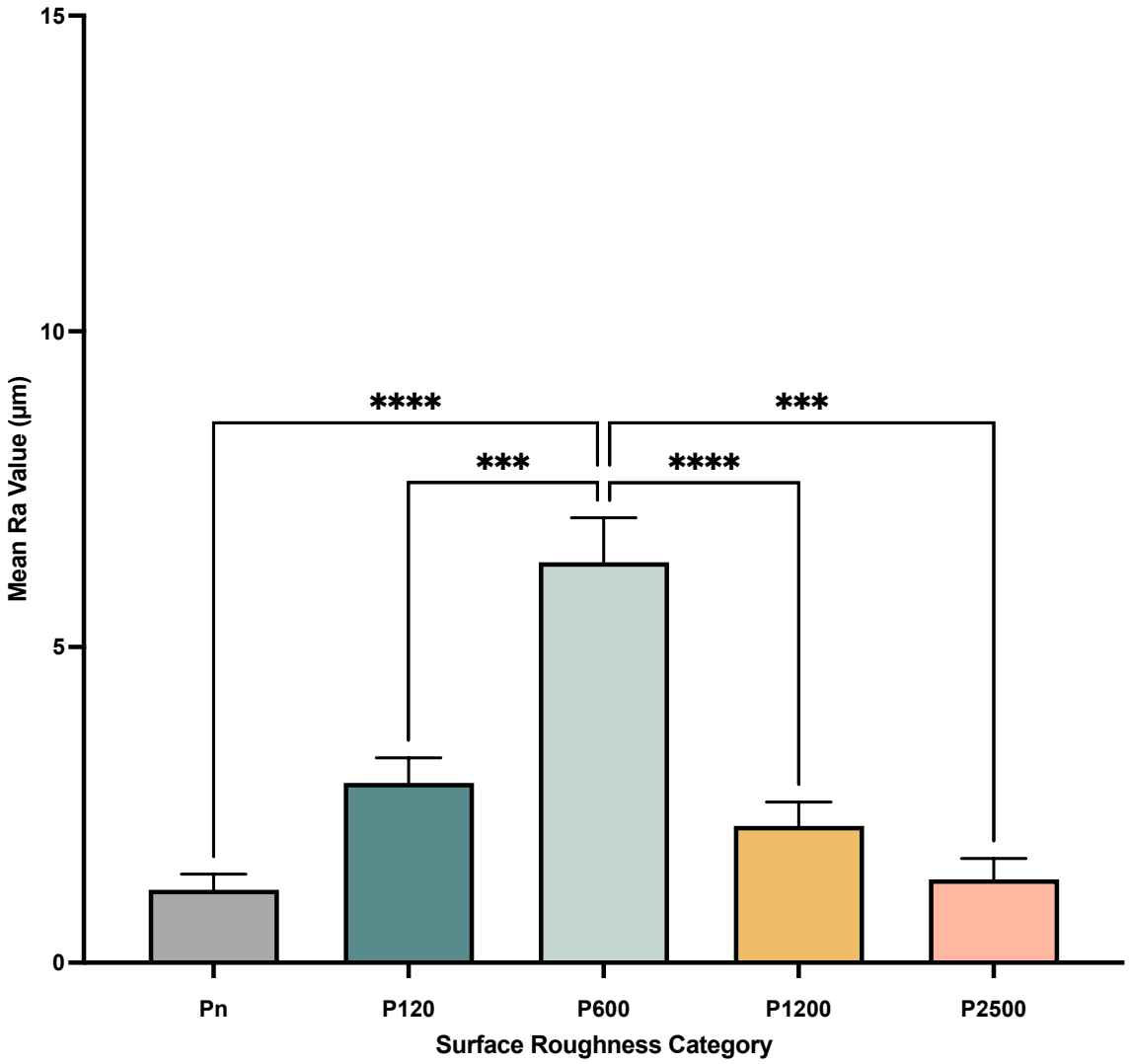

Figure 3.3. Mean surface roughness measurements of each polymethyl methacrylate (PMMA) surface roughness category measured for a 100 µm^2 area using atomic force microscopy. The surface of PMMA coupons were polished to create different categories of surface roughness. AFM was used to measure randomly selected 100 µm^2 areas across the surface that were then averaged to obtain a mean Ra value (µm) for each surface roughness category. Data presented as mean ± standard error of the mean. *n*(Pn) = 5, *n*(P120) = 4, *n*(P600) = 5, *n*(P1200) = 5, *n*(P2500) = 2. Statistical significance was determined using one-way ANOVA (F (4, 16) = 20.42, $P \leq 0.0001$) with Tukey Post-Hoc test for comparison between groups *** indicates $P \leq 0.001$ and **** indicates $P \leq 0.0001$.

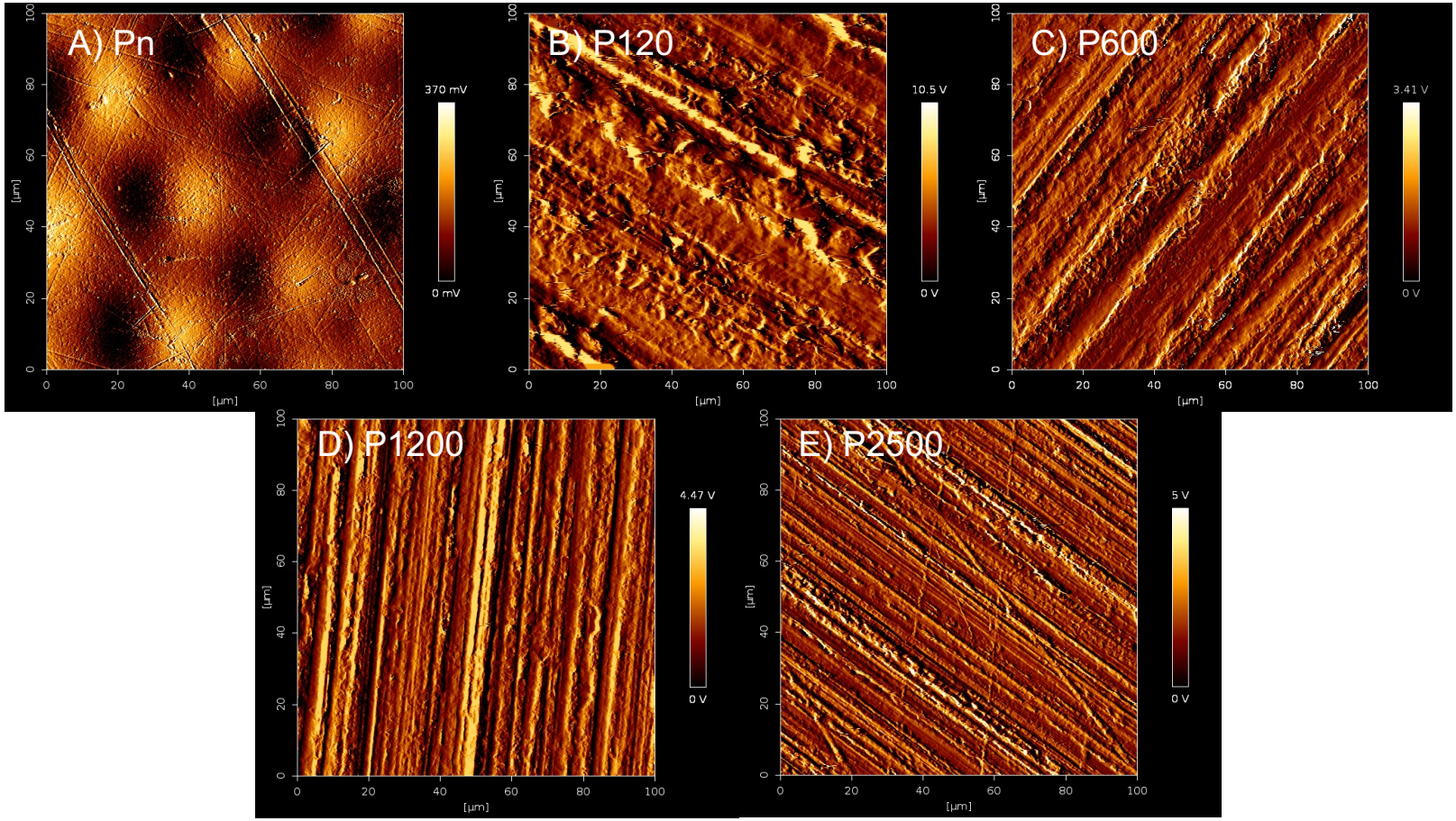

Figure 3.4. Representative images of the polymethyl methacrylate (PMMA) surface for each roughness category. PMMA coupons from each of the different roughness categories were mounted on an AFM Nanowizard 4 stage and imaged using an MSNL-10 cantilever with a spring constant of 0.1 N/m. Images were taken of 10,000 µm^2 areas to reveal the topology of the surface. Error signal images are presented, which gives a visual representation of the surface.

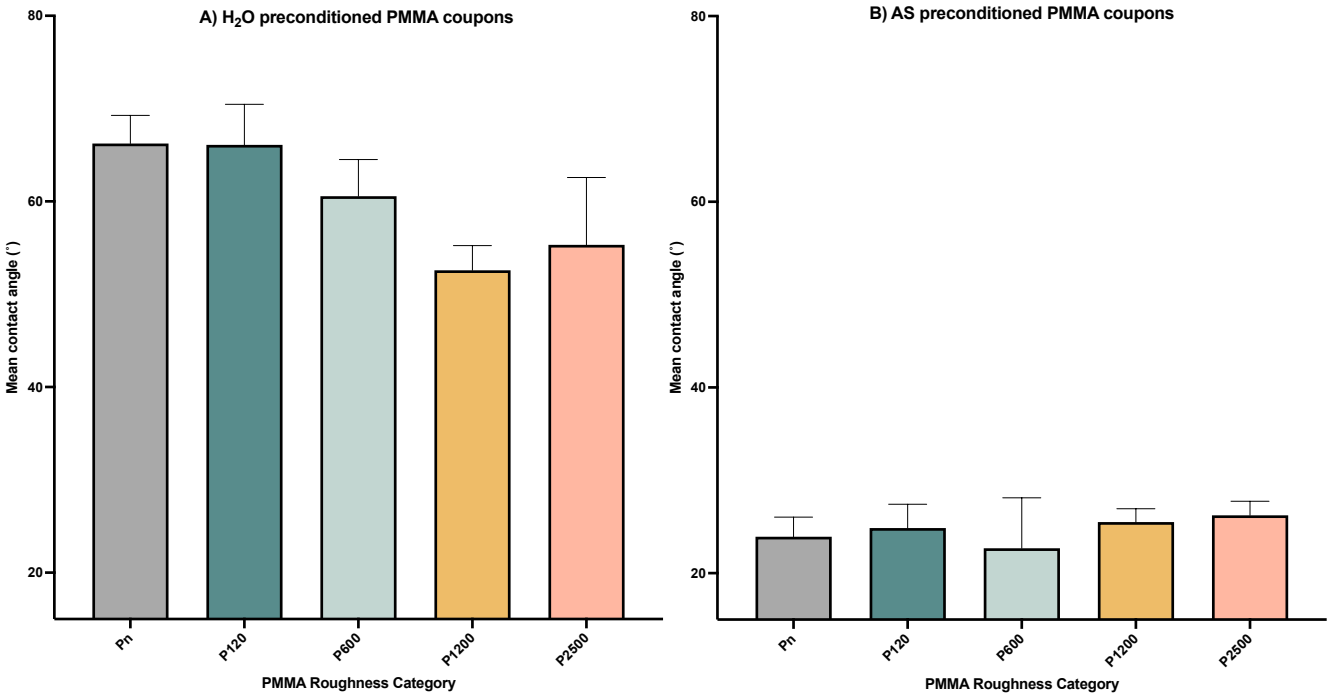

Figure 3.5. Hydrophobicity of each surface roughness category measured as mean contact angle (°). PMMA coupons from each different roughness category were preconditioned in either H_2O (A) or artificial saliva (B). A contact angle goniometer was used to measure the mean contact angle using the sessile drop method which was indicative of hydrophobicity. Data presented as mean ± standard error of the mean. *n*(Pn) = 6, *n*(P120) = 4, *n*(P600) = 5, *n*(P1200) = 6, *n*(P2500) = 4. No significant differences were found between the roughness categories using One-Way ANOVA (F (4, 20) = 0.2061, $P \leq 0.9320$) with Tukey's post-hoc test.

3.3.2. Adherence of *Candida albicans* to PMMA surfaces of differing surface roughness.

Adherence of *C. albicans* SC5314 to PMMA surfaces varied depending on levels of roughness with several significant differences evident between the categories (Figure 3.6. (H (4) = 140.8, $P < 0.0001$)). As the grade of silicone carbide paper used for polishing became finer, the greater the surface area coverage by *C. albicans* SC5314 after 90 min was encountered. The surface area coverage of *C. albicans* SC5314 was highest for P2500 surfaces (6.5%) and lowest for P120 surfaces (0.4%). The unabraded Pn surface had a level of *C. albicans* adherence (0.8%) that was higher than P120, but lower than the P600 surfaces. The Pn, P120 and P600 surfaces were not significantly different from each other in terms of *C. albicans* SC5314 adherence after 90 min. However, in terms of *C. albicans* adherence, all three surfaces were significantly lower ($P \leq 0.0001$) than P1200 and P2500 surfaces; the P1200 and P2500 surfaces were not significantly different from each other. Representative images of *C. albicans* SC5314 adherence on the surface roughness categories are presented in Figure 3.7. In the 90 min samples, the smaller the diameter of the grit paper used was found to increase *C. albicans* adherence to the surface.

Candida albicans ΔALS3 exhibited a different pattern of adherence to PMMA surfaces of different roughness categories compared with *C. albicans* SC5314. There was a decrease in adherence from Pn to P120 to P600 (2%, 1.5% and 0.5%, respectively) and an increase from P600 to P1200 to P2500 (0.5%, 3.1% and 4.8%, respectively (Figure 3.8). The difference between Pn and P120 surfaces was not significant, which was also the case for P1200 and P2500 surfaces. All other differences in adherence to the roughness categories were significant according to the Kruskal-Wallis test (H (4) = 94.19, $P \leq 0.0001$) with Dunn's post-hoc test of multiple comparisons (Figure 3.8). Adherence of *C. albicans* SC5314 and *C. albicans* ΔALS3 after 90 min incubation showed no significant differences in surface area coverage for every roughness category (Table 3.3).

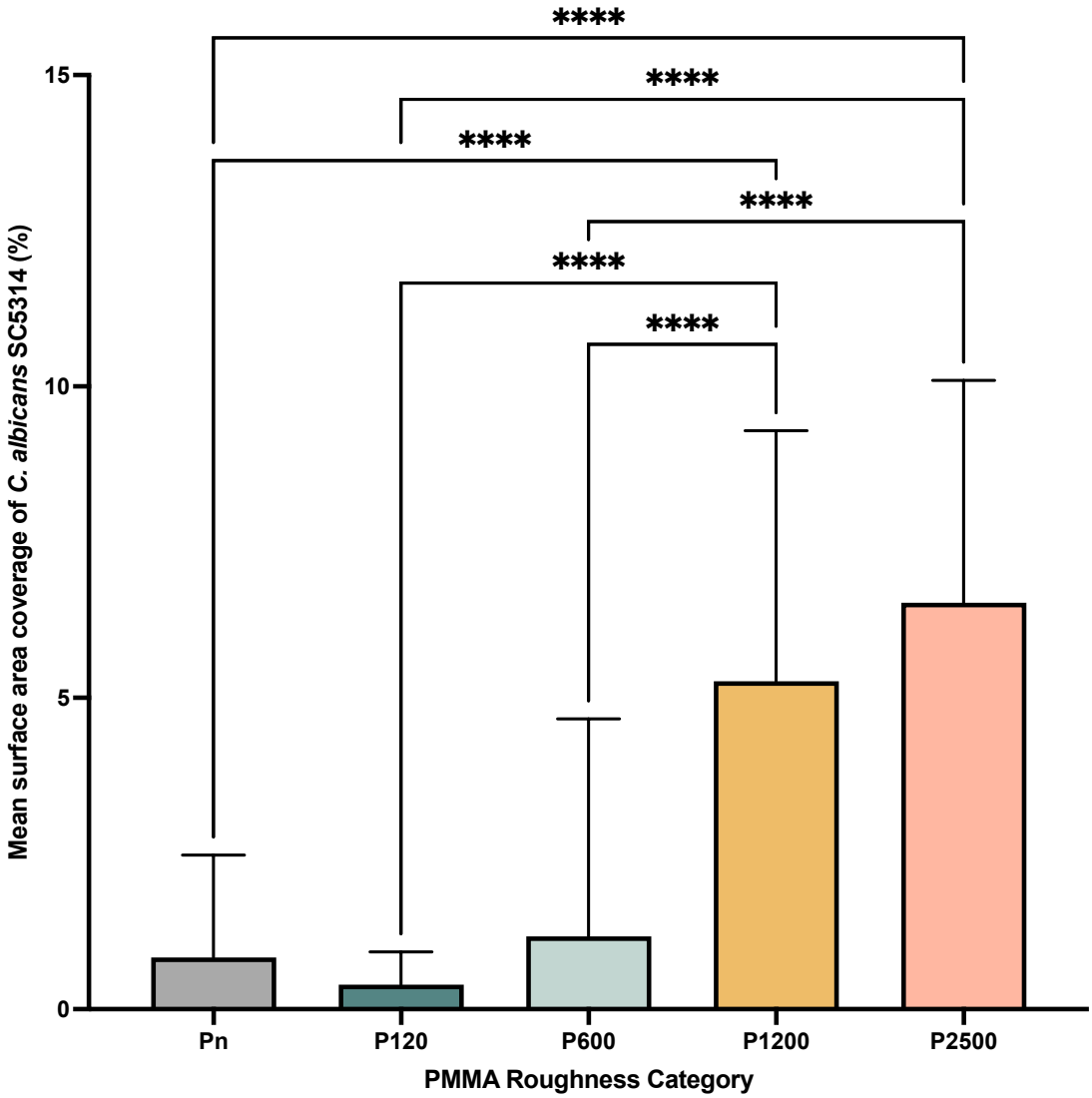

Figure 3.6. Mean level of adherence of *C. albicans* SC5314 on each polymethyl methacrylate (PMMA) roughness category measured as percentage area coverage. *Candida albicans* SC5314 was added to the surface of artificial saliva preconditioned PMMA coupons from each roughness category and incubated for 90 min. Fluorescence microscopy was used to obtain images that were analysed to obtain the area of surface coverage by *C. albicans.* Data presented as mean ± standard error of the mean. Statistical significance was determined using the non-parametric Kruskal-Wallis test (H (4) = 140.8, $P \leq 0.0001$) with Dunn's post-hoc test of multiple comparisons to show significance between groups. Each category $n = 45$. **** indicates $P \leq 0.0001$.

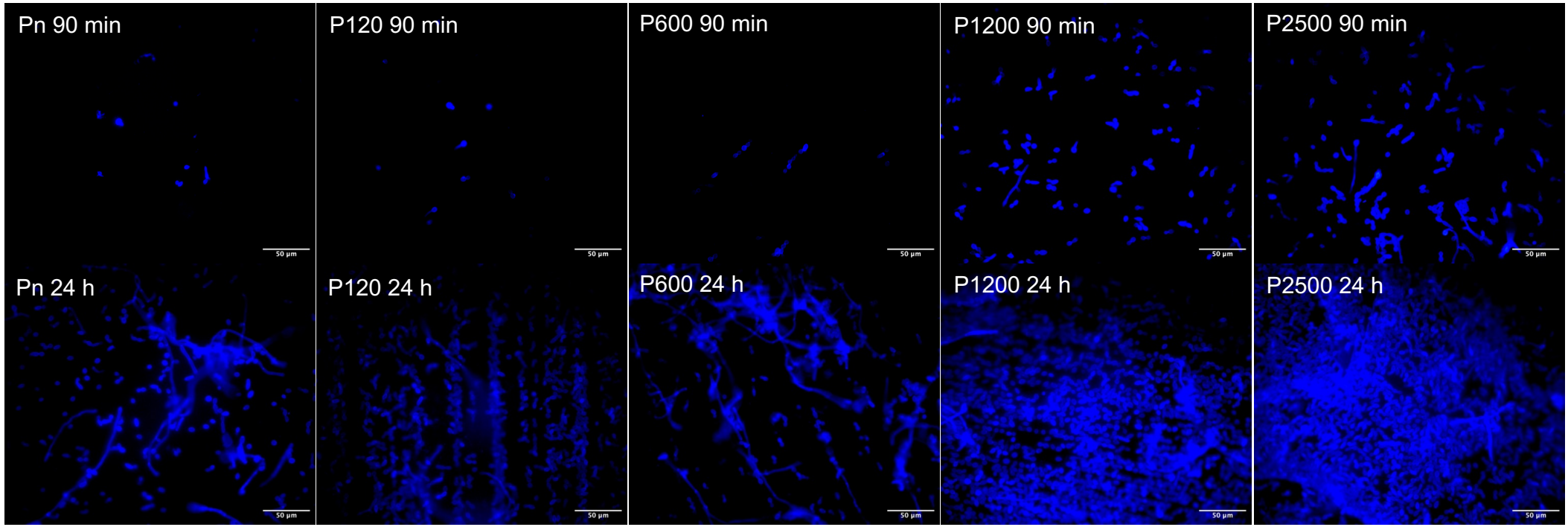

Figure 3.7. Representative images of *C. albicans* SC5314 surface coverage after 90 min (top row) and 24 h (bottom row) incubation on different categories of polymethyl methacrylate (PMMA) surface roughness. *C. albicans* SC5314 was added to the surface of artificial saliva preconditioned PMMA coupons from each roughness category and incubated for 90 min and 24 h. *Candida albicans* SC5314 fluoresces blue from calcofluor white staining. *Candida albicans* at 24 h appears to be following scratches in the surface, and was particularly evident in the P120, P600 and P1200 images. Images were at x400 total magnification. Scale bars are 50 μm.

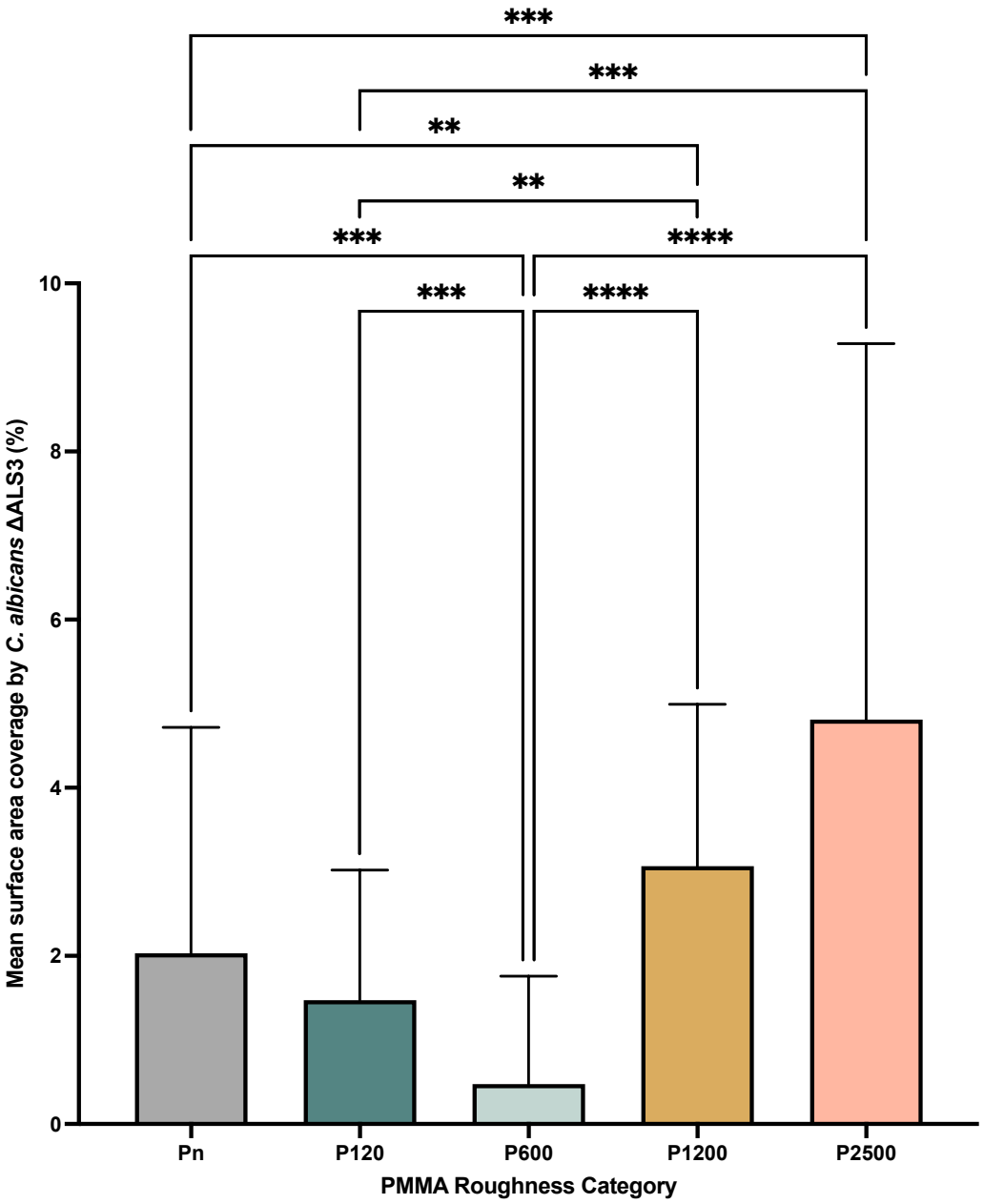

Figure 3.8. Mean level of adherence of *C. albicans* ΔALS3 on each polymethyl methacrylate (PMMA) roughness category expressed as percentage area coverage. *Candida albicans* ΔALS3 was added to the surface of artificial saliva preconditioned PMMA coupons from each roughness category and incubated for 90 min. Fluorescence microscopy was used to obtain images that were analysed to obtain the area of surface coverage by *C. albicans.* Data is presented as mean ± standard error of the mean. Statistical significance was determined using the non-parametric Kruskal-Wallis test (H (4) = 94.19, $P \leq 0.0001$) with Dunn's post-hoc test of multiple comparisons. Each category n = 45. ** indicates $P \leq 0.01$. *** indicates $P \leq 0.001$. **** $P \leq 0.0001$.

Table 3.3. Comparison between *C. albicans* SC5314 and *C. albicans* ΔALS3 adherence (90 min) and biofilm development (24 h) measured as surface area coverage (%). The mean surface area coverage (%) and the standard error of the mean for each roughness category and strain is included in the table. Significant differences between *C. albicans* SC5314 and *C. albicans* ΔALS3 for each roughness category were determined using the Kruskal-Wallis test with Dunn's post-hoc test for multiple comparisons. (*) indicates that the result reached the threshold for significance ($P \leq 0.05$).

.

	Surface area coverage (%) of *Candida albicans* after 90 min					**Surface area coverage (%) of *Candida albicans* after 24 h**				
	SC5314		**ΔALS3**			**SC5314**		**ΔALS3**		
Roughness category	Mean (%)	Std. Error of Mean	Mean (%)	Std. Error of Mean	*P* values (Dunn's post-hoc test)	Mean (%)	Std. Error of Mean	Mean (%)	Std. Error of Mean	*P* values (Dunn's post-hoc test)
Pn	0.83	0.25	2.03	0.40	$P \leq 0.9999$	14.94	1.86	22.83	3.34	$P \leq 0.9999$
P120	0.39	0.08	1.47	0.23	$P \leq 0.0687$	30.52	2.45	15.00	1.90	$P \leq 0.0249$*
P600	1.17	0.52	0.48	0.19	$P \leq 0.9999$	14.11	2.58	4.94	1.01	$P \leq 0.0582$
P1200	5.27	0.60	3.07	0.29	$P \leq 0.9999$	43.41	3.07	9.12	1.54	$P \leq 0.0001$*
P2500	6.53	0.53	4.81	0.67	$P \leq 0.9999$	50.24	2.79	23.52	3.05	$P \leq 0.0001$*

3.3.3. Surface area coverage of *Candidia albicans* to PMMA surfaces of different surface roughness after 24 h

Representative images of *C. albicans* SC5314 surface coverage after 24 h on the different roughness categories of PMMA are presented in Figure 3.7. Increased *C. albicans* coverage was evident as the grit size of the abrasive paper used to abrade the surface becomes finer. Also, *C. albicans* appeared to be colonising along the topological features of the surfaces that had been created by abrasion (Figure 3.7).

In the case of *C. albicans* SC5314 surface coverage after 24 h (Figure 3.9), there was a general trend that as the grit of the abrasive paper used (Table 3.3) to roughen the surface decreased, its surface coverage increased. There was a reduction in the surface area coverage on the P600 surfaces, which was the lowest mean surface coverage (14.1%) but was similar to the Pn surfaces (14.9%). Highest *Candida* surface area coverage (50.2%) was on the P2500 surfaces.

Changing the roughness of the PMMA surfaces led to significant differences in the mean surface area covered by *C. albicans* SC5314 (H (4) = 93.25, $P < 0.0001$). Levels of significant difference between each of the groups are presented in Figure 3.9. Pn and P600 surfaces had similar levels of *C. albicans* SC5314 surface area coverage, with both categories being significantly lower than the P120 (Pn $P \leq 0.0078$, P600 $P \leq 0.0001$), P1200 (both comparisons $P \leq 0.0001$), and P2500 (both comparisons $P \leq 0.0001$) surfaces. In addition, P120 surfaces had significantly lower *C. albicans* SC5314 mean surface area coverage than the P2500 surfaces ($P \leq 0.003$).

Candida albicans ΔALS3 had similar patterns of surface area coverage between the roughness categories at 24 h compared with 90 min (Figure 3.10 and Figure 3.8). At 24 h, decreasing *C. albicans* ΔALS3 surface area coverage was evident from Pn to P120 to P600 (22.8%, 15% and 4.9%). The surface area coverage of *C. albicans* ΔALS3 increased from P600 to P1200 to P2500 (4.9%, 9.1% and 23.5%, respectively). The P600 surfaces had significantly lower surface coverage by *C. albicans* ΔALS3 compared with Pn, P120 and P2500 surfaces ($P \leq 0.0001$ for all comparisons). P1200 surfaces also had significantly lower *C. albicans* ΔALS3 on the surfaces compared with Pn ($P \leq 0.0014$), P120 ($P \leq 0.0199$) and P2500 ($P \leq 0.0005$). Pn and P120 surfaces were not significantly different from

each other in terms of *C. albicans* ΔALS3 coverage after 24 h ($P \leq 0.9999$), as was the case with P600 and P1200 surfaces ($P \leq 0.3165$).

The 24 h surface area coverage of *C. albicans* SC5314 and *C. albicans* ΔALS3 was compared. *Candida albicans* SC5314 showed significantly higher surface coverage than the *C. albicans* ΔALS3 on the P120 ($P \leq 0.0249$), P1200 ($P \leq 0.0001$), and P2500 ($P \leq 0.0001$) surfaces (Table 3.3). The P600 surface had the same pattern of higher coverage by *C. albicans* SC5314 compared with *C. albicans* ΔALS3, but this was not significant ($P \leq 0.0582$).

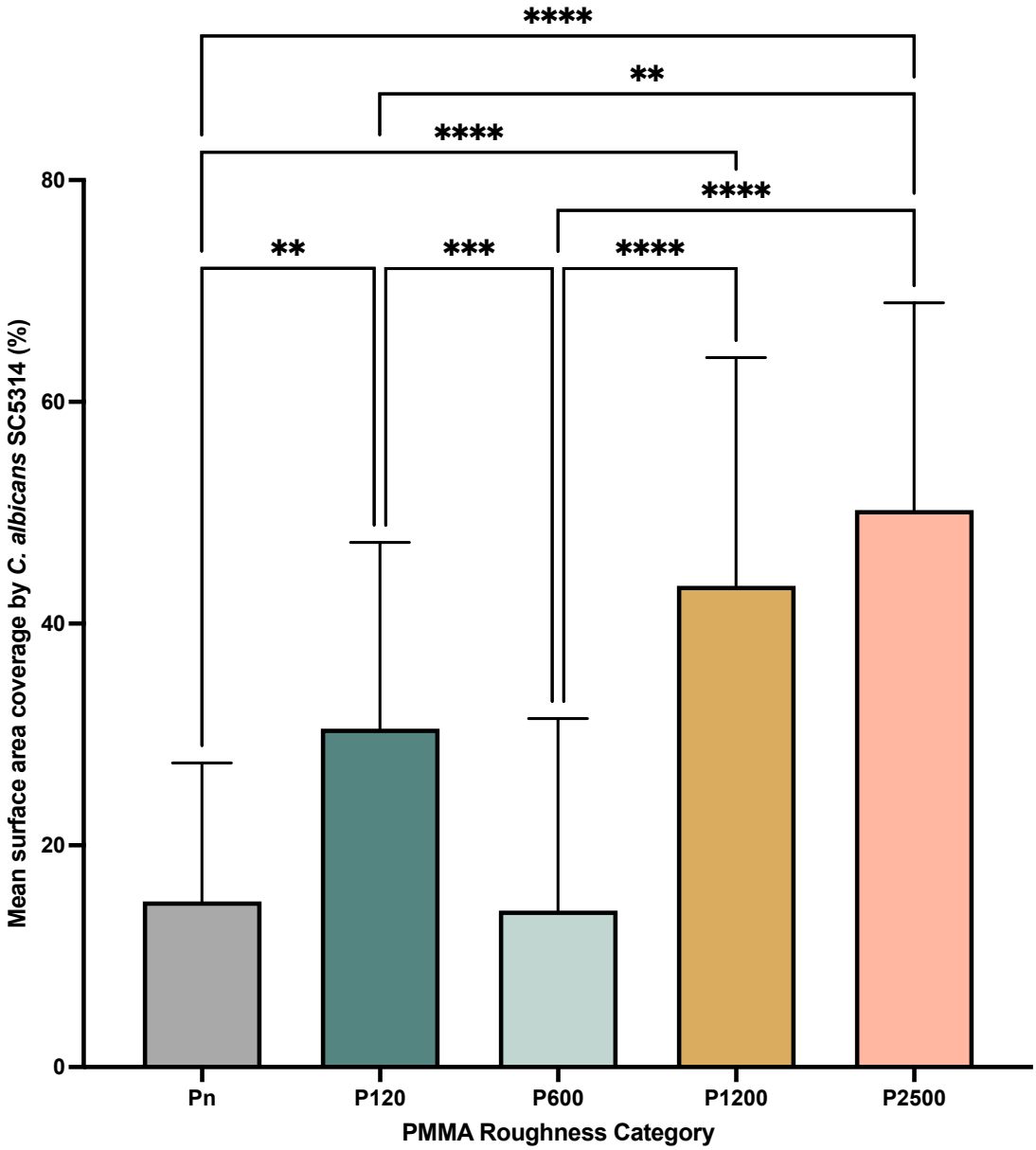

Figure 3.9. Mean surface area coverage (%) by *C. albicans* SC5314 on each polymethyl methacrylate (PMMA) roughness category after 24 h incubation. *C. albicans* SC5314 was added to the surface of artificial saliva preconditioned PMMA coupons from each roughness category and incubated for 90 min. Fluorescence microscopy was used to obtain images that were analysed to obtain the area of surface coverage by *C. albicans.* Data presented as mean ± standard error of the mean. Each category n = 45. Statistical significance was determined using Kruskal-Wallis (H (4) = 93.25, $P \leq 0.0001$) with Dunn's post-hoc test. ** indicates $P \leq 0.01$. *** indicates $P \leq 0.001$. **** indicates $P \leq 0.0001$

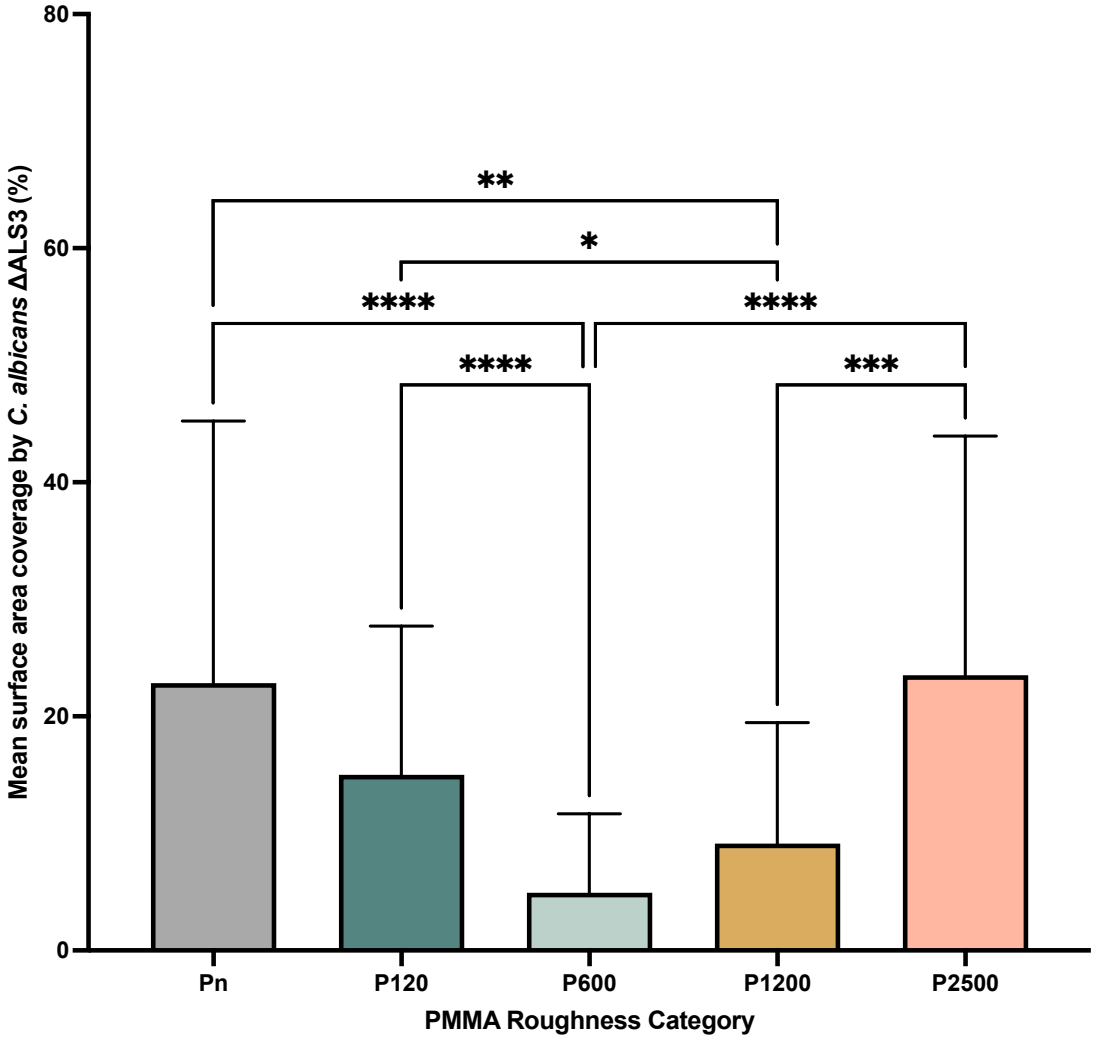

Figure 3.10. Mean surface area coverage (%) by *C. albicans* ΔALS3 on each polymethyl methacrylate (PMMA) roughness category after 24 h incubation. *C. albicans* ΔALS3 was added to the surface of artificial saliva preconditioned PMMA coupons from each roughness category and incubated for 90 min. Fluorescence microscopy was used to obtain images that were analysed to obtain the area of surface coverage by *C. albicans.* Data presented as mean ± standard error of the mean. Each category n = 45. Statistical significance was determined using Kruskal-Wallis (H (4) = 59.10, $P \leq 0.0001$) with Dunn's post-hoc test. * indicates $P \leq 0.05$. ** indicates $P \leq 0.01$. *** indicates $P \leq 0.001$. **** indicates $P \leq 0.0001$.

3.4. Discussion

The research presented in this chapter sought to determine whether the roughness of acrylic surfaces altered levels of adhesion and biofilm formation by *C. albicans.* A previous review on the effect of substratum topography on microbial retention concluded that effects of surface topography on microbial retention was a complex phenomenon, that was likely affected by hydrophilicity and conditioning films (Whitehead and Verran 2006).

In the present studies, different PMMA surface roughness significantly affected *C. albicans* SC5314 adherence. Higher *C. albicans* adherence was associated with surfaces prepared using abrasive paper of finer grit sizes. Highest adherence was for surfaces abraded using silicon carbide paper of grit size P2500 (equivalent to 8.4 ± 0.5 μm grit diameter). This diameter was most comparable to the typical size of a *C. albicans* yeast, which has a mean size of 6.6 μm (Mukaremera et al. 2017). It is readily conceivable that retention of *C. albicans* yeast would be highest in the P2500 surface topography based on relative pore sizer and physical entrapment. Materials with larger topographical irregularities would be less likely to physically entrap yeast cells. This view was supported by previous research, where a strong correlation has been found between PMMA surface roughness and adherence of *C. albicans* (Murat et al. 2019). Additionally, adherence of cells to a surface was dependent on the comparative cell size and the topological feature size (Whitehead and Verran 2006). *Candida parapsilosis* exhibits variability in cell length and there was a strong correlation between its cell length and adhesion to acrylic surfaces (Panagoda and Samaranayake 1998). Adherence of rod-shaped bacteria on stainless steel surfaces has also revealed that rougher and flatter surfaces led to increased retention and that bacterial cells were retained within surface features a similar size to the cells (Medilanski et al. 2002).

Candida exhibit high intra-species variation in adhesion which may be attributed to differences in cell length, their ability to exhibit polymorphism and relative cell hydrophobicity (Panagoda et al. 1998). Of note is that there is a reported correlation between the presence ALS3 and the hydrophobicity of filamentous forms of *C. albicans*. which has been attributed to hydrophobic TR domains (Beaussart et al. 2012). This could have affected the adherence of C. *albicans*

ΔALS3 relative to that of the wildtype *C. albicans* SC5314. Interestingly, *C. albicans* SC5314 and *C. albicans* ΔALS3 did not exhibit the same pattern of responses to different surface categories for three of the categories at the 24 h timepoint. After 24 h, biofilm development of *C. albicans* SC5314 produced a similar profile of adherence as for 90 min and for 24 h adherence of *C. albicans* ΔALS3. The P120 category differed by having higher *C. albicans* surface coverage relative to P600 surfaces. This finding contradicted *in vitro* and in clinical studies that reported increasing roughness associated with increased adherence (Quirynen and Bollen 1995; Radford et al. 1998; Taylor et al. 1998; Pereira-cenci et al. 2008; Zamperini et al. 2010). However, when assessing a highly polymorphic species such as *C. albicans* this is perhaps understandable. Although previous studies reported that surface roughness was the single most important adherence parameter, other factors such as the dimensions of surface features, hydrophobicity and charge will also contribute (Quirynen and Bollen 1995; Hilbert et al. 2003; Verran et al. 2010)

Although there was an association between *C. albicans* SC5314 adherence and biofilm levels with the diameter of the grit used to create surfaces, this did not correspond to the measured Ra values of mean surface roughness. All surface roughness measurements, with the exception of P2500, as determined by the profilometer, and for P600 as measured by AFM, were too small for retention of an mean yeast cell size (6.6 μm (Mukaremera et al. 2017)). It is important to note that *C. albicans* cell size is variable, especially when consideration is given to its polymorphic properties. *Candida albicans* yeast can transform to hyphal and pseudohyphal (elongated yeast) forms. The presence of a range of fungal unit sizes and shapes might allow for retained organisms to subsequently grow along surface imperfections via thigmotropism. Thigmotropism by *C. albicans* is when the direction of growth responds to contact with surface topography. This in turn would potentially increase surface area contact and protection from any shear forces (Watts et al. 1998; Brand et al. 2007; Williams et al. 2011; Gow and Yadav 2017).

Since the Ra of the acrylic surfaces were typically smaller in size to average size of the cells this might account for the fact that increased roughness did not result in an associated increase in adherence. Taylor et al. (1998) reported that roughened cobalt-chromium alloy and dental acrylic resin surfaces had greater retention of *C. albicans* than smoother surfaces. *Candida albicans* had increased

retention on surfaces when the Ra value increased from 0.15 to 3.53 μm. It was stated that the *C. albicans* cells required larger surface defects than the oral bacteria tested to enhance retention based on relatively larger cell size (4 μm) of *Candida*. Other studies have confirmed these findings by identifying threshold roughness values, and increasing roughness beyond these reduces the amount of protection from shear forces and enhances the cleanability of the surfaces (Pier-Francesco et al. 2006; Verran et al. 2010).

Adherence and biofilm coverage by *Candida albicans* ΔALS3, and biofilm coverage by *C. albicans* SC5314 wildtype showed similar hierarchical profiles based on AFM determined surface roughness. However, these findings were opposite to those anticipated from the profilometer data. It was evident that with higher AFM Ra values, reduced *C. albicans* ΔALS3 surface coverage for adherence and biofilm development occurred. Compared to profilometer Ra values, *C. albicans* ΔALS3 surface colonisation supported previous studies where increased roughness enhanced adherence and biofilm levels. The discrepancy with the profilometer data could be that the surface roughness was determined on a much larger scale whilst the AFM measurements related to an 100 μm^2 area might be a more appropriate scale to measure as this is the roughness that *C. albicans* will interface with (Aguayo et al. 2017). In addition, AFM measurements could only be obtained in areas suitable for the cantilever, creating a bias in the area selected for measurement, which could have avoided areas of large variability in roughness.

Previous research has indicated that hydrophobicity and surface-free energy are important factors in *Candida* adherence (Panagoda et al. 1998; Kang et al. 2013). However, other research states there is no correlation between hydrophobicity and the adherence of *C. albicans* on PMMA (Murat et al. 2019).The observed changes in adherence and biofilm development presented here were unlikely to be attributed to hydrophobicity which was not significantly different between surfaces. In addition, all experiments were conducted using AS pre-conditioned PMMA, which may standardise the surface-free energy of the materials (Sipahi et al. 2001; Kang et al. 2013).

Ra is a value widely used to represent average surface roughness. This measurement involves consideration of surface peaks and troughs and the deviation from the mean line. It is the average of these values that determines the Ra, which is usually reported in μm. Higher deviations are associated with rougher surfaces and where the Ra is small, the surface is considered smooth. Ra values are useful to assess the general roughness of a surface. However, they are derived from an average of a given length or area, which means the Ra does not measure the entire surface, which is most often highly variable. Therefore using Ra as a roughness indicator might omit important surface features and reduce accuracy of measurement in the presence of large 'peaks and troughs' (Whitehead and Verran 2006). While Ra is useful to provide an indication of surface roughness, it does not measure the size and characteristics of topological features which are important in microbial retention (Taylor et al. 1998; Whitehead et al. 2005; Whitehead and Verran 2006). Measuring surface roughness is dependent on the area and scale measured and various methods can be employed. For example, methods include physical stylus profilometry, laser/optical profilometer, and AFM (Verran et al. 2001; Mahross et al. 2015; Cavalcanti et al. 2016a; Aguayo et al. 2017). Profilometer measurements used in this study were from a mean average of 5 mm transects and the AFM measurements of a 100 μm^2 area. These methods were not in agreement over which surfaces were rougher which likely relates the scale of measurement which limits direct comparisons. Both the stylus profilometer and AFM measurements were dependent on the instruments being able to maintain contact with the surface throughout the measurement reading. If there were large variations and topological features present, contact could be disrupted. To overcome this, a laser profilometer could be used instead as it is a non-contact method. The AFM cantilever tip had difficulty maintaining surface contact for some measurements, which meant alternative areas were required to be measured and this was evident when measuring the P2500 surfaces. Therefore, the AFM measurements would have an innate bias for areas, based on where the cantilever tip could record measurements of the full area. Studies that have explored relationships between microbial retention and surface roughness use different methods of surface abrasion, which complicates comparison of studies.

To conclude, the level of PMMA surface roughness was found to affect *C. albicans* adherence and biofilm coverage. This effect was not, however, a continuous one that was associated with the measured Ra. The results indicate the optimum level of surface roughness and topological features that reduce *Candida* adherence and were likely dependent on relative cell size. Knowing the surface roughness that promotes retention of problematic organisms such as *C. albicans* could inform denture manufacturers in their denture developmental processes. However, minimising unnecessary roughening of denture surfaces, and the appropriate use of denture maintenance regimes with non-abrasive cleansing methods would still be important factors to limit *Candida* colonisation.

CHAPTER 4: Effect of Selected Oral Bacteria on *Candida albicans* within Biofilms

4.1. Introduction

Numerous environmental niches exist in the oral cavity that are suitable for colonisation by microorganisms. Examples include the hard non-shedding enamel surfaces of teeth, the mucosal surfaces of the hard and soft palates, the tongue, the buccal mucosa and any introduced orthodontic and prosthodontic appliances. Maintaining stable microbial communities at these sites is essential for microbial persistence (Wright et al. 2013). The distinct environmental conditions encountered at different oral colonisation sites leads to a diverse and highly complex microbial network that play a vital role in the regulation of both oral health and disease.

In addition, the oral microbial community has been shown to influence the local environment to improve its own survival needs and this in turn reduces the likelihood of colonisation by exogenous microorganisms that may be pathogenic (He et al. 2014). Competitive exclusion of non-oral microorganisms occurs from a range of mechanisms along with the continuous recruitment of beneficial oral microorganisms. Kuramitsu et al. (2007) outlined five distinct types of competitive interactions between oral bacteria which included nutrient competition, synergy, antagonism, neutralisation of virulence factors and interference of signalling mechanisms. Inter-species interactions are instrumental to the maintenance of the microbial community via specific inter-microbial adhesion, cell signalling through cell-to-cell contact, metabolic interaction and quorum sensing (Wright et al. 2013). This complex system in a ‘healthy mouth’ is termed normobiosis and occurs when interactions are self-regulated and balanced (Hooks and O’Malley 2017; Baraniya et al. 2022). A change to this balance may mean that self-regulation no longer occurs and certain groups of microorganisms become disproportionate in their number or activity, thus resulting in dysbiosis. Dysbiosis is the state that can lead to occurrence of oral diseases including dental caries, periodontal diseases and candidosis (Zaura et al. 2017; Bostanci et al. 2021).

To elucidate the relationships that occur between microbial species in these complex microbial networks first requires an understanding of how smaller groups can affect each other. In the case of *Candida albicans* and associated oral infections, the importance of oral bacteria in preventing infection is clearly evident

in *Candida*-associated denture stomatitis (Williams et al. 2011). For example, *S. salivarius* has exhibited the ability to reduce symptoms of denture stomatitis and reduce counts of *C. albicans in vivo* (Passariello et al. 2020). In contrast, *in vitro* interactions between oral bacteria and *C. albicans* have been shown to promote initiation of a more pathogenic *C. albicans* phenotype that would conceivably be more likely to lead to infection when translated to the *in vivo* situation (Cavalcanti et al. 2016a; Morse et al. 2019). For example, the co-culture of *C. albicans* with specific oral bacteria; *Streptococcus sanguinis, Streptococcus gordonii, Actinomyces viscosus* and *Actinomyces odontolyticus,* on denture acrylic surfaces leads to heightened virulence of *C. albicans* in terms of upregulation of virulence-associated genes and an increase in hyphal morphology, which is considered the more virulent morphological form (Cavalcanti et al. 2016a; Morse et al. 2018).

Oral bacteria produce a range of signalling factors that influence biofilm formation and morphogenesis of *C. albicans* to more filamentous and virulent forms (Wright et al. 2013). For example, biofilms of *C. albicans* with *Streptococcus sanguinis* and *S. mutans* have led to the up-regulation of *C. albicans* virulence genes involved in adhesion (Als3), production of hydrolytic enzymes (Sap2 and Sap6), and hyphal development (Hwp1) (Cavalcanti et al. 2016a; Morse et al. 2018). Significantly increased hyphal production (which is an important virulence factor) was also shown when *C. albicans* was grown in polymicrobial biofilms containing *S. sanguinis, S. gordonii, A. viscosus* and *A. odontolyticus* (Morse et al. 2018). Antagonism between *Streptococcus* species such as *S. mutans, S. gordonii* and *S. sanguinis* often results in elevated levels of hydrogen peroxide, especially in more aerobic conditions, and has been shown to induce *C. albicans* hyphal development (Kreth et al. 2005; Nasution et al. 2008).

Interactions between several *Streptococcus* species and *C. albicans* have been studied, however the relationships are still not fully understood. Research into interactions between *S. gordonii* and *C. albicans* has been undertaken with the aim of understanding both oral, and vaginal health (Silverman et al. 2010; Pidwill et al. 2018). One well-explained mechanism of the interaction between these two species that promotes co-colonisation relates to a physical receptor-mediated interaction. This occurs between *C. albicans* agglutinin-like sequence 3 (Als3) and SspA and SspB proteins of *S. gordonii* (Bamford et al. 2009; Silverman et al. 2010;

Bamford et al. 2015). The role of Als3 in the interaction has been supported through use of an Als3 deleted mutant *C. albicans* strain which was unable to form biofilms and did not facilitate hyphal adhesion of *S. gordonii* (Silverman et al. 2010; Pidwill et al. 2018). These results were supported by studies involving expression of the *C. albicans* Als3 protein in *S. cerevisiae*, which facilitated *S. gordonii* binding to Als3 expressing *Saccharomyces cerevisiae* (Silverman et al. 2010). Synergy between *C. albicans* and *S. gordonii* has also been shown to result in increased biofilm biomass and increased hyphal morphology due to both physical interaction and diffusible chemical signals during biofilm development (Bamford et al. 2009). Diffusible signals included autoinducer 2 from *S. gordonii* which was found to contribute to suppression of the *Candida* quorum sensing molecule farnesol, which inhibited hyphal formation and biofilm production, meaning that the presence of *S. gordonii* increased both *Candida* biofilm and hyphae (Bamford et al. 2009).

Understanding how *C. albicans* interacts with and responds to the presence of oral streptococci that frequently co-exist with the fungus at oral sites would provide insight into better understanding of the risk factors for oral disease and potentially inform improved interventions and mechanisms of disease prevention.

4.1.1. Aims and Objectives

The primary aims of the research in the research in this chapter were to:

1. Identify the effect of specific oral *Streptococcus* species in dual species biofilms on *C. albicans* biofilm formation and hyphal transformation.
2. Investigate potential mechanisms of bacterial and *C. albicans* interaction, by assessing whether modulation in *C. albicans* responses occurs through chemical effects or physical (cell-to-cell) interaction.

4.2. Materials and Methods

4.2.1. Selection and culture conditions of microorganisms

4.2.1.1. Candida albicans

Candida albicans SC5314 was selected for this research given the previous extensive study of this strain and the availability of specific mutant variants (Zhao et al. 2006; Silverman et al. 2010; Pidwill et al. 2018). *Candida albicans* SC5314 UB1941 *Δals3*/*als3* (ΔALS3) was also used. Details of these strains and culture conditions are provided in section 2.2.1 and section 3.2.1. All *Candida* cultures were standardised prior to use, unless otherwise specified, using a spectrophotometer (DiluPhotometer™, Implen, Westlake Village, CA, USA) to an OD_{600} of 1 ± 0.05 (equivalent to 10^6 cells/mL) in Yeast Nitrogen Base (YNB) without amino acids (BD Difco™) supplemented with 0.67 g D-glucose, 0.1 mg L-histidine, 0.2 mg L-methionine and 0.2 mg L-tryptophan per L (Thermo-Fisher Scientific).

4.2.1.2. Bacterial species and strains

Four bacterial species, *S. sanguinis, S. gordonii, S. salivarius,* and *S. mutans* (Table 4.1) were used as potential modulators of *C. albicans* SC5314 growth, biofilm development and morphological changes. Experiments were conducted using dual- and single-species biofilms.

Table 4.1. *Streptococcus* species used to investigate interactions and specific effects on *Candida albicans* SC5314. ^{T} indicates the strain is a designated type strain.

Bacterial species	Strain reference	Culture conditions
***Streptococcus sanguinis*^{T}**	NCTC 7863	Facultative anaerobe, 37°C, 5% (v/v) CO_2
***Streptococcus gordonii*^{T}**	NCTC 7865	Facultative anaerobe, 37°C, 5% (v/v) CO_2
***Streptococcus salivarius*^{T}**	DSM 20560	Facultative anaerobe, 37°C, 5% (v/v) CO_2
***Streptococcus mutans*^{T}**	DSM 20523	Facultative anaerobe, 37°C, 5% (v/v) CO_2

4.2.1.2.1. Bacterial culture conditions and standardisation of inocula

Facultative anaerobic bacterial species (Table 4.1) were cultured on trypticase soy agar (TSA; Sigma) for 24 h at 37°C in 5% (v/v) CO_2. Culture stocks of each strain were stored at -80°C and streak plates from these were retained at 4°C for up to 4 weeks. For liquid cultures, 10 mL of trypticase soy broth (TSB; Sigma) was inoculated with 1-2 colonies and incubated at 37°C in 5% (v/v) CO_2 for 16-18 h.

Prior to inoculation for experiments, 16-18 h cultures were centrifuged at 1700 x *g* for 10 min. The supernatant was discarded and 10 mL of YNB was added to the cell pellet, which was resuspended by gentle repeated pipetting. The culture was then standardised to an optical density of 0.5 OD_{600} (± 0.05) (equivalent to approximately 5 x 10^7 cells/mL), using a spectrophotometer (DiluPhotometer™, Implen, Westlake Village, CA, USA).

4.2.1.2.2. Confirmation of *Streptococcus* species identification

Bacteria were from previous culture stocks stored at the School of Dentistry, Cardiff University, except for *S. sanguinis* NCTC 7863 and *S. gordonii* NCTC 7865 which were purchased from Public Health England culture collections (Salisbury, UK).

Gram staining, followed by light microscopy imaging using an Olympus Ax70 upright microscope, and PAX-it imaging software (PAX cam) was used to confirm that the cultures were Gram-positive with a coccus morphology. Two colonies were used to produce streak plates on Mitis Salivarius Agar (MSA), and these were incubated in 5% (v/v) CO_2 at 37°C for 24 to 48 h. On MSA, *S. salivarius* colonies were presumptively identified as large, pale-blue, mucoid colonies with a glistening appearance. *S. mutans* formed raised, convex, undulate, opaque, pale-blue colonies that were granular in appearance. *S. sanguinis* also generated raised colonies, but these were smooth and embedded in the agar. A colony from each species was also added to hydrogen peroxide to confirm a negative catalase reaction.

4.2.2. Preparation of denture material as the substratum for biofilm growth.

4.2.2.1. Production of polymethyl methacrylate (PMMA) coupons

Polymethyl methacrylate (PMMA) is a thermoplastic used to construct denture prostheses and orthodontic retainers. PMMA was used as the solid substratum to grow mono- and polymicrobial biofilms. PMMA coupons were prepared as described in section 2.2.2.1.

4.2.2.2. Preconditioning of PMMA coupons in artificial saliva

Artificial saliva (AS) was prepared based on a previously published composition (Cavalcanti et al. 2014; Morse et al. 2019) and used to precondition the PMMA coupons as described in section 2.2.2.2.1. AS was selected for preconditioning the acrylic to provide a more standardised surface with closer similarity to that encountered *in vivo*.

4.2.3. Effect of *Streptococcus* species on *Candida albicans* in biofilms

4.2.3.1. Effect of bacteria on *Candida albicans* adherence and biofilm formation on PMMA coupons

The standardised preparations of *C. albicans* and each separate bacterial species were mixed at a 2:1 ratio (*Candida:*Bacteria). *C. albicans* without bacteria, and bacteria only preparations were also used at the same total volume as the mixed samples. Preparations were incubated at 37°C in a 5% (v/v) CO_2 incubator for 1.5 h to facilitate planktonic interaction. After incubation, a 100-µL volume of microbial suspension was then added to the appropriate wells of the 24-well plate that contained 1900 µL of YNB and a sterile PMMA coupon preconditioned with AS. Coupons were either singly inoculated with *C. albicans,* the bacterial species, or with dual species combinations of *C. albicans* with each bacterial species. Negative controls to ensure absence of contamination contained 100 µL of YNB and were devoid of microorganisms. The 24-well plates were incubated at 37°C in 5% (v/v) CO_2 for 24 h and 72 h. For 72 h incubations, a 2 ml volume of YNB medium was changed at 24 h intervals. This was done by careful pipetting to the side of the PMMA coupon. After incubation, analysis included enumeration of recovered colony forming units (CFU) from the coupon surface and confocal laser scanning microscopy (CLSM) to ascertain abundance and morphologies of *C. albicans*. Coupons were placed in PBS for the number of recovered CFU/mL to be determined by culture of serial dilutions on appropriate agar media. Selected PMMA coupons were fixed by gentle immersion for 15 min in 10% (v/v) formalin buffered saline (Sigma-Aldrich) prior to being transferred to 1 mL PBS and stored at 2-5°C overnight (14-15 h). Fixed specimens were subsequently imaged by CLSM using peptide nucleic acid-fluorescence *in situ* hybridisation (PNA-FISH) in combination with propidium iodide as a counterstain.

4.2.3.2. Measurement of recovered colony forming units (CFU) from dual species biofilms after 24 h and 72 h

To determine the recovered CFU/mL from biofilms of the *C. albicans* and *Streptococcus* species, an adapted Miles and Misra method (Miles *et al.* 1938) was

used (Figure 4.1). Each coupon was placed in 2 mL of PBS and vortex mixed for 2 min. The PBS was then serial decimally diluted and 5 µl of the diluted preparations plated on to agar media as outlined in Figure 4.1, with each demarked column designated for a specific dilution. The agar plate was held vertically to allow the sample to run down the plate to a demarcation indicated by the dashed line (Fig. 4.1). Enumeration of *C. albicans* CFU was on SDA (Lab M, Heywood, UK) supplemented with 1 mg/mL chloramphenicol (Thermofisher). Enumeration of *Streptococcus* species was on TSA containing 250 U/mL Nystatin (Thermofisher). The plates were dried horizontally prior to inversion and incubation. Incubation of *Streptococcus* species was in 5% (v/v) CO_2 at 37°C for 24 h. *C. albicans* was similarly incubated, but without addition of 5% (v/v) CO_2. Resultant colonies were enumerated, and the number of recovered CFU/mL determined.

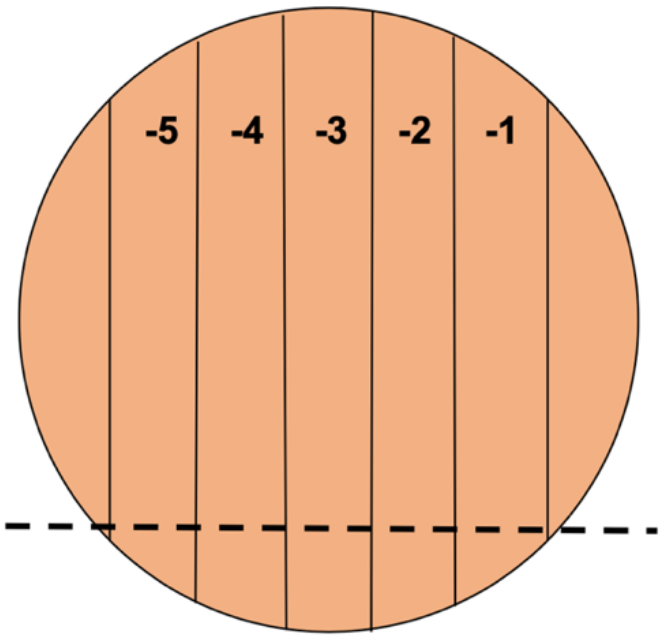

Figure 4.1. Schematic diagram of an agar plate used for the adapted Miles and Misra method. (Miles et al. 1938) The agar plate was divided into columns for different dilutions to be included on the same plate. The dashed line indicates the furthest point the dilutions were allowed to run, as past this point the samples would spread around the perimeter of the plate and were no longer usable. The indicated numbers represent 10-fold dilutions, and the position of the numbers indicate where the samples were pipetted on the plate.

4.2.3.3. Fluorescence microscopy of PMMA coupons after CFU/mL recovery

After the coupons were used to recover the CFU/mL of *C. albicans,* an Olympus Ax70 upright fluorescence microscope was used to examine remaining cells on the surface of the coupon. Live/Dead BacLight Bacterial Viability kit (Thermofisher) was used to stain the cells remaining on the PMMA surface. The live/dead filter cube was used to visualise the cells and PAX-it imaging software (PAX cam) employed to obtain example fluorescence micrographs.

4.2.3.4. Peptide nucleic acid-fluorescence *in situ* hybridisation (PNA-FISH) analysis of dual species biofilms.

The methodology for PNA-FISH for the biofilms was adapted from approaches used in the Microbial Diseases Research Group of the School of Dentistry at Cardiff University and as previously published (Perry-O'Keefe et al. 2001; Cavalcanti et al. 2014; Kim and Brehm-Stecher 2015; Morse 2017; Sands et al. 2017). A custom PNA probe for *C. albicans* was obtained (Cambridge Research Biochemicals Discovery, UK) using the sequence [N-terminus OO-`cgg cca taa aga cct` C-terminus] which had previously been published and optimised by Kim and Brehm-Stecher (2015). This probe was tagged with 5-carboxyfluorescein (FAM) at the N-terminus.

Lyophilised PNA probe stocks were aseptically reconstituted in nuclease-free water with gentle pipetting. To ensure complete probe suspension the preparations were heated to 50°C in a water bath for 5 min as recommended by the manufacturer. Aliquoted stocks of 200 µL at 10 µM were created and stored in the dark at -20°C. During experiments, probes were also protected from light as much as possible, including the use of foil covered microcentrifuge tubes. Stocks were diluted to a working of concentration of 500 nM using PNA hybridisation buffer (20 mM Tris-HCl (pH 9.0), 2 mM EDTA, 100 mM NaCl, and 0.5% SDS) (Perry-O'Keefe et al. 2001; Kim and Brehm-Stecher 2015). Fifty µL of the PNA hybridisation buffer containing the probe was added to the surface of the formalin fixed PMMA coupon and incubated at 55°C for 1 h in a humidified box in a hybridisation oven (SI30H, Stuart). The coupons were then flooded with 200 µL of pre-heated PNA wash buffer (10 mM TRIS (pH 8), 1 mM EDTA) and incubated 15 min at 55°C. This wash step

was conducted twice, after which the coupons were retained on glass slides using Blu Tack (Bostik) which was required to immobilise the sample for imaging. Vectashield® Antifade Mounting Medium (25 µL) with propidium iodide (PI) (Vectorlabs, Orton Southgate, UK) was applied to the coupon surface and enclosed with a 13 mm diameter circular borosilicate glass coverslip (VWR). PI functioned as a counterstain to visualise bacteria.

4.2.3.5. Effect of bacterial spent culture medium on *C. albicans* in biofilms.

4.2.3.5.1. Spent media collection.

Bacterial species were cultured for 16-18 h in 15 mL of TSB at 37ºC with 5% (v/v) CO_2 and the cultures were centrifuged (1200 x *g* for 10 min) to pellet cells. The supernatant was removed and 15 mL of YNB added for a second incubation for 24 h at 37ºC with 5% (v/v) CO_2. After 24 h incubation the cultures were centrifuged again (1200 x *g* for 10 min), and the supernatant collected and filtered using a Minisart™ NML Syringe Filter (Sartorius) with a pore size of 0.2 µm before being stored at 2- 4ºC until needed. This process was also performed for *C. albicans* SC5314, which served as a spent medium control.

4.2.3.5.2. Effect of spent medium on *C. albicans* in biofilms.

PMMA coupons preconditioned in AS were rinsed with dH_2O and aseptically added to the wells of 24-well plates. A 1900 µL volume of 24 h spent medium was added to each well and this was done in triplicate for each species. YNB medium was used as a positive control. One hundred µl of standardised (OD_{600nm} 1 ± 0.1) inoculum was added to each well. Incubation was for 24 h and 72 h at 37ºC in 5% (v/v) CO_2. Coupons were aseptically transferred to a new 24 well plate that contained 1 mL of 10% (w/v) neutral buffered formalin solution for 15 min, before being transferred to 24 well plates containing PBS. These coupons were then stored at 2- 4ºC prior to imaging. A drop of calcofluor white 50% (v/v) solution (Sigma) was added to the surface of the PMMA coupon, which was embedded in Blu Tack® (Bostik) to ensure the coupons were immobilised for imaging. The coupon surface was sealed with a 13 mm diameter circular borosilicate glass coverslip (VWR) in readiness for CLSM.

4.2.3.6. Confocal Laser Scanning Microscopy (CLSM) of dual species and spent media samples.

CLSM was performed using a Zeiss LSM880 Airyscan Fast system upright confocal microscope controlled by Zen Black software (Zen 2.3 SP1 FP3 (black) Version: 14.0.20.201) at the Cardiff University Bioimaging Hub. The excitation spectra and emission filters used for the dual species and spent media experiments are presented in Table 4.2. Dual species experiments utilised the 5-carboxyfluorescein (FAM) fluorophore for *C. albicans* and propidium iodide as a counterstain. For spent media samples, calcofluor white was used for *C. albicans* staining. Three-dimensional Z-stacks were obtained using the Plan-Apochromat 63x/1.4 oil objective lens from five randomly selected areas of each coupon at intervals of 0.43 µm with a scanning resolution of 1024 x 1024 pixels and x4 line averaging.

Table 4.2. Excitation and emission spectra for dual species and spent media experiments confocal laser scanning microscopy (CLSM)

Target Species	Fluorophore/ Stain	Excitation Wavelength (nm)	Emission Frequency (nm)
***Candida albicans* SC5314**	5-carboxyfluorescein (FAM)	493	517
***Candida albicans* SC5314**	Calcofluor White	380	475
***Streptococcus* species**	Propidium Iodide	535	617

4.2.3.7. Confocal Laser Scanning Microscopy (CLSM) image analysis

CLSM Z-stacks were converted into maximum intensity projection TIFF files using FIJI ImageJ Software (Version:2.0.0-rc-69/1.52p Build: 269a0ad53f). The software processed the Z-stacks slices into a single 2D image, which reflected a top-down view of the surface and was then used for analysis through the green channel. The percentage area coverage by *C. albicans* on the coupon surface (x63 objective lens, maximum intensity projection files) was assessed. A macro was used to

convert the files to 8-bit, thresholding using “moments” and the percentage coverage of the field of view determined using the set measurements area. The mean percentage area coverage was determined using the output of five fields of view per coupon and across the replicates.

The area of *C. albicans* filamentous forms including true hyphae, pseudohyphae and elongated cells was determined using the freehand drawing tool in FIJI ImageJ software to draw around the filamentous forms and using the ‘Measure’ function to calculate the area within the drawn areas of each field of view. The area measurement was then converted into a percentage of the frame and averaged between the replicates.

Statistical analyses of the results from the CLSM images for percentage area coverage and the area occupied by filamentous forms was determined using One-Way ANOVA with Tukey post-hoc test to compare means between groups or Kruskal-Wallis test with Dunn’s test for multiple comparisons depending on whether the data was normally distributed. Prism 9 for macOS (GraphPad Prism 9.4.0 (453) GraphPad Software, San Diego, California USA, www.graphpad.com) software was also used for statistical analysis and construction of graphs.

4.2.3.8. Interactions between *Streptococcus* species and *Candida albicans* filamentous forms

Following 16-18 h of growth, microbial cultures were centrifuged and re-eluted in YNB as previously stated (section 4.2.1). Prior to standardisation of the *Streptococcus* in YNB, 1 mL of 1 mg/mL fluorescein isothiocyanate (FITC) (Thermofisher) solution in carbonate buffer was added to each cell pellet and thoroughly mixed by repeat pipetting. Samples were placed on a tube roller (Starlab, Milton Keynes, UK) ~ 50 rev/min for 30 min at room temperature. Three washes using 5 mL of carbonate buffer and centrifugation at 1200 x *g* for 5 min were undertaken and the supernatant was discarded each time. After the third wash, the pellets were resuspended in YNB and standardised as previously described (section 4.2.1).

The standardised preparation of wild type *C. albicans* SC5314 or *C. albicans* Δ*ALS3*/*ALS3* and the FITC stained bacteria were mixed at a 2:1 ratio. Preparations

were incubated at 37°C in a 5% (v/v) CO_2 incubator for 1.5 h to facilitate interactions. Twenty µL of each sample was added to a microscope slide with 5 µL of calcofluor white (Sigma) 50% (v/v) in water. Fluorescence microscopy was used to image specifically the filamentous forms of *C. albicans* in both the wild-type and mutant samples.

4.2.3.9. Fluorescence microscopy of interactions between *C. albicans* and planktonic cultures of *Streptococcus* species.

Fluorescence micrographs were obtained using an oil immersion lens at x1000 total magnification, on an Olympus Ax70 upright fluorescence microscope, running PAX-it imaging software (PAX cam). A DAPI/Hoechst filter cube was used to image *C. albicans* stained with 50% (v/v) calcofluor white solution (Sigma). The live/dead filter cube was used to image the FITC stained bacteria.

4.2.3.10. Fluorescence microscopy micrograph image analysis

Las X software (Leica) was used to overlay the calcofluor white and FITC stained images for each frame. The area of *C. albicans* filamentous forms including true hyphae, pseudohyphae and elongated cells was determined using the freehand drawing tool in FIJI ImageJ to draw around the filamentous forms and using the 'Measure' function to calculate the area within the drawn areas of each frame. The bacteria that were proximal and therefore associated with the filamentous regions were manually counted. A judgement was made to count bacterial cells in very close proximity to the filamentous forms as the images were a construct of the overlays of two images, and this allowed for slight movement that may have occurred during the overlay process. For each sample, the mean number of bacterial cells per 100 μm^2 of filamentous forms of *C. albicans* was calculated. After determining the data did not exhibit normal distribution, the non-parametric Mann-Whitney U test was used to determine any differences between the wild-type and mutant strains of *C. albicans* for each bacterial species.

4.3. Results

4.3.1. Effect of dual species biofilms on PMMA surfaces on the abundance, surface area coverage and the filamentous morphology of *C. albicans* SC5314 after 24 h and 72 h growth.

The number of colony forming units (CFU) recovered from the PMMA coupons was used to determine the abundance of viable microbial cells (Table 4.3). From the dual species and *C. albicans* single species control biofilms, recovered CFU/mL was determined to assess whether the presence of the individual *Streptococcus* species affected the abundance of *C. albicans* SC5314 after 24 h and 72 h. In comparison to the *C. albicans* single species biofilm after 24 h, a significant increase in recovered CFU/mL of *C. albicans* was found in the biofilms grown with *S. gordonii* ($P \leq 0.0022$), *S. salivarius* ($P \leq 0.0004$) and *S. mutans* ($P \leq 0.0001$) (Figure 4.2). An increase in the *C. albicans* recovered CFU/mL was also observed in dual species biofilms with *S. sanguinis* even though this did not meet the threshold of being statistically significant ($P \leq 0.1639$). In these samples, the mean recovered CFU/mL for *C. albicans* increased from 4.82E+05 CFU/mL in the single species biofilm to 2.51E+07 CFU/mL when grown with *S. salivarius*.

In 72 h biofilms, the mean *C. albicans* recovered CFU/mL was higher for all dual species biofilms compared with the *C. albicans* SC5314 single species biofilm (Figure 4.3). This increase was statistically significant with *S. salivarius* and *S. sanguinis* ($P \leq 0.0279$ and $P \leq 0.0049$, respectively).

After recovery of CFUs, the cells on the PMMA coupons were stained using Live/Dead BacLight Bacterial Viability Kit (Invitrogen™) and imaged using fluorescence microscopy which revealed adhered cells remaining on the surface (Figure 4.4). All coupons still had cells remaining adhered to the PMMA surface after attempted recovery. Very few bacterial cells were observed remaining on the dual species coupons after recovery compared to a large number observed on the bacteria only coupon surfaces. In dual species biofilms, a recovered CFU/mL for the bacterial cells was not obtained due to a lack of growth on the agar plates,

whereas the recovered CFU/mL was determined for the bacterial single species biofilms (bacterial recovered CFU/mL data not presented).

Table 4.3. *C. albicans* recovered colony forming units (CFU)/mL for the 24 h and 72 h timepoints. The mean *C. albicans* recovered CFU/mL and the standard error of the mean (SEM) are presented in the table.

	***C. albicans* SC5314 recovered CFU/mL**			
	24 h		72 h	
	Mean	SEM	Mean	SEM
C. albicans SC5314 only	4.82E+05	5.03E+04	3.02E+06	3.50E+05
C. albicans SC5314 and *S. gordonii*	9.33E+06	2.58E+06	6.22E+06	1.18E+06
C. albicans SC5314 and *S. salivarius*	2.51E+07	1.07E+07	1.04E+07	2.21E+06
C. albicans SC5314 and *S. sanguinis*	3.56E+06	6.48E+05	1.20E+07	2.45E+06
C. albicans SC5314 and *S. mutans*	1.00E+07	1.89E+06	7.11E+06	1.42E+06

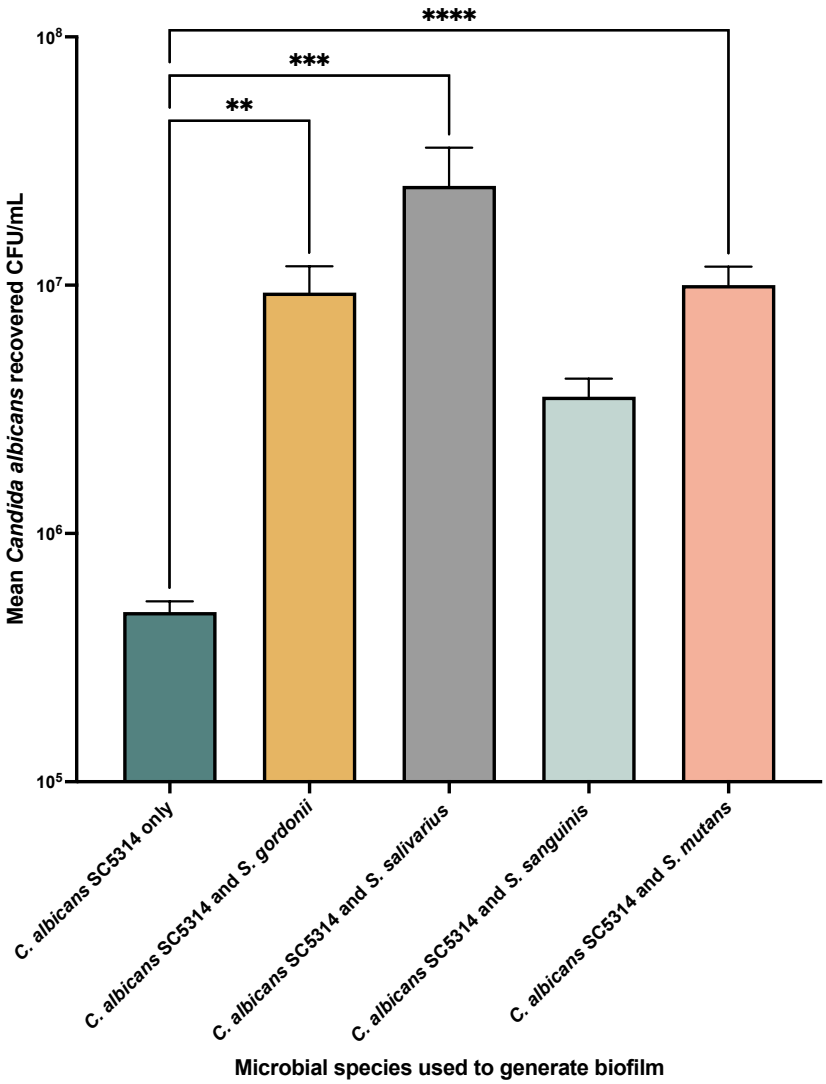

Figure 4.2. *Candida albicans* recovered colony forming units (CFU)/mL from dual species biofilms and a single species *C. albicans* biofilm control after 24 h growth on polymethyl methacrylate (PMMA). Cells were recovered from the PMMA surface of the sample coupons via vortexing in PBS, diluted and grown on SDA plates supplemented with 1 mg/mL chloramphenicol for 24 h. Resultant colonies of *C. albicans* SC5314 were enumerated after 24 h incubation at 37°C. The mean was determined from 3 replicates counted from each of the 3 replicate coupons. Each category n = 9. Data presented as mean ± standard error of the mean. Statistical significance between the biofilms for the amount of *Candida* recovered CFU/mL was determined using the non-parametric Kruskal-Wallis test (H (4) = 26.38, $P \leq 0.0001$) with Dunn's test for multiple comparisons the results of which are annotated on the graph. * $P \leq 0.05$. ** $P \leq 0.01$. *** $P \leq 0.001$. **** $P \leq 0.0001$

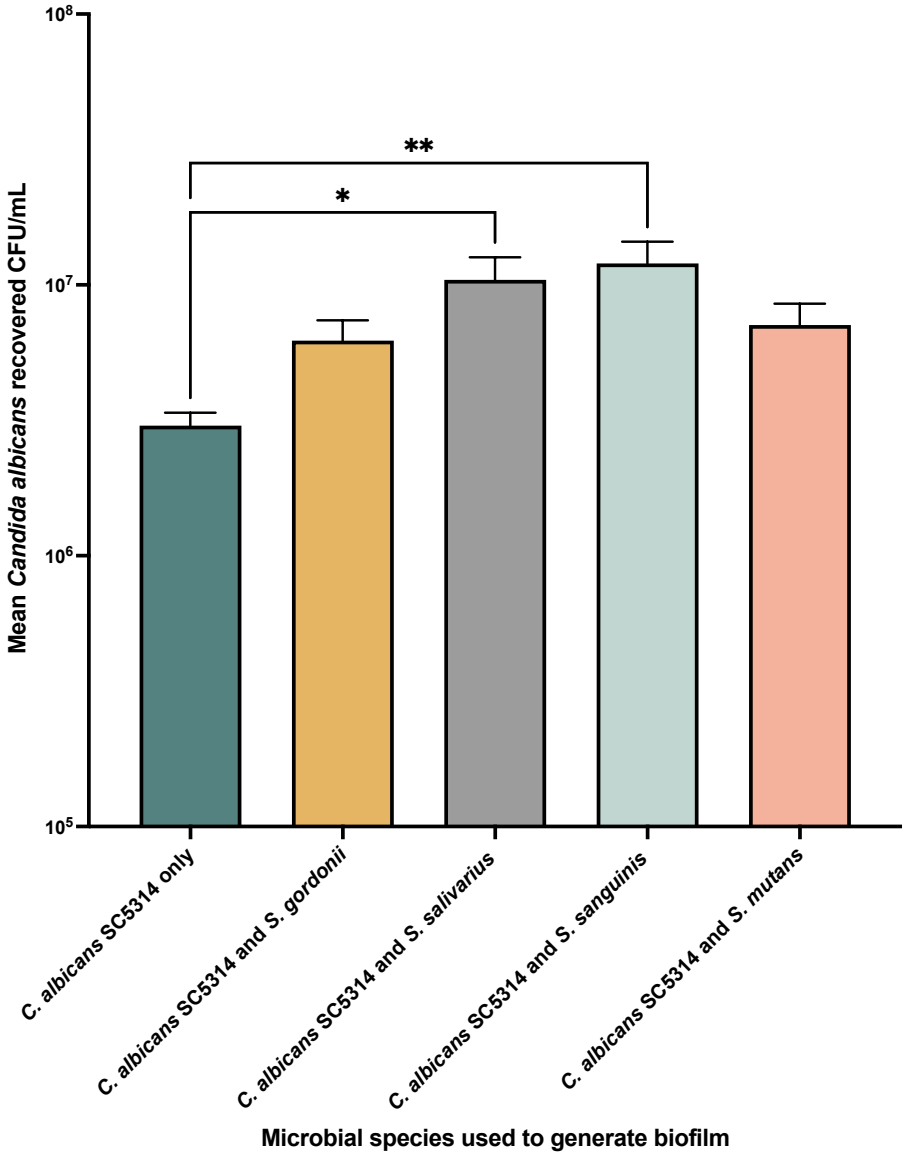

Figure 4.3. *Candida albicans* recovered colony forming units (CFU)/mL from dual species biofilms and a single species *C. albicans* biofilm control after 72 h growth on polymethyl methacrylate (PMMA). Cells were recovered from the PMMA surface of the sample coupons via vortexing in PBS, diluted and grown on SDA plates supplemented with 1 mg/mL chloramphenicol for 24 h. Resultant colonies of *C. albicans* SC5314 were enumerated after 24 h growth incubation at 37°C. The mean was determined from 3 replicates counted from each of the 3 replicate coupons. Each category $n = 9$. Data presented as mean ± standard error of the mean. Statistical significance was determined using one-way ANOVA test (F (4, 40) = 4.382, $P \leq 0.0049$) with Tukey's test for multiple comparisons the results of which are annotated on the graph. * $P \leq 0.05$. ** $P \leq 0.01$. *** $P \leq 0.001$. **** $P \leq 0.0001$

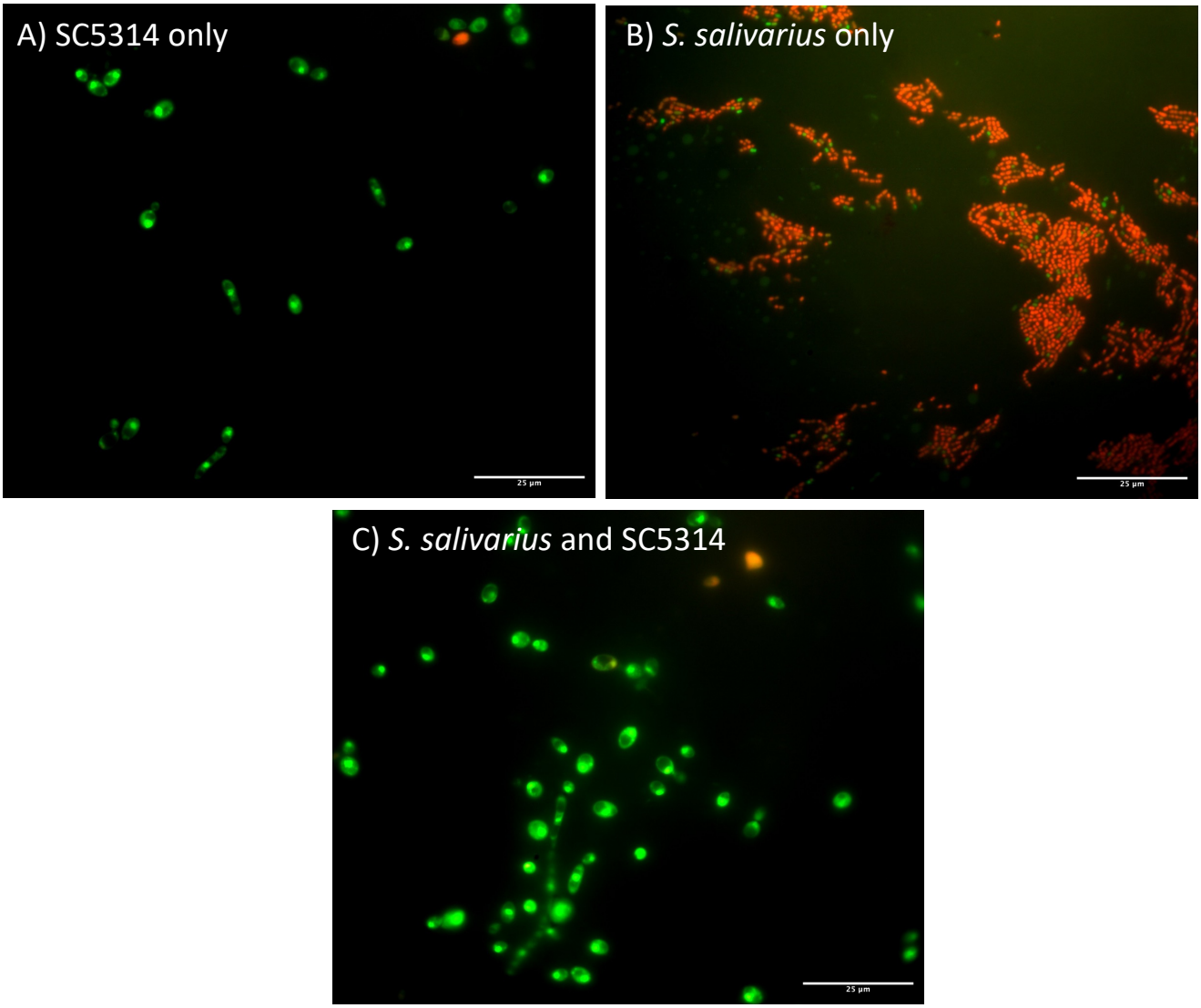

Figure 4.4. Fluorescence micrographs of the cells remaining on the 72 h polymethyl methacrylate (PMMA) coupon surface after recovery for colony forming units (CFU)/mL determination. Coupons were vortex mixed to remove cells to determine the CFU/mL. The surface of the PMMA coupon was then stained using live/dead staining to assess what remained on the surface. Green indicates viable cells. Red indicates dead cells. Scale bars are 25 µm.

In addition to determining the recovered CFU/mL, microscopy methods were also used to investigate whether the presence of the *Streptococcus* species modulated *C. albicans* abundance and surface area coverage in biofilms (Table 4.4, Figure 4.5). Analysis of the CLSM images found that after 24 h of growth on PMMA (Figure 4.6), the mean surface area covered by *C. albicans* SC5314 was statistically higher in the dual species biofilm with *S. salivarius* than for *C. albicans* single species controls ($P \leq 0.0229$). The dual species biofilm with the *S. salivarius* was also significantly higher than the dual species biofilms with *S. gordonii* ($P \leq 0.0001$) and *S. mutans* ($P \leq 0.001$) dual species biofilms. Significantly increased *C. albicans* surface area coverage was also found when *C. albicans* was grown with *S. sanguinis* compared with *S. gordonii* ($P \leq 0.015$), but there was no significant difference between the dual species biofilm containing *S. sanguinis* compared to the single species *C. albicans* positive control. *C. albicans* grown for 24 h in dual species biofilms with *S. gordonii* and *S. mutans* resulted in reduction in the amount of *C. albicans* mean surface area coverage compared with all three other biofilms. In contrast to the 24 h timepoint, CLSM image analysis of the samples grown for 72 h showed no significant differences in the mean percentage area covered by *C. albicans* SC5314 between any of the dual species' biofilms, or the single species positive control (Figure 4.7). The range of surface area coverage after 72h incubation was 2.18% (*S. sanguinis* dual species biofilm) to 4.04% (*S. salivarius* dual species biofilm).

Table 4.4. Summary of the surface area coverage by *C. albicans* results for the dual species biofilm experiments for 24 h and 72 h timepoints. The mean surface area of *C. albicans* and the standard error of the mean (SEM) are presented in the table.

	Surface area coverage by *C. albicans* SC5314 (%)			
	24 h		72 h	
	Mean	SEM	Mean	SEM
C. albicans SC5314 only	9.24	0.95	2.19	0.23
C. albicans SC5314 and *S. gordonii*	4.23	0.48	3.20	0.56
C. albicans SC5314 and *S. salivarius*	16.81	2.12	4.04	1.31
C. albicans SC5314 and *S. sanguinis*	13.75	2.76	2.18	0.41
C. albicans SC5314 and *S. mutans*	5.97	1.48	3.36	0.57

Filamentous morphology data for the dual species biofilms at 24 h (Table 4.5), showed there was an increase in *C. albicans* filamentous morphotypes in the *S. salivarius* dual species biofilms compared to all other biofilms (Figure 4.8). Both *S. gordonii* (3.25%) and *S. mutans* (3.64%) dual species biofilms had a similar level of filamentous forms, which was less than the single species *C. albicans* biofilm control (6.02%). The *S. salivarius* (15.2%) and *S. sanguinis* (10.01%) dual species biofilms both exhibited increased filamentous morphology compared to the *C. albicans* only biofilm.

For the 72 h timepoint, no statistically significant differences were found for the mean percentage area of filamentous morphology between any of the different biofilm compositions (Figure 4.9). The highest percentage area of filamentous morphotypes was observed in the *C. albicans* with *S. sanguinis* biofilm (1.61%) and the lowest was in the *C. albicans* with *S. mutans* biofilm (0.48%). The mean area of filamentous forms remained relatively consistent between the different types of biofilms (range of 0.3%) except for the *S. mutans* dual biofilm filamentous decrease to 0.48%.

Table 4.5. Summary of results for the area of *C. albicans* filamentous forms in the dual species biofilm experiments for 24 h and 72 h timepoints. The mean percentage area of *C. albicans* filamentous forms and the standard error of the mean (SEM) are presented in the table.

	***C. albicans* filamentous morphology area (%)**			
	24 h		**72 h**	
	Mean	**SEM**	**Mean**	**SEM**
C. albicans SC5314 only	6.02	1.36	1.31	0.43
C. albicans SC5314 and *S. gordonii*	3.25	0.82	1.52	0.43
C. albicans SC5314 and *S. salivarius*	15.20	5.30	1.40	0.60
C. albicans SC5314 and *S. sanguinis*	10.01	2.69	1.61	0.74
C. albicans SC5314 and *S. mutans*	3.64	1.06	0.48	0.34

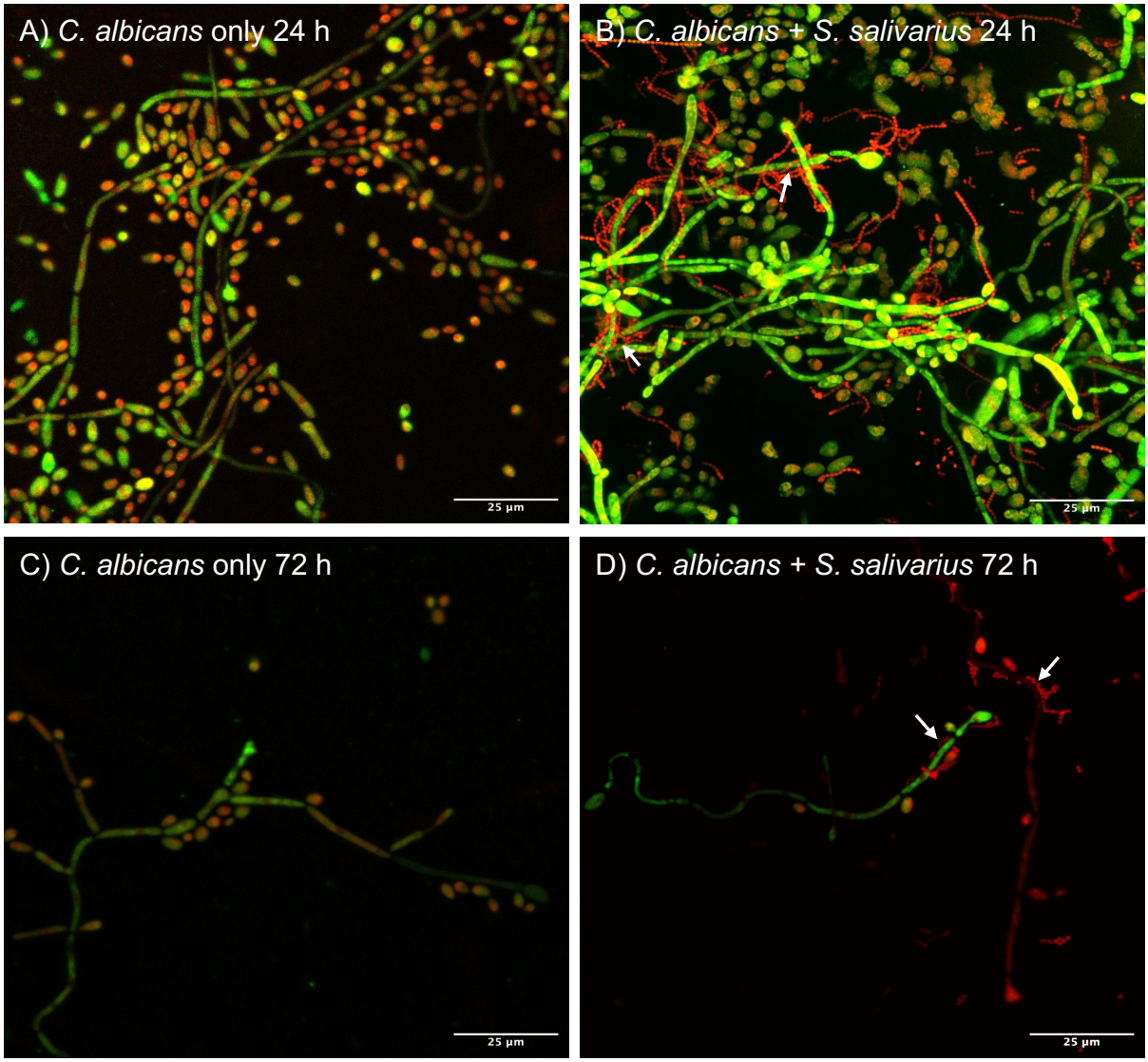

Figure 4.5. Representative images of dual species biofilms grown on polymethyl methacrylate (PMMA) for 24 and 72 h. *C. albicans* SC5314 was grown in a single biofilm for 24 h (A) and 72 h (C) and grown in dual biofilms with *S. salivarius* for 24 h (B) and 72 h (D). *C. albicans* was stained with PNA probes (green) and the samples were counterstained with propidium iodide staining the bacteria red only and the *Candida* also retains the red stain but are distinguishable by size and morphology. Maximum projection images were created from CLSM z-stack files. White arrows indicate examples if where the bacteria are attaching to the hyphal forms of *C. albicans.* Scale bars are 25 µm.

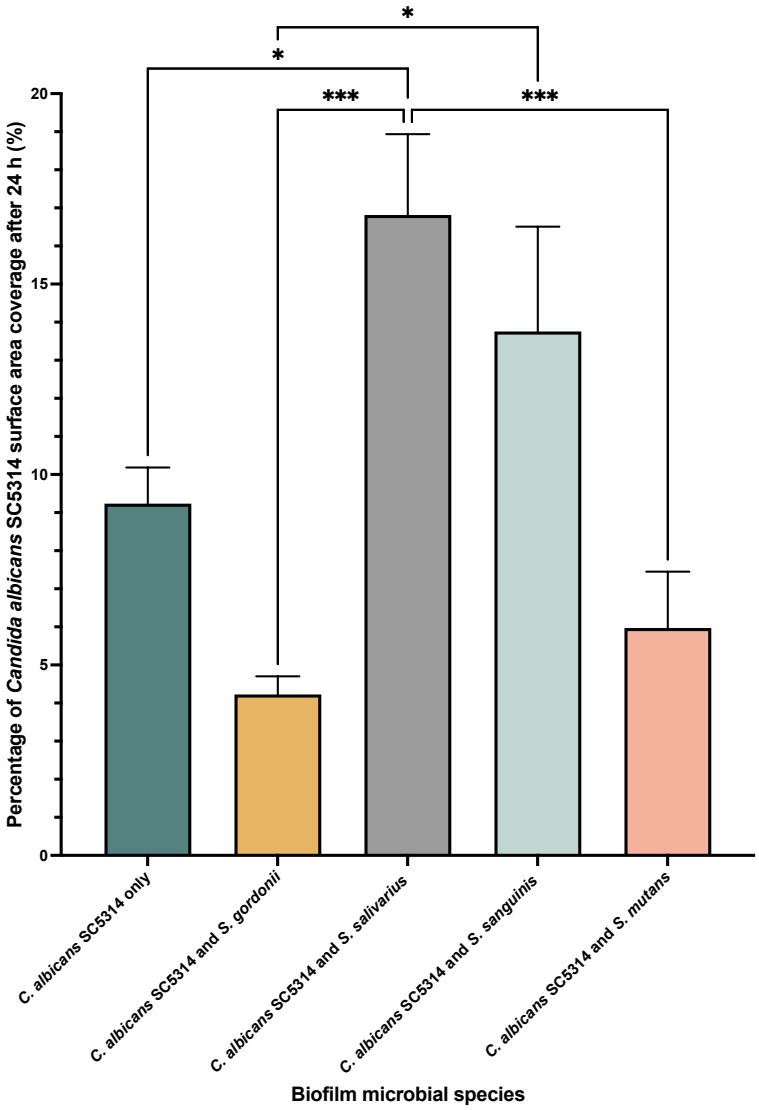

Figure 4.6. Mean percentage of surface area coverage by *Candida albicans* SC5314 in single and dual species biofilms grown on polymethyl methacrylate (PMMA) for 24 h. Each biofilm contains *C. albicans* SC5314 and one of the following Streptococcal species: *S. gordonii, S. salivarius, S. sanguinis* and *S. mutans.* There is also a *C. albicans* SC5314 single species biofilm control. The mean percentage area coverage by SC5314 was determined through analysis of the CLSM images. Data presented as mean ± standard error of the mean. *C. albicans* only n = 59, *C. albicans* and *S. gordonii* n = 16, *C. albicans* and *S. salivarius* n = 15, *C. albicans* and *S. sanguinis* n = 15, *C. albicans* and *S. mutans* n = 15. Statistical significance was determined using the non-parametric Kruskal-Wallis test (H (4) = 26.70, $P \leq 0.0001$) with Dunn's test for multiple comparisons the results of which are annotated on the graph. * $P \leq 0.05$. ** $P \leq 0.01$. *** $P \leq 0.001$. **** $P \leq 0.0001$

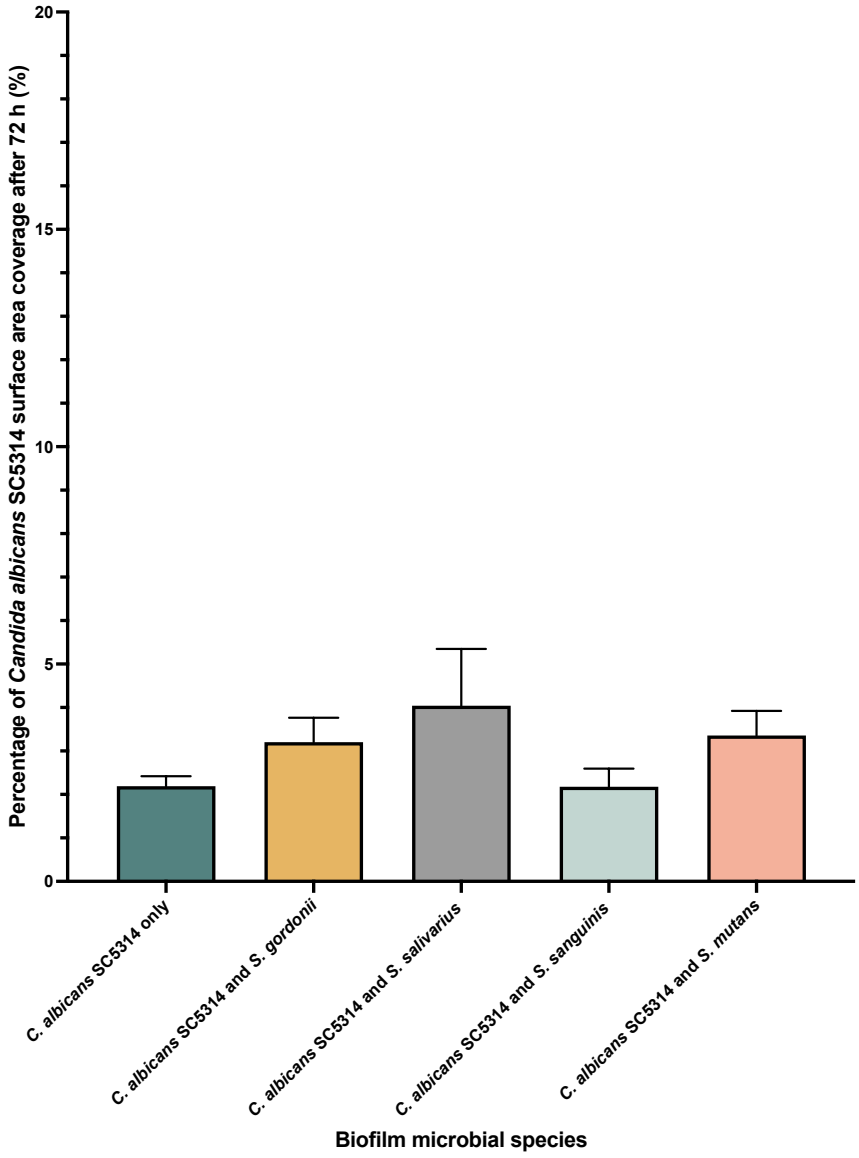

Figure 4.7. Mean percentage of surface area coverage by *Candida albicans* SC5314 in single and dual species biofilms grown on polymethyl methacrylate (PMMA) for 72 h. Each biofilm contains *C. albicans* SC5314 and one of the following Streptococcal species: *S. gordonii, S. salivarius, S. sanguinis* and *S. mutans.* There is also a *C. albicans* SC5314 single species biofilm control. The mean percentage area coverage by SC5314 was determined through analysis of the CLSM images. Data presented as mean ± standard error of the mean. *C. albicans* only n = 50, *C. albicans* and *S. gordonii* n = 19, *C. albicans* and *S. salivarius* n = 16, *C. albicans* and *S. sanguinis* n = 16, *C. albicans* and *S. mutans* n = 16. Statistical significance was determined using the non-parametric Kruskal-Wallis test (H (4) = 4.541, $P \leq 0.3377$) with Dunn's test for multiple comparisons. No significant differences were found between the groups.

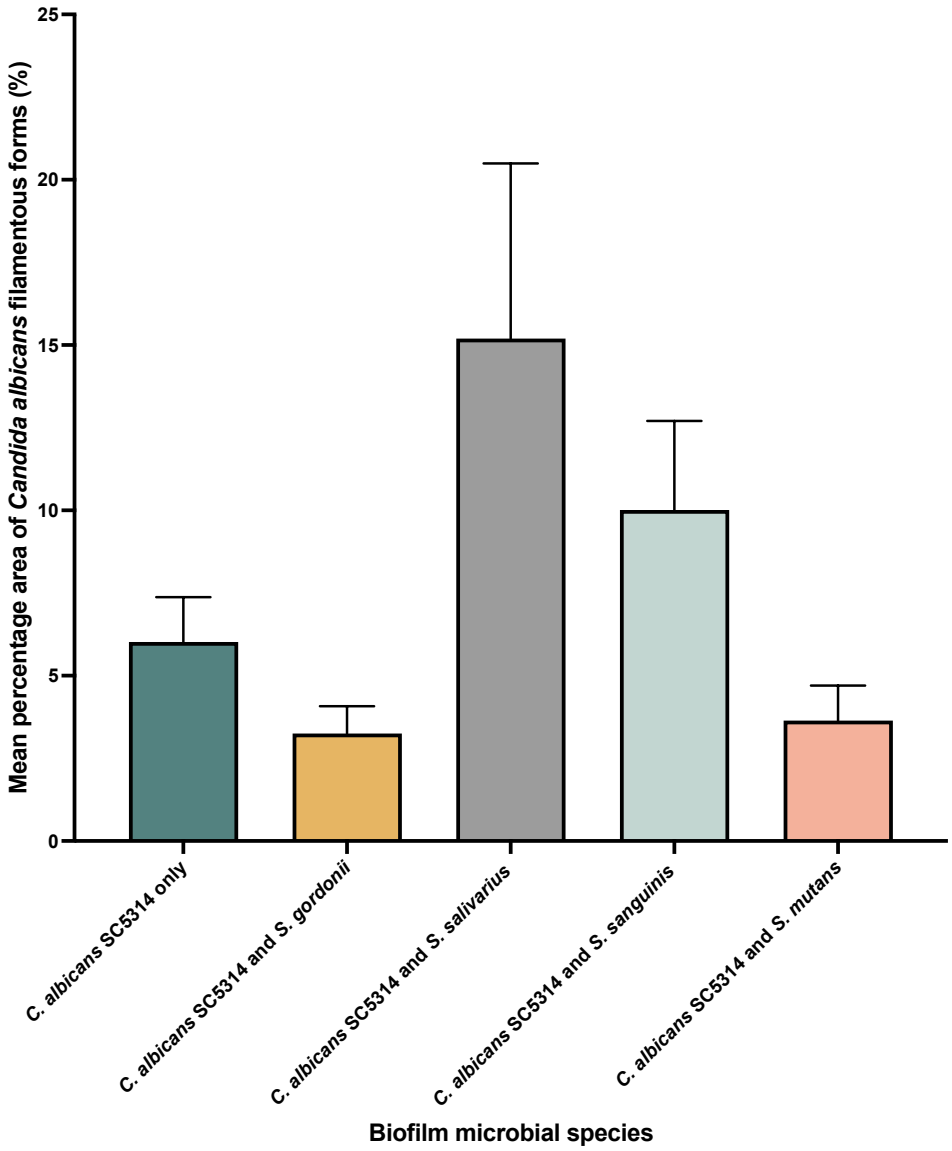

Figure 4.8. Mean percentage area of *Candida albicans* SC5314 filamentous forms in dual species biofilms grown on polymethyl methacrylate (PMMA) surfaces after 24 h. Each biofilm contains *C. albicans* SC5314 and one of the following Streptococcal species: *S. gordonii, S. salivarius, S. sanguinis* and *S. mutans.* There is also a *C. albicans* SC5314 single species biofilm control. The mean percentage area of *C. albicans* SC5314 filamentous forms was determined through analysis of the CLSM images. Data presented as mean ± standard error of the mean. *C. albicans* only $n = 11$, *C. albicans* and *S. gordonii* $n = 6$, *C. albicans* and *S. salivarius* $n = 6$, *C. albicans* and *S. sanguinis* $n = 6$, *C. albicans* and *S. mutans* $n = 6$. Statistical significance was determined using the non-parametric Kruskal-Wallis test ($H(4) = 11.39$, $P \leq 0.0225$) with Dunn's test for multiple comparisons. No significant differences were found between the groups.

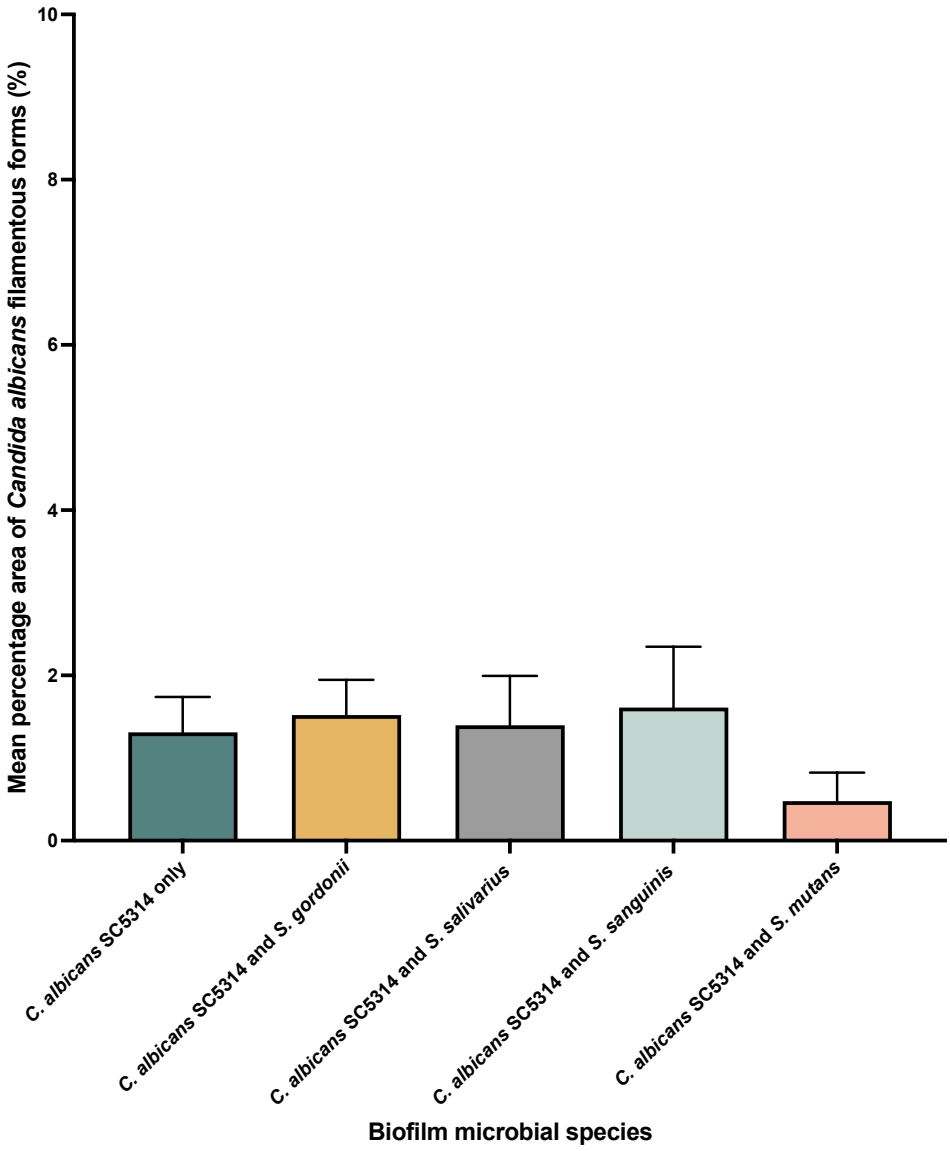

Figure 4.9. Mean percentage area of Candida albicans SC5314 filamentous forms in dual species biofilms grown on polymethyl methacrylate (PMMA) surfaces after 72 h. Each biofilm contains *C. albicans* SC5314 and one of the following Streptococcal species: *S. mutans, S. salivarius, S. sanguinis* and S*. gordonii.* There is also a *C. albicans* SC5314 single species biofilm control. The mean percentage area of filamentous forms of *C. albicans* SC5314 was determined through analysis of the CLSM images. Data presented as mean ± standard error of the mean. *C. albicans* only *n* = 8, *C. albicans* and *S. gordonii n* = 16, *C. albicans* and *S. salivarius n* = 15, *C. albicans* and *S. sanguinis n* = 15, *C. albicans* and *S. mutans n* = 15. Statistical significance was determined using one-way ANOVA test ($F(4, 27) = 0.7195$, $P \leq 0.5861$) with Tukey's test for multiple comparisons. No significant differences were found.

4.3.2. Effect of bacterial spent medium on *C. albicans* adherence, biofilm formation and morphology

Spent medium collected from the growth of the four different *Streptococcus* species and *C. albicans* SC5314 was used as the medium for the growth of *C. albicans* to test whether effects observed in the dual species biofilm experiments could be attributed to competition of resources, secreted components or changes to the environment caused by the *Streptococcus* species. The control *C. albicans* biofilm grown in fresh medium had a high level of surface coverage which is clearly observed in the 24 h time point representative images (Figure 4.10). This observation was supported by the surface area coverage analysis that showed *C. albicans* in every type of spent media exhibited significantly lower levels of surface area coverage than the control biofilm (Figure 4.11). At the 72 h timepoint, while all spent media were observed to lead to an increase in surface area compared to the control, there were no statistically significant differences (Figure 4.12). A summary of the results can be found in Table 4.6.

Table 4.6. Summary of the surface area coverage by *C. albicans* results for the spent media experiments for 24 h and 72 h timepoints. The mean surface area of *C. albicans* and the standard error of the mean (SEM) are presented in the table.

	Surface area coverage by *C. albicans* SC5314 (%)			
	24 h		**72 h**	
	Mean	**SEM**	**Mean**	**SEM**
Control	40.83	4.24	6.65	1.24
C. albicans SC5314 spent media	5.35	1.05	13.19	1.68
S. gordonii spent media	4.97	0.98	15.56	2.53
S. salivarius spent media	8.60	2.17	16.55	2.30
S. sanguinis spent media	7.85	1.39	18.71	2.42
S. mutans spent media	13.40	2.42	11.24	2.04

Analysis of *C. albicans* morphological changes in spent media experiments (Table 4.7), showed that there were no significant differences in the mean percentage

area of filamentous forms of *C. albicans* (Figure 4.13). The control and the spent medium from *C. albicans* SC5314 had similar levels of *C. albicans* with a filamentous morphology (4.03% and 3.87%, respectively), whereas the spent media from the *Streptococcus* species had around half the area of filamentous forms though this was not deemed statistically significant. At the 72 h timepoint (Figure 4.14), the spent media from *S. salivarius, S. sanguinis* and *S. mutans* all yielded significantly fewer filamentous forms of *C. albicans* compared to the control ($P \leq 0.0076$, $P \leq 0.0031$ and $P \leq 0.0126$, respectively). However, the *S. gordonii* spent medium (3.41%) caused a slight increase in *C. albicans* filamentous morphology compared to the control (2.19%).

Table 4.7. Summary of results for the area of *C. albicans* filamentous forms in the spent media experiments for 24 h and 72 h timepoints. The mean percentage area of *C. albicans* filamentous forms and the standard error of the mean (SEM) are presented in the table.

	***C. albicans* filamentous morphology area (%)**			
	24 h		**72 h**	
	Mean	**SEM**	**Mean**	**SEM**
Control	4.03	1.02	2.19	0.69
C. albicans SC5314 spent media	3.87	1.02	0.65	0.17
S. gordonii spent media	1.34	0.43	3.41	2.99
S. salivarius spent media	2.52	0.54	0.25	0.11
S. sanguinis spent media	1.94	0.34	0.18	0.11
S. mutans spent media	1.55	0.46	0.24	0.11

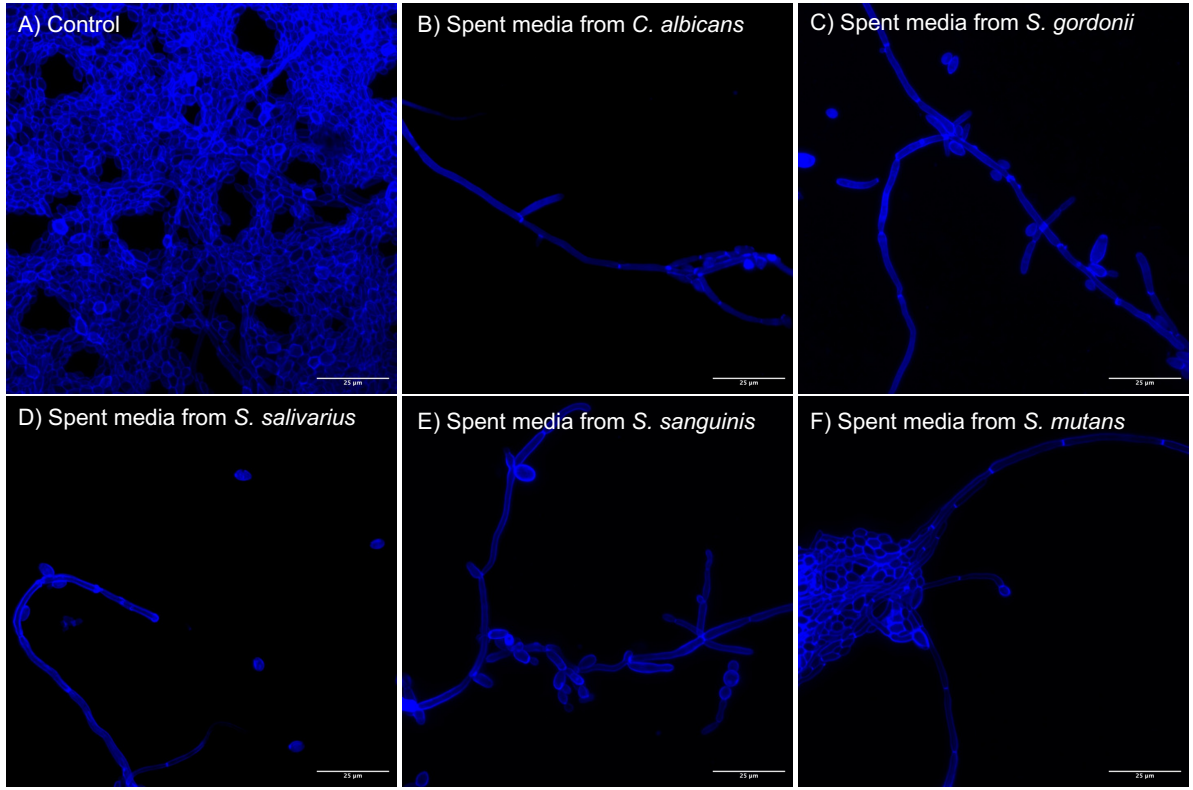

Figure 4.10. Representative images of the *Candida albicans* SC5314 grown for 24 h in spent media from different species and a no spent media control on polymethyl methacrylate (PMMA) coupon surfaces. Spent medium was collected from *C. albicans* SC5314 (B), *S. gordonii* (C), *S. salivarius* (D), *S. sanguinis* (E) *and S. mutans* (F) planktonic cultures after 24 h. *Candida albicans* SC5314 was then grown on PMMA for 24 h in the spent media before fixation in formal-buffered saline, staining with calcofluor white and imaged as z-stacks using CLSM. A 'no spent media' control was included that was grown in fresh media (A). Presented here are representative examples for each condition of max projection images created from the z-stacks that were subsequently used for analysis. Scale bars are 25 μm.

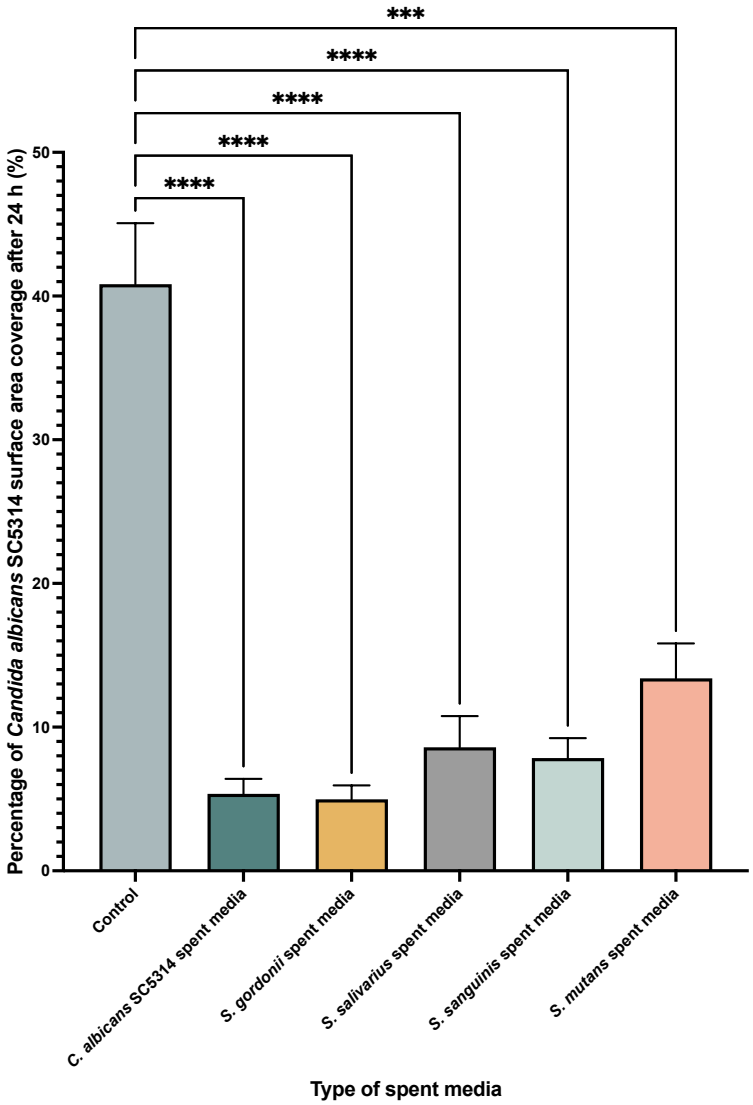

Figure 4.11. Mean percentage of surface area coverage by *Candida albicans* SC5314 grown for 24 h on polymethyl methacrylate (PMMA) with spent media from different species and a media control. *C. albicans* was grown in spent media collected from *C. albicans* SC5314, *S. gordonii, S. salivarius, S. sanguinis* and *S. mutans.* The positive control was grown in fresh media. The mean percentage area coverage by SC5314 was determined through analysis of the CLSM images. Data presented as mean ± standard error of the mean. Control n = 15, spent medium from *C. albicans* n = 32, spent medium from *S. gordonii* n= 43, spent medium from *S. salivarius* n = 45, spent medium from *S. sanguinis* n = 40, spent medium from *S. mutans* n = 45. Statistical significance was determined using the non-parametric Kruskal-Wallis test (H (5) = 40.02, $P \leq 0.0001$) with Dunn's test for multiple comparisons the results of which are annotated on the graph. * $P \leq 0.05$. ** $P \leq 0.01$. *** $P \leq 0.001$. **** $P \leq 0.0001$

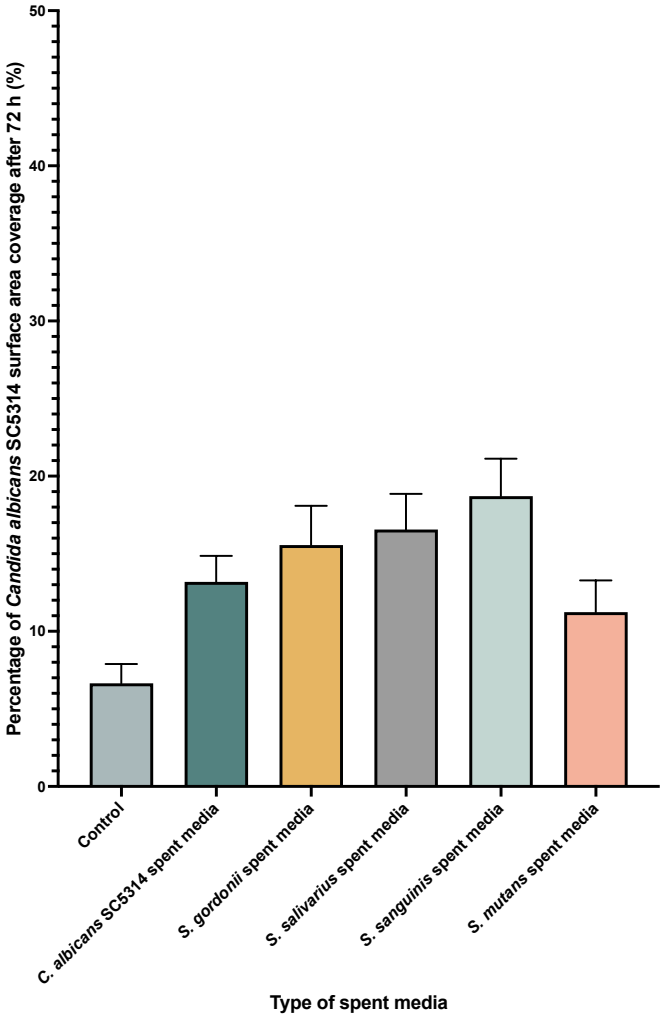

Figure 4.12. Mean percentage of surface area coverage by *Candida albicans* SC5314 grown for 72 h on polymethyl methacrylate (PMMA) with spent media from different species and a media control. *C. albicans* was grown in spent media collected from *C. albicans* SC5314, *S. gordonii, S. salivarius, S. sanguinis* and *S. mutans.* The positive control was grown in fresh media. The mean percentage area coverage by SC5314 was determined through analysis of the CLSM images. Data presented as mean ± standard error of the mean. Control n = 15, spent medium from *C. albicans* n = 42, spent medium from *S. gordonii* n= 41, spent medium from *S. salivarius* n = 35, spent medium from *S. sanguinis* n = 45, spent medium from *S. mutans* n = 42. Statistical significance was determined using the non-parametric Kruskal-Wallis test (H (5) = 11.72, $P \leq 0.0388$) with Dunn's test for multiple comparisons. No significant differences were found between the groups.

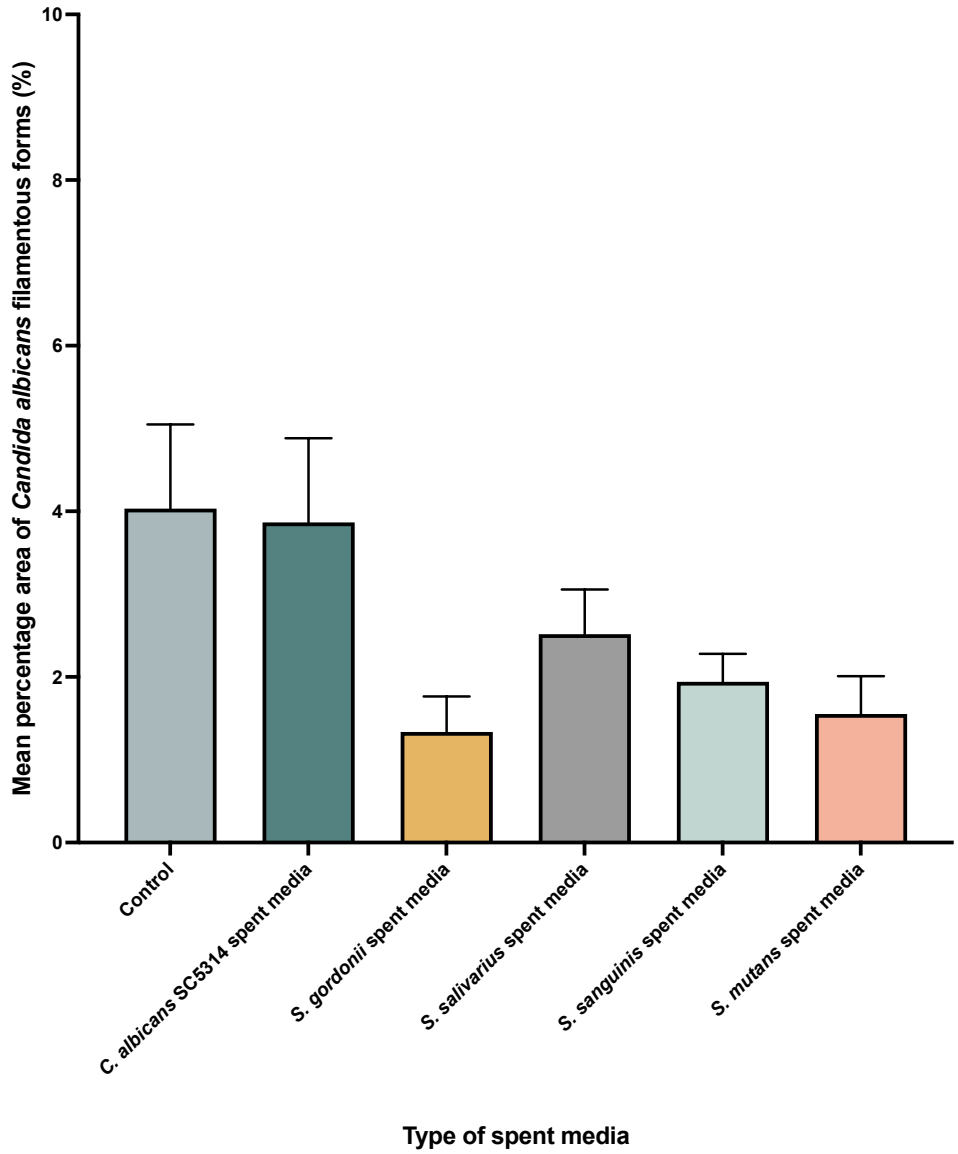

Figure 4.13. Mean percentage area of *Candida albicans* SC5314 filamentous forms grown in different types of spent media on polymethyl methacrylate (PMMA) surfaces for 24 h. *C. albicans* was grown in spent media collected from *C. albicans* SC5314, *S. gordonii, S. salivarius, S. sanguinis* and *S. mutans.* The positive control was grown in fresh media. The mean percentage area of *C. albicans* SC5314 filamentous forms was determined through analysis of the CLSM images. Data presented as mean ± standard error of the mean. Control n = 20, spent medium from *C. albicans* n = 19, spent medium from *S. gordonii* n= 19, spent medium from *S. salivarius* n = 18, spent medium from *S. sanguinis* n = 18, spent medium from *S. mutans* n = 18. Statistical significance was determined using the non-parametric Kruskal-Wallis test (H (5) = 7.625, $P \leq 0.1781$) with Dunn's test for multiple comparisons. No significant differences were found between the groups.

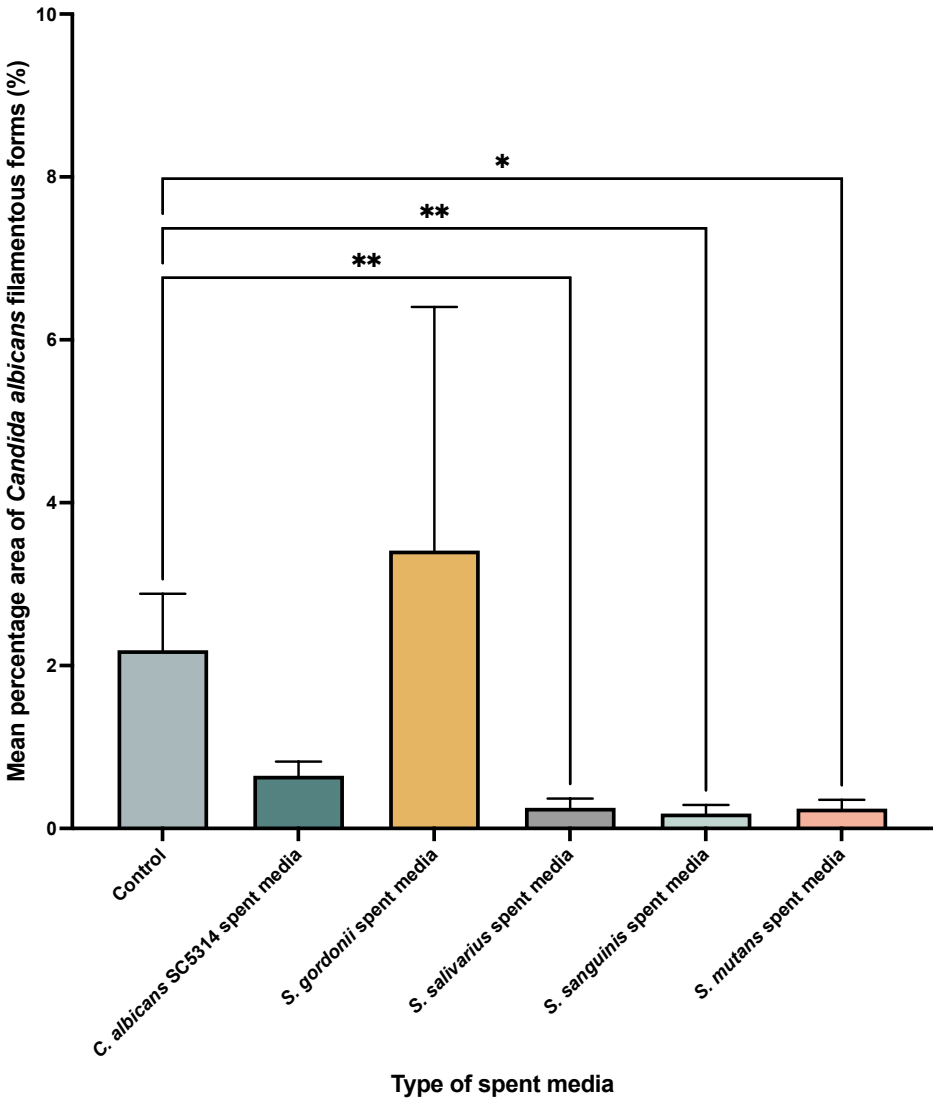

Figure 4.14. Mean percentage area of *Candida albicans* SC5314 filamentous forms grown in different types of spent media on polymethyl methacrylate (PMMA) surfaces for 72 h. *C. albicans* was grown in spent media collected from *C. albicans* SC5314, *S. gordonii, S. salivarius, S. sanguinis* and *S. mutans.* The positive control was grown in fresh media. The mean percentage area of *C. albicans* SC5314 filamentous forms was determined through analysis of the CLSM images. Data presented as mean ± standard error of the mean. Control n = 13, spent medium from *C. albicans* n = 18, spent medium from *S. gordonii* n= 18, spent medium from *S. salivarius* n = 18, spent medium from *S. sanguinis* n = 18, spent medium from *S. mutans* n = 18. Statistical significance was determined using the non-parametric Kruskal-Wallis test (H (5) = 21.79, $P \leq 0.0006$) with Dunn's test for multiple comparisons the results of which are annotated on the graph. * $P \leq 0.05$. ** $P \leq 0.01$. *** $P \leq 0.001$. **** $P \leq 0.0001$

4.3.3. Interactions between planktonic *Streptococcus* species and *Candida albicans* filamentous morphological forms

Representative fluorescence micrographs of the filamentous forms of *C. albicans* SC5314 WT and the *C. albicans* ΔALS3 mutant strain with *S. gordonii* (Figure 4.15), *S. salivarius* (Figure 4.16), *S. sanguinis* (Figure 4.17), and *S. mutans* (Figure 4.18) show the association between with two species with and without the Als3 adhesin.

Cells of *S. gordonii* (Figure 4.19), *S. salivarius* (Figure 4.20) and *S. sanguinis* (Figure 4.21) all exhibited greater association with filamentous forms (hyphae, pseudohyphae and elongated forms) of the wild-type *C. albicans* SC5314 than the *C. albicans Δals3/Δals3* mutant strain. This was significantly so for the *S. gordonii* (Mann–Whitney $U = 30$, $n_1 = 15$ $n_2 = 15$, $P < 0.0003$ two-tailed) and *S. salivarius* (Mann–Whitney $U = 57$, $n_1 = 15$ $n_2 = 15$, $P < 0.0202$ two-tailed) species.

Streptococcus mutans had significantly (Mann–Whitney $U = 50$, $n_1 = 15$ $n_2 = 15$, $P < 0.0086$ two-tailed) more cells associated with the filamentous forms of *C. albicans* ΔALS3 mutant strain (Mean = 5.88 cells/100μm^2) than with *C. albicans* SC5314 WT (Mean = 14.74 cells/100μm^2) strain (Figure 4.22).

Table 4.8. Summary of results for the interactions between the streptococcal species and both the *C. albicans* wild type and Als3 mutant strains. Mean number of bacterial cells associated with 100 μm^2 of *C. albicans* filamentous morphotypes and the standard error of the mean (SEM) are presented.

	Mean number of bacterial cells associated with 100 μm^2 filamentous morphotypes of *C. albicans*			
	***C. albicans* SC5314**		***C. albicans* ΔALS3**	
	Mean	SEM	Mean	SEM
S. gordonii	11.19	2.24	2.65	0.66
S. salivarius	8.76	2.17	2.62	0.63
S. sanguinis	12.37	2.66	6.86	1.06
S. mutans	5.88	1.70	14.74	3.00

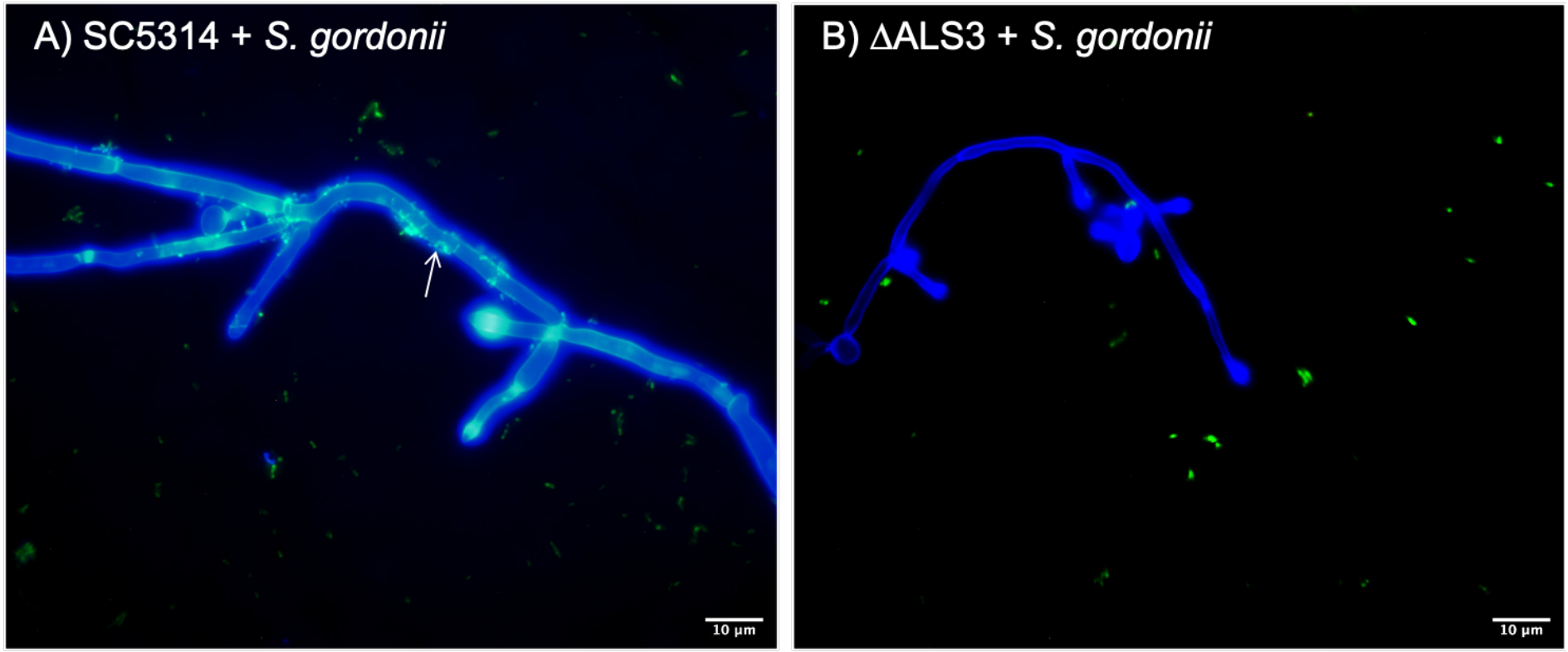

Figure 4.15. Representative fluorescence micrographs of planktonic interactions between *Streptococcus gordonii* and the filamentous forms of a wild type and mutant strain of *Candida albicans*. Bacteria cells were pre-stained with FITC (green) and incubated for 90 min at 37°C and 5% CO_2 with either *C. albicans* SC5314 wild type (A) or the ΔALS3 mutant strain (B). *C. albicans* was stained with calcofluor white (blue). The white arrow indicates an example of where the bacterial cells are in close proximity to the hyphal forms of *C. albicans.* Scale bars are 10 µm.

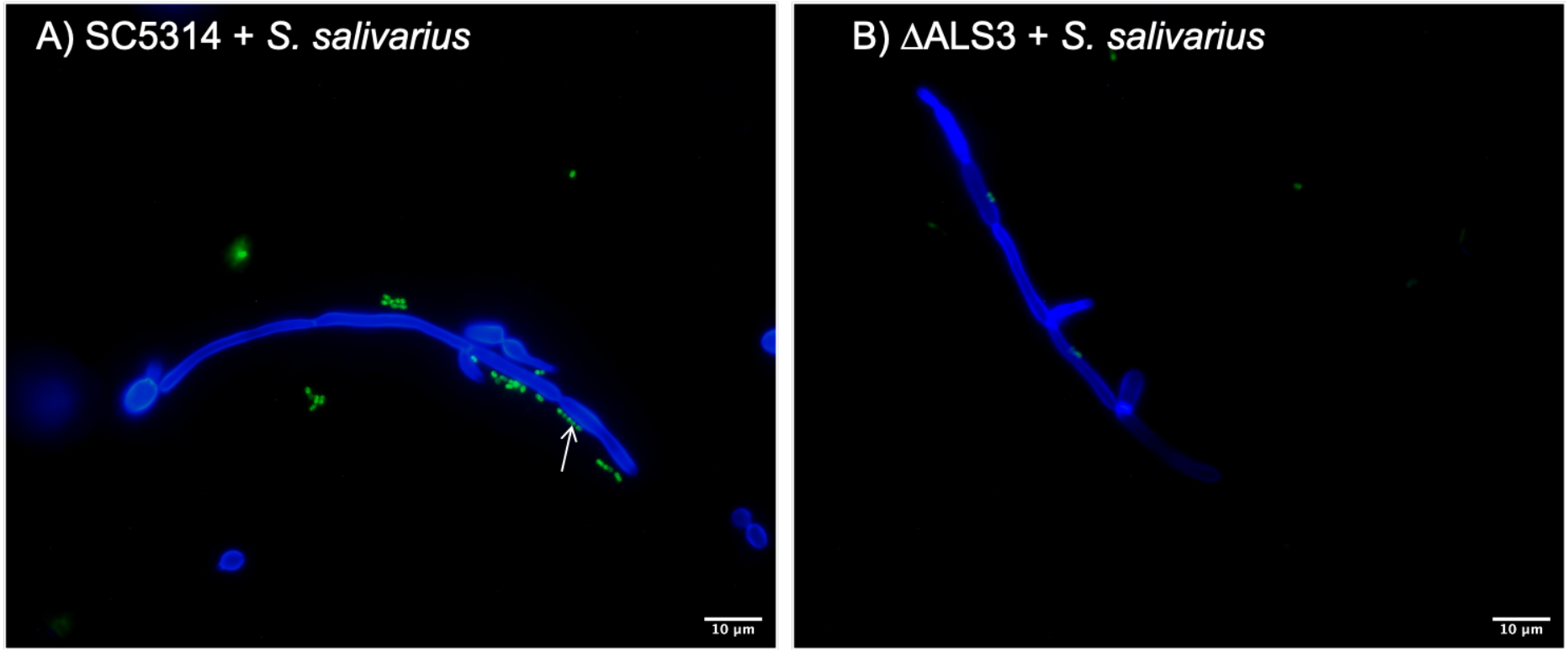

Figure 4.16. Representative fluorescence micrographs of planktonic interactions between *Streptococcus salivarius* and the filamentous forms of a wild type and mutant strain of *Candida albicans*. Bacteria cells were pre-stained with FITC (green) and incubated for 90 min at 37°C and 5% CO_2 with either *C. albicans* SC5314 wild type (A) or the ΔALS3 mutant strain (B). *C. albicans* was stained with calcofluor white (blue). The white arrow indicates an example of where the bacterial cells are in close proximity to the hyphal forms of *C. albicans.* Scale bars are 10 µm.

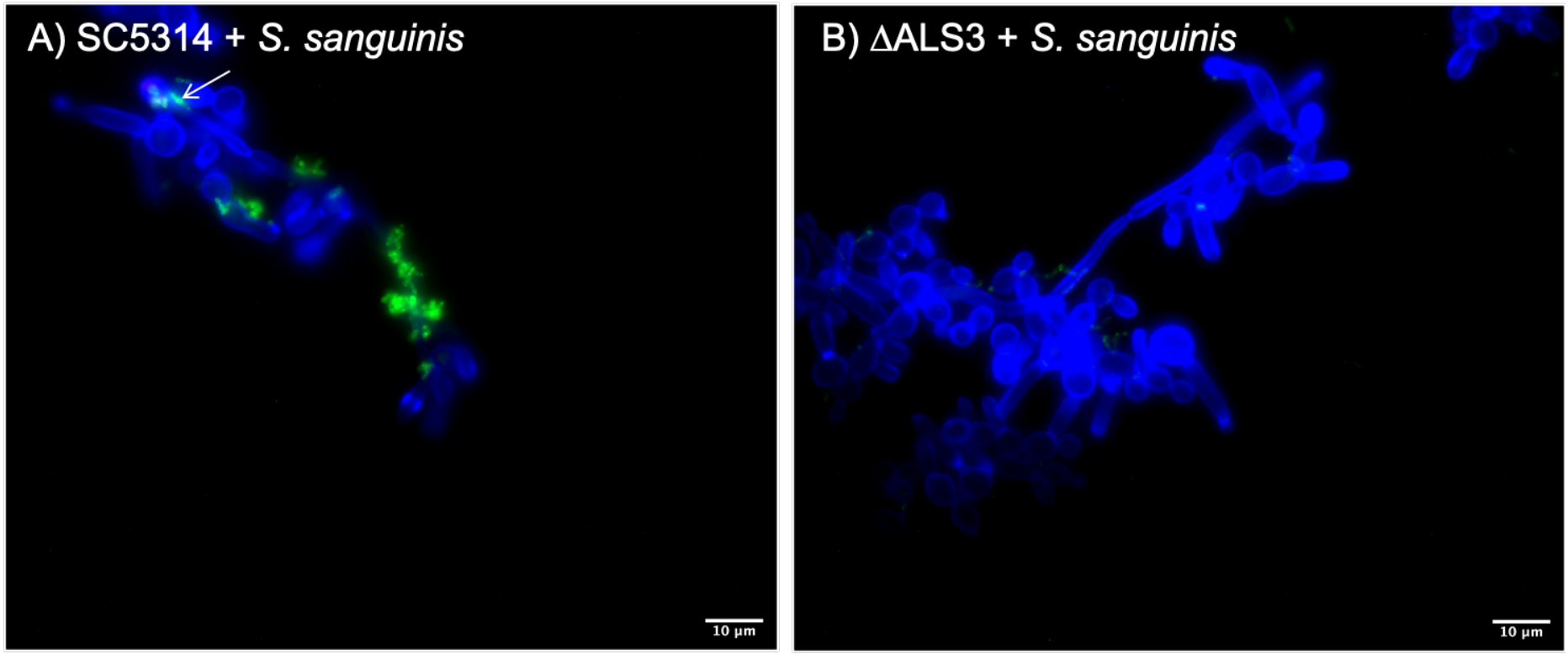

Figure 4.17. Representative fluorescence micrographs of planktonic interactions between *Streptococcus sanguinis* and the filamentous forms of a wild type and mutant strain of *Candida albicans*. Bacteria cells were pre-stained with FITC (green) and incubated for 90 min at 37°C and 5% CO_2 with either *C. albicans* SC5314 wild type (A) or the ΔALS3 mutant strain (B). *C. albicans* was stained with calcofluor white (blue). The white arrow indicates an example of where the bacterial cells are in close proximity to the hyphal forms of *C. albicans.* Scale bars are 10 µm.

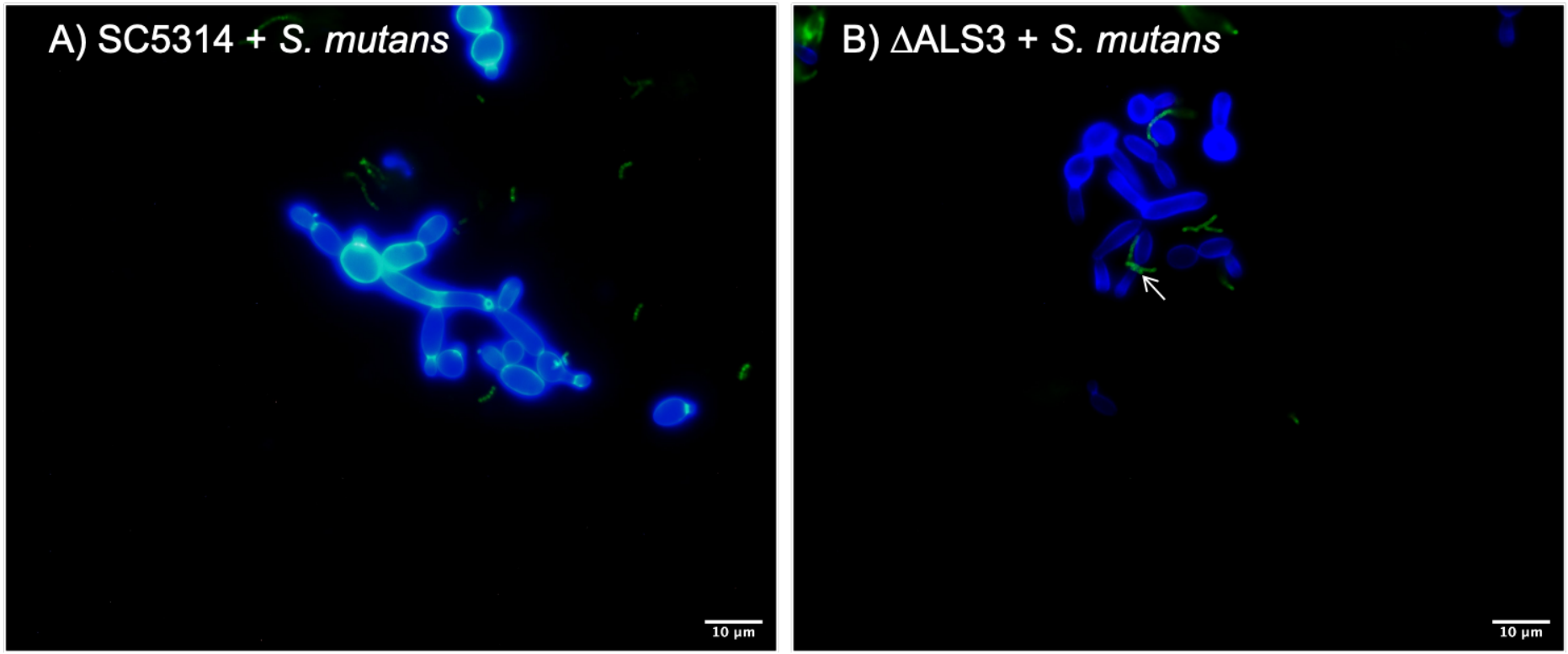

Figure 4.18. Representative fluorescence micrographs of planktonic interactions between *Streptococcus mutans* and the filamentous forms of a wild type and mutant strain of *Candida albicans*. Bacteria cells were pre-stained with FITC (green) and incubated for 90 min at 37°C and 5% CO_2 with either *C. albicans* SC5314 wild type (A) or the ΔALS3 mutant strain (B). *C. albicans* was stained with calcofluor white (blue). The white arrow indicates an example of where the bacterial cells are in close proximity to the hyphal forms of *C. albicans.* Scale bars are 10 µm.

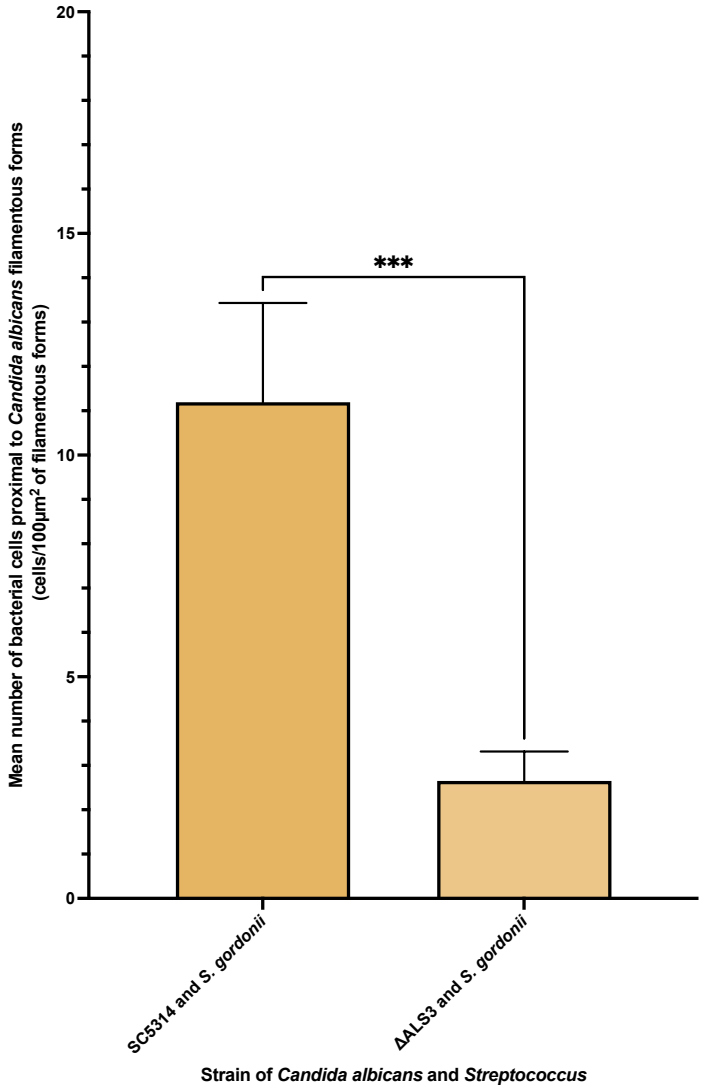

Figure 4.19. Mean number of *Streptococcus gordonii* cells associated with *Candida albicans* filamentous forms (bacterial cells/100 μm^2). *Streptococcus gordonii* was incubated for 90 min at 37°C and 5% CO_2 planktonically with either *C. albicans* SC5314 wild type (A) or the *C. albicans* ΔALS3 mutant strain (B). *Streptococcus gordonii* cells were stained with FITC (green) and *C. albicans* was stained with calcofluor white (blue). Fluorescence microscopy was used to image the *C. albicans* filamentous forms and the number of bacterial cells proximal to the filamentous forms of *C. albicans* were enumerated and standardised as mean number of cells/100 μm^2 of filamentous forms of *C. albicans.* Data presented as mean ± standard error of the mean. Each group n = 15. Statistical significance was determined using the Mann Whitney U test (Mann–Whitney U = 30, n_1 = 15 n_2 = 15, P < 0.0003 two-tailed). * $P \leq 0.05$. ** $P \leq 0.01$. *** $P \leq 0.001$. **** $P \leq 0.0001$

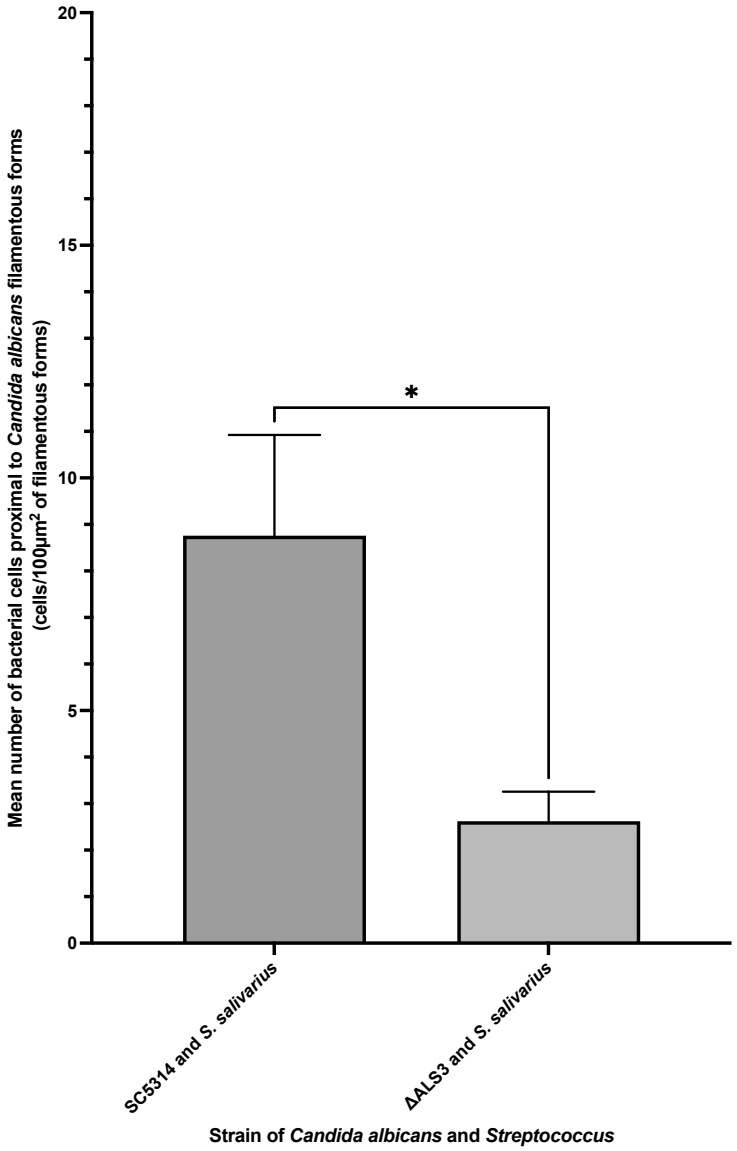

Figure 4.20. Mean number of *Streptococcus salivarius* cells associated with *Candida albicans* filamentous forms (bacterial cells/100 µm^2). *Streptococcus salivarius* was incubated for 90 min at 37°C and 5% CO_2 planktonically with either *C. albicans* SC5314 wild type (A) or the ΔALS3 mutant strain (B). *Streptococcus salivarius* cells were stained with FITC (green) and *C. albicans* was stained with calcofluor white (blue). Fluorescence microscopy was used to image the *C. albicans* filamentous forms and the number of bacterial cells proximal to the filamentous forms of *C. albicans* were enumerated and standardised as mean number of cells/100 µm^2 of filamentous forms of *C. albicans.* Data presented as mean ± standard error of the mean. Each group *n* = 15. Statistical significance was determined using the Mann Whitney U test (Mann–Whitney U = 57, n_1 = 15 n_2 = 15, P < 0.0202 two-tailed). * $P \leq 0.05$. ** $P \leq 0.01$. *** $P \leq 0.001$. **** $P \leq 0.0001$

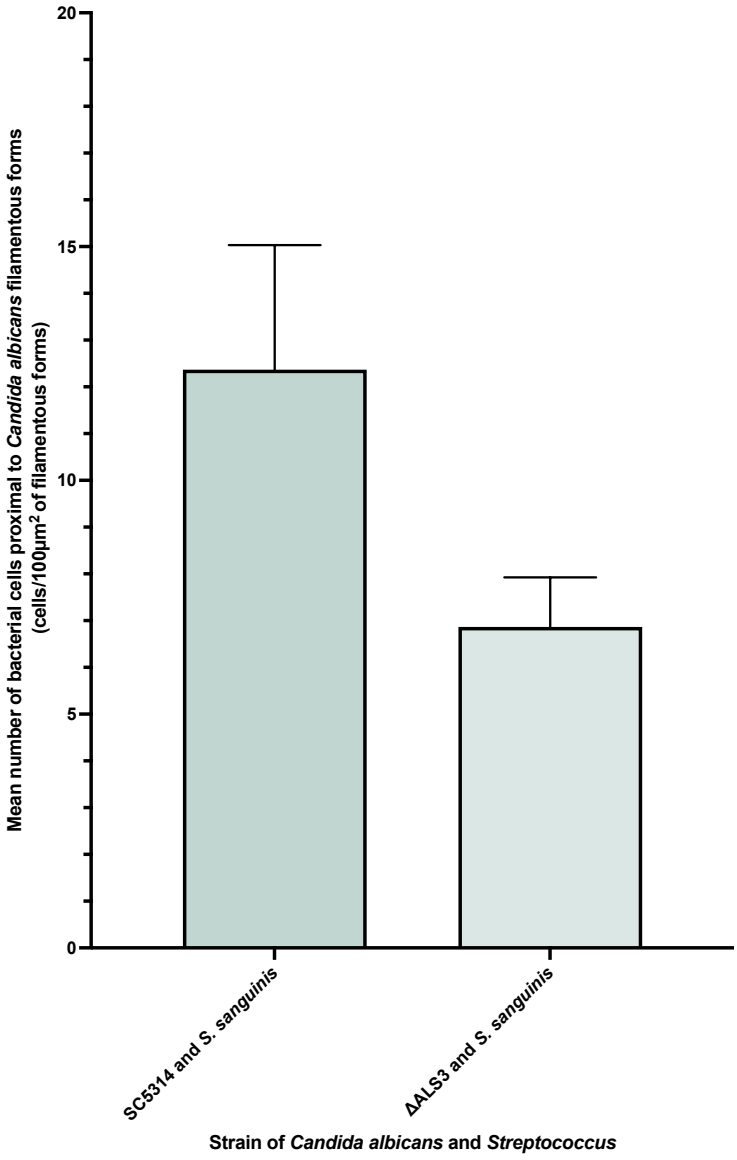

Figure 4.21. Mean number of *Streptococcus sanguinis* cells associated with *Candida albicans* filamentous forms (bacterial cells/100 µm^2). *S. sanguinis* was incubated for 90 min at 37°C and 5% CO_2 planktonically with either *C. albicans* SC5314 wild type (A) or the ΔALS3 mutant strain (B). *S. sanguinis* cells were stained with FITC (green) and *C. albicans* was stained with calcofluor white (blue). Fluorescence microscopy was used to image the *C. albicans* filamentous forms and the number of bacterial cells proximal to the filamentous forms of *C. albicans* were enumerated and standardised as mean number of cells/100 µm^2 of filamentous forms of *C. albicans.* Data presented as mean ± standard error of the mean. Each group *n* = 15. Statistical significance was determined using the Mann Whitney U test (Mann–Whitney U = 77, n_1 = 15 n_2 = 15, P < 0.1485 two-tailed). No significant difference was found between the groups.

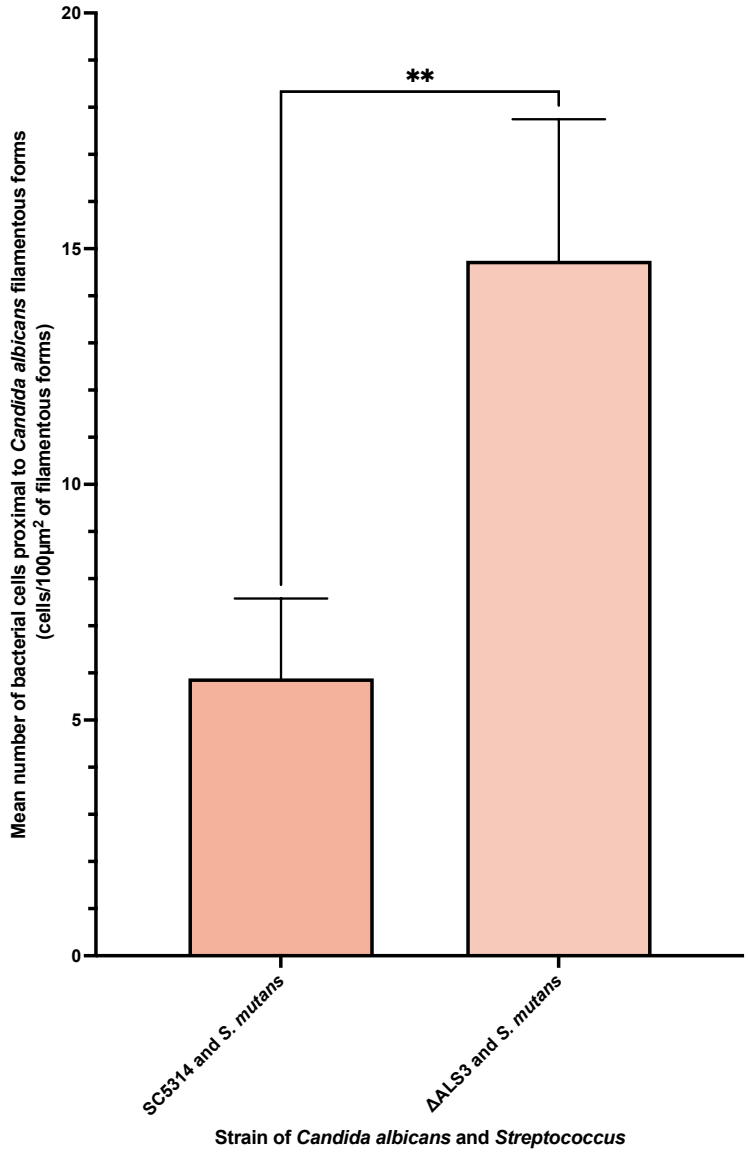

Figure 4.22. Mean number of *Streptococcus mutans* cells associated with *Candida albicans* filamentous forms (bacterial cells/100 μm^2). *Streptococcus mutans* was incubated for 90 min at 37°C and 5% CO_2 planktonically with either *C. albicans* SC5314 wild type (A) or the ΔALS3 mutant strain (B). *Streptococcus mutans* cells were stained with FITC (green) and *C. albicans* was stained with calcofluor white (blue). Fluorescence microscopy was used to image the *C. albicans* filamentous forms and the number of bacterial cells proximal to the filamentous forms of *C. albicans* were enumerated and standardised as mean number of cells/100 μm^2 of filamentous forms of *C. albicans.* Data presented as mean ± standard error of the mean. Each group *n* = 15. Statistical significance was determined using the Mann Whitney U test (Mann–Whitney U = 50, n_1 = 15 n_2 = 15, P < 0.0089 two-tailed). * $P \leq 0.05$. ** $P \leq 0.01$. *** $P \leq 0.001$. **** $P \leq 0.0001$

4.4. Discussion

A risk factor for *Candida*-associated denture stomatitis is occurrence of higher numbers of *Candida* on denture surfaces. Therefore, it is important to investigate the factors which promote increased *Candida* denture surface colonisation. Previous research has found that some oral bacterial species not only increased the abundance of *C. albicans* in the oral cavity, but also promoted the more pathogenic filamentous forms of *C. albicans* that could lead to invasive candidosis (Morse et al. 2019). The research presented in this Chapter aimed to investigate the effect of single oral *Streptococcus* species on *C. albicans* in terms of abundance and morphology and assess whether effects required the presence of live cells and the *C. albicans* Als3 adhesin.

The presence of *Streptococcus* species increased the number of *C. albicans* CFUs that were recovered from 24 h and 72 h biofilms. It is important to highlight that the data is based on a recovered CFU/mL as the samples were grown adhering to PMMA surfaces and therefore the results were dependent on the effective removal of the cells from the surface. However, this was anticipated to have been equal in all conditions and therefore still representative. CFU determination was used as it is still considered the gold standard for the quantification of biofilms and viable cell abundance, even though it is both time consuming and uses a lot of resources (Thieme et al. 2021). Imaging the surfaces post-recovery revealed cells remaining on the surfaces which appeared to be proportionate to the results and deemed to be a reasonable level of error.

Surface area analysis of CLSM images was also used to assess the abundance of *C. albicans* present on the denture material in the dual species experiments. *Streptococcus* species were found to increase the biofilm surface area coverage by *C. albicans* in 24 h biofilms. For 72 h biofilms, no significant difference in surface area coverage was found between the biofilms. Previous research on the interactions between *C. albicans* and Mitis Group *Streptococcus* (MSG) which included dual species biofilms with *S. gordonii* and *S. sanguinis* on a titanium-mucosal interface, revealed that after 72 h *C. albicans* biovolume and biomass was reduced by both *S. gordonii* and *S. sanguinis* (Souza et al. 2020). Significantly decreased *C. albicans* biomass was also found in 72 h dual species biofilms with

S. salivarius though the effect was shown to be dependent on the strain of *C. albicans* present (Mokhtar et al. 2021). However, *S. mutans* has been reported to increase the amount of *C. albicans* in 24 h dual species biofilms in comparison to single species controls (Sztajer et al. 2014).

The presence of MSG has also been shown to increase *C. albicans* tissue invasion and upregulation of hyphal specific virulence associated genes, *efg1,* Hyphal Wall Protein 1 (*hwp1*), and agglutinin-like sequence 3 (*als3*) at 72 h, but not at 24 h (Souza et al. 2020). This supports our findings that the dual species 24 h biofilms resulted in an increase in *C. albicans* filamentous morphology with the *S. salivarius* and *S. sanguinis* strains which was not statistically significant, but suggests this may have been the start of upregulation of genes that promote hyphal formation. However, *S. salivarius* has previously been shown to inhibit hyphal formation of *C. albicans* when incubated for 16 h and this interaction occurred through binding of *S. salivarius* to *C. albicans* (Ishijima et al. 2012)

For 72 h dual species biofilms, there was a consistent level of filamentous forms across the different biofilms, showing increased levels compared to the single species control, apart for *S. mutans* which led to reduced *C. albicans* filamentous morphologies. This was supported by the findings of Souza *et al.* (2020) which found an increase in *C. albicans* hyphal associated gene expression at 72 h, which could lead to an increase in filamentous forms. The reduction of *C. albicans* filamentous forms with *S. mutans* was also supported by previous research showing that *S. mutans* inhibited germ tube formation, the initial phase of *C. albic*ans hyphal transition (Jarosz et al. 2009). However, this was found to only occur with spent medium that was collected during the exponential phase of growth *i.e.* spent media collected from 4 h cultures and was attributed to the quorum-sensing molecule, competence-stimulating peptide (CSP) that was produced during this phase of growth (Jarosz et al. 2009).

The addition of spent media from the different *Streptococcus* species was also examined in this research to assess possible effects of secreted factors and changes in the media, such as resource depletion. This would also give insight as to whether live streptococcal cells needed to be present to facilitate changes in *C. albicans* abundance and morphology. High *C. albicans* surface area coverage was

observed after 24 h in control single species *C. albicans* biofilms. The presence of spent media from any species, including *C. albicans*, resulted in significantly lower surface area coverage by *C. albicans* compared to controls. This was expected due to likely stress responses to spent media through depleted nutritional resources and higher concentrations of waste products. However, another study found that spent media from a mixed biofilm of *C. albicans* and *S. gordonii* and single species did not affect *C. albicans* growth on titanium surfaces (Souza et al. 2020). However, this was assessed at 72 h which supports our results that there were no significant differences in *C. albicans* surface area coverage observed in the 72 h spent media samples. The 72 h fresh medium control had a lower level of *C. albicans* surface area coverage than spent media biofilms. The spent media from *S. mutans* led to lower levels of *C. albicans* surface area coverage than the other *Streptococcus* species but was still higher than the control.

After 24 h, spent media from *Streptococcus* species or *C. albicans* had no significant effect on *C. albicans* hyphal development relative to the *C. albicans* control biofilm. After 72 h, spent media from *S. gordonii* led to increased *C. albicans* filamentation compared to the control. At this time, spent media from the other *Streptococcus* species significantly reduced *C. albicans* filamentous morphology. Purified competence stimulating peptide from *S. gordonii* has been shown to have no effect on *C. albicans* hyphal formation, but inhibited single species biofilm formation by *C. albicans* (Jack et al. 2015). This contrasts with the competence-stimulating peptide produced by *S. mutans* in 4 h spent media, which has bacteriocin activity and inhibited *C. albicans* hyphal development (Jarosz et al. 2009; Sztajer et al. 2014). Spent media (4 h) from *Streptococcus salivarius* was also found to inhibit germ tube formation by 45%, but no effect was found with 24 h spent medium (Jarosz et al. 2009). This supports the current findings which found no significant differences in *C. albicans* filamentation in 24 h biofilms, using 24 h spent media. However, it does not explain the significant decrease in filamentous morphology at 72 h. *Streptococcus mutans* inhibits *C. albicans* hyphal formation through a fatty acid signalling molecule called trans-2- decenoic acid (SDSF) which is also produced by *S. sanguinis* (Vílchez et al. 2010), and perhaps this may contribute to decreased filamentous morphology observed at 72 h.

Previous research has indicated physical cell-to-cell interactions between *C. albicans* and *S. gordonii* requires the *Candida* adhesin Als3 (Silverman et al. 2010; Wright et al. 2013). Therefore, these present studies also aimed to assess the role of Als3 in bacterial interactions with *C. albicans* SC5314. Experiments sought to determine if more streptococcal adhesion occurred with *C. albicans* filamentous forms containing Als3. The presence of Als3 in *C. albicans* significantly increased the number of *S. gordonii, S. salivarius* and *S. sanguinis* bacteria cells associated with the filamentous forms, but the opposite occurred with *S. mutans.* Interactions between *S. mutans* and *C. albicans* are known to be independent of Als3 (Yang et al. 2018), however in the present study, significantly higher association occurred with the *C. albicans* Als3 deleted mutant compared with the wild-type. The presence of Als3 in *C. albicans* hyphae increases cell surface hydrophobicity, which is thought to be due to exposure of hydrophobic tandem repeats (TR) domains of the Als3 adhesin (Beaussart et al. 2012). The lack of Als3 could lower hydrophobicity making these more preferential for *S. mutans* binding compared with the wild-type. Although, there are no reported changes to the regulation of other genes in the Als3 knockout, there could be a mechanism whereby the deletion of Als3 has caused up- or downregulation of other genes that potentially influenced interactions with *S. mutans*. Future work could assess further the relationship between the Als3 deleted mutant *C. albicans* strain and *S. mutans*. It would be beneficial to replicate the dual species biofilm experiments with the *C. albicans* Als3 mutant strain to see how interactions with the *Streptococcus* species is affected, however the mutant strain is unable to form biofilms, as the filamentous forms initially attach but rapidly detach from surfaces (Silverman et al. 2010).

In conclusion, specific oral *Streptococcus* species increased the quantity of *C. albicans* in *in vitro* biofilms on PMMA surfaces. The effect was not evident with spent culture media, suggesting that bacterial cells were required for this effect. No significant changes in terms of filamentous morphology occurred due to presence of the *Streptococcus* species, despite increased *C. albicans* filamentous morphotypes occurring with *S. salivarius* and *S. sanguinis*. Spent media from the *Streptococcus* species significantly lowered *C. albicans* filamentation after 72 h, apart from *S. gordonii* spent medium, which led to an increase. All the *Streptococcus* species bound to filamentous forms of *C. albicans,* and this

appeared to be mediated by the Als3 adhesin of *C. albicans*, except for *S. mutans* whose interaction with *C. albicans* is independent of Als3. These findings are important if they are extrapolatable to *in vivo* conditions since co-occurrence of *C. albicans* with *Streptococcus* on denture material would increase levels of *C. albicans* and promote infection. Therefore, management strategies for *C. albicans* oral biofilm infections should also consider bacterial presence to mitigate their contribution to *Candida* infection.

CHAPTER 5: Effect of Complex Microbial Biofilms Derived from Saliva on the Quantity and Morphology of *Candida albicans*

5.1. Introduction

The oral cavity provides many niches that support extensive networks of commensal microorganisms in interconnected communities, and collectively this is termed the oral microbiome (Yamashita and Takeshita 2017). Historically, microbiologists have attempted to identify specific species as causative agents of oral diseases, for example *Streptococcus mutans* as a cause of dental caries (Loesche et al. 1975). This view is the 'Specific Plaque Hypothesis', which states that rather than just accumulation of plaque causing infection (Non-Specific Plaque Hypothesis), only a selected number of species are involved in infection (Loesche 1976; Rosier et al. 2014). Normally, the oral microbiota is resilient to minor ecological changes, as this symbiotic community can self-regulate and maintain itself to provide a healthy oral environment (Rosier et al. 2018). However, in cases where environmental changes cause longer-term imbalance or dysbiosis to the community, pathogens can become predominant leading to infections (Marsh 1994; Rosier et al. 2014). This is known as the 'Ecological Plaque Hypothesis', which incorporates principles from both the Non-Specific Plaque Hypothesis and the Specific Plaque Hypothesis (Rosier et al. 2014). However, it is now recognised that the complexity of the microbiome as a whole, has a role in the modulation of dental caries. The presence of *S. mutans* alone is not sufficient to explain instigation of disease (Philip et al. 2018). As scientific advancement, specifically new molecular approaches, has occurred, the increasing complexity of the microbiome of human hosts has been recognised along with the role it plays in human physical and mental health (Huttenhower et al. 2012). Additionally, Hajishengallis et al. (2012) outlined the Keystone-Pathogen Hypothesis stating that it is not necessarily the abundance of species that may be responsible for causing disease, but instead the presence of specific species that have the ability to push the microbiota into dysbiosis and interfere with the host immune system.

As discussed in Chapter 4, studies have previously examined interactions of selected groups of bacterial species with *Candida albicans,* but this is a small part of the whole picture (Wright et al. 2013; Cavalcanti et al. 2016a; Cavalcanti et al. 2017; Morse et al. 2019). In order to study the wider picture, microbiome research is moving more towards culture-independent techniques, especially through use of metagenomics (Lazarevic et al. 2012; Segata et al. 2012). The definition of

metagenomics is the direct genetic analysis of genomes within an environmental sample (Thomas et al. 2012). The use of culture-independent techniques is important; the human oral microbiome is one of the most studied human microbial communities, nevertheless it has been shown that approximately a third of the 700 bacterial species identified in the human oral cavity had not been cultivated in 2010 (Chen et al. 2010; Lazarevic et al. 2012). As previously mentioned in Chapter 1, The Human Oral Microbiome Database V3 (eHOMD) database (v9.15) collates the sequences of oral bacterial species and currently there are 774 oral bacterial species (Dewhirst et al. 2010; Human Oral Microbiome Database: HOMD. Accessed [02/03/2023]).

Metagenomic approaches have been used to investigate the community composition in the oral cavity for non-caries and caries environments, where clustering analysis showed that there was a distinct bacterial consortium associated with each of the conditions (Alcaraz et al. 2012). These findings were supported by another metagenomics study, which demonstrated a reduction in microbial diversity in subjects with dental caries (Lee et al. 2016).

Oral bacterial communities that inhabit supragingival plaque, tongue plaque, and saliva are distinct from one another in terms of community composition (Hall et al. 2017). Saliva is an important niche in the oral cavity that has its own defined microbiome comprised of microorganisms shed from oral surfaces and salivary antimicrobials which are crucial for the maintenance of symbiosis between the host and the microbiota (Marsh et al. 2016b; Belstrøm 2020). Saliva is not only an essential coating for surfaces in the oral cavity, but it is key for physiological processes including mastication, swallowing and speech and contains important biological constituents (Belstrøm 2020). In early plaque biofilm development, saliva is the sole source of nutrition for microorganisms, providing salivary mucins and glycoproteins (Jakubovics 2015). The salivary microbiome can reflect oral and general health status and contains a diverse microbiota (Hasan et al. 2014; Belstrøm 2020). The salivary microbiome is distinct from other microbiomes in the human body, and exhibits individualised differences in taxonomic composition and diversity (Cameron et al. 2015; Hall et al. 2017; Shaw et al. 2017). Ecological factors that impact on the saliva microbiome include the climate zones in which people live (Li et al. 2014; Bhushan et al. 2019), diet (De Filippis et al. 2014;

Hansen et al. 2018; Lassalle et al. 2018), dentate status (De Waal et al. 2014; Mason et al. 2018; Gazdeck et al. 2019) and dental development (Crielaard et al. 2011).

Early life development of the salivary microbiome is impacted by ecological perturbations such as mode of birth delivery, breastfeeding duration and antibiotic treatment (Dzidic et al. 2018). Individualisation of the salivary microbiome was shown by a periodic, longitudinal sequencing study of the same individuals for over a year (Cameron et al. 2015). The salivary microbiome is sufficiently diverse between individuals that Illumina® high-throughput sequencing has demonstrated differentiation even between identical twins and provided information on lifestyle factors based on microbial composition (Nasidze et al. 2009; Leake et al. 2016; Shaw et al. 2017). Studies have been conducted that determine changes in the salivary microbiome across a range of host variables including aging (Schwartz et al. 2021), occurrence of diabetes (Bostanci et al. 2021), the menstrual cycle (Bostanci et al. 2021), obesity (Wu et al. 2018), carcinomas (Wolf et al. 2017; Rai et al. 2021), dental caries (Jiang et al. 2016), gastroesophageal reflux (Kawar et al. 2021) and individuals who smoke (Suzuki et al. 2022), amongst many others. Studies suggest that these definitions may provide features in the microbiome that can be used as identifying tools of lifestyle factors and conditions (Wolf et al. 2017). A pilot study has found differences in the salivary microbiome between oral and oropharyngeal squamous cell carcinoma patients and healthy controls (Wolf et al. 2017). Further research is required, but there is evidence to support that salivary microbial biomarkers may lead to better understanding of the disease pathobiology, disease detection, and identify potential therapeutic interventions (Wolf et al. 2017). Liu *et al.* (2021) presented a promising salivary microbiome based auxiliary diagnostic model for type 2 diabetes. Differences in the saliva microbiome of patients with type-2 diabetes and healthy controls was used to develop a diagnostic tool for type-2 diabetes with 80% accuracy (Liu et al. 2021). All this research shows the significance and relevance of microbiome composition in a wide range of fields and why further microbiome exploration is beneficial.

The research within this chapter investigated whether the *in vitro* bacterial biofilm derived from human saliva from separate individuals could differentially influence *Candida albicans* surface colonisation, biofilm growth and morphology, properties

which may be indicative of pathogenicity. The individuality of salivary microbiomes might infer that each biofilm would elicit a varied response from *C. albicans*. The hypothesis is that microbiome differences between saliva from separate individuals will have different bacterial compositions in *in vitro* biofilms and these have a impact on *C. albicans* biofilm behaviour.

5.1.1. Aims and Objectives

The primary aims of this chapter were to:

1. Assess whether the bacterial microbiome of *in vitro* biofilms from human saliva samples from different individuals influenced *Candida albicans* growth and morphology which would be indicative of pathogenicity.
2. Assess whether the *in vitro* biofilms derived from human saliva had differences in bacterial composition that may account for observed differences elicited by *C. albicans*.

5.2. Materials and Methods

5.2.1. Culture conditions for *Candida albicans*

Candida albicans SC5314-GFP was gifted from Dr Angela Nobbs at Bristol University and used for this research. Green fluorescent protein (GFP) expression by this strain would enable its detection and analysis following its artificial contamination in a biofilm derived from whole saliva. This was important, as such biofilms could potentially contain *C. albicans* originating from the saliva. *Candida albicans* SC5314-GFP was cultured as described in section 2.2.1 in supplemented YNB medium for 16-18 h at 37°C with the addition of 5% CO_2.

5.2.2. Saliva collection and processing

Ethical approval for saliva collection and use in this research was obtained from the Dental School Research Ethics Committee at Cardiff University (DSREC reference: 2110a). Saliva was collected from seven self-declared healthy individuals on the day of experimentation (six female and one male). Three volunteers made a second donation of saliva. Samples ES006 and ES006-2 were collected from the same volunteer one month apart. Samples ES001 and ES001-2 were collected 6 months apart and samples ES002 and ES002-2 were 5 months apart. The ES001-2 and ES002-2 samples were used for metagenomic sequencing experiments and not analysed in the other experiments. A total of 5-10 mL of saliva was collected from each volunteer, and guidance on saliva collection was as previously described (Bhattarai et al. 2018). On the day of collection, the saliva sample was standardised to an OD_{600nm} of 1 ± 0.5 using a spectrophotometer (DiluPhotometer™, Implen, Westlake Village, CA, USA). Half of the sample was set aside and designated ‘whole saliva’ while the other half was centrifuged at 3200 rpm for 10 min. The supernatant of this centrifuged saliva was then filtered through a Sterivex™-GP 0.22 µm filter unit (Merck Millipore, Burlington, Massachusetts, United States) and was subsequently referred to as ‘filtered saliva’. One hundred µL of filtered saliva was cultured on SDA and TSA to confirm absence of microorganisms. The whole saliva (100 µl) was plated on SDA supplemented with 1 mg/ml of chloramphenicol to detect possible *C. albicans* presence in saliva samples.

5.2.3. Saliva biofilms artificially contaminated with *Candida albicans*

Biofilms were grown in a CBR 90 Standard CDC Biofilm Reactor® (BioSurface Technologies Corporation, Montana, USA) system (Figure 5.1). Polycarbonate disc coupons with a diameter of 12.7 mm and of 3.8 mm thickness (RD128-PC, BioSurface Technologies Corporation) were autoclaved in dH_2O for 5 min at 121°C, before being added to the rod holders of the CDC reactor and the whole apparatus was sterilised by autoclaving. A 400-mL volume of sterile, 10% (w/v) strength TSB (3 g/L) was added to each CDC bioreactor along with 1 mL of *C. albicans* SC5314-GFP standardised to an OD_{600nm} of 1 ± 0.5. For each saliva sample, two CDC bioreactors were employed, with 4 mL of either whole saliva or filtered saliva used to separately inoculate each bioreactor. CDC bioreactors were placed on magnetic stirrer plates and incubated at 37°C for 24 h. After incubation, the CDC rods containing the coupons were immersed in PBS before the coupons were removed into a sterile petri dish. From each CDC bioreactor, three coupons were placed in 1 mL of PBS and stored at 4°C prior to imaging by confocal laser scanning microscopy (CLSM). Another three coupons were placed in DNA/RNA Shield buffer (Zymo Research), vortex mixed and stored at -20°C. A further three coupons were fixed in 10% (w/v) formal buffered saline for 15-30 min before being placed in PBS and stored at 4°C prior to being processed for Scanning Electron Microscopy. Figure 5.1 summarises the research workflow.

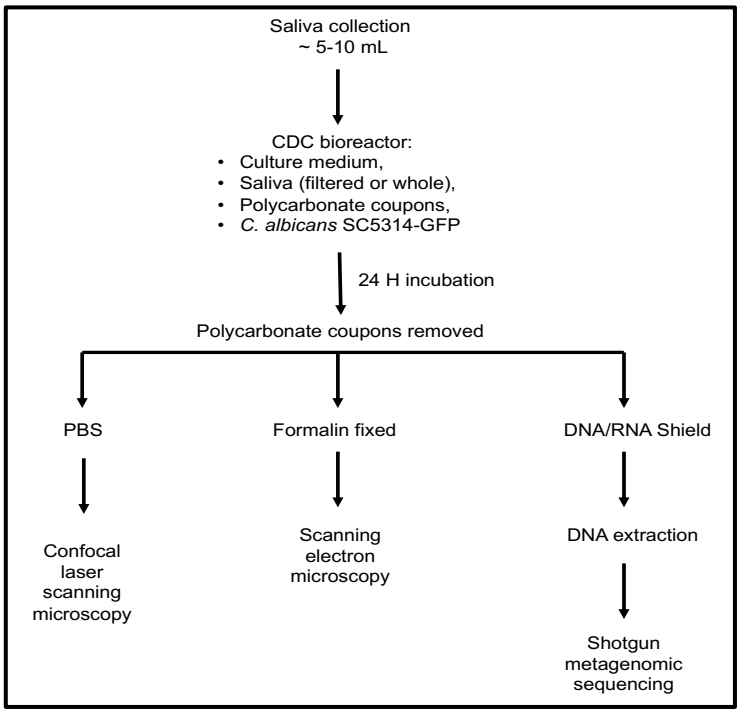

Figure 5.1. Overview of methodology for growth and analysis of saliva derived biofilms artificially contaminated with *C. albicans* SC5314-GFP.

5.2.4. Confocal laser scanning microscopy of saliva biofilms on polycarbonate disc coupons

Biofilms on coupons were imaged using a Zeiss LSM880 Airyscan Fast system upright confocal microscope controlled by Zen Black software (Zen 2.3 SP1 FP3 (black) Version: 14.0.20.201) at the Cardiff University Bioimaging Hub. No staining was required as only the SC5314-GFP strain was detected. The excitation spectra and emission filters used were 488 nm and 509 nm, respectively. Three-dimensional Z-stacks were captured using the Plan-Apochromat 40x/1.4 oil immersion objective lens from five randomly selected areas of each coupon at intervals of 1 µm with a scanning resolution of 1024-1024 pixels and x4 line averaging. Resultant z-stacks were processed using Zen Black software into maximum intensity projection TIFF images that were analysed using ImageJ2 software (Version 2.3.0) to determine the percentage of area coverage of *C. albicans* averaged across each coupon. Imaris viewer 9.9.1 software was used to render 3D view images of the z-stacks using the MIP mode and the snapshot function was used to produce representative images of the samples.

5.2.5. Quantification of *C. albicans* hyphae in saliva derived biofilms

The area of *C. albicans* filamentous forms in biofilms was determined using the freehand drawing tool in Fiji ImageJ software (Version:2.0.0-rc-69/1.52p Build: 269a0ad53f) to draw around the filamentous forms and using 'Measure' to calculate the resulting occupied area within each frame. The measured area of filamentous forms and total surface area were used to determine the percentage area covered by *C. albicans* filaments. The fields of view analysed from each coupon for hyphal analysis were randomly selected.

5.2.6. Statistical analysis of differences in *C. albicans* area coverage in biofilms

GraphPad Prism 9 (Version 9.4.0) was used to collate data, produce graphs, and run statistical analyses including normality testing and to determine whether there were statistically significant differences in *C. albicans* SC5314-GFP percentage area surface coverage between samples. When the data was not Gaussian (normally distributed) based on Shapiro-wilk and Q-Q plots, a non-parametric Mann Whitney U test was performed. When samples were normally distributed, a student's t-test was used. Comparison between biofilms of all whole saliva samples and between filtered saliva samples were assessed for statistical significance using One-Way ANOVA with Tukey's post-hoc test or Kruskal-Wallis test with Dunn's test for multiple comparisons depending on whether the data was normally distributed. Comparison was also conducted between the ES006 and ES006-2 samples, which were collected from the same volunteer, one month apart and statistical significance between the data was determined using a One-Way ANOVA with Tukey's post hoc test for multiple comparisons.

5.2.7. Scanning Electron Microscopy (S.E.M) of saliva derived biofilms on polycarbonate disc coupons.

S.E.M was undertaken with assistance of Mrs Wendy Rowe at Cardiff University School of Dentistry. Formalin fixed samples were rinsed three times with PBS for 15 min before being dehydrated in an ethanol gradient series (50%, 70%, 90% and

100%) for 15 min at each concentration. The 100% ethanol step was repeated for a further 15 min before the samples were air dried. The polycarbonate coupons were then attached to S.E.M stubs and splutter coated in gold before being imaged on a Tescan VAGA SEM system, at 5-10kV.

5.2.8. Metagenomic analysis

5.2.8.1. DNA extraction from saliva-derived biofilms for low DNA yielding samples.

DNA extraction was initially undertaken using the DNeasy Blood and Tissue kit (Qiagen) following manufacturer's instructions for extraction from animal saliva. However, Qubit measurements (5.2.8.2) of DNA extractions determined that DNA concentrations were initially too low for input into the library preparation and sequencing. Therefore, an alternate method for DNA extraction was performed using the DNeasy® PowerBiofilm® Kit (Qiagen) as per manufacturer's instructions. Coupons exposed to the same saliva inoculum were pooled and the surface of each coupon scraped to increase biofilm removal into solution. For example, the three replicates of the ES001 whole saliva coupons from the same CDC bioreactor were thawed, vortex mixed and the solution from all samples centrifuged to a pellet. The exception to this was the ES002-2 and ES001-2 samples where instead of three coupons being pooled the number was increased to 18 coupons. Polycarbonate coupons in RNA/DNA shield solution were thawed and vortex mixed for ~30 s. One mL at a time was taken for DNA extraction and placed in a 2 mL microcentrifuge tube and centrifuged at 8000 x *g* for 5 min to pellet until all of the material was pelleted. The weight of each pellet was recorded. The pellet was resuspended in 350 µL of MBL solution and transferred to the PowerBiofilm bead tube and 100 µL of solution FB added. The tube was vortex mixed before being incubated at 65°C for 5 min. The tubes were placed in a FastPrep-24 Sample Preparation System Homogenizer (MP Biomedicals) at 6.0 m/s for 30 s, repeated five times with 3-5 min intervals between to ensure over heating did not occur. All centrifugations were at 13,000 x *g* unless otherwise stated. The tubes were centrifuged for 1 min and the supernatant transferred to new 2 mL collection tubes. Two hundred µL of solution IRS was added and vortex mixed before incubation at 2-8°C for 5 min. After incubation the tubes were centrifuged for 1 min and the

supernatant transferred to a new collection tube before 900 µL of solution MR was added and vortex mixed briefly. All of the sample was added to an MB spin column 650 µL and centrifuged for 1 min and the flow through discarded. The MB spin column was added to a new collection tube and 650 µL of solution PW added, and centrifuged for 1 min. The flow through was discard before 650 µL of ethanol was added and centrifuged for a further 1 min. The flow through was discarded before a second centrifugation for 2 min to ensure all the ethanol was removed from the spin column. The spin column was placed in a new collection tube and 100 µL of solution EB added to the middle of the filter membrane of the spin column, and centrifuged for 1 min. The spin column was discarded and the flow through containing extracted DNA was stored at -20°C. Samples were then delivered to the Cardiff University Biosciences Genomics Hub for sequencing.

5.2.8.2. Qubit measurements

Samples were quantified using the Qubit™ dsDNA HS assay kit (Invitrogen) as per manufacturer's instructions. The standards were prepared for calibration of the Qubit™ Fluorometer. The Qubit™ working solution was then prepared by the Qubit™ dsDNA HS reagent 1:200 in the Qubit™ dsDNA HS buffer. Ten µL of each Qubit™ standard was added to the appropriate tube. Five µL of each DNA extraction sample and 195 µL of the Qubit™ working solution were added to appropriate tubes and vortex mixed for 3-5 s. All tubes, including the standards, were incubated for 2 min at room temperature. Standards and samples were then measured using the Qubit™ Fluorometer, the output of which is given in ng/µL.

5.2.8.3. Metagenomic sequencing of saliva derived *in vitro* biofilms.

Extracted DNA samples were transferred to Cardiff University School of Biosciences Genomics Hub for shotgun whole genome sequencing. An overview of the sequencing workflow is given in Figure 5.2. Illumina® DNA PCR free library preparation was used to prepare libraries which were then quantified using the qPCR Collibri™ library quantification kit (Thermo Fisher Scientific) as per manufacturer's instructions. Either the low input (< 100 ng total DNA) procedure or the standard preparation (>100 ng total DNA) was used. Libraries were then pooled to equimolar concentrations. The pool was then run on a Miseq Nano 300 cycle cartridge to check pooling and success of the library preparation. Libraries were

repooled based on the cluster formation from the Nano run. The new pool was then run on an SP 300 cycle v1.5 Nova Seq cartridge to sequence at the required depth of 20M reads per sample.

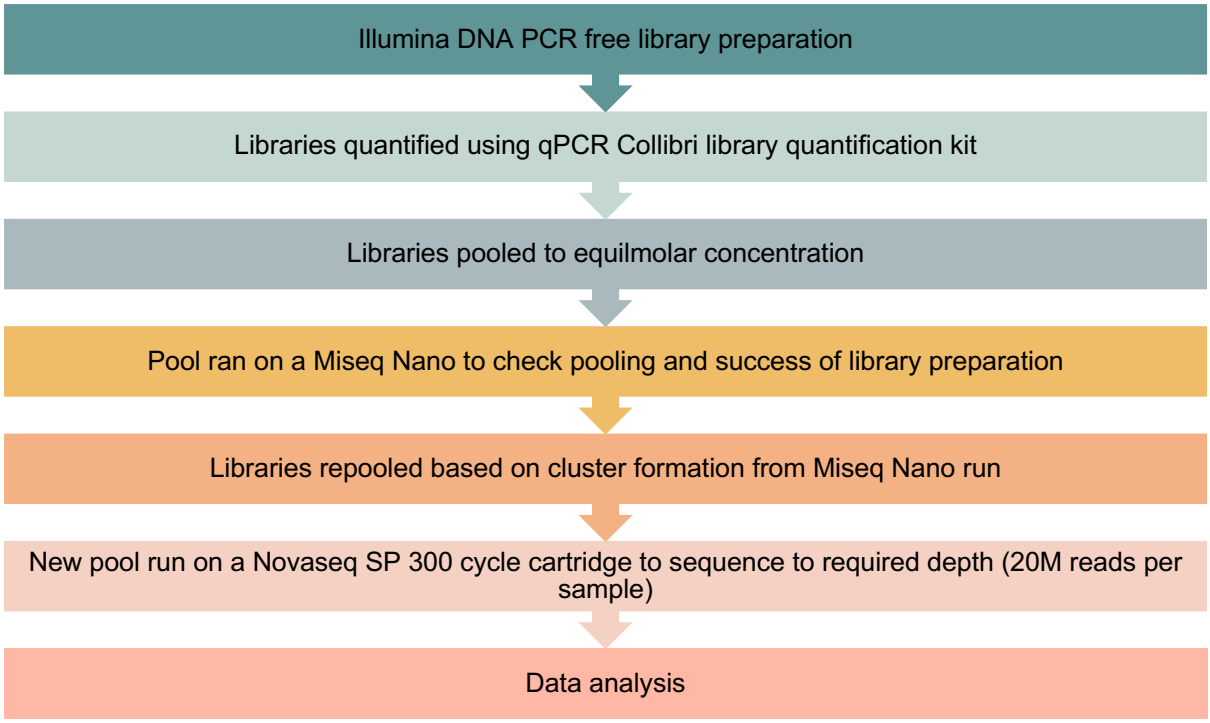

Figure 5.2. Overview of the metagenomic sequencing process conducted at the School of Biosciences Genomics Hub at Cardiff University.

5.2.8.4. Metagenomic sequencing analysis

Firstly, the sequences required demultiplexing and conversion into fastq files, which was undertaken by Prof. Peter Kille (Cardiff University, School of Biosciences). Data analysis was conducted using Kraken2, which used *k*-mers to identify the taxonomy of the sequences in the samples by finding the lowest common ancestor that contains that *k*-mer (Wood and Salzberg 2014). The Krona interactive metagenomics tool (Ondov et al. 2011) was used to visualise the kraken output. The Kraken output was also run through the Pavian R package and a MultiQC (v1.9) report was created.

All the bacterial species were selected from the excel file created from the kraken output of all organisms found in the samples. Any cells that had 'NA' (not applicable), were replaced with a 0 (zero). The top 500 species were selected for analysis, and the abundance values converted into percentages. The top 500

species data and the metadata from the study was input into STAMP software (Parks et al. 2014). STAMP software was used to conduct statistical analyses between samples, testing the difference between proportions using the Storey FDR correction (Velsko et al. 2019). Some figures from the top 500 bacterial species were also constructed using Microsoft Excel. Assistance in using STAMP was provided by Dr Ann Smith (School of Health and Social Wellbeing, University of the West of England, Bristol).

5.3. Results

5.3.1. Surface area coverage of *Candida albican*s SC5314-GFP in biofilms derived from saliva.

Percentage surface area coverage of *C. albicans* SC5314-GFP in *in vitro* biofilms generated from whole and filtered saliva inocula was measured (Table 5.1). Representative images and S.E.M scans for one saliva sample is presented in Figure 5.3. Biofilms derived from three saliva samples ES001, ES003 and ES004 (Figure 5.4a. A, B and C) showed significantly lower surface area coverage of C. albicans SC5314-GFP when grown in the whole saliva derived biofilm compared with the corresponding filtered saliva ($P \leq 0.0006$, $P \leq 0.0003$, and $P \leq 0.0001$, respectively). In contrast, an opposite effect was observed in biofilms from saliva samples ES005, ES002 and ES007 (Figure 5.4a. and Figure 5.4b.). In these biofilms, those from whole saliva had a significantly higher *C. albicans* SC5314-GFP surface area coverage than the corresponding filtered saliva biofilms ($P \leq 0.0002$, $P \leq 0.0002$, and $P \leq 0.0008$, respectively). The surface area coverage by *C. albicans* SC5314-GFP in the biofilm from saliva ES006 (Figure 5.4b.) exhibited no difference between whole (6.45%) and filtered saliva (8.97%). Biofilms from saliva ES006-2 (Figure 5.4b.), which was collected from the same volunteer as ES006, also showed equivalent levels of surface coverage by *C. albicans* SC5314-GFP in the whole and filtered saliva derived biofilms (7.41%). In terms of surface area covered by *C. albicans* SC5314-GFP, saliva samples ES006 and ES006-2 yielded consistent results with no significant differences (Figure 5.5). This was true for both whole and filtered saliva biofilms. There were small differences in *C. albicans* SC5314-GFP surface area coverage for ES006 and ES006-2 whole saliva samples (6.45% and 7.40%, respectively) and filtered saliva biofilms taken one month apart (8.97% and 7.41%, respectively).

Table 5.1. Mean surface area covered by *C. albicans* in filtered and whole saliva-derived biofilms. The mean surface area of *C. albicans* and the standard error of the mean (SEM) are presented in the table. *ES006-2 was collected from the same participant as sample ES006.

	Surface area coverage by *C. albicans* (%)			
	Filtered Saliva Biofilm		**Whole Saliva Biofilm**	
Saliva sample	**Mean**	**SEM**	**Mean**	**SEM**
ES001	12.65	1.99	4.36	0.82
ES002	2.85	0.83	7.97	0.83
ES003	4.13	0.46	1.47	0.45
ES004	13.85	3.41	0.60	0.15
ES005	4.09	0.79	16.94	2.97
ES006	8.97	0.96	6.45	0.96
ES007	2.99	0.24	8.67	1.49
ES006-2*	7.41	1.29	7.41	1.17

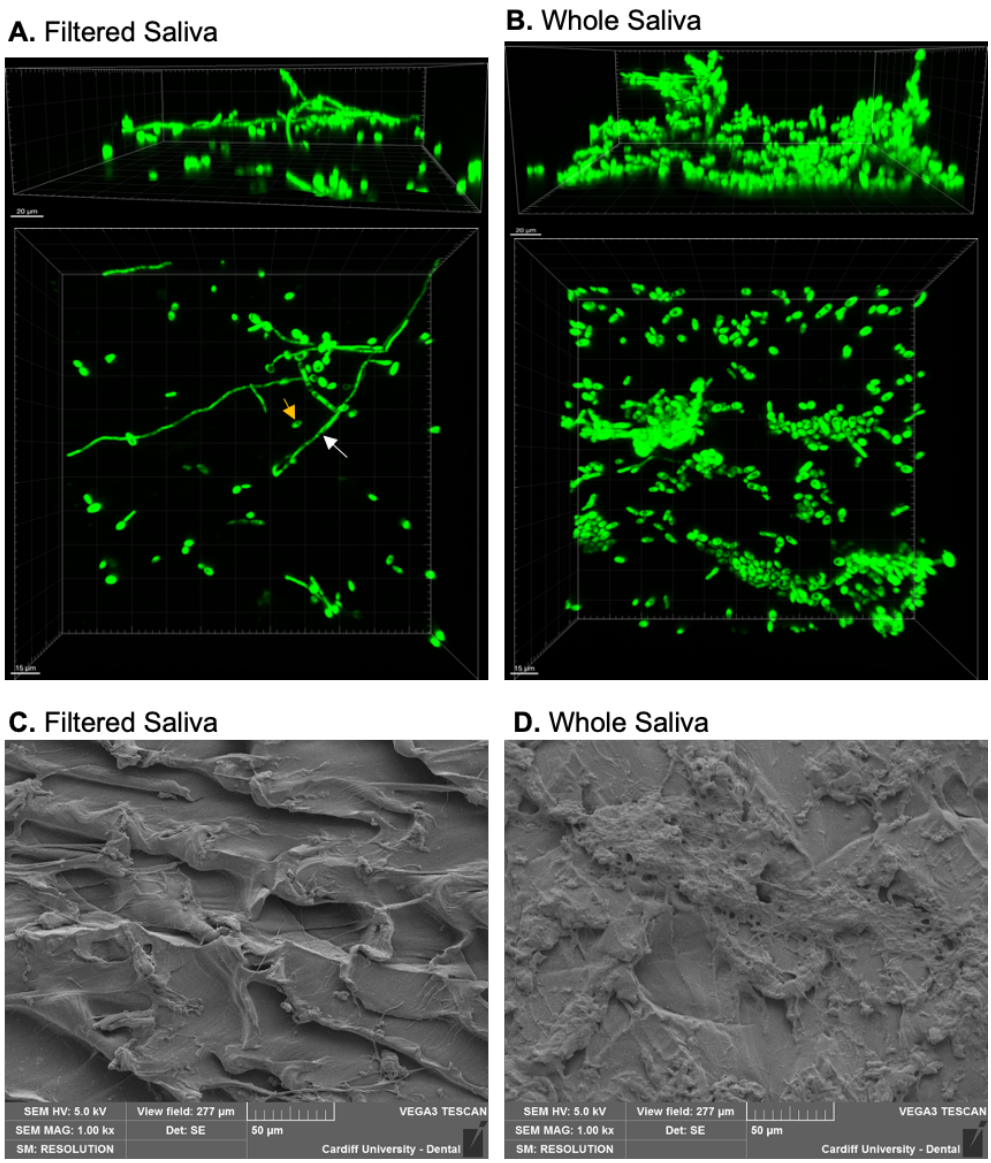

Figure 5.3. Representative 3D projection images of *C. albicans* SC5314-GFP in biofilms from ES007 filtered (A) and whole saliva (B). Representative S.E.M images of ES007 filtered saliva (C) and whole saliva (D) on the polycarbonate coupon surface. For the 3D projection images, both a side view and a top-down view were created on Imaris software from the CLSM z-stack images. The white arrow indicates a hyphal cell, and the orange arrow indicates a yeast morphological form. Scale bars in the side view images are 20 µm and the scale bars for the top-down views are 15 µm. S.E.M images show the topology of the surface to be irregular and the presence of cells can be seen on the surfaces.

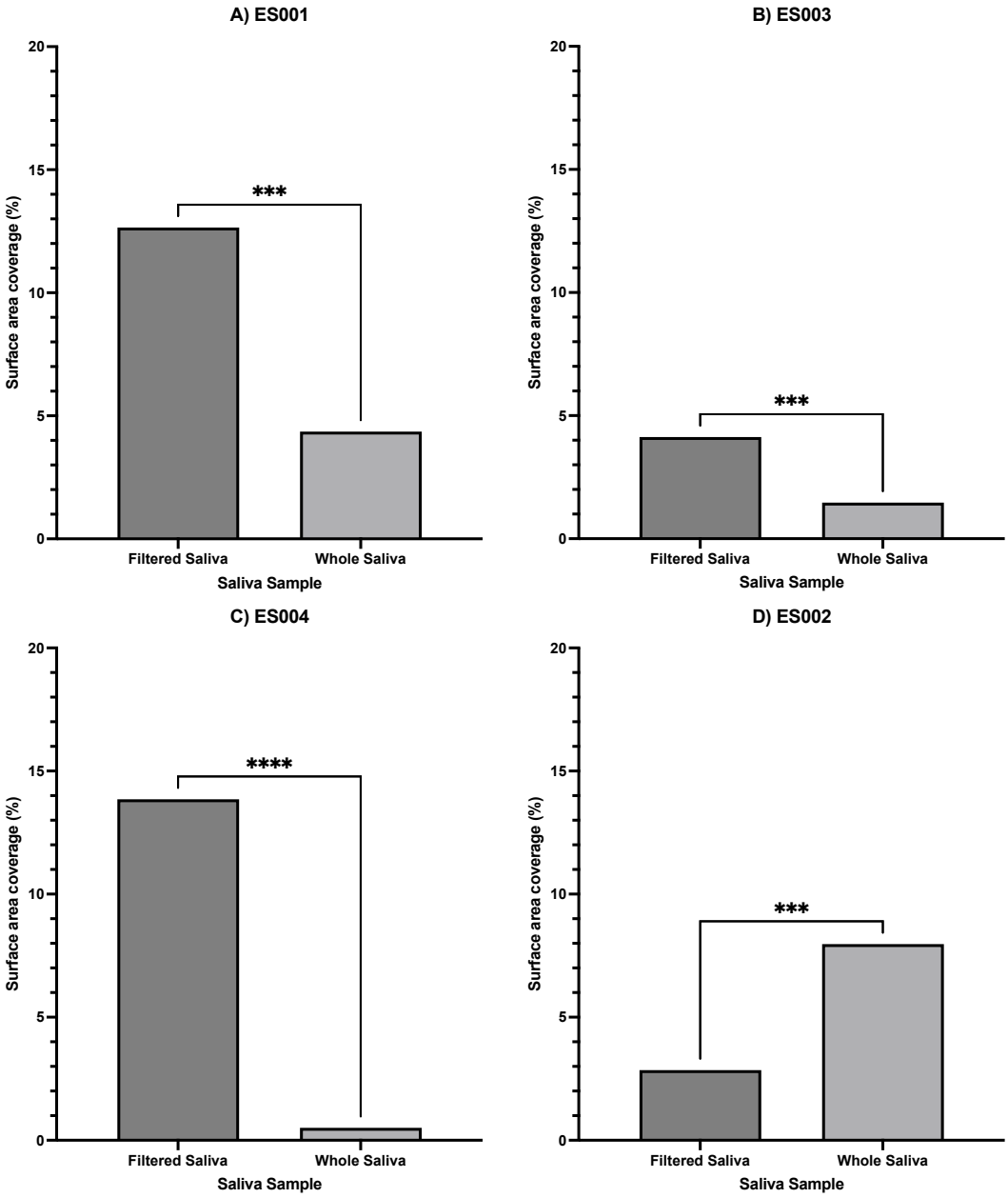

Figure 5.4a. Mean percentage surface area coverage of *Candida albicans*-GFP on polycarbonate coupon surfaces grown with whole saliva compared to filtered saliva from ES001 (A), ES003 (B), ES004 (C) and ES002 (D). Saliva samples were collected from volunteers, artificially contaminated with *C. albicans* SC5314-GFP and used to grow biofilms on the same day as collection. Max projection images from the CLSM z-stacks were analysed to determine the percentage surface area coverage of the *C. albicans* SC5314-GFP strain. Significance was tested using an unpaired t-test except for C) ES004 where the Mann-Whitney U test was used. * $P \leq 0.05$. ** $P \leq 0.01$. *** $P \leq 0.001$. **** $P \leq 0.0001$..

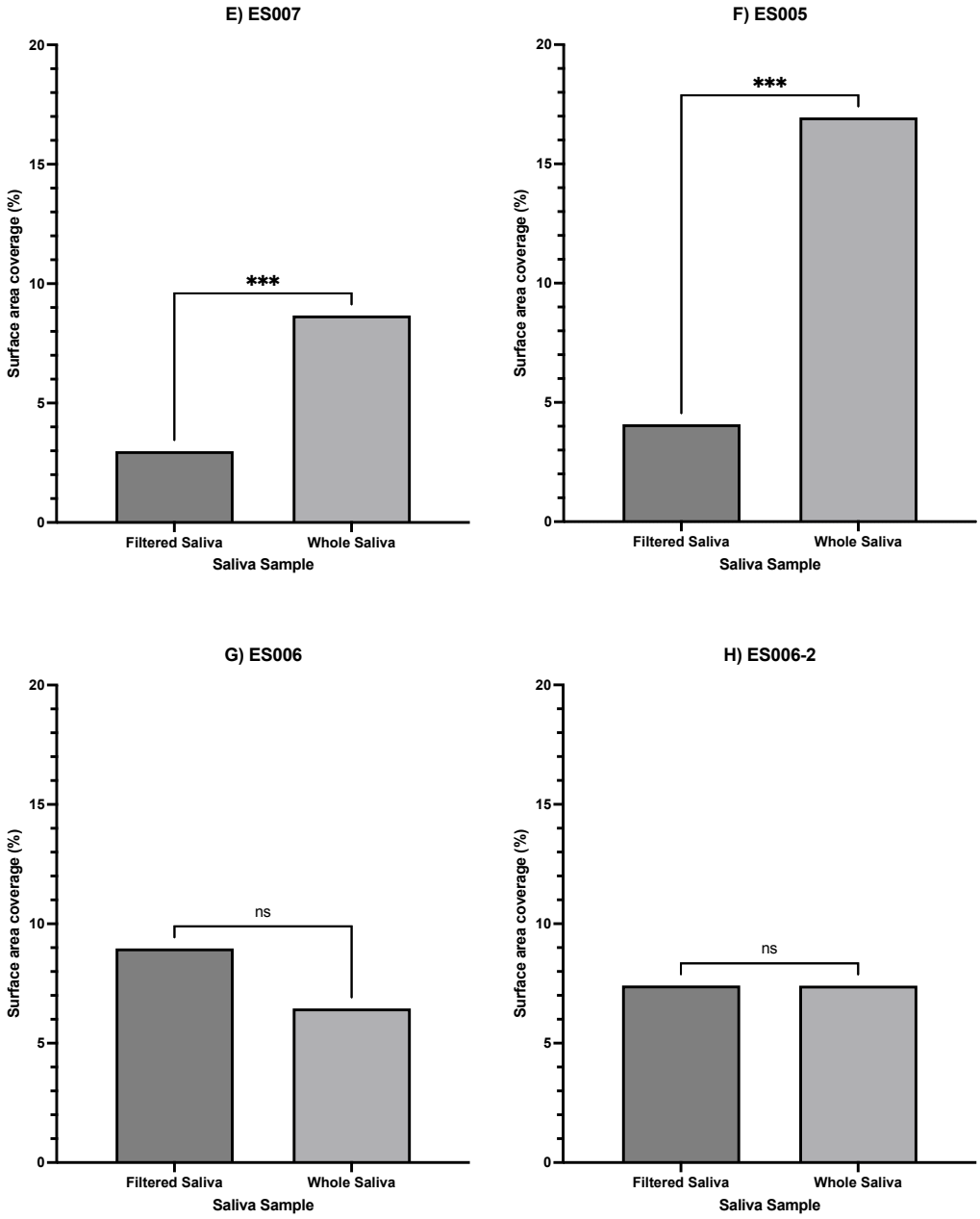

Figure 5.4b. Mean percentage surface area coverage of *Candida albicans*-GFP on polycarbonate coupon surfaces grown with whole saliva compared to filtered saliva from ES007 (E), ES005 (F), ES006 (G) and ES006-2 (H). Saliva samples were collected from volunteers, artificially contaminated with *C. albicans* SC5314-GFP and used to grow biofilms on the same day as collection. Max projection images from the CLSM z-stacks were analysed to determine the percentage surface area coverage of the *C. albicans* SC5314-GFP strain. Significance was tested using an unpaired t-test except for F) ES005 where the Mann-Whitney U test was used. ns = no significance * $P \leq 0.05$. ** $P \leq 0.01$. *** $P \leq 0.001$. **** $P \leq 0.0001$.

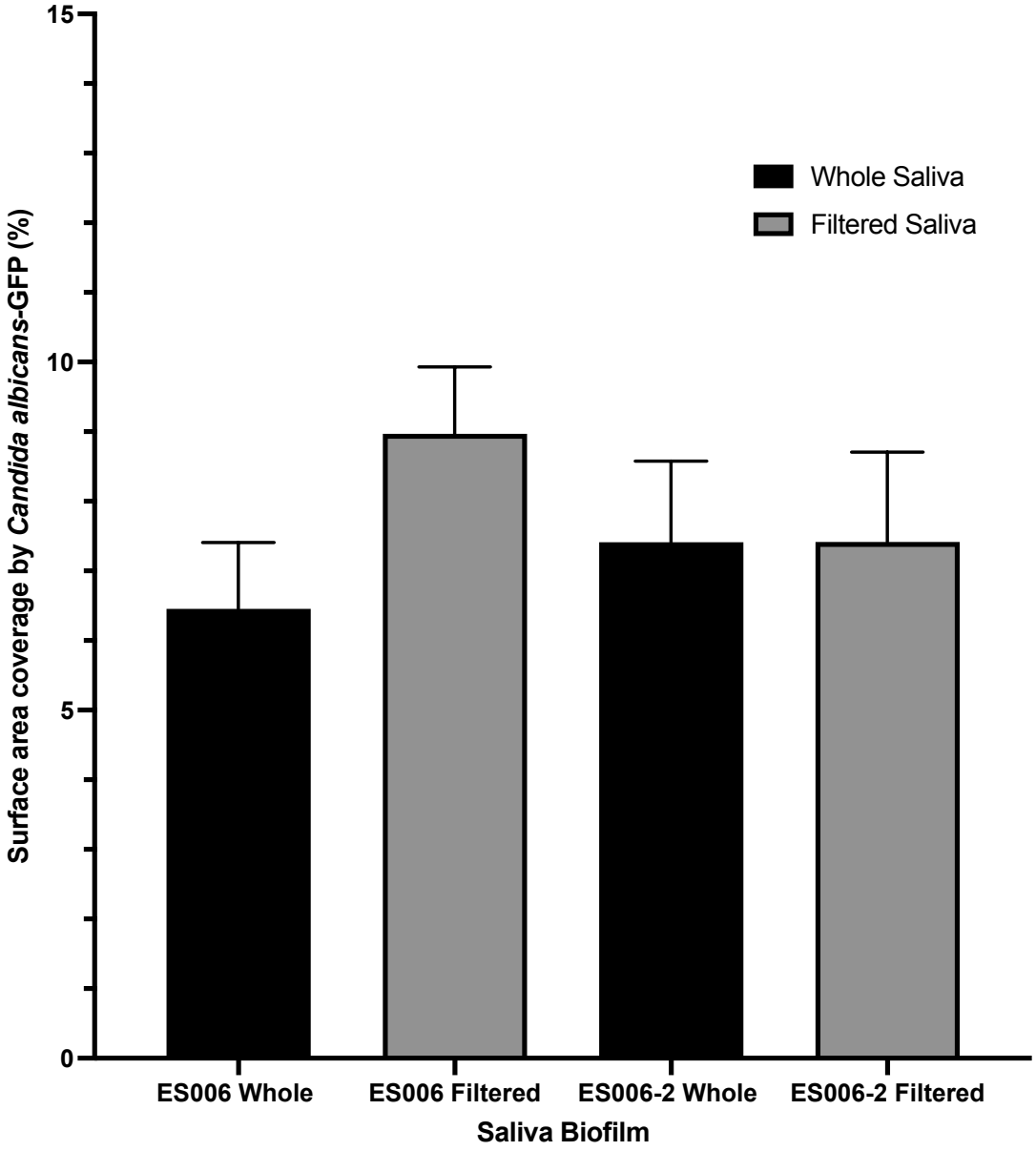

Figure 5.5. Mean percentage surface area coverage by *C. albicans* SC5314-GFP in biofilms derived from ES006 and ES006-2 saliva. The two saliva samples were collected from the same individual one month apart and biofilms were grown the same day as collection. Both the whole and filtered saliva were artificially contaminated with *C. albicans* SC5314-GFP. Max projection images from the CLSM z-stacks were analysed to determine the percentage surface area coverage of the GFP strain. Significance was tested using One-Way ANOVA (F (3, 56) = 0.890, $P \leq 0.4520$) with Tukey's post hoc test for multiple comparisons. No statistical significance was found between the groups.

Comparison between surface area coverage by *C. albicans* in whole saliva derived biofilms from the different volunteers was undertaken (Figure 5.6). The biofilm derived from saliva ES006-2 was not included in the comparison, as it was taken from the same volunteer as saliva ES006. When comparing whole saliva biofilms from individual samples, several significant differences were evident (Figure 5.6). The ES004-whole saliva biofilm had the lowest level of mean surface area coverage by *C. albicans* SC5314-GFP (0.60%), which was significantly lower than five of the other whole saliva biofilm samples *i.e.,* ES005 ($P \leq 0.0001$), ES006 ($P \leq 0.0011$), ES002 ($P \leq 0.0001$), ES001 ($P \leq 0.0448$) and ES007 ($P \leq 0.0001$). The ES003-whole saliva derived biofilm exhibited the second lowest surface area coverage (1.47%) and this was significantly different from biofilms from whole saliva ES002 ($P \leq 0.0013$), ES005 ($P \leq 0.0001$), ES006 ($P \leq 0.0325$) and ES007 ($P \leq 0.0021$). In addition, the ES005-whole saliva biofilm had a significantly higher *C. albicans* SC5314-GFP surface area coverage than for the ES001-whole saliva biofilm ($P \leq 0.0219$). The biofilm from ES005-whole saliva had the highest *C. albicans* SC5314-GFP percentage surface area coverage (16.94%) compared with whole saliva derived biofilms from all other individuals.

Of the filtered saliva-derived biofilms (Table 5.1), the highest *C. albicans* SC5314-GFP percentage surface area coverage was for saliva samples ES001 (12.65%) and ES004 (13.85%) (Figure 5.7). Biofilms from ES002 -filtered (2.85%) and ES007-filtered (2.99%) saliva had the lowest percentage *C. albicans* SC5314-GFP surface area coverage. Comparison of the percentage surface area coverage by *C. albicans* SC5314-GFP in biofilms of filtered saliva showed several significant differences (Figure 5.7). Biofilm from ES001-filtered saliva had significantly higher surface area coverage of *C. albicans* SC5314-GFP than biofilms from ES002 -filtered ($P \leq 0.0001$), ES005-filtered ($P \leq 0.0399$) and ES007-filtered ($P \leq 0.0042$) saliva. The ES002 -filtered saliva biofilm also showed significantly lower surface coverage by *C. albicans* SC5314-GFP than biofilms from ES004-filtered ($P \leq 0.0008$) and ES006-filtered ($P \leq 0.0009$) saliva. Similarly to the ES002 -filtered saliva biofilm, biofilm from ES007-filtered saliva also exhibited significantly lower percentage surface area coverage of *C. albicans* SC5314-GFP than biofilms from ES004-filtered ($P \leq 0.0235$) and ES006-filtered ($P \leq 0.0276$) saliva samples.

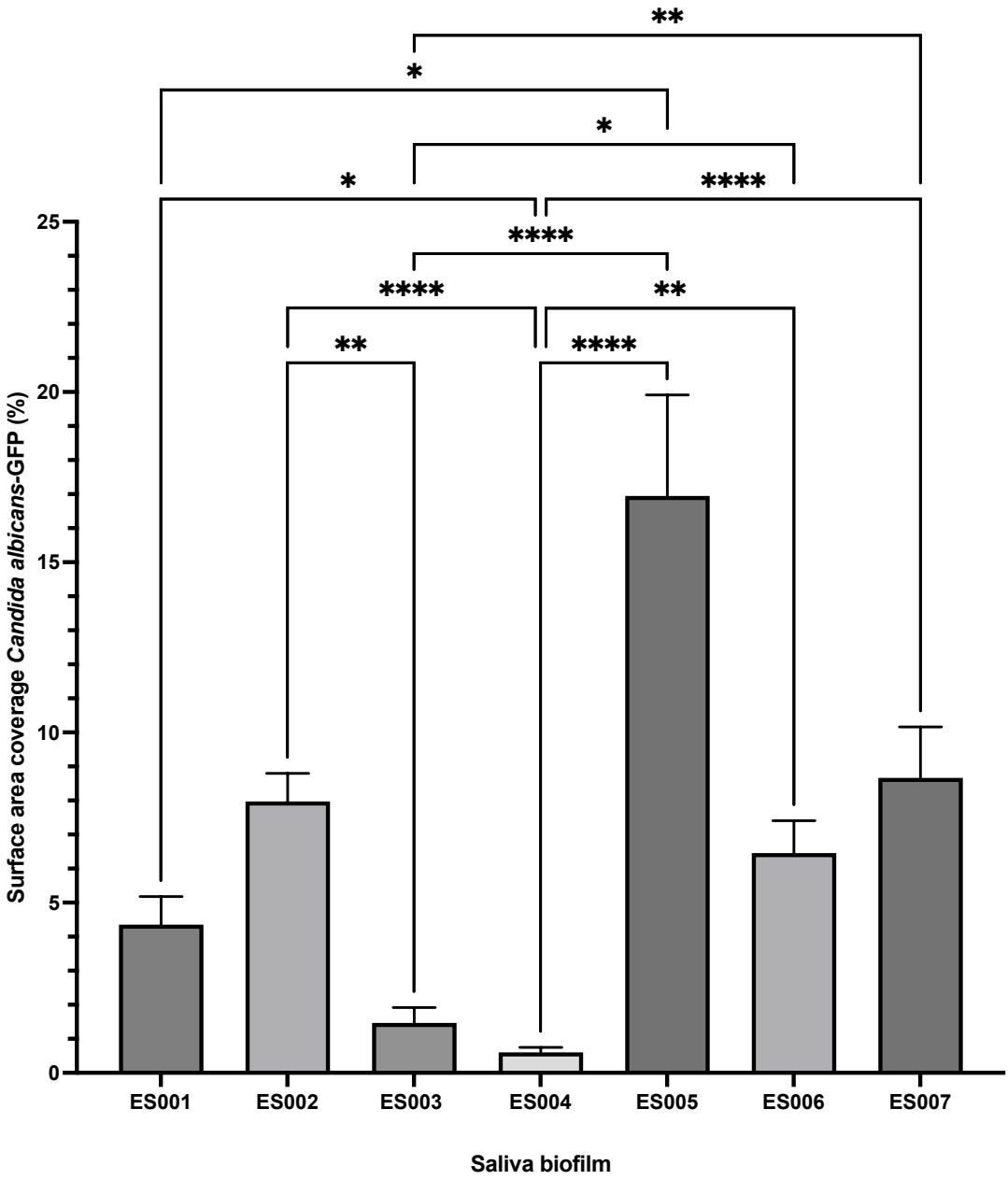

Figure 5.6. Mean percentage surface area coverage of *Candida albicans*-GFP in biofilms derived from seven different whole saliva samples artificially contaminated with *C. albicans* SC5314-GFP. Saliva samples were collected from the volunteers, artificially contaminated with *C. albicans* SC5314-GFP and used to grow biofilms on the same day as collection. Max projection images from the CLSM z-stacks were analysed to determine the percentage surface area coverage of the *C. albicans* SC5314-GFP strain. Significance was tested using Kruskal-Wallis test (H (6) = 63.13, $P \leq 0.0001$) with Dunn's multiple comparisons test. * $P \leq 0.05$. ** $P \leq 0.01$. *** $P \leq 0.001$. **** $P \leq 0.0001$.

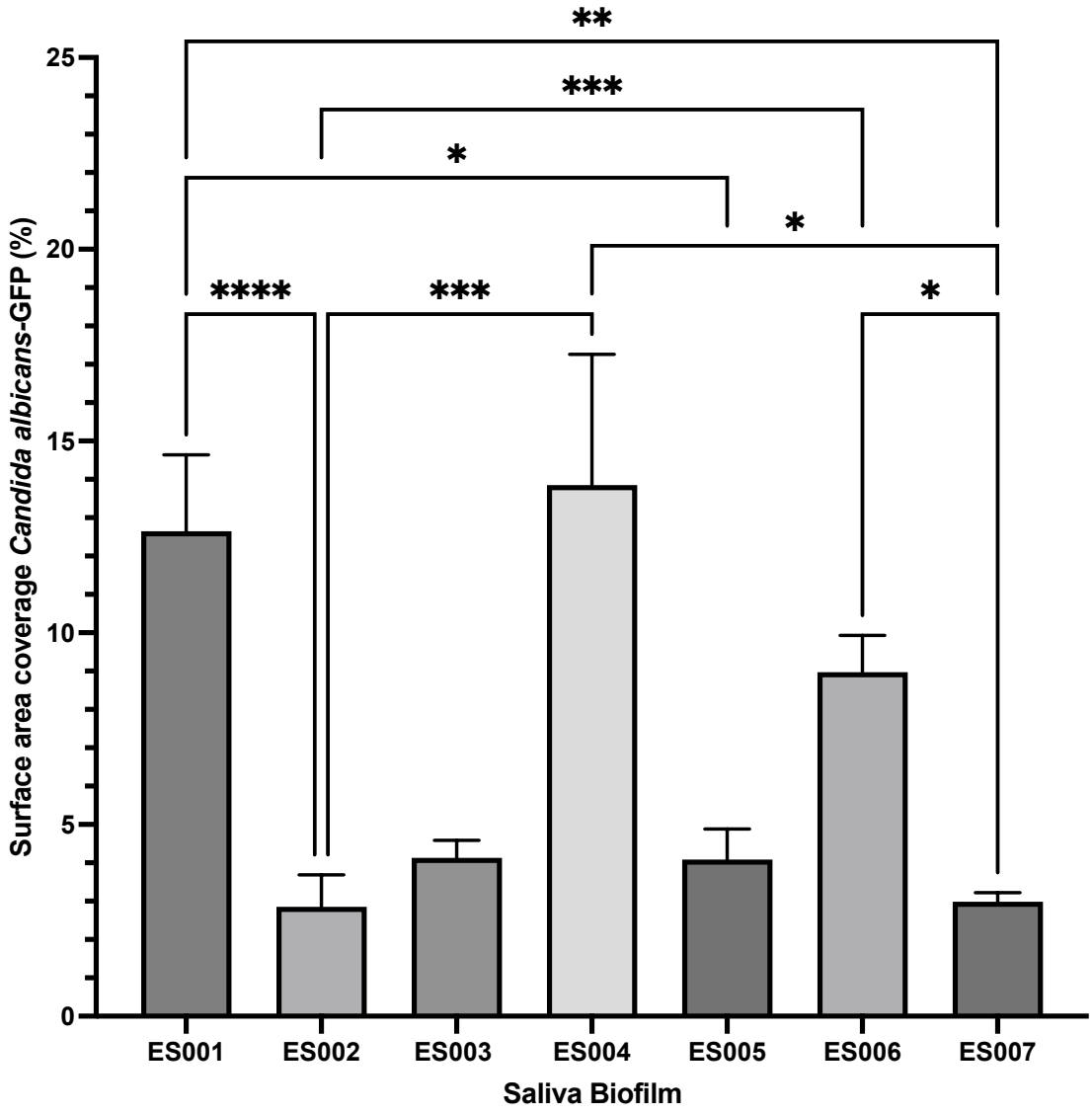

Figure 5.7. Mean percentage surface area coverage of *Candida albicans*-GFP in biofilms derived from seven different filtered saliva samples artificially contaminated with *C. albicans* SC5314-GFP. Saliva samples were collected from volunteers, filtered, artificially contaminated with *C. albicans* SC5314-GFP and used to grow biofilms on the same day as collection. Max projection images from the CLSM z-stacks were analysed to determine the percentage surface area coverage of the *C. albicans* SC5314-GFP strain. Significance was tested using Kruskal-Wallis test (H (6) = 39.68, $P \leq 0.0001$) with Dunn's multiple comparisons test. * $P \leq 0.05$. ** $P \leq 0.01$. *** $P \leq 0.001$. **** $P \leq 0.0001$.

5.3.2. *Candida albican*s SC5314-GFP filamentous morphological types in biofilms derived from saliva.

The effect of saliva from different volunteers on the abundance of filamentous forms of *C. albicans* was investigated (Table 5.2). The percentage area of filamentous forms of *C. albicans* SC5314-GFP was compared for biofilms derived from the whole and filtered saliva from each volunteer (Table 5.2, Figure 5.8 and Figure 5.). Only two of the saliva samples (ES007 and ES006) yielded biofilms that had a significant difference in the area of *C. albicans* SC5314-GFP filamentous forms in the whole saliva compared to filtered saliva derived biofilms ($P \leq 0.0089$ and $P \leq 0.0357$, respectively). In biofilms from ES007 and ES006 saliva samples (Figure 5.), the filtered saliva biofilm had a significantly higher level of *C. albicans* filamentous forms. All other samples were not significantly different, although in the ES005-saliva derived biofilms the whole saliva had a higher level of filamentous forms (0.093%) than the filtered saliva biofilms (0.0014%). The ES004-saliva biofilms showed a slight decrease in area of filamentous forms in the whole saliva compared to the filtered (0.015% and 0.036%, respectively). ES001, ES003, ES002 and ES006-2 saliva biofilms, all had consistent levels of *C. albicans* filamentous forms between the whole and filtered saliva biofilms (Figure 5.8 and Figure 5.). The quantity of *C. albicans* filamentous forms was compared for the ES006 and ES006-2 samples (Figure 5.9) and was significantly higher in the biofilm from the ES006-filtered saliva than in the biofilm from the whole ES006 saliva and biofilms derived from the ES006-2 whole and filtered saliva ($P \leq 0.0045$ and $P \leq 0.0061$, respectively).

Biofilms from the whole saliva of each volunteer mainly exhibited a consistent level of filamentous forms of *C. albicans* ranging from 0.0052% to 0.0145% (Figure 5.10). An exception was ES005, which was higher at 0.093%, although not deemed to be statistically significant. Comparison between mean areas of filamentous forms of the *C. albicans* between filtered saliva from the different volunteers showed no significant differences (Figure 5.11). However, biofilms derived from the ES006, ES004 and ES007 saliva all had observably higher areas of *C. albicans* filamentous forms than ES001, ES002, ES003 and ES005 biofilms. Saliva ES006 biofilm had the highest *C. albicans* filamentous morphology percentage area (0.073%) and ES005 had the lowest (0.0014%).

Table 5.2. Mean percentage area of *C. albicans* filamentous morphologies in filtered and whole saliva-derived biofilms. The mean percentage area of *C. albicans* filamentous forms and the standard error of the mean (SEM) are presented in the table. ***** ES006-2 was collected from the same participant as sample ES006.

	***C. albicans* filamentous morphology area (%)**			
	Filtered Saliva Biofilm		**Whole Saliva Biofilm**	
Saliva sample	**Mean**	**SEM**	**Mean**	**SEM**
ES001	0.0070	0.0026	0.0052	0.0033
ES002	0.0028	0.0028	0.0080	0.0060
ES003	0.0094	0.0028	0.0106	0.0084
ES004	0.0364	0.0304	0.0145	0.0063
ES005	0.0014	0.0001	0.0930	0.0453
ES006	0.0729	0.0175	0.0126	0.0082
ES007	0.0264	0.0017	0.0116	0.0026
ES006-2*	0.0064	0.0030	0.0031	0.0017

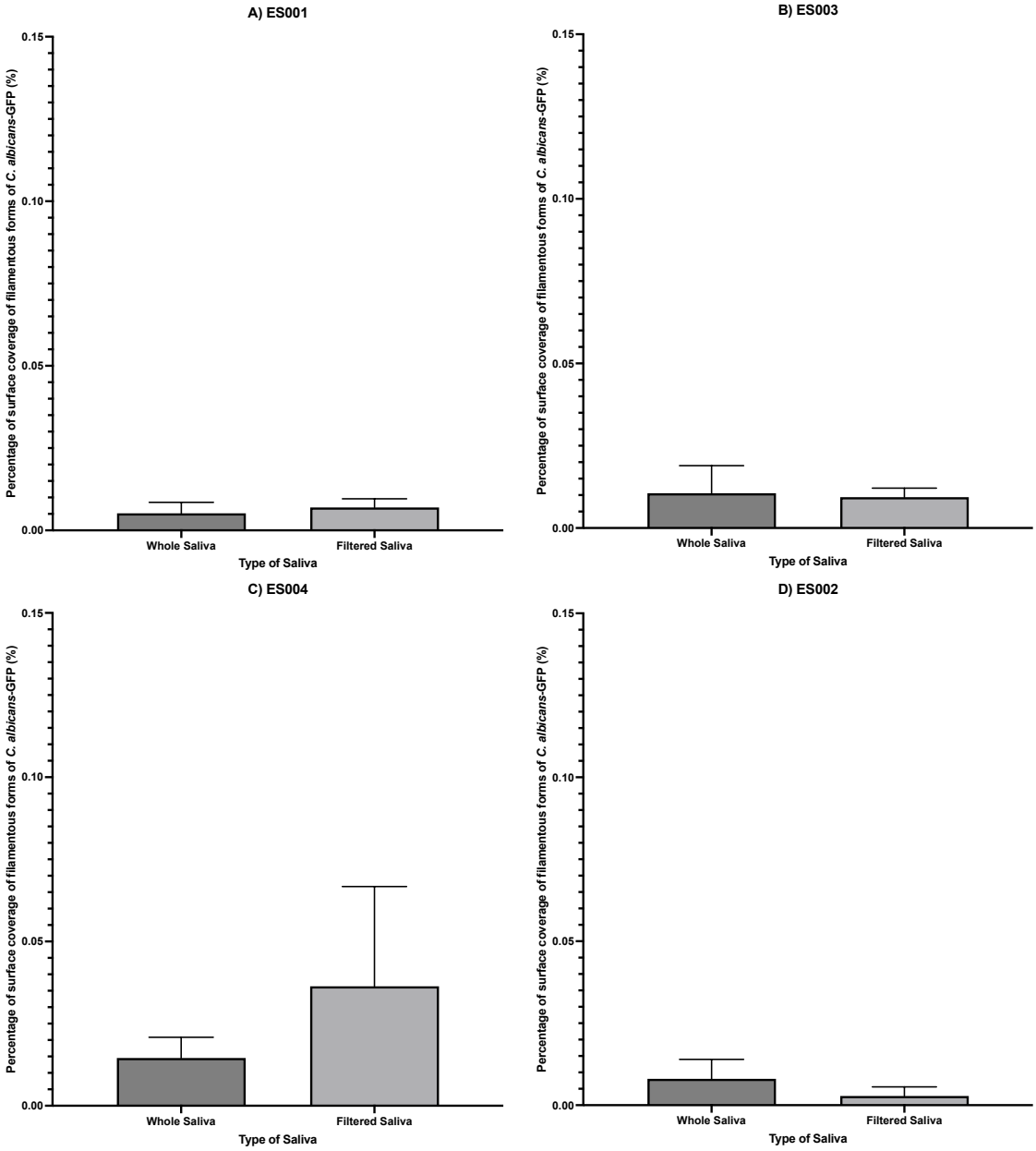

Figure 5.8a. Mean percentage area of *Candida albicans*-GFP filamentous forms on polycarbonate coupon surfaces grown with whole saliva compared to filtered saliva from ES001 (A), ES003 (B), ES004 (C) and ES002 (D). Saliva samples were collected from volunteers, artificially contaminated with *C. albicans* SC5314-GFP and used to grow biofilms on the same day as collection. Max projection images from the CLSM z-stacks were analysed to determine the percentage surface area coverage by the filamentous morphological forms of the GFP strain. Statistical significance was tested using an unpaired *t*-test. No significant differences were found.

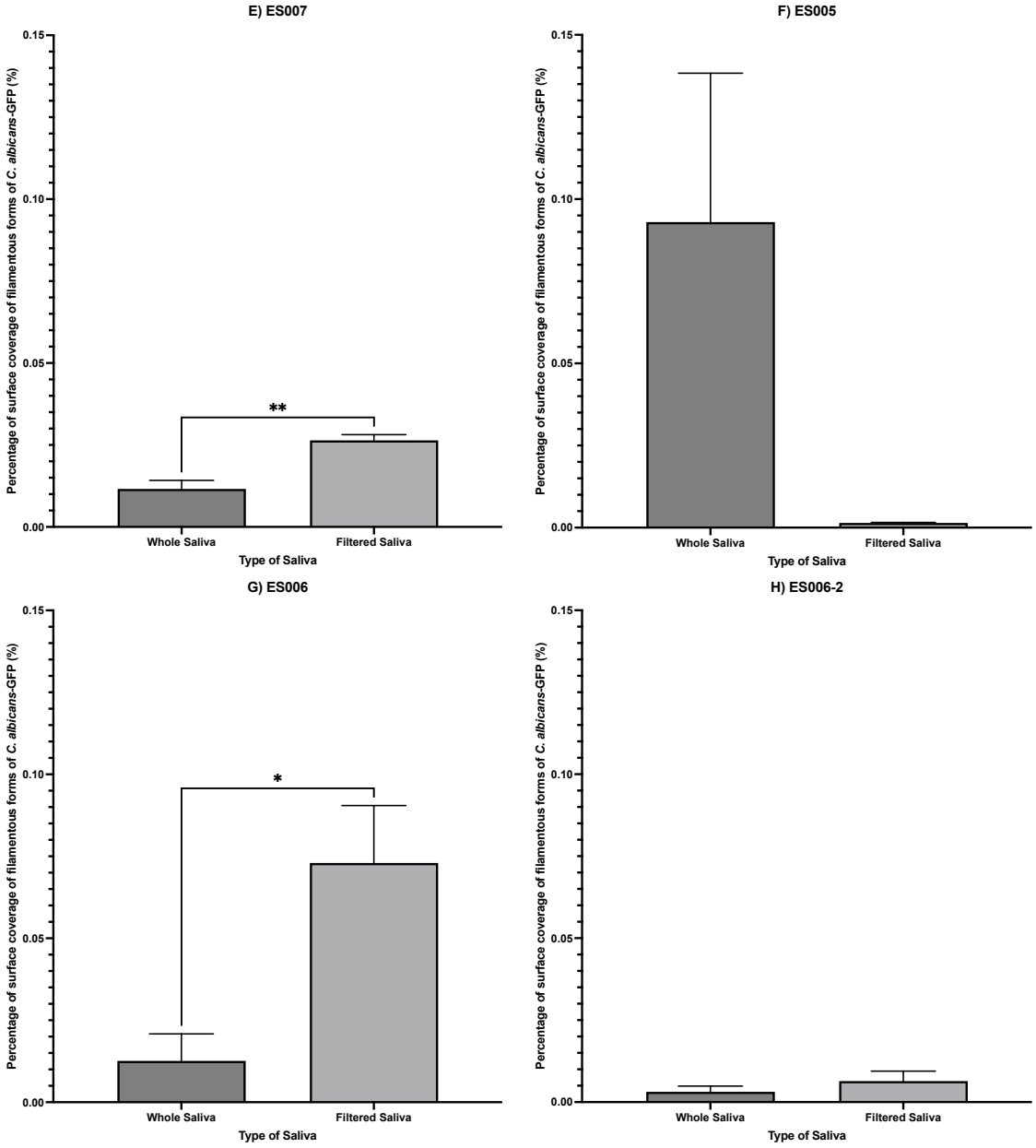

Figure 5.8b. Mean percentage area of *Candida albicans*-GFP filamentous forms on polycarbonate coupon surfaces grown with whole saliva compared to filtered saliva from ES007 (E), ES005 (F), ES006 (G) and ES006-2 (H). Saliva samples were collected from volunteers, artificially contaminated with *C. albicans* SC5314-GFP and used to grow biofilms on the same day as collection. Max projection images from the CLSM z-stacks were analysed to determine the percentage surface area coverage by the filamentous morphological forms of the GFP strain. Statistical significance was tested using an unpaired *t*-test. * $P \leq 0.05$. ** $P \leq 0.01$. *** $P \leq 0.001$. **** $P \leq 0.0001$.

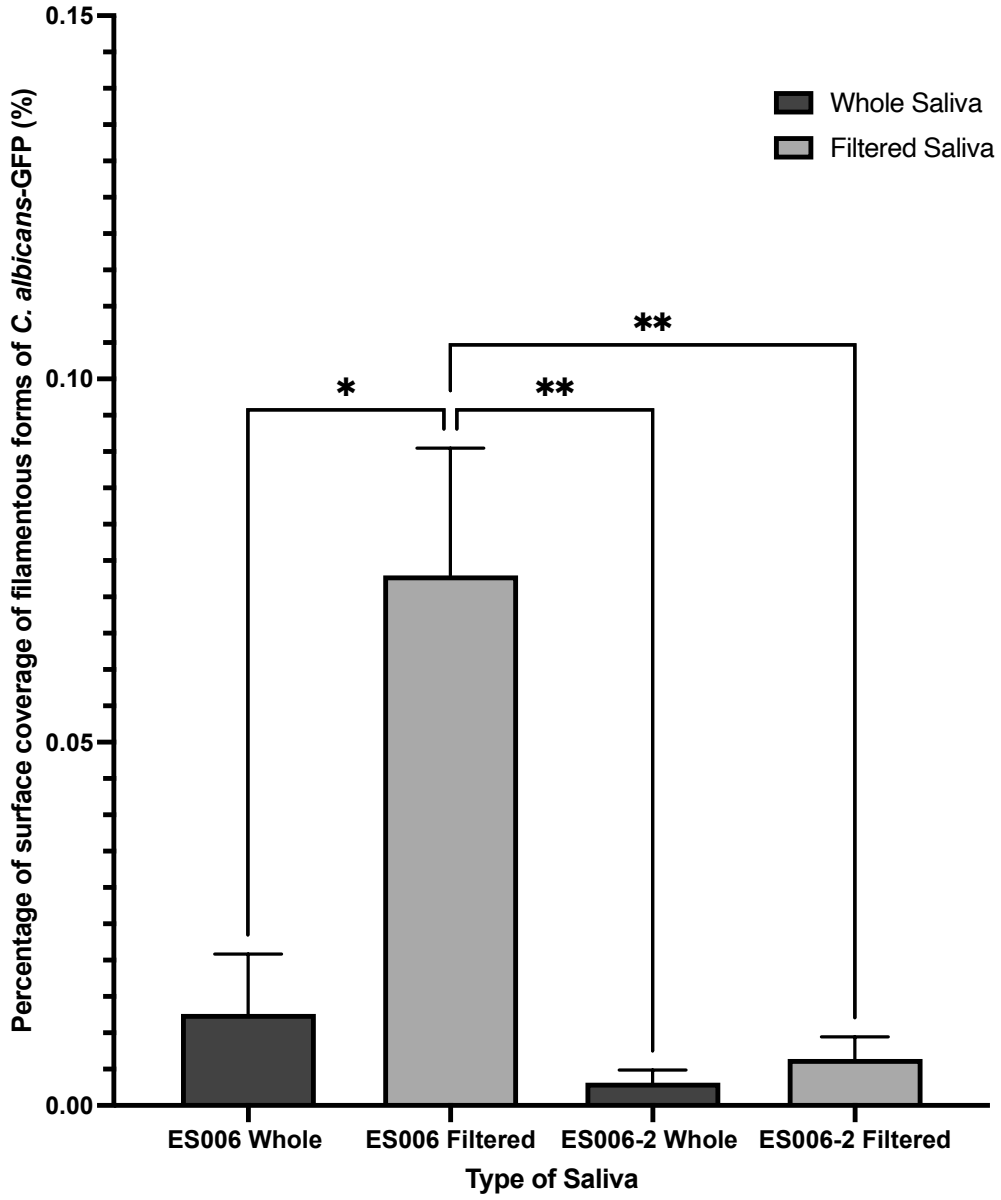

Figure 5.9. Mean percentage area of *Candida albicans*-GFP filamentous forms in biofilms derived from ES006 and ES006-2 saliva artificially contaminated with *C. albicans* SC5314-GFP. The two saliva samples were collected from the same individual one month apart and biofilms were grown the same day as collection. Both the whole and filtered saliva were artificially contaminated with *C. albicans* SC5314-GFP. Max projection images from the CLSM z-stacks were analysed to determine the percentage surface area coverage by the filamentous morphological forms of the GFP strain. Statistical significance was tested using One-Way ANOVA (F (3, 8) = 11.25, $P \leq 0.0031$) with Tukey's post hoc test for multiple comparisons. * $P \leq 0.05$. ** $P \leq 0.01$. *** $P \leq 0.001$. **** $P \leq 0.0001$.

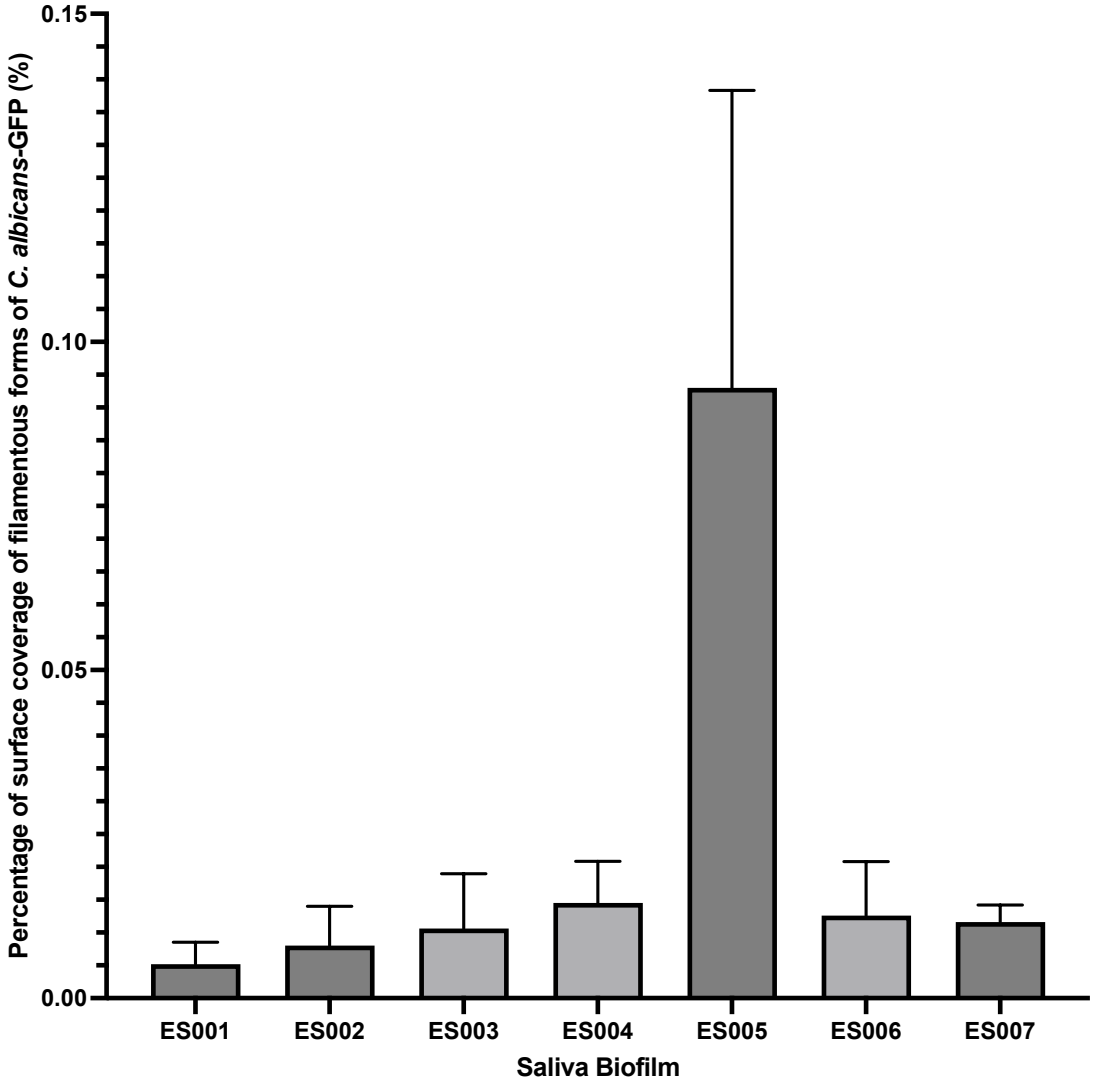

Figure 5.10. Mean percentage area of *Candida albicans*-GFP filamentous forms in biofilms derived from whole saliva artificially contaminated with *C. albicans* SC5314-GFP. Saliva samples were collected from volunteers, artificially contaminated with *C. albicans* SC5314-GFP and used to grow biofilms on the same day as collection. Max projection images from the CLSM z-stacks were analysed to determine the percentage surface area coverage by the filamentous morphological forms of the GFP strain. Statistical significance was tested using Kruskal-Wallis test (H (6) = 5.764, $P \leq 0.4502$) with Dunn's multiple comparisons test. No statistical significance was found between the groups.

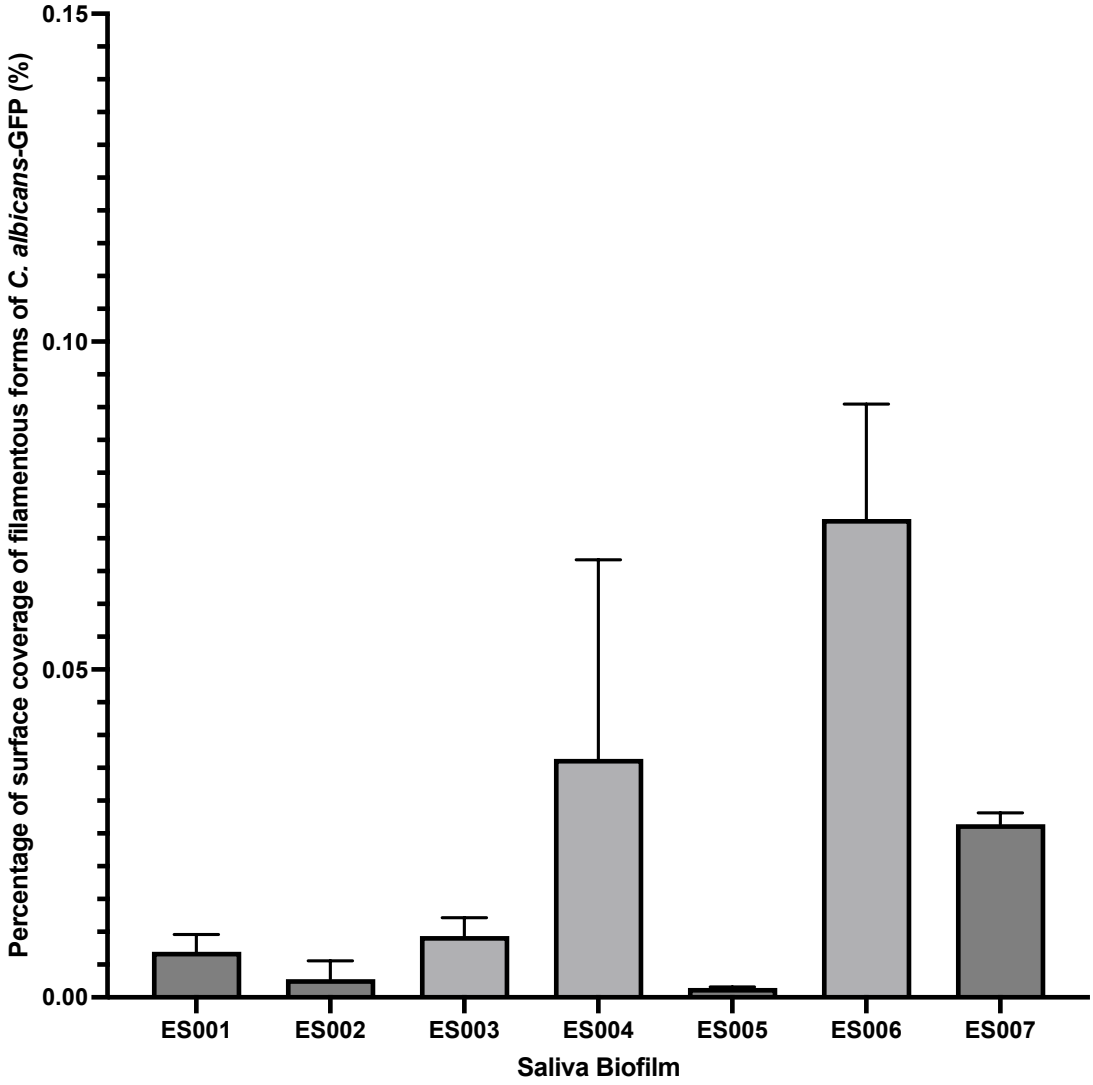

Figure 5.11. Mean percentage area of *Candida albicans*-GFP filamentous forms in biofilms derived from filtered saliva artificially contaminated with *C. albicans* SC5314-GFP. Saliva samples were collected from volunteers, filtered, artificially contaminated with *C. albicans* SC5314-GFP and used to grow biofilms on the same day as collection. Max projection images from the CLSM z-stacks were analysed to determine the percentage surface area coverage of the *C. albicans* SC5314-GFP strain. Significance was tested using Kruskal-Wallis test ($H(6) = 14.24$, $P \leq 0.0270$) with Dunn's multiple comparisons test. * $P \leq 0.05$. ** $P \leq 0.01$. *** $P \leq 0.001$. **** $P \leq 0.0001$.

5.3.3. Metagenomic shotgun sequencing

All 18 biofilm samples, ES001 – ES007 and ES006-2 whole and filtered saliva samples plus whole saliva samples of ES001-2 and ES002-2 (Table 5.3), were successfully sequenced with very good quality calls for the FastQC sequence, mean quality scores and per sequence quality scores in the MultiQC report. A total 6,383 species of bacteria were identified in the 18 samples and an example of the bacterial diversity seen in the whole saliva-derived biofilms samples is shown in Figure 5.12. The percentage of reads that were classified, and the percentage that were classified as bacterial reads in each sample, are summarised in Table 5.3. The biofilms from filtered saliva showed that around 90% of the raw sequence reads were unclassified. Importantly, the database through which the data was run did not include fungi and so the unclassified reads likely included *C. albicans* that had been added to the samples, and potentially other fungal species. The exception to this was the ES007 filtered saliva biofilm sample, which only had 43.97% of the reads unclassified and 53.86% of the classified reads were bacterial. The filtered saliva biofilms were expected to have some bacterial DNA present, as this would not have been removed by filtration. However, the ES007 filtered saliva biofilm sample was different in terms of classification of percentages compared to the other filtered saliva biofilm samples.

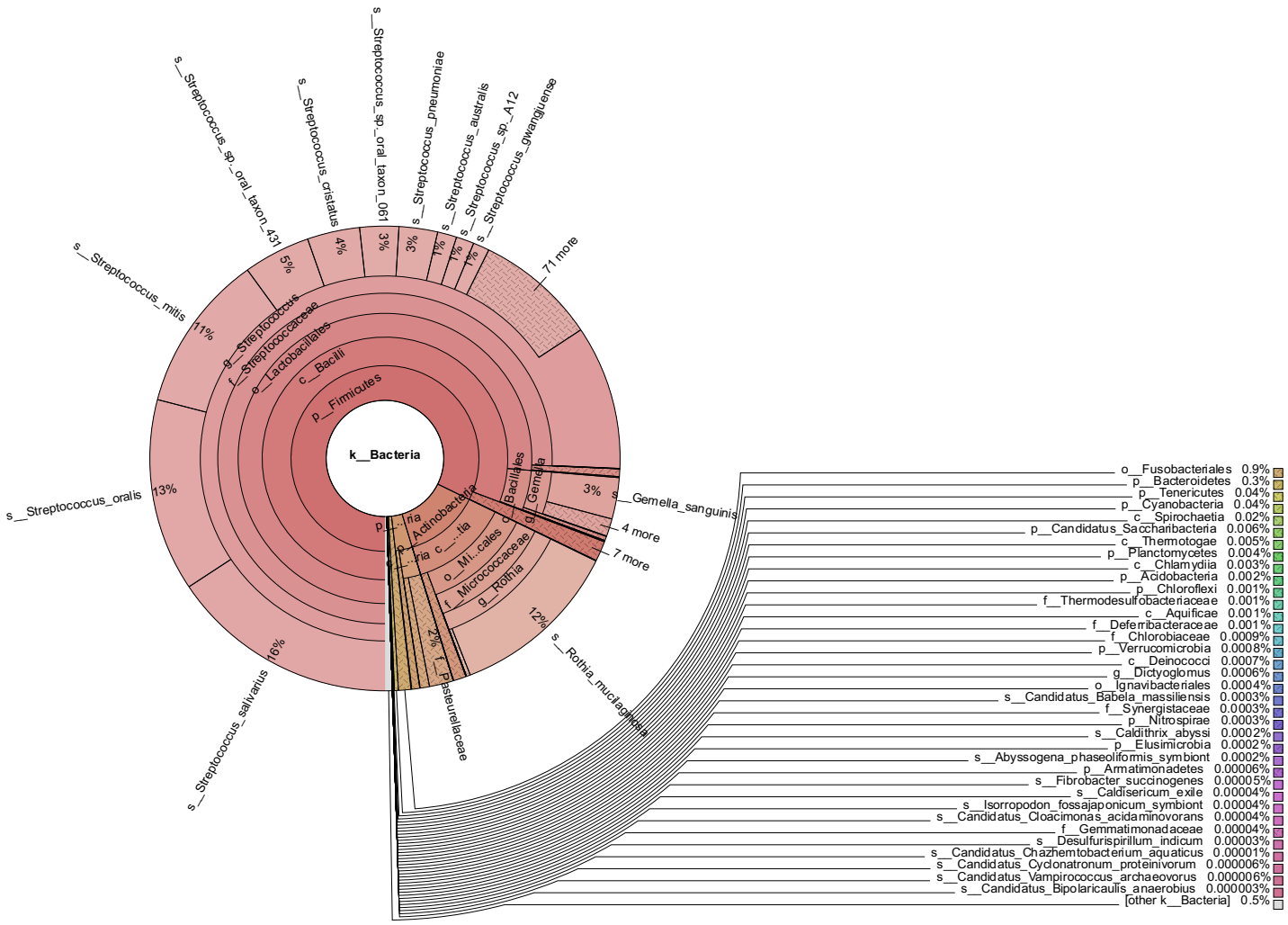

Figure 5.12. Snapshot of the Krona visualisation of the bacteria in the ES005 whole saliva-derived biofilm. Presented as an example of the bacterial diversity seen in the whole saliva-derived biofilm samples.

Table 5.3. Summary of the raw number of reads and read classification for each sample from the MultiQC report. The table shows the number of raw reads and the percentage of those reads that were able to be classified for each saliva-derived biofilm. The table also shows the percentage of reads that were classified as bacterial reads.

Name	Number of raw reads	Classified reads	Unclassified reads	Bacterial reads
ES006 Filtered	48,888,526	9.452%	90.55%	4.414%
ES006 Whole	58,840,152	78.55%	21.45%	77.33%
ES006-2 Filtered	49,217,433	8.976%	91.02%	4.207%
ES006-2 Whole	48,943,147	85.56%	14.44%	84.78%
ES003 Filtered	32,672,766	9.485%	90.51%	4.427%
ES003 Whole	45,577,326	89.98%	10.02%	89.32%
ES002 Filtered	43,940,376	9.307%	90.69%	4.452%
ES002 Whole	55,470,256	75.79%	24.21%	74.58%
ES002-2 Whole	40,893,472	86.56%	13.44%	86.07%
ES007 Filtered	45,827,153	56.03%	43.97%	53.68%
ES007 Whole	31,904,699	68.94%	31.06%	67.46%
ES001 Filtered	24,698,059	10.01%	89.99%	5.178%
ES001 Whole	66,764,692	88.02%	11.98%	87.37%
ES001-2 Whole	40,413,612	87.99%	12.01%	87.63%
ES005 Filtered	37,872,513	8.947%	91.05%	4.001%
ES005 Whole	48,009,278	72.68%	27.32%	71.14%
ES004 Filtered	39,850,158	9.442%	90.56%	4.423%
ES004 Whole	46,222,550	89.22%	10.78%	88.99%

The top 500 bacterial species were analysed to assess compositional changes between the samples (Figure 5.13). The proportion of the top 500 species showed that *Streptococcus salivarius, Streptococcus oralis, Streptococcus mitis, Rothia mucilaginosa* and *Streptococcus parasanguinis* were on average the top five species in the biofilms (Table 5.4 and Table 5.5). The top 5 species made up 53.58% (ES007) to 74.24% (ES001-2) of the abundance of the bacterial species in the whole saliva-derived biofilm samples. Of note was that species used in experiments in Chapter 4, namely *S. salivarius, S. gordonii, S. sanguinis,* and *S. mutans,* were all present in the top 500 species of the 10 whole saliva-derived biofilm samples, and on average were ranked as 1st, 22nd, 27th, and 59th of the most abundant species, respectively (Table 5.4).

A principal component analysis (PCA) was conducted to assess how the whole saliva-derived biofilms clustered in terms of composition of the top 500 species/genera (Figure 5.14). PCA showed a lack of clustering, indicating the samples were quite distinct from each other, especially ES003. From this analysis, it can be inferred that ES004, ES002 and ES006 were more similar to each other, and that ES001, ES005 and ES007 were more similar to each other in the composition of the top 500 species, but there was no clear overlapping and clustering.

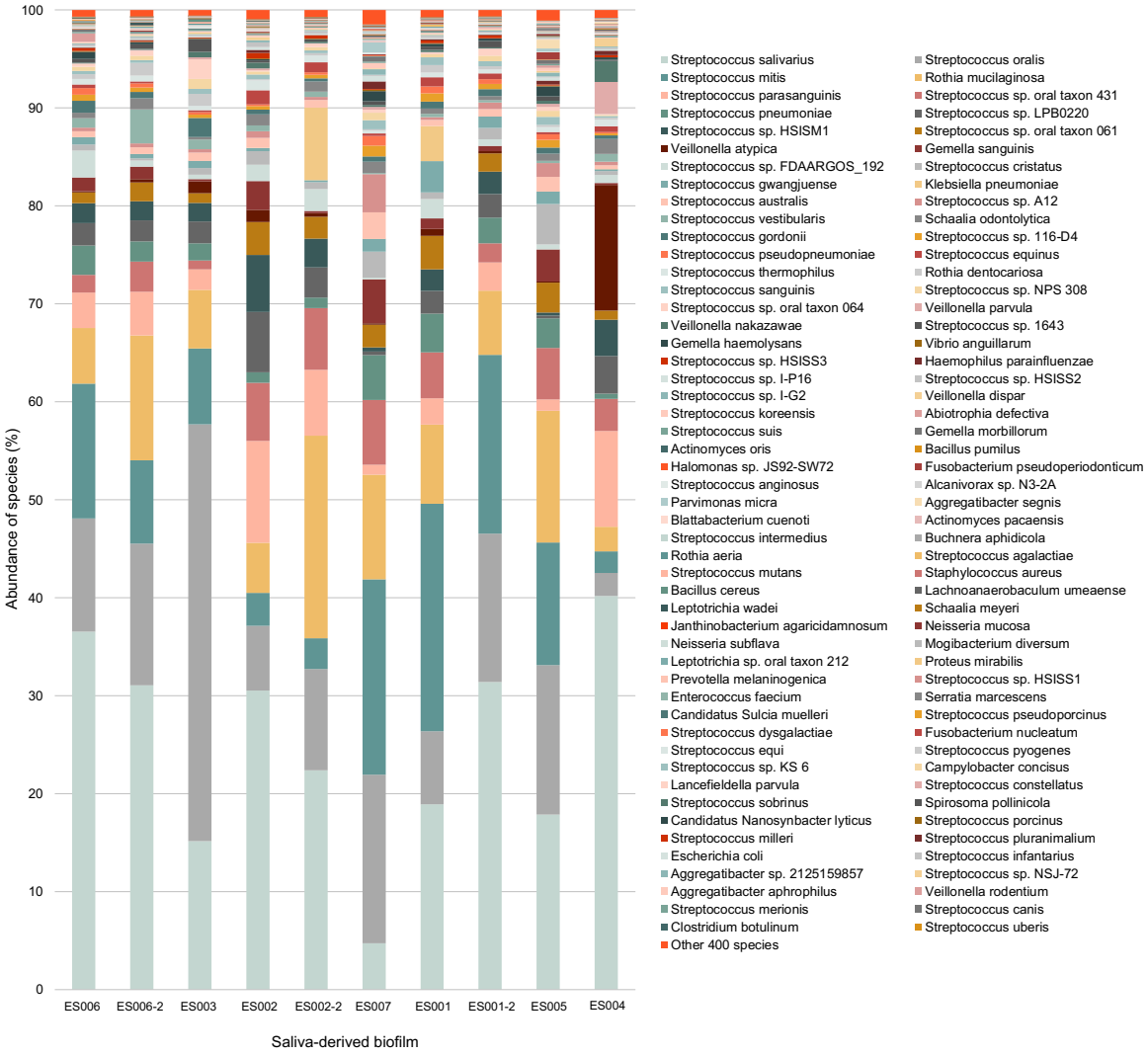

Figure 5.13. Proportion (%) of the top 500 bacterial species in each whole saliva-derived biofilm sample. Percentages were calculated for the abundance of the top 500 bacterial species in each whole saliva-derived biofilm. The top 100 species made up of the top 98.43 – 99.56% of the top 500 species and the last 400 species were combined into a single group for the construction of this figure. The 100 species included are labelled in the legend on the right-hand side.

Table 5.4. Summary of selected bacterial species abundance across 10 whole saliva-derived biofilm samples from the top 500 bacterial species data.

Bacterial Species	Rank In Top 500 Species	Mean Abundance (%)	SEM	Range (%)
Streptococcus salivarius	1	24.87	3.46	31.83
Streptococcus oralis	2	14.30	3.46	40.23
Streptococcus mitis	3	11.26	2.37	21.00
Rothia mucilaginosa	4	9.15	1.69	18.17
Streptococcus parasanguinis	5	4.48	1.07	9.36
Streptococcus gordonii	22	0.76	0.15	1.62
Streptococcus sanguinis	27	0.51	0.08	0.78
Streptococcus mutans	59	0.05	0.01	0.14

Table 5.5. Proportions of the top five most proportionate species in the top 500 ranked species of each of the whole saliva-derived biofilms.

	Proportion of the 5 most proportionate species in the whole saliva-derived biofilm samples (%)									
Species	**ES001**	**ES002**	**ES003**	**ES004**	**ES005**	**ES006**	**ES007**	**ES001-2**	**ES002-2**	**ES006-2**
S. salivarius	18.90	30.51	15.14	40.19	17.87	36.54	4.71	31.38	22.37	31.05
S. oralis	7.48	6.62	42.56	2.33	15.25	11.56	17.21	15.16	10.36	14.47
S. mitis	23.21	3.37	7.74	2.21	12.51	13.75	19.96	18.26	3.13	8.50
R. mucilaginosa	8.10	5.10	6.01	2.51	13.46	5.69	10.67	6.53	20.68	12.74
S. parasanguinis	2.67	10.38	2.07	9.79	1.16	3.61	1.02	2.91	6.73	4.48
Total proportion	60.35	55.99	73.51	57.02	60.25	71.14	53.58	74.24	63.27	71.24

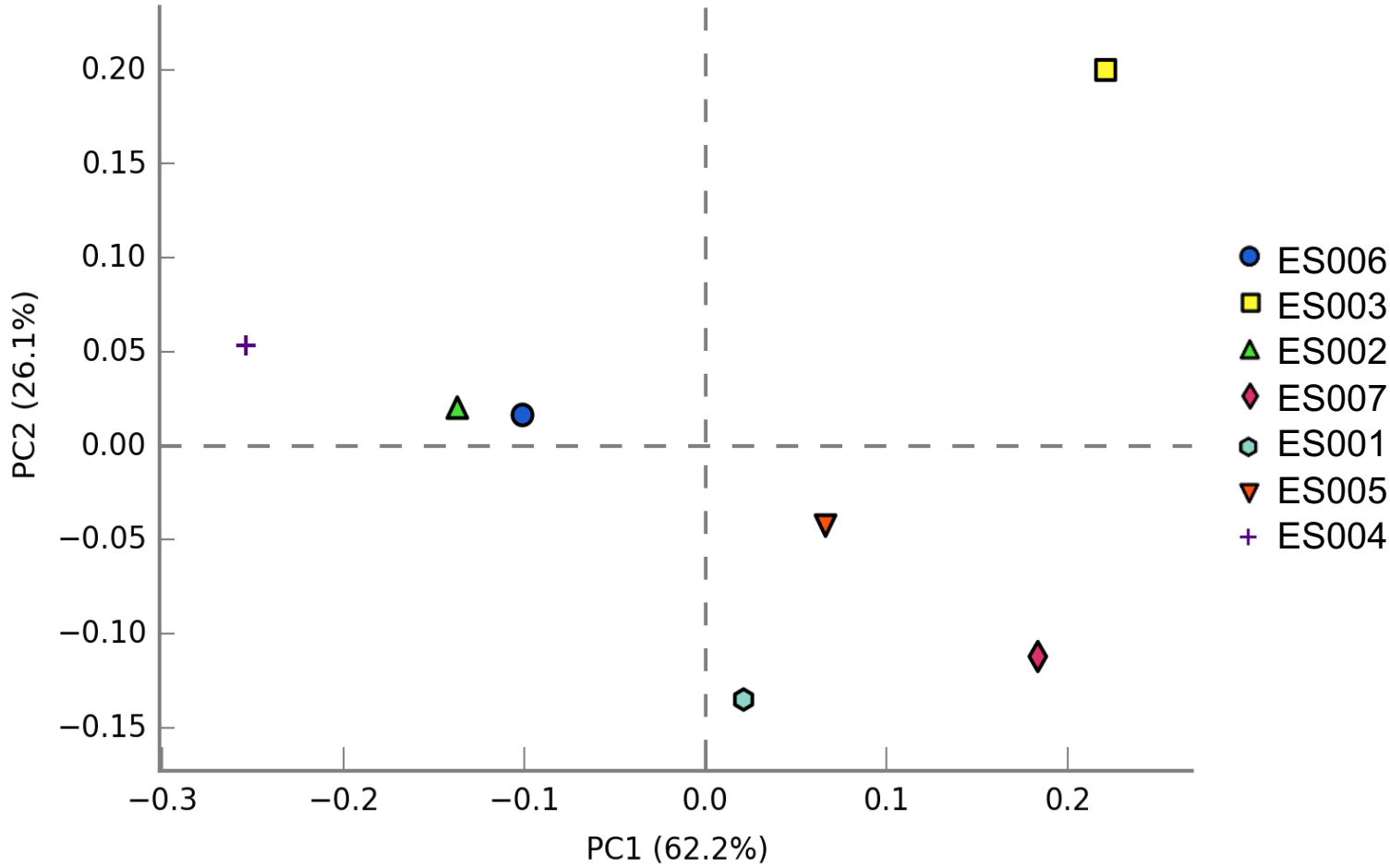

Figure 5.14. Principal component analysis (PCA) plot comparing species-level taxonomic profiles of seven whole saliva-derived biofilms. The top 500 bacterial species were compared using STAMP to perform PCA.

5.3.3.1. Comparisons between the proportions of the top 500 species in selected whole saliva-derived biofilm samples.

Assessment of the differences between the proportions of the top 500 species in the whole-saliva derived biofilms was conducted. The ES005 and the ES004 whole saliva derived-biofilm samples were selected for comparison as they exhibited the highest and lowest level of surface area coverage of *C. albicans*. No significant differences were found in the proportions of the top 500 species in these biofilms. To identify differences that did not reach the threshold for statistical significance, statistical tests were run without the multiple test correction and some differences were highlighted between the ES004 and ES005 whole saliva-derived biofilms for six of the 500 species (Figure 5.15). *S. salivarius, Veillonella atypica and S. parasanginius* were a greater proportion in the ES004 biofilm than the ES005 biofilm. Conversely, *Rothia mucilaginosa, S. oralis* and *S. mitis* were all greater in proportion in the ES005 compared to the ES004 biofilm. Even though the results are not statistically significant they could represent a biological significance.

In addition, ES005 and ES001 whole saliva derived-biofilm samples were also compared as biofilms from those samples exhibited the highest and lowest levels of filamentous forms of *C. albicans*, respectively. No significant differences were found in the proportion of the top 500 bacterial species in those biofilms. Testing differences in proportions without a statistical correction resulted in a difference in the *Streptococcus mitis* proportions, with the ES001 whole saliva-derived biofilm having a greater proportion of *S. mitis* than the ES005 sample.

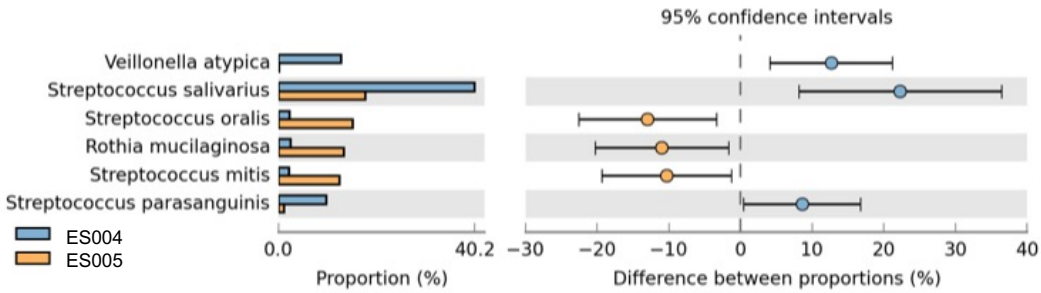

Figure 5.15. Comparison between the proportion of the top 500 species in the ES004 or ES005 whole saliva-derived biofilms. Analysis was conducted using STAMP differences in proportions test with no correction to highlight whether there may be differences that are not statistically significant but could be biologically significant. The blue bars indicate the ES004 whole saliva-derived biofilm sample and the orange bars indicate ES005 whole saliva-derived biofilm sample. These differences were not deemed statistically significant.

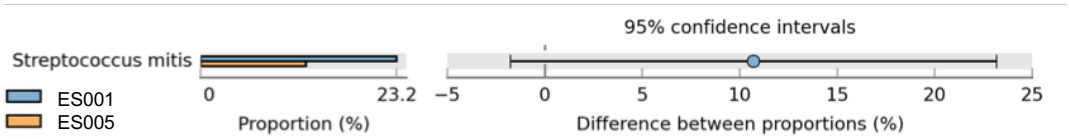

Figure 5.16. Comparison between the proportion of the top 500 species in the ES005 and ES001 whole saliva-derived biofilms. Analysis was conducted using STAMP differences in proportions test with no correction to highlight whether there may be differences that are not statistically significant but could be biologically significant. The blue bars indicate the ES001 whole saliva-derived biofilm sample and the orange bars indicate ES005 whole saliva-derived biofilm sample. These differences were not deemed statistically significant.

5.3.3.2. Comparison of the differences in proportion of the top 500 species in the whole saliva-derived biofilms that were taken from the same individual at two different timepoints.

Comparisons were made between biofilms from samples that were taken from the same individual at two separate timepoints: ES006 and ES006-2, ES001 and ES001-2, and ES002 and ES002-2. No significant differences were found in proportions of the top 500 species in any of these samples. For the ES006 and ES006-2 whole saliva-derived biofilms, comparison of proportions showed no significant differences. Therefore, the proportions of the top 500 species in these samples were similar from both collections of saliva from the same individual used to inoculate the biofilm. However, some differences were detected when no correction was implemented in the ES001 and ES001-2 comparisons for the top 500 species differences in the proportions test (Figure 5.17). *Streptococcus salivarius* was a greater proportion of the ES001-2 sample than the ES001 sample. Additionally, when no correction was implemented in the ES002 and ES002-2 comparisons, *Rothia mucilaginosa* and *Klebsiella pneumoniae* species were both found to be a greater proportion of the ES002-2 sample (20.68% and 7.40%, respectively) than the ES002 sample (5.10% and 0.0169%, respectively) (Figure 5.18). *K. pneumoniae* was found at the highest proportion in the ES002-2 sample and second highest in the ES001 sample (3.59%); the remaining eight whole saliva-derived samples had low levels between 0.0004% and 0.0169%. However, these differences were not significant and overall bacterial proportions in the biofilms from the saliva of the same individual showed stability between collection time points.

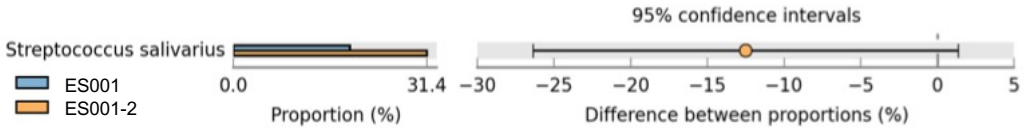

Figure 5.17. Comparison between the proportion of the top 500 species in the ES001 and ES001-2 whole saliva-derived biofilms. Analysis was conducted using STAMP differences in proportions test with no correction. The blue bars indicate the ES001 whole saliva-derived biofilm sample and the orange bars indicate ES001-2 whole saliva-derived biofilm sample.

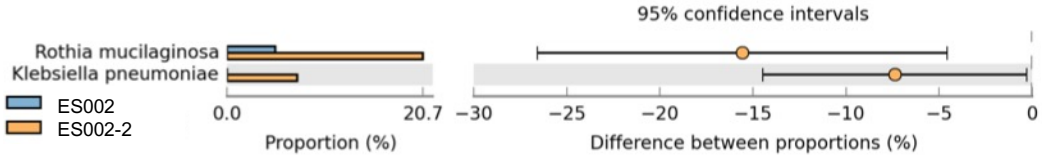

Figure 5.18. Comparison between the proportion of the top 500 species in the ES002 and ES002-2 whole saliva-derived biofilms. Analysis was conducted using STAMP differences in proportions test with no correction. The blue bars indicate the ES002 whole saliva-derived biofilm sample, and the orange bars indicate ES002-2 whole saliva-derived biofilm sample.

5.4. Discussion

Knowledge of how the highly complex and diverse oral microbial community influences *C. albicans* is important for understanding the risk factors of oral *Candida*-associated infections. The aims of this study were to determine whether biofilms derived from the saliva of separate healthy individuals differentially affected *C. albicans*, and whether these biofilms had different bacterial compositions. Previous studies frequently pool saliva from many individuals to form saliva derived biofilms (Edlund et al. 2013; Janus et al. 2017). However, research indicates that the salivary microbiome is highly individualised in people (Hall et al. 2017). This study investigated the effect of relatively complex *in vitro* biofilms on the growth and morphology of *C. albicans* to gain a better understanding of how different healthy people may vary in susceptibility to *C. albicans* infection based on the composition of their oral microbiomes. Biofilms grown from saliva inocula would select only cultivatable microorganisms and those able to adhere to the polycarbonate coupon supported biofilms. The biofilms were grown in an aerobic environment for 24 h, which may also affect the biofilm composition by limiting numbers of slow-growing and anaerobic species.

Whole and filtered saliva-derived biofilms were compared. The filtered saliva-biofilms acted as controls and represented only the effects of filterable saliva molecules rather live microbial cells. The absence of microorganisms in the filtered saliva was confirmed with no growth observed on TSA and SDA plates. Whole saliva would be indicative of the impact that both microbial cells and salivary components had on *C. albicans*. Comparing the whole and filtered saliva biofilms from each individual indicated that the live microbial cells integrated into biofilms had different effects on surface area coverage and extent of filamentous morphology *C. albicans* SC5314-GFP. Depending on the source of the saliva, some biofilms exhibited significantly higher *C. albicans*, whilst other biofilms had significantly lower surface area coverage than filtered saliva controls. These findings suggest that the biofilm microbiome originating from the saliva was a contributor to the changes observed for *C. albicans* in the biofilms.

Different effects on the *C. albicans* with saliva from different volunteers indicates that the composition of the microbiome itself was important. This was further

supported by the surface area coverage of *C. albicans* being significantly different depending on the individual the whole saliva was obtained from. Significant differences were also found when comparing the filtered saliva-derived biofilms, highlighting that the salivary components also varied between individuals and had an effect on the *C. albicans* surface area coverage. These findings indicate that saliva from healthy individuals varied both in salivary components and microbial content. Evidence from previous research does support that the salivary microbiome is different between individuals (Belstrøm 2020).

As *C. albicans* filamentous morphotypes are more associated with virulence (Kumamoto and Vinces 2005b), the amount of filamentous morphology present was used to determine whether the saliva from different healthy individuals could potentially influence the virulence of *C. albicans*. In most of the saliva-derived biofilms, the amount of filamentous morphology observed in the whole saliva compared to the filtered saliva biofilms was relatively similar, apart from significant differences observed for ES007 and ES006 derived biofilms. These biofilms showed significantly higher quantities of *C. albicans* filamentous morphology in the filtered saliva-derived biofilm. This suggests that morphology was perhaps influenced more by salivary components and could possibly indicate that hyphal levels in these saliva samples were reduced to a lower level when microbial cells were present. The ES005 whole saliva exhibited higher levels of filamentous forms. However, this was not statistically significant possibly due to greater variability in the ES005 filamentous morphology data as shown by the standard error of the mean. The whole saliva-derived biofilm from different individuals did not exhibit significant differences in filamentous morphology, remaining consistent between the saliva from different individuals. The ES005 whole saliva-derived biofilm also displayed higher levels of filamentous *C. albicans*, than the other biofilms, but this was not statistically significant. Filtered-saliva derived biofilms also did not show statistically significant changes in the levels of filamentous morphology between the saliva from different individuals. Notably, the amount of filamentous morphology observed across the filtered saliva derived biofilms was less consistent than between the whole saliva biofilm samples. However, even though they are not statistically different there could still be biologically significance in the results and could indicate the possibility of promoting infection.

Whole genome shotgun metagenomic sequencing was used to investigate whether differences in bacterial composition in whole saliva-derived biofilms could be responsible for differential effects on *C. albicans.* A large number of the sequence reads were unclassified, this was partly due to the database used for analysis not including fungal data. Future work should involve incorporating a fungal database not only to determine the proportion of the biofilm that was *C. albicans* SC5314, but also whether *C. albicans* or other fungal species were already present in the samples. It could be hypothesised that samples which already contained *C. albicans* may have resulted in a difference in the response of *C. albicans* SC5314. Conceivably, prior interaction between *C. albicans* existing in saliva and the bacteria could have altered the microbiome before experiments were undertaken and be 'primed' to interact with *C. albicans*.

The top 500 bacterial species were used to compare bacterial biofilm composition. All four *Streptococcus* species used in Chapter 4 were found to be present in the biofilms based on sequencing. The majority of the bacterial biofilm composition (53.58% to 74.24%) of whole saliva-derived biofilms consisted of the top five bacterial species, namely *S. salivarius, S. oralis, S. mitis, R. mucilaginosa* and *S. parasanguinis*. Notably, the highest ranked species in whole-saliva derived biofilms was *S. salivarius,* which was found in Chapter 4 to increase *C. albicans* surface area and filamentous morphology in dual species biofilms. This finding was supported by Edlund *et al.* (2013), who also reported that *S. salivarius* was the most abundant species in biofilms developed in an *in vitro* human oral microbiome model which was derived from human saliva but pooled from multiple individuals. Additionally, Edlund *et al.* (2013) found that *S. parasanguinis* was the most dominant species in the first 3 h of development and whilst it then decreased in proportion, it remained as one of the top five most abundant species in the biofilms. However, they found that the top 5 bacterial species in their biofilms at 16 h and 48 h, were *S. salivarius, Lactobacillus fermentum, Streptococcus vestibularis, Streptococcus parasanguinis* and *Klebsiella pneumoniae.* This previous study did not have a 24 h assessment so was not directly comparable to the findings presented here. This study pooled saliva from multiple individuals and did not investigate differences between saliva from different individuals. Differences in the most abundant species could be due to the presence of *C. albicans.* Previous

research states that the presence of *C. albicans* changes the bacterial microbiome of early *in vitro* biofilms (Janus et al. 2017). However, they state that the presence of *C. albicans* allowed for colonisation of facultative and strict anaerobic bacteria under oxygen rich conditions and biofilms without *C. albicans* contained more *Neisseria, Rothia,* and *Streptococcus* species. None of the top five species reported here were considered to be abnormal or unexpected for a saliva-derived biofilm, and all are common residents of the oral cavity (Yamashita and Takeshita 2017; Zaura et al. 2017; Coker et al. 2022).

Sequencing of ES004 and ES005 saliva derived biofilms was used for comparison, as these exhibited the highest and lowest levels of *C. albicans* surface area coverage. Results showed that there were no overall significant differences in the proportions out of the top 500 bacterial species present. However, there was a difference found in the proportions of six of the species, which included all the species ranked as the five most proportionate species. While not statistically significant, this could indicate possible biological significance in contributing to the effects observed on *C. albicans.* ES005 and ES001 derived biofilms were also selected for comparison as these resulted in the highest and lowest amounts of *C. albicans* filamentous morphologies. For these, the only difference detected was between the *S. mitis* proportions, where the ES001 biofilm had higher *S. mitis* and the lowest level of *C. albicans* filamentous forms. Research does show that *S. mitis* is capable of inhibiting hyphal production (do Rosário Palma et al. 2019).

PCA showed distinction between the different whole saliva-derived biofilms through lack of clustering, however, the PCA did not show significance. Previous research has highlighted that the salivary microbiome is highly individualised (Hasan et al. 2014; Hall et al. 2017; Belstrøm 2020). Cameron et al. (2015), found there were seasonal changes were observed in the salivary microbiome over a one-year period in terms of taxonomic composition and diversity but that changes appeared to be from individual differences rather than temporal changes. Stability has been found to be mostly temporary but there are personal features that persist over time (Hall *et al.* 2017). The source subjects in the study of Hall et al. (2017) were able to be identified from the profile of their oral microbiota one year later from the variable microorganisms present. They found supportive evidence for the fact that the healthy oral microbiota is both homeostatic and dynamic, bringing

together research from both sides of this debate (Darveau 2010; Ursell et al. 2012; Zarco et al. 2012; Xu et al. 2015). Saliva from different individuals has been shown to form biofilms of different microbial composition (Cieplik et al. 2019). The clustering of taxa in a PCA was observed to be based on the individual the saliva was collected from more than the oral niche (saliva, subgingival plaque, tongue and tonsils) (Cieplik et al. 2019). However, these biofilms were grown for a much longer period of time for 14 and 28 days.

The comparable results from the ES006 and ES006-2 samples that were obtained from the same individual one month apart would tentatively support previous research that the salivary microbiome is consistent over time. However, there was an exception in relation to the levels of filamentous morphology in the filtered saliva from the second collection (ES006-2), which was significantly different from all three other conditions; ES006 whole, ES006 filtered and the ES006-2 whole samples. A possible explanation of this finding is that the significantly higher hyphal proportion was due to a salivary component that was negated by the presence of microorganisms in the microbiome. The fact that the whole saliva effect on *C. albicans* was the same for the ES006 and ES006-2 samples suggests stability in the composition of the microbiome. This was supported by metagenomic sequencing where comparison of the proportions of the top 500 bacterial species showed no significant differences. This suggests that the saliva from this individual was the same at both collection times.

The biofilms derived from ES002 and ES002-2, and also ES001 and ES001-2 salivas, were also compared as these were also from the same individuals, but after a longer period of time (5 months and 6 months apart, respectively). It is also important to note that the methodology was slightly different in that the second samples (designated 002) were sequenced from pooling a larger number of coupons and, therefore, there was more starting material. However, the analyses were assessing proportional differences. There were no statistically significant differences observed between the ES002 and ES002-2, or ES001 and ES001-2 samples, however, unlike with the ES006 and ES006-2 samples, some differences were found when no multiple test correction was implemented. In the ES001and ES001-2 samples, the proportion of *S. salivarius* was higher in the second sample (ES001-2) and this could be relevant as in Chapter 4 *S. salivarius* when grown with

C. albicans resulted in an increase in filamentous forms of. *C. albicans*. Unfortunately, the ES001-2 and ES002-2 were not included in the experiments that determined effects on *C. albicans* because they were taken at a later date and only collected for sequencing to ensure enough material for sequencing analysis. Therefore, it cannot be determined whether this increased proportion of *S. salivarius* would have resulted in increased filamentous forms in these experiments. The EW derived biofilms also revealed some differences with *Rothia mucilaginosa* and *Klebsiella pneumoniae* being higher in proportion in the ES002-2 samples. It was perhaps unexpected to detect *K. pneumoniae* at such a high prevalence in this sample as it was only present in small proportions in the rest of the samples. However, *K. pneumoniae* is known to occur in the oral microbiome (Li et al. 2014) and *in vitro* models have reported *K. pneumoniae* growing in human saliva-derived biofilms at a quite high proportions and is one of the top five most abundant microbial species (Edlund et al. 2013). Overall, when saliva was collected from the same individual at different time points exhibited stability in the bacterial composition of the biofilms.

Hall *et al.* (2017) describes a "core" microbiota and a "variable" microbiota in the salivary microbiome that is more personal to subject, persists over time and creates a unique microbial fingerprint by which an individual can be identified (Turnbaugh et al. 2007; Zarco et al. 2012). The research showed that some personalised features were maintained over time regardless of the rate of community drift which was not consistent between individuals. The most abundant microorganisms are the most resistant to change, with rarer microorganisms more likely to shift and be more transient (Shade et al. 2014; Lynch and Neufeld 2015; Hall et al. 2017). This finding could explain the consistency of the top five species in the whole saliva-derived biofilms encountered in this research. However, it could also be that these species are more proportionate because they were selected for by the material of the surface (polycarbonate) and the culture conditions used. For example, Li et al. (2021), showed that reconstructed human gingiva, titanium and hydroxyapatite surfaces formed biofilms with different microbial composition even though the saliva was obtained from the same individual. Future work could involve looking at whether the proportions of bacterial species in the saliva-derived biofilms reflect the proportions found in the original saliva. The variable microbiota is considered

to be mostly functionally redundant meaning their influence is mitigated by other factors or other species are carrying out the same function (Turnbaugh et al. 2007). However, these species could have an important influence that is yet to be elucidated. This study in terms of the metagenomic sequencing focused on composition of the whole saliva-derived biofilm by proportion to determine whether proportion would be related to the effect seen. However, it could be that the more variable microorganisms have an impact on *C. albicans* surface colonisation and hyphal morphology, as the saliva from each individual elicited a significantly different response on *C. albicans*.

However, the above comparisons were based on differences in proportions, but research has proposed that it may not be the most abundant species which are important, but the activity that is present and possibly the presence of keystone species (Hajishengallis et al. 2012). It could also be that proportionally there were no differences between the bacterial composition in biofilms, however, localisation and proximity of specific species may lead to altered interactions and effects. This could be investigated through looking at the functional capacity of the salivary microbiome through metabolomics or which could be explored using the metagenomic data that has been obtained in this research. Now that the species present in highest proportions in biofilms derived from the saliva of individuals using this methodology is known, future research could use species specific staining/probes to assess localisation within biofilms. In addition, the individual effects on *C. albicans* of each of these species (*S. salivarius, S. oralis, S. mitis, R. mucilaginosa* and *S. parasanguinis*) could be assessed.

Future work could aim to combine metagenomic results with metatranscriptomics and metabolomics to assess not only taxonomic composition and diversity, but the functional aspect of the influence they are having and what they are expressing and bringing to the environment. The whole genome metagenomic sequencing obtained herein has only been used for species assessment and is available for analysis in subsequent work. In such studies genes of interest whose presence may be more important than the abundance of species could be determined. The depth of the sequencing performed is of sufficient quality to allow more sophisticated analysis, for example using metagenome-assembled genomes (MAGs) to assemble the microbes, contextualise them and their functions of

interest (Zhu et al. 2022; Gurbich et al. 2023). The sequencing data has also been run through the MEGARes AMR++ v3.0 pipeline (Bonin et al. 2023), however, this is beyond the scope of this thesis so the output has not yet been analysed but may be relevant in future work.

In conclusion, biofilms from whole saliva encompassing both salivary components and microbial cells from different individuals promoted changes in *C. albicans* surface area coverage. However, *C. albicans* filamentous morphology was mostly unaffected by the saliva from the different individuals, resulting in relatively consistent levels of filamentous forms suggesting that virulence was not significantly increased in any specific sample. Sequence analysis of the bacterial species in the biofilms found that there were no statistically significant differences in the proportions of the top 500 bacterial species. More research is required to elucidate how the oral microbiome may modulate behaviour of *C. albicans* and which species may increase risk of *Candida*-associated infections.

CHAPTER 6: General Discussion

6.1. General Discussion

Candida as a genus comprises over 350 species which are found ubiquitously in the environment, within animal hosts and in industrial settings (Williams and Lewis 2011). In the case of humans, *Candida* are known to colonise the skin, gut and moist mucosal surfaces, primarily of the mouth and vagina (Gulati and Nobile 2016; Lohse et al. 2018). To facilitate colonisation of the host, *Candida* has inherent mechanisms to adhere and form biofilms, acquire nutrition from the immediate environment and successfully compete with other microorganisms as well as resist host responses to eradicate it (Williams and Lewis 2011; Dadar et al. 2018; Abuhajar et al. 2023).

Whilst *Candida* is normally a harmless member of the normal microbiota, it is an opportunistic pathogen and under certain conditions of host debilitation can cause infection (Williams and Lewis 2011; Abuhajar et al. 2023). In 2022, the World Health Organisation composed a priority list to indicate the importance of research development and public health action for fungal pathogens, and *C. albicans* was one of four species placed in the critical priority category (World Health Organization 2022). Most frequently, *Candida* infections are superficial and managed by control of risk factors and topical antifungals. However, in immunocompromised patients, serious systemic disease can occur with high morbidity and mortality rates (Kadosh 2019; Abuhajar et al. 2023). Whilst several *Candida* species can cause human infection (candidosis), the most frequent cause is *C. albicans* (Ramage et al. 2006; Williams and Lewis 2011; Abuhajar et al. 2023). Unsurprisingly, this species is also reported to have highest expression of putative virulence factors, such as production of secreted aspartyl proteinases (SAPs), phospholipases (PLs), and hyphal transformation (Kumamoto and Vinces 2005b; Williams et al. 2011). Despite possessing virulence attributes, infection by *C. albicans* does not typically occur in otherwise healthy individuals and this highlights the importance of additional host factors in the initiation of disease. Known risk factors for oral candidosis include a high carbohydrate diet, nutritional deficiency, local and systemic immunodeficiencies, extremes of age (new-born and elderly), the wearing of a denture prothesis alongside poor oral hygiene, hormonal imbalances and receipt of a broad-spectrum antibiotic (Shulman et al. 2005; Abuhajar et al. 2023). The latter is potentially indicative of the competition afforded by oral bacteria that might control *Candida* numbers and behaviour at oral sites.

Clearly, a wide range of variables can ultimately impact on the transition of *C. albicans* from a harmless oral commensal microorganism to one that is responsible for human infection. The overarching aim of the research presented was to explore several of these potential variables and their impact on the *in vitro* behaviour *of C. albicans* in terms of biofilm formation and development. Selected variables were the conditioning films for oral surfaces (Chapter 2), the topography of these surfaces (Chapter 3), the effect of individual species of oral bacteria within the biofilm (Chapter 4), and consideration of a more complex microbial community derived from whole human saliva (Chapter 5). An understanding of how these variables impacted upon *Candida* biofilm development was important as the knowledge generated could be used to inform both on the prevention of infection and its subsequent management.

Research exploring the effect of surface conditioning used acrylic (polymethyl methacrylate; PMMA) as the surface material. This was considered clinically relevant because of the use of acrylic within dentures and the high prevalence of chronic erythematous candidosis amongst denture wearers (Williams and Lewis 2011; Abuhajar et al. 2023). An artificial saliva (AS) was incorporated as a preconditioning medium to create an environment more mimetic of the oral cavity. Given the higher incidence of oral candidosis, including chronic erythematous candidosis amongst tobacco smokers (Barbeau et al. 2003), it was hypothesised that the addition of tobacco components to precondition the acrylic surfaces would increase *C. albicans* virulence compared to controls. Tobacco condensate has been found to increase *C. albicans* biofilm thickness, induce hyphal transition and increase cell surface hydrophobicity (Awad and Karuppayil 2018; Gunasegar and Himratul-aznita 2019). *C. albicans* can also be successfully grown on tobacco agar which can be utilised to differentiate *C. albicans* from *C. dubliniensis* using phenotypic traits (Khan et al. 2004)

The use of five different strains of *C. albicans* highlighted the diversity of this species, as strain dependent responses were encountered in terms of adherence, biofilm development and hyphal transformation. Evidence to support the hypothesis that a tobacco condensate (TC) would promote *C. albicans* virulence was seen with *C. albicans* 705/93. This was a clinically isolated strain and was found to demonstrate higher hyphal transformation after 24 h of growth on the TC treated acrylic.

It was expected that preconditioning with AS would cause a significant difference in adherence as previous research using the same AS formulation with PMMA significantly increased adherence to PMMA surfaces (Morse 2017). However, this research used a different strain of *C. albicans* and as shown the effect was strain dependent. Two clinical *C. albicans* strains did show increased surface coverage on the AS-preconditioned surfaces compared to water and TC treated surfaces. This could have been due the AS surfaces being significantly more hydrophilic, but it was interesting that not all *C. albicans* strains responded similarly. Cell surface hydrophobicity does vary dependent on the cell wall components present and is influenced by environmental factors (Panagoda et al. 1998; Ellepola et al. 2013; Danchik and Casadevall 2021). Variation in the literature concerning the adherence of *C. albicans* adherence due to saliva, both artificial and natural, preconditioning of surfaces *in vitro* may be due to the diversity and high intra-species variation of *C. albicans* (Hirakawa et al. 2015).

Another potential surface variable that could conceivably impact on the behaviour of *C. albicans* in biofilms is the material surface topography. In the case of denture acrylic, whilst smooth and highly polished surfaces may originally be produced, these can become abraded based on intake of abrasive foods, and physical damage from handling or cleaning with abrasive products (Nikawa et al. 2003). Several studies have examined the impact of different surface topographies on adherence of oral microorganisms including *Candida* to acrylic and also bacteria to titanium (Radford et al. 1998; Nevzatoğlu et al. 2007). Results have indicated that there is an optimum size of surface irregularity that promotes adherence which is typically associated to the size of the microbial cell under study (Whitehead et al. 2004; Whitehead et al. 2005). In the research presented in Chapter 3, a range of acrylic surface topographies were produced by abrasion with different grades of polishing sandpapers. Results showed that these surfaces were different in respect of subsequent *C. albicans* adherence and biofilm formation. There was no direct correlation between colonisation and mean roughness value, which indicated that once an optimal mean roughness size was present, increasing or decreasing the roughness would negate its effects. Importantly, the retention of *C. albicans* within surface scratches was clearly evident in the micrographs generated and would likely represent problematic regions for any cleansing regimes.

Interestingly, previous studies have suggested that changing surface roughness can alter hydrophobicity, which in turn can affect microbial adherence (Mouhat et al. 2020). It has been observed that the more hydrophobic the denture-base surface (exact material not disclosed) the greater the level of adhesion of *C. albicans* (Minagi et al. 1985). Significant differences in hydrophobicity between surfaces of varying surface roughness categories were not encountered in this research. However, it was interesting to note that differences in adherence and biofilm formation between the wild type *C. albicans* SC5413 and its Als3 deleted mutant occurred. This could, in part, relate to relative differences in cell surface hydrophobicity between the strains. The Als3 protein has been suggested to present hydrophobic domains that facilitate adherence (Beaussart et al. 2012). Measurement of cell surface hydrophobicity was not undertaken in this research and is an area for further work. However, in contrast other studies have found that hydrophobicity of PMMA surfaces does not correlate with *C. albicans* adherence (Murat et al. 2019). Another consideration of surface topography that could indirectly effect biofilm development would be higher retention of organic debris within surface irregularities. These areas could serve as 'seeding' regions with greater capacity for biofilm regrowth following inadequate surface cleansing (Vila et al. 2020).

The hypothesis that differentially abraded surfaces would alter adherence of *C. albicans* was confirmed, though there was not a direct relationship between increasing roughness and adherence. Instead, findings supported those in the literature that stated that there was an optimum level of roughness and size of topological features for increased adhesion and retention (Whitehead and Verran 2006). However, it is important to note that abrasion of surfaces inevitably results in variation in roughness and size of topological features. The roughness was categorised by measuring the m Ra values and this has widely been used as a descriptor of surface roughness, not only in research but also in manufacturing and production industries (Rodriguez Fereira et al. 2011). Ra values do not however represent the extreme deviations on the surface that may impact on adherence and retention of *C. albicans* (Rodriguez Fereira et al. 2011). The optimum level of roughness for microbial cell adhesion and retention appears to be related to cell size (Whitehead et al. 2004). However, it would be difficult to define the optimum pore/surface feature size for increased *C. albicans* adherence given the highly polymorphic nature of this species yielding differently sized

fungal units (yeast and hyphae). It is also possible that the size of surface features that increases *C. albicans* adherence may be lower than the comparative size of *C. albicans* cells due to microbial interactions. Future work could explore the effect of *C. albicans* adherence on surfaces of different roughness in combination with selected bacterial species that have been shown to increase abundance of *C. albicans* on denture material surfaces. Oral *Streptococcus* species were found to increase *C. albicans* colonisation (Chapter 4), therefore, it could be hypothesised that if the adherence and retention of oral *Streptococcus* species was increased by smaller topological features, this may result in increased *C. albicans* presence due to interactions with *Streptococcus* cells. This would have clinical implications for the level of wear and roughness that enhances microbial adherence and retention may be lower than currently expected, which may increase the risk of infection and inform the level at which denture replacement may be advised due to levels of abrasion and damage.

Having assessed non-biological effects of conditioning and abiotic surface abrasion, it was important to evaluate the role that other microorganisms could play in the behaviour of *C. albicans* within biofilms, and this was the focus of Chapters 4 and 5. The complexity of the oral microbiome and the networks of interaction that occur are extensive. Hypotheses of infection range from 1) the presence of single species being causative agents for infections, 2) groups of the most abundant species interacting, and 3) to the presence of keystone species not necessarily being the most abundant but coordinating oral microbiota in infection (Rosier et al. 2014). Investigating these complex network requires understanding interactions between single species that can then be considered in more complex systems in ecological studies (Zengler and Zaramela 2018). Understanding such a network of interactions would have implications in terms of prognosis and management of biofilm infections, not only in the mouth but also other biofilm infections. Findings from *in vitro* studies could be extrapolated to other microbiomes at different body sites, thereby having wider implications for human health.

Investigating interactions between *C. albicans* and four selected oral *Streptococcus* species aimed to describe what would occur without interference of other members in a complex network and how these interactions may occur. The *Streptococcus* species selected for study are recognised as primary colonisers of the oral cavity to which *C. albicans* can bind, to facilitate its adherence and biofilm formation (Álvarez et al. 2022).

In addition, previous research has found that oral *Streptococcus* species can promote *C. albicans* hyphal production through suppression of farnesol-mediated inhibition (Bamford et al. 2009; Ponde et al. 2021). It was hypothesised therefore that dual species biofilms would increase colonisation of *C. albicans* on acrylic surfaces and occurrence of hyphal forms associated with increased pathogenicity. All four *Streptococcus* species studied, *S. mutans, S, gordonii, S. salivarius* and *S. sanguinis,* resulted in an increase in *C. albicans* colonisation when grown in dual species compared to single species controls at 24 h. The same result was not found using spent medium from the same species, indicating that live cells were required for this effect to be observed.

Interactions between *S. gordonii* and *C. albicans* have previously been studied due to implications not only in the oral cavity, but also in vaginal health. This interaction has been described as being facilitated through the Als3 adhesin of *C. albicans* and the SspA and SspB proteins of *S. gordonii* (Silverman et al. 2010). Therefore, an Als3 deleted mutant was used in these studies to ascertain whether changes would occur without the adhesin present and whether other selected species of *Streptococcus* exhibited the same effect. The hypothesis was that physical interaction between filamentous forms of the wild-type *C. albicans* would be higher than for the mutant *C. albicans* strain lacking Als3. In these studies, this hypothesis was supported for *S. gordonii, S. sanguinis* and *S. salivarius* though not for *S. mutans.* This was expected due to interactions between *C. albicans* and *S. mutans* previously being described as being independent of Als3 (Hwang et al. 2017; Yang et al. 2018). Interaction in biofilms *in vivo* involve *C. albicans* cell wall mannans binding to an *S. mutans* secreted exoenzyme beta glucosyltransferase (GtfB) that results in enhanced production of the glucan-matrix and modulates bacterial-fungal association (Hwang et al. 2017). Another pathway of interaction between *S. mutans* and *C. albicans* has reportedly been mediated through *S. mutans* antigen I/II and also independent of Als1 and Als3 (Yang et al. 2018).

Further research into whether biofilm development by the *C. albicans* Als3 mutant was affected by the presence of the individual *Streptococcus* species would have been useful. However, the Als3 mutant strain has previously been found to be unable to form biofilms; while the cells initially attach the hyphal forms then ‘lift away’ from

surfaces which would interfere with findings and also reaffirming the importance of Als3 in adherence and biofilm formation (Silverman et al. 2010).

A limitation of this research was that the biofilms at the 72 h timepoint were exposed to disruption of the biofilm during media changes which was limited as much as possible but could have caused loss of material. Though this was the same for the controls and still representative in future studies, it may be better to use an alternative method such as using a CDC bioreactor as was used in Chapter 5. Using the CDC bioreactor for these experiments would have been more time consuming as a bioreactor would have been needed for each condition reducing the throughput of samples. However, biofilms grown in a CDC bioreactor batch or continuous flow system may be more representative as they form more robust biofilms due to experiencing shear flow throughout growth (Bowen et al. 2018; Johnson et al. 2021; Lindsay et al. 2022).

After investigating the effects of selected individual oral species on *C. albicans*, a more complex biofilm derived from whole human saliva was used study the impact on *C. albicans* biofilm colonisation and morphology and ascertain if saliva from different individuals led to differences in these effects. This would help determine whether the salivary microbiome and components from healthy individuals might be a contributing factor in why some individuals are more susceptible to *Candida* infections than others.

Each saliva sample, (filtered or whole) affected the biofilm colonisation of *C. albicans* on surfaces differently. Significantly elevated quantities of *C. albicans* in biofilms were found when using either filtered or whole saliva from the same individuals. This showed that the presence of microbial cells influenced to *C. albicans* levels on surfaces. The area of *C. albicans* on surfaces was also significantly different between filtered and whole saliva for different individuals. However, no differences in the *C. albicans* morphology between (saliva filtered or whole) from different individuals occurred. There was slightly more variation in the area of filamentous morphology between filtered saliva biofilms from different individuals than for the whole salivas which could suggest that the presence of live bacteria may regulate *C. albicans* hyphal transition. Two saliva biofilms had significantly fewer hyphal morphology in the whole compared to the filtered saliva, supporting this hypothesis.

To explore differences in saliva derived biofilms in respect of the bacterial microbiome, whole genome shotgun metagenomic sequencing was undertaken. The bacterial species present in the whole saliva-derived biofilms appeared similar with the top five bacterial species accounting for the majority of the bacterial component of the biofilms (53.58% to 74.24%). *Streptococcus salivarius* was the most abundant species in all whole-saliva derived biofilms and in Chapter 4 this species increased *C. albicans* colonisation and hyphal morphology. If the most abundant species was responsible for causing effects, it would have been expected that all the whole-saliva derived biofilms would have had this effect. However, there were no significant differences in the top 500 species of the whole-saliva biofilm, demonstrating the highest and lowest abundance of *C. albicans* on the surfaces, and also the highest and lowest levels of filamentous morphology. This suggests that effects on *Candida* were not due to differences in abundance of bacteria species. It may be that the effects on *C. albicans* were not caused by a more abundant species, but possibly due to localisation of species. Biofilms are highly heterogenous, with species not being equally distributed. Also, *Streptococcus* species, including *S. salivarius* interact with *C. albicans* both physically and chemically through QS molecules, which may contribute to the differences between filtered saliva biofilms if QS molecules (*e.g.* autoinducer-2) were present in the filtered saliva samples (Sztajer et al. 2008). All four bacterial species used in Chapter 4 were detected in whole saliva-derived biofilms, as well as many other *Streptococcus* species that may have elicited similar effects. Further research is required to understand which bacterial species may contribute to the effects on *C. albicans.* It may be that rather than species abundance it is the levels of specific gene expression from multiple species that is the determining factor on affecting *C. albicans*.

To conclude, overall findings showed that *C. albicans* responded to environmental factors in a strain dependent manner for surface conditioning and the influence of tobacco condensates. Surface roughness of dentures was an important factor for *C. albicans* adherence and colonisation, which could imply that dentures with a high level of surface abrasion should be replaced to reduce *Candida* colonisation and risk of infection. In terms of microbial interactions, the four *Streptococcus* species investigated, namely *S. mutans, S, gordonii, S. salivarius* and *S. sanguinis,* increased *C. albicans* colonisation on acrylic surfaces and this could have resulted from physical interaction as the same effects did not occur using spent medium. Use of the *C.*

albicans Als3 mutant strain showed that *S, gordonii, S. salivarius* and *S. sanguinis* had higher localisation to the filamentous forms when Als3 was present, supporting previous research that this hyphal specific adhesin is involved in physical interactions of bacteria with *C. albicans.* However, *S. mutans* had higher localisation with the Als3 mutant strain than the wild-type. It is unknown why it was higher on the mutant, but it is known that *S. mutans* interactions with *C. albicans* do not involve Als3. Biofilms from the saliva from healthy individuals had different effects on *C. albicans* and were seen with biofilms from filtered and whole saliva. Differences were seen in the presence and absence of bacteria, confirming that both live cells and salivary components contribute to effects. Analysis of metagenomic sequencing suggested that abundance/proportion of bacterial species was not a determining factor on *C. albicans* surface area coverage or filamentous morphology. The primary aim of this thesis was to determine whether key properties of *C. albicans* such as biofilm forming ability and morphological transformation in biofilms are modulated by specific local environment factors including surface conditioning, surface roughness and the presence of oral bacterial species. These factors were found to influence *C. albicans* properties and should therefore be taken into consideration in the management of *C. albicans* in the oral cavity and *Candida*-associated denture stomatitis.

Bibliography

Aas, J.A., Paster, B.J., Stokes, L.N., Olsen, I. and Dewhirst, F.E. 2005. Defining the normal bacterial flora of the oral cavity. *Journal of Clinical Microbiology* 43(11), pp. 5721–5732. doi: 10.1128/JCM.43.11.5721-5732.2005.

Abelson, D.C. 1981. Denture plaque and denture cleansers. *The Journal of Prosthetic Dentistry* 45(4), pp. 376–379. doi: 10.1016/0022-3913(81)90094-9.

Abranches, J. et al. 2018. Biology of oral streptococci. *Gram-Positive Pathogens*, pp. 426–434. doi: 10.1128/9781683670131.ch26.

Abuhajar, E., Ali, K., Zulfiqar, G., Al Ansari, K., Raja, H.Z., Bishti, S. and Anweigi, L. 2023. Management of Chronic Atrophic Candidiasis (Denture Stomatitis)-A Narrative Review. *International journal of environmental research and public health* 20(4). doi: 10.3390/ijerph20043029.

Adler, C.J. et al. 2013. Sequencing ancient calcified dental plaque shows changes in oral microbiota with dietary shifts of the Neolithic and Industrial revolutions. *Nature Genetics* 45(4), pp. 450–455. doi: 10.1038/ng.2536.

Aguayo, S. et al. 2017. Early Adhesion of *Candida albicans* onto Dental Acrylic Surfaces. *Journal of Dental Research* 96(8), pp. 917–923. doi: 10.1177/0022034517706354.

Akram, Z., Al-Kheraif, A.A., Kellesarian, S. V., Vohra, F. and Javed, F. 2018. Comparison of oral *Candida* carriage in waterpipe smokers, cigarette smokers, and non-smokers. *Journal of Oral Science* 60(1), pp. 115–120. doi: 10.2334/josnusd.17-0090.

Alanazi, H., Semlali, A., Chmielewski, W. and Rouabhia, M. 2019. E-cigarettes increase *Candida albicans* growth and modulate its interaction with gingival epithelial cells. *International Journal of Environmental Research and Public Health* 16(2), pp. 1–18. doi: 10.3390/ijerph16020294.

Alanazi, H., Semlali, A., Perraud, L., Chmielewski, W., Zakrzewski, A. and Rouabhia, M. 2014. Cigarette Smoke-Exposed *Candida albicans* Increased Chitin Production and Modulated Human Fibroblast Cell Responses. *BioMed Research International* 2014. doi: 10.1155/2014/963156.

Alcaraz, L.D., Belda-Ferre, P., Cabrera-Rubio, R., Romero, H., Simón-Soro, Á., Pignatelli, M. and Mira, A. 2012. Identifying a healthy oral microbiome through metagenomics. *Clinical Microbiology and Infection* 18(SUPPL. 4), pp. 54–57. doi: 10.1111/j.1469-0691.2012.03857.x.

Allison, R.T. and Douglas, W.H. 1973. Micro-colonization of the denture-fitting surface by *Candida albicans*. *Journal of Dentistry* 1(5), pp. 198–201. doi: 10.1016/0300-5712(73)90059-6.

de Almeida, P.D.V., Grégio, A.M.T., Machado, M.A.N., Lima, A.A.S. de and Azevedo, L.R. 2008. Saliva composition and functions: a comprehensive review. *The journal of contemporary dental practice* 9(3), pp. 72–80.

Álvarez, S., Leiva-Sabadini, C., Schuh, C.M.A.P. and Aguayo, S. 2022. Bacterial

adhesion to collagens: implications for biofilm formation and disease progression in the oral cavity. *Critical Reviews in Microbiology* 48(1), pp. 83–95. doi: 10.1080/1040841X.2021.1944054.

Alves, C.T., Wei, X.Q., Silva, S., Azeredo, J., Henriques, M. and Williams, D.W. 2014. *Candida albicans* promotes invasion and colonisation of *Candida glabrata* in a reconstituted human vaginal epithelium. *Journal of Infection* 69(4), pp. 396–407. doi: 10.1016/j.jinf.2014.06.002.

An, S., Evans, J.L., Hamlet, S. and Love, R.M. 2021. Overview of incorporation of inorganic antimicrobial materials in denture base resin: A scoping review. *Journal of Prosthetic Dentistry*, pp. 1–10. doi: 10.1016/j.prosdent.2021.09.004.

Andes, D. 2003. In vivo pharmacodynamics of antifungal drugs in treatment of candidiasis. *Antimicrobial Agents and Chemotherapy* 47(4), pp. 1179–1186. doi: 10.1128/AAC.47.4.1179-1186.2003.

Awad, A. and Karuppayil, S. 2018. Tobacco Extract Induces Yeast to Hyphal form Transition in the Human Pathogen , *Candida albicans*. *American Journal of Clinical Microbiology and Antimicrobials* 1(3), pp. 1–6.

Axe, A.S., Varghese, R., Bosma, M., Kitson, N. and Bradshaw, D.J. 2016. Dental health professional recommendation and consumer habits in denture cleansing. *Journal of Prosthetic Dentistry* 115(2), pp. 183–188. doi: 10.1016/j.prosdent.2015.08.007.

Bamford, C. V., D'Mello, A., Nobbs, A.H., Dutton, L.C., Vickerman, M.M. and Jenkinson, H.F. 2009. *Streptococcus gordonii* modulates *Candida albicans* biofilm formation through intergeneric communication. *Infection and Immunity* 77(9), pp. 3696–3704. doi: 10.1128/IAI.00438-09.

Bamford, C. V., Nobbs, A.H., Barbour, M.E., Lamont, R.J. and Jenkinson, H.F. 2015. Functional regions of *Candida albicans* hyphal cell wall protein Als3 that determine interaction with the oral bacterium *Streptococcus gordonii*. *Microbiology (United Kingdom)* 161(1). doi: 10.1099/mic.0.083378-0.

Baraniya, D. et al. 2022. Optimization of conditions for in vitro modeling of subgingival normobiosis and dysbiosis. *Frontiers in Microbiology* 13(November), pp. 1–10. doi: 10.3389/fmicb.2022.1031029.

Barbeau, J. et al. 2003. Reassessing the presence of *Candida albicans* in denture-related stomatitis. *Oral Surgery, Oral Medicine, Oral Pathology, Oral Radiology, and Endodontics* 95(1), pp. 51–59. doi: 10.1067/moe.2003.44.

Barraud, N., Hassett, D.J., Hwang, S.H., Rice, S.A., Kjelleberg, S. and Webb, J.S. 2006. Involvement of nitric oxide in biofilm dispersal of *Pseudomonas aeruginosa*. *Journal of Bacteriology* 188(21), pp. 7344–7353. doi: 10.1128/JB.00779-06.

Beaussart, A., Alsteens, D., El-Kirat-Chatel, S., Lipke, P.N., Kucharíková, S., Van Dijck, P. and Dufrêne, Y.F. 2012. Single-Molecule Imaging and Functional Analysis of Als Adhesins and Mannans during *Candida albicans* Morphogenesis. *ACS Nano* 6(12), pp. 10950–10964. doi: 10.1021/nn304505s.

Belstrøm, D. 2020. The salivary microbiota in health and disease. *Journal of Oral Microbiology* 12(1). doi: 10.1080/20002297.2020.1723975.

Benoit, D.S.W., Sims, K.R. and Fraser, D. 2019. Nanoparticles for Oral Biofilm Treatments. *ACS Nano* 13(5), pp. 4869–4875. doi: 10.1021/acsnano.9b02816.

Berger, D., Rakhamimova, A., Pollack, A. and Loewy, Z. 2018. Oral Biofilms : Development , Control , and Analysis. pp. 1–8. doi: 10.3390/ht7030024.

Besemer, K., Peter, H., Logue, J.B., Langenheder, S., Lindström, E.S., Tranvik, L.J. and Battin, T.J. 2012. Unraveling assembly of stream biofilm communities. *ISME Journal* 6(8), pp. 1459–1468. doi: 10.1038/ismej.2011.205.

Bhattarai, K.R., Kim, H.R. and Chae, H.J. 2018. Compliance with saliva collection protocol in healthy volunteers: Strategies for managing risk and errors. *International Journal of Medical Sciences* 15(8), pp. 823–831. doi: 10.7150/ijms.25146.

Bhushan, B., Yadav, A.P., Singh, S.B. and Ganju, L. 2019. Diversity and functional analysis of salivary microflora of Indian Antarctic expeditionaries. *Journal of Oral Microbiology* 11(1). doi: 10.1080/20002297.2019.1581513.

Bik, E.M. et al. 2010. Bacterial diversity in the oral cavity of 10 healthy individuals. *ISME Journal* 4(8), pp. 962–974. doi: 10.1038/ismej.2010.30.

Bjarnsholt, T. et al. 2013. The *in vivo* biofilm. *Trends in Microbiology* 21(9), pp. 466–474. doi: 10.1016/j.tim.2013.06.002.

Bollen, C.M.L., Papaioanno, W., Eldere, J. Van, Schepers, E., Quirynen, M. and Steenberghe, D. Van. 1996. The influence of abutment surface roughness on plaque accumulation and peri-implant mucositis. *Clinical Oral Implants Research* 7, pp. 201–211. doi: https://doi.org/10.1034/j.1600-0501.1996.070302.x.

Bonin, N. et al. 2023. MEGARes and AMR++, v3.0: an updated comprehensive database of antimicrobial resistance determinants and an improved software pipeline for classification using high-throughput sequencing. *Nucleic acids research* 51(D1), pp. D744–D752. doi: 10.1093/nar/gkac1047.

Bostanci, N. et al. 2021. Dysbiosis of the Human Oral Microbiome During the Menstrual Cycle and Vulnerability to the External Exposures of Smoking and Dietary Sugar. *Frontiers in Cellular and Infection Microbiology* 11(March), pp. 1–14. doi: 10.3389/fcimb.2021.625229.

Bowen, W.H., Burne, R.A., Wu, H. and Koo, H. 2018. Oral Biofilms: Pathogens, Matrix, and Polymicrobial Interactions in Microenvironments. *Trends in Microbiology* 26(3). doi: 10.1016/j.tim.2017.09.008.

Brand, A., Shanks, S., Duncan, V.M.S., Yang, M., Mackenzie, K. and Gow, N.A.R. 2007. Report Hyphal Orientation of *Candida albicans* Is Regulated by a Calcium-Dependent Mechanism. 17(4), pp. 347–352. doi: 10.1016/j.cub.2006.12.043.

Britannica, T.E. of E. 2022. mouth.

Brown, A.J.P., Brown, G.D., Netea, M.G. and Gow, N.A.R. 2014. Metabolism impacts upon *candida* immunogenicity and pathogenicity at multiple levels. *Trends in Microbiology* 22(11), pp. 614–622. doi: 10.1016/j.tim.2014.07.001.

Bruder-Nascimento, A., Camargo, C.H., Mondelli, A.L., Sugizaki, M.F., Sadatsune, T. and Bagagli, E. 2014. *Candida* species biofilm and *Candida albicans* ALS3 polymorphisms in clinical isolates. *Brazilian Journal of Microbiology* 45(4), pp. 1371–

1377. doi: 10.1590/S1517-83822014000400030.

Cameron, S.J.S., Huws, S.A., Hegarty, M.J., Smith, D.P.M. and Mur, L.A.J. 2015. The human salivary microbiome exhibits temporal stability in bacterial diversity. *FEMS Microbiology Ecology* 91(9), pp. 1–9. doi: 10.1093/femsec/fiv091.

Campanha, N.H., Pavarina, A.C., Jorge, J.H., Vergani, C.E., MacHado, A.L. and Giampaolo, E.T. 2012. The effect of long-term disinfection procedures on hardness property of resin denture teeth. *Gerodontology* 29(2), pp. 571–576. doi: 10.1111/j.1741-2358.2011.00520.x.

Cannon, R.D., Holmes, A.R., Mason, A.B. and Monk, B.C. 1995. *Concise Review Oral Candida: Clearance, Colonization, or Candidiasis?*

Cavalcanti, I.M.G., Del Bel Cury, A.A., Jenkinson, H.F. and Nobbs, A.H. 2017. Interactions between *Streptococcus oralis, Actinomyces oris,* and *Candida albicans* in the development of multispecies oral microbial biofilms on salivary pellicle. *Molecular Oral Microbiology* 32(1), pp. 60–73. doi: 10.1111/omi.12154.

Cavalcanti, Y.W. et al. 2014. Virulence and pathogenicity of *Candida albicans* is enhanced in biofilms containing oral bacteria. *Biofouling* 31(1), pp. 27–38. doi: 10.1080/08927014.2014.996143.

Cavalcanti, Y.W., Wilson, M., Lewis, M., Del-Bel-Cury, A.A., da Silva, W.J. and Williams, D.W. 2016a. Modulation of *Candida albicans* virulence by bacterial biofilms on titanium surfaces. *Biofouling* 32(2), pp. 123–134. doi: 10.1080/08927014.2015.1125472.

Cavalcanti, Y.W., Wilson, M., Lewis, M., Williams, D., Senna, P.M., Del-Bel-Cury, A.A. and Da Silva, W.J. 2016b. Salivary pellicles equalise surfaces' charges and modulate the virulence of *Candida albicans* biofilm. *Archives of Oral Biology* 66, pp. 129–140. doi: 10.1016/j.archoralbio.2016.02.016.

Chang, Y.H., Lee, C.Y., Hsu, M.S., Du, J.K., Chen, K.K. and Wu, J.H. 2021. Effect of toothbrush/dentifrice abrasion on weight variation, surface roughness, surface morphology and hardness of conventional and cad/cam denture base materials. *Dental Materials Journal* 40(1), pp. 220–227. doi: 10.4012/dmj.2019-226.

Chaouachi, K.T. 2007. The narghile (hookah, shisha, goza) epidemic and the need for clearing up confusion and solving problems related with model building of social situations. *TheScientificWorldJournal* 7, pp. 1691–1696. doi: 10.1100/tsw.2007.255.

Chen, T., Yu, W.H., Izard, J., Baranova, O. V., Lakshmanan, A. and Dewhirst, F.E. 2010. The Human Oral Microbiome Database: a web accessible resource for investigating oral microbe taxonomic and genomic information. *Database : the journal of biological databases and curation* 2010, pp. 1–10. doi: 10.1093/database/baq013.

Chua, S.L. et al. 2014. Dispersed cells represent a distinct stage in the transition from bacterial biofilm to planktonic lifestyles. *Nature Communications* 5, pp. 1–12. doi: 10.1038/ncomms5462.

Cieplik, F. et al. 2019. Microcosm biofilms cultured from different oral niches in periodontitis patients. *Journal of Oral Microbiology* 11(1). doi: 10.1080/20022727.2018.1551596.

Clemens, K.J., Caillé, S., Stinus, L. and Cador, M. 2009. The addition of five minor

tobacco alkaloids increases nicotine-induced hyperactivity, sensitization and intravenous self-administration in rats. *International Journal of Neuropsychopharmacology* 12(10), pp. 1355–1366. doi: 10.1017/S1461145709000273.

Coker, M.O. et al. 2022. Metagenomic analysis reveals associations between salivary microbiota and body composition in early childhood. *Scientific Reports* (0123456789), pp. 1–15. doi: 10.1038/s41598-022-14668-y.

Costello, E.K., Lauber, C.L., Hamady, M., Fierer, N., Gordon, J.I. and Knight, R. 2009. Bacterial Community Variation in Human Body Habitats Across Space and Time. *Science* 326(5960), pp. 1694–1697. doi: 10.1126/science.1177486.

Costello, E.K., Stagaman, K., Dethlefsen, L., Bohannan, B.J.M. and Relman, D.A. 2012. The Application of Ecological Theory Toward an Understanding of the Human Microbiome. *Science* 336(6086), pp. 1255–1262. doi: 10.1126/science.1224203.

Crielaard, W., Zaura, E., Schuller, A.A., Huse, S.M., Montijn, R.C. and Keijser, B.J.F. 2011. Exploring the oral microbiota of children at various developmental stages of their dentition in the relation to their oral health. *BMC Medical Genomics* 4(1), p. 22. doi: 10.1186/1755-8794-4-22.

Dadar, M., Tiwari, R., Karthik, K., Chakraborty, S., Shahali, Y. and Dhama, K. 2018. *Candida albicans* - Biology, molecular characterization, pathogenicity, and advances in diagnosis and control – An update. *Microbial Pathogenesis* 117(February), pp. 128–138. doi: 10.1016/j.micpath.2018.02.028.

Danchik, C. and Casadevall, A. 2021. Role of Cell Surface Hydrophobicity in the Pathogenesis of Medically-Significant Fungi. *Frontiers in Cellular and Infection Microbiology* 10(January), pp. 1–7. doi: 10.3389/fcimb.2020.594973.

Darveau, R.P. 2010. Periodontitis: A polymicrobial disruption of host homeostasis. *Nature Reviews Microbiology* 8(7), pp. 481–490. doi: 10.1038/nrmicro2337.

Davies, D.G. and Marques, C.N.H. 2009. A fatty acid messenger is responsible for inducing dispersion in microbial biofilms. *Journal of Bacteriology* 191(5), pp. 1393–1403. doi: 10.1128/JB.01214-08.

Davies, J.M., Stacey, A.J. and Gilligan, C.A. 1999. *Candida albicans* hyphal invasion: Thigmotropism or chemotropism? *FEMS Microbiology Letters* 171(2), pp. 245–249. doi: 10.1016/S0378-1097(98)00600-4.

Dawes, C. et al. 2015. The functions of human saliva: A review sponsored by the World Workshop on Oral Medicine VI. *Archives of Oral Biology* 60(6), pp. 863–874. doi: 10.1016/j.archoralbio.2015.03.004.

Dawes, C. and Wong, D.T.W. 2019. Role of Saliva and Salivary Diagnostics in the Advancement of Oral Health. *Journal of Dental Research* 98(2), pp. 133–141. doi: 10.1177/0022034518816961.

Deng, K., Jiang, W., Jiang, Y., Deng, Q., Cao, J., Yang, W. and Zhao, X. 2021. ALS3 Expression as an Indicator for *Candida albicans* Biofilm Formation and Drug Resistance. *Frontiers in Microbiology* 12(April), pp. 1–10. doi: 10.3389/fmicb.2021.655242.

Desai, J. V. 2018. *Candida albicans* hyphae: From growth initiation to invasion. *Journal*

of Fungi 4(1). doi: 10.3390/jof4010010.

Desmond, P., Best, J.P., Morgenroth, E. and Derlon, N. 2018. Linking composition of extracellular polymeric substances (EPS) to the physical structure and hydraulic resistance of membrane biofilms. *Water Research* 132, pp. 211–221. doi: 10.1016/j.watres.2017.12.058.

Dewhirst, F.E. et al. 2010. The human oral microbiome. *Journal of Bacteriology* 192(19), pp. 5002–5017. doi: 10.1128/JB.00542-10.

Diaz-Torres, M.L. et al. 2006. Determining the antibiotic resistance potential of the indigenous oral microbiota of humans using ametagenomic approach. *FEMS Microbiology Letters* 258(2), pp. 257–262. doi: 10.1111/j.1574-6968.2006.00221.x.

Diaz, P.I., Strausbaugh, L.D. and Dongari-Bagtzoglou, A. 2014. Fungal-bacterial interactions and their relevance to oral health: Linking the clinic and the bench. *Frontiers in Cellular and Infection Microbiology* 4(JUL), pp. 1–6. doi: 10.3389/fcimb.2014.00101.

Division, U.N.D. of E. and S.A.P. 2019. *World population prospects 2019*.

Dodds, M., Roland, S., Edgar, M. and Thornhill, M. 2015. Saliva A review of its role in maintaining oral health and preventing dental disease. *BDJ Team* 2(1–8), pp. 1–3. doi: 10.1038/bdjteam.2015.123.

Dodds, M.W.J., Johnson, D.A. and Yeh, C.K. 2005. Health benefits of saliva: A review. *Journal of Dentistry* 33(3 SPEC. ISS.), pp. 223–233. doi: 10.1016/j.jdent.2004.10.009.

Dzidic, M., Collado, M.C., Abrahamsson, T., Artacho, A., Stensson, M., Jenmalm, M.C. and Mira, A. 2018. Oral microbiome development during childhood: an ecological succession influenced by postnatal factors and associated with tooth decay. *ISME Journal* 12(9), pp. 2292–2306. doi: 10.1038/s41396-018-0204-z.

Edgerton, M. and Levine, M.J. 1992. Characterization of acquired denture pellicle from healthy and stomatitis patients. *The Journal of Prosthetic Dentistry* 68(4), pp. 683–691. doi: 10.1016/0022-3913(92)90387-P.

Edlund, A. et al. 2013. An in vitro biofilm model system maintaining a highly reproducible species and metabolic diversity approaching that of the human oral microbiome. pp. 1–17.

Eliades, T., Eliades, G. and Brantley, W.A. 1995. Microbial attachment on orthodontic appliances: I. Wettability and early pellicle formation on bracket materials. *American Journal of Orthodontics and Dentofacial Orthopedics* 108(4), pp. 351–360. doi: 10.1016/S0889-5406(95)70032-3.

Ellepola, A.N.B., Joseph, B.K. and Khan, Z.U. 2013. Changes in the cell surface hydrophobicity of oral *candida albicans* from smokers, diabetics, asthmatics, and healthy individuals following limited exposure to chlorhexidine gluconate. *Medical Principles and Practice* 22(3), pp. 250–254. doi: 10.1159/000345641.

Fidel Jr, P.L. 2006. *Candida*-Host Interactions in HIV Disease: Relationships in Oropharyngeal Candidiasis. *Adv Dent Res* 19, pp. 80–84.

De Filippis, F. et al. 2014. The same microbiota and a potentially discriminant metabolome in the saliva of omnivore, ovo-lacto-vegetarian and vegan individuals.

PLoS ONE 9(11). doi: 10.1371/journal.pone.0112373.

Fischer, N.G. and Aparicio, C. 2021. The salivary pellicle on dental biomaterials. *Colloids and Surfaces B: Biointerfaces* 200. doi: 10.1016/j.colsurfb.2021.111570.

Flemming, H.C., Neu, T.R. and Wozniak, D.J. 2007. The EPS matrix: The "House of Biofilm Cells." *Journal of Bacteriology* 189(22), pp. 7945–7947. doi: 10.1128/JB.00858-07.

Flemming, H.C. and Wingender, J. 2010. The biofilm matrix. *Nature Reviews Microbiology* 8(9), pp. 623–633. doi: 10.1038/nrmicro2415.

Flemming, H.C., Wingender, J., Szewzyk, U., Steinberg, P., Rice, S.A. and Kjelleberg, S. 2016. Biofilms: An emergent form of bacterial life. *Nature Reviews Microbiology* 14(9), pp. 563–575. doi: 10.1038/nrmicro.2016.94.

Force, R.W. and Nahata, M.C. 1995. Salivary Concentrations of Ketoconazole and Fluconazole: Implications for Drug Efficacy in Oropharyngeal and Esophageal Candidiasis. *Annals of Pharmacotherapy* 29(1), pp. 10–15. doi: 10.1177/106002809502900102.

Fourie, R., Ells, R., Swart, C.W., Sebolai, O.M., Albertyn, J. and Pohl, C.H. 2016. *Candida albicans* and *Pseudomonas aeruginosa* interaction, with focus on the role of eicosanoids. *Frontiers in Physiology* 7(FEB). doi: 10.3389/fphys.2016.00064.

Frade, J.P. and Arthington-Skaggs, B.A. 2010. Effect of serum and surface characteristics on *Candida albicans* biofilm formation. *Mycoses* 54(4), pp. 154–162. doi: 10.1111/j.1439-0507.2010.01862.x.

Garcia, L. 2014. Synergism Testing: Broth Microdilution Checkerboard and Broth Macrodilution Methods. In: *Clinical Microbiology Procedures Handbook*. pp. 5.16.1-5.16.23. doi: 10.1128/9781555818814.ch5.16.

Gazdeck, R.K., Fruscione, S.R., Adami, G.R., Zhou, Y., Cooper, L.F. and Schwartz, J.L. 2019. Diversity of the oral microbiome between dentate and edentulous individuals. *Oral Diseases* 25(3), pp. 911–918. doi: 10.1111/odi.13039.

Ghannoum, M.A. 2000. Potential role of phospholipases in virulence and fungal pathogenesis. *Clinical Microbiology Reviews* 13(1), pp. 122–143. doi: 10.1128/CMR.13.1.122-143.2000.

Gow, N.A.R. and Hube, B. 2012. Importance of the *Candida albicans* cell wall during commensalism and infection. *Current Opinion in Microbiology* 15(4), pp. 406–412. doi: 10.1016/j.mib.2012.04.005.

Gow, N.A.R. and Yadav, B. 2017. Microbe profile: *Candida* albicans: A shape-changing, opportunistic pathogenic fungus of humans. *Microbiology (United Kingdom)* 163(8), pp. 1145–1147. doi: 10.1099/mic.0.000499.

Gregoire, S. et al. 2011. Role of ghlucosyltransferase B in interactions of Candida albicans with *Streptococcus mutans* and with an experimental pellicle on hydroxyapatite surfaces. *Applied and Environmental Microbiology* 77(18), pp. 6357–6367. doi: 10.1128/AEM.05203-11.

Gulati, M. and Nobile, C.J. 2016. *Candida albicans* biofilms: development, regulation, and molecular mechanisms. *Microbes and Infection* 18(5), pp. 310–321. doi:

10.1016/j.micinf.2016.01.002.

Gunaratnam, G., Dudek, J., Jung, P., Becker, S.L., Jacobs, K., Bischoff, M. and Hannig, M. 2021. Quantification of the adhesion strength of *Candida albicans* to tooth enamel. *Microorganisms* 9(11), pp. 1–12. doi: 10.3390/microorganisms9112213.

Gunasegar, S. and Himratul-aznita, W.H. 2019. Nicotine enhances the thickness of biofilm and adherence of *Candida albicans* ATCC 14053 and *Candida parapsilosis* ATCC 22019. (July 2018), pp. 1–11. doi: 10.1093/femsyr/foy123.

Gunasegar, S. and Himratul-Aznita, W.H. 2017. Gunasegar, S. and Himratul-Aznita, W.H. 2017. Influence of nicotine on the adherence of *Candida albicans* ATCC 14053 and *Candida parapsilosis* ATCC 22019 and expression of selected binding-related genes. Biotechnology and Biotechnological Equipment 31(4), p. *Biotechnology and Biotechnological Equipment* 31(4), pp. 807–814. doi: 10.1080/13102818.2017.1334593.

Gurbich, T.A. et al. 2023. MGnify Genomes: A Resource for Biome-specific Microbial Genome Catalogues. *Journal of Molecular Biology* (xxxx), p. 168016. doi: 10.1016/j.jmb.2023.168016.

Hajishengallis, G., Darveau, R.P. and Curtis, M.A. 2012. The keystone-pathogen hypothesis. *Nature Reviews Microbiology* 10(10), pp. 717–725. doi: 10.1038/nrmicro2873.

Hall-Stoodley, L. and Stoodley, P. 2002. Developmental regulation of microbial biofilms. *Current Opinion in Biotechnology* 13(3), pp. 228–233. doi: 10.1016/S0958-1669(02)00318-X.

Hall, M.W. et al. 2017. Inter-personal diversity and temporal dynamics of dental, tongue, and salivary microbiota in the healthy oral cavity. *npj Biofilms and Microbiomes* 3(1), pp. 0–1. doi: 10.1038/s41522-016-0011-0.

Hannah, V.E., O'Donnell, L., Robertson, D. and Ramage, G. 2017. Denture Stomatitis: Causes, Cures and Prevention. *Primary dental journal* 6(4), pp. 46–51. doi: 10.1308/205016817822230175.

Hansen, T.H. et al. 2018. Impact of a vegan diet on the human salivary microbiota. *Scientific Reports* 8(1), pp. 1–11. doi: 10.1038/s41598-018-24207-3.

Harimawan, A., Rajasekar, A. and Ting, Y.P. 2011. Bacteria attachment to surfaces - AFM force spectroscopy and physicochemical analyses. *Journal of Colloid and Interface Science* 364(1), pp. 213–218. doi: 10.1016/j.jcis.2011.08.021.

Harriott, M.M. and Noverr, M.C. 2011. Importance of *Candida*-bacterial polymicrobial biofilms in disease. *Trends Microbiol.* 19(11), pp. 557–563. doi: 10.1038/nature08365.Reconstructing.

Hasan, N.A. et al. 2014. Microbial community profiling of human saliva using shotgun metagenomic sequencing. *PLoS ONE* 9(5). doi: 10.1371/journal.pone.0097699.

He, X., McLean, J.S., Guo, L., Lux, R. and Shi, W. 2014. The social structure of microbial community involved in colonization resistance. *ISME Journal* 8(3), pp. 564–574. doi: 10.1038/ismej.2013.172.

Hilbert, L.R., Bagge-ravn, D., Kold, J. and Gram, L. 2003. Influence of surface

roughness of stainless steel on microbial adhesion and corrosion resistance. 52, pp. 175–185. doi: 10.1016/S0964-8305(03)00104-5.

Hirakawa, M.P. et al. 2015. Genetic and phenotypic intra-species variation in *Candida albicans*. *Genome Research* 25(3), pp. 413–425. doi: 10.1101/gr.174623.114.

Hogan, D. a. 2002. *Pseudomonas-Candida* Interactions: An Ecological Role for Virulence Factors. *Science* 296(5576), pp. 2229–2232. doi: 10.1126/science.1070784.

Hogan, D.A., Vik, Å. and Kolter, R. 2004. A *Pseudomonas aeruginosa* quorum-sensing molecule influences *Candida albicans* morphology. *Molecular Microbiology* 54(5), pp. 1212–1223. doi: 10.1111/j.1365-2958.2004.04349.x.

Hooks, K.B. and O'Malley, M.A. 2017. Dysbiosis and its discontents. *mBio* 8(5). doi: 10.1128/mBio.01492-17.

Hornby, J.M. et al. 2001. Quorum Sensing in the Dimorphic Fungus *Candida albicans* Is Mediated by Farnesol. *Applied and Environmental Microbiology* 67(7), pp. 2982–2992. doi: 10.1128/AEM.67.7.2982-2992.2001.

Hoyer, L.L. and Cota, E. 2016. *Candida albicans* agglutinin-like sequence (Als) family vignettes: A review of als protein structure and function. *Frontiers in Microbiology* 7(MAR), pp. 1–16. doi: 10.3389/fmicb.2016.00280.

Hoyer, L.L., Oh, S.H., Jones, R. and Cota, E. 2014. A proposed mechanism for the interaction between the *Candida albicans* Als3 adhesin and streptococcal cell wall proteins. *Frontiers in Microbiology* 5(OCT), pp. 1–7. doi: 10.3389/fmicb.2014.00564.

Human Oral Microbiome Database: HOMD. [no date]. Available at: www.homd.org [Accessed: 2 March 2023].

Humphrey and Williamson, R.T. 2001. A review of saliva Normal composition, flow, and function. Journal of Prosthetic Dentistry.pdf. *The Journal of Prosthetic Dentistry* 85(2), pp. 162–169.

Hunter, P. 2008. The mob response. *EMBO reports* 9(4), pp. 314–317. doi: 10.1038/embor.2008.43.

Huttenhower, C. et al. 2012. Structure, function and diversity of the healthy human microbiome. *Nature* 486(7402), pp. 207–214. doi: 10.1038/nature11234.

Hwang, G., Liu, Y., Kim, D., Li, Y., Krysan, D.J. and Koo, H. 2017. *Candida albicans* mannans mediate *Streptococcus mutans* exoenzyme GtfB binding to modulate cross-kingdom biofilm development in vivo. *PLoS Pathogens* 13(6). doi: 10.1371/journal.ppat.1006407.

Iinuma, T. et al. 2015. Denture wearing during sleep doubles the risk of pneumonia in the very elderly. *Journal of Dental Research* 94(March), pp. 28S-36S. doi: 10.1177/0022034514552493.

Ishijima, S.A., Hayama, K., Burton, J.P., Reid, G., Okada, M., Matsushita, Y. and Abe, S. 2012. Effect of Streptococcus salivarius K12 on the In vitro growth of *Candida albicans* and its protective effect in an oral candidiasis model. *Applied and Environmental Microbiology* 78(7), pp. 2190–2199. doi: 10.1128/AEM.07055-11.

Jack, A.A., Daniels, D.E., Jepson, M.A., Margaret Vickerman, M., Lamont, R.J., Jenkinson, H.F. and Nobbs, A.H. 2015. *Streptococcus gordonii* comCDE (competence) operon modulates biofilm formation with *Candida albicans*. *Microbiology (United Kingdom)* 161(2), pp. 411–421. doi: 10.1099/mic.0.000010.

Jacob, P., Yu, L., Shulgin, A.T. and Benowitz, N.L. 1999. Minor tobacco alkaloids as biomarkers for tobacco use: Comparison of users of cigarettes, smokeless tobacco, cigars, and pipes. *American Journal of Public Health* 89(5), pp. 731–736. doi: 10.2105/AJPH.89.5.731.

Jakubovics, N.S. 2015. Saliva as the sole nutritional source in the development of multispecies communities in dental plaque. *Metabolism and Bacterial Pathogenesis*, pp. 263–277. doi: 10.1128/9781555818883.ch12.

Janus, M.M., Crielaard, W., Volgenant, C.M.C., van der Veen, M.H., Brandt, B.W. and Krom, B.P. 2017. *Candida albicans* alters the bacterial microbiome of early in vitro oral biofilms. *Journal of Oral Microbiology* 9(1), p. 1270613. doi: 10.1080/20002297.2016.1270613.

Jarosz, L.M., Deng, D.M., Van Der Mei, H.C., Crielaard, W. and Krom, B.P. 2009. *Streptococcus mutans* competence-stimulating peptide inhibits *Candida albicans* hypha formation. *Eukaryotic Cell* 8(11), pp. 1658–1664. doi: 10.1128/EC.00070-09.

Jenkinson, H.F. 2011. Beyond the oral microbiome. *Environmental Microbiology* 13(12), pp. 3077–3087. doi: 10.1111/j.1462-2920.2011.02573.x.

Ji, L., Melkonian, G., Riveles, K. and Talbot, P. 2002. Identification of pyridine compounds in cigarette smoke solution that inhibit growth of the chick chorioallantoic membrane. *Toxicological Sciences* 69(1), pp. 217–225. doi: 10.1093/toxsci/69.1.217.

Jiang, S., Gao, X., Jin, L. and Lo, E.C.M. 2016. Salivary microbiome diversity in caries-free and caries-affected children. *International Journal of Molecular Sciences* 17(12). doi: 10.3390/ijms17121978.

Johnson, E., Petersen, T. and Goeres, D.M. 2021. Characterizing the shearing stresses within the CDC biofilm reactor using computational fluid dynamics. *Microorganisms* 9(8). doi: 10.3390/microorganisms9081709.

Kaci, G. et al. 2014. Anti-inflammatory properties of *Streptococcus salivarius*, a commensal bacterium of the oral cavity and digestive tract. *Applied and Environmental Microbiology* 80(3), pp. 928–934. doi: 10.1128/AEM.03133-13.

Kadosh, D. 2019. Regulatory mechanisms controlling morphology and pathogenesis in *Candida albicans*. *Current Opinion in Microbiology* 52, pp. 27–34. doi: 10.1016/j.mib.2019.04.005.

Kang, S., Lee, H., Hong, S., Kim, K. and Kwon, T. 2013. Influence of surface characteristics on the adhesion of *Candida albicans* to various denture lining materials. 6357. doi: 10.3109/00016357.2012.671360.

Kaplan, J.B. 2010. Biofilm Dispersal: Mechanisms, Clinical Implications, and Potential Therapeutic Uses. *Journal of Dental Research* 89(3), pp. 205–218. doi: 10.1177/0022034509359403.

Karakis, D., Akay, C., Oncul, B., Rad, A.Y. and Dogan, A. 2016. Effectiveness of disinfectants on the adherence of *Candida albicans* to denture base resins with

different surface textures. *Journal of Oral Science* 58(3), pp. 431–437. doi: 10.2334/josnusd.15-0642.

Kawar, N. et al. 2021. Salivary microbiome with gastroesophageal reflux disease and treatment. *Scientific Reports* 11(1), pp. 1–8. doi: 10.1038/s41598-020-80170-y.

Keijser, B.J.F. et al. 2008. Pyrosequencinq analysis of the oral microflora of healthy adults. *Journal of Dental Research* 87(11), pp. 1016–1020. doi: 10.1177/154405910808701104.

Kerr, J.E. and Tribble, G.D. 2015. Salivary Diagnostics and the Oral Microbiome BT - Advances in Salivary Diagnostics. In: Streckfus, C. F. ed. Berlin, Heidelberg: Springer Berlin Heidelberg, pp. 83–119. doi: 10.1007/978-3-662-45399-5_5.

Khan, Z.U., Ahmad, S., Mokaddas, E. and Chandy, R. 2004. Tobacco Agar , a New Medium for Differentiating *Candida dubliniensis* from *Candida albicans*. *Journal of Clinical Microbiology* 42(10), pp. 4796–4798. doi: 10.1128/JCM.42.10.4796.

Kikuchi, M., Ghani, F. and Watanabe, M. 1999. Method for enhancing retention in complete denture bases. *Journal of Prosthetic Dentistry* 81(4), pp. 399–403. doi: 10.1016/S0022-3913(99)80005-5.

Kim, D. et al. 2018. Bacterial-derived exopolysaccharides enhance antifungal drug tolerance in a cross-kingdom oral biofilm. *The ISME Journal* 12(6), pp. 1427–1442. doi: 10.1038/s41396-018-0113-1.

Kim, H.J. and Brehm-Stecher, B.F. 2015. Design and evaluation of peptide nucleic acid probes for specific identification of *Candida albicans*. *Journal of Clinical Microbiology* 53(2), pp. 511–521. doi: 10.1128/JCM.02417-14.

Kim, H.Y., Märtson, A.G., Dreesen, E., Spriet, I., Wicha, S.G., McLachlan, A.J. and Alffenaar, J.W. 2020. Saliva for Precision Dosing of Antifungal Drugs: Saliva Population PK Model for Voriconazole Based on a Systematic Review. *Frontiers in Pharmacology* 11(June). doi: 10.3389/fphar.2020.00894.

Köhler, J.R., Casadevall, A. and Perfect, J. 2015. The spectrum of fungi that infects humans. *Cold Spring Harbor Perspectives in Medicine* 5(1), pp. 1–22. doi: 10.1101/cshperspect.a019273.

Kolenbrander, P.E., Palmer, R.J., Periasamy, S. and Jakubovics, N.S. 2010. Oral multispecies biofilm development and the key role of cell-cell distance. *Nature Reviews Microbiology* 8(7), pp. 471–480. doi: 10.1038/nrmicro2381.

Kreth, J., Merritt, J., Shi, W. and Qi, F. 2005. Competition and coexistence between *Streptococcus mutans* and *Streptococcus sanguinis* in the dental biofilm. *Journal of Bacteriology* 187(21), pp. 7193–7203. doi: 10.1128/JB.187.21.7193-7203.2005.

Kuhar, M. and Funduk, N. 2005. Effects of polishing techniques on the surface roughness of acrylic denture base resins. *Journal of Prosthetic Dentistry* 93(1), pp. 76–85. doi: 10.1016/j.prosdent.2004.10.002.

Kumamoto, C.A. and Vinces, M.D. 2005a. Alternative *Candida albicans* lifestyles: Growth on surfaces. *Annual Review of Microbiology* 59, pp. 113–133. doi: 10.1146/annurev.micro.59.030804.121034.

Kumamoto, C.A. and Vinces, M.D. 2005b. Contributions of hyphae and hypha-co-

regulated genes to *Candida albicans* virulence. *Cellular Microbiology* 7(11), pp. 1546–1554. doi: 10.1111/j.1462-5822.2005.00616.x.

Kuramitsu, H.K., He, X., Lux, R., Anderson, M.H. and Shi, W. 2007. Interspecies Interactions within Oral Microbial Communities. *Microbiology and Molecular Biology Reviews* 71(4), pp. 653–670. doi: 10.1128/mmbr.00024-07.

Lassalle, F. et al. 2018. Oral microbiomes from hunter-gatherers and traditional farmers reveal shifts in commensal balance and pathogen load linked to diet. *Molecular Ecology* 27(1), pp. 182–195. doi: 10.1111/mec.14435.

Lazarevic, V. et al. 2012. Analysis of the salivary microbiome using culture-independent techniques. *Journal of Clinical Bioinformatics* 2(1), pp. 1–8. doi: 10.1186/2043-9113-2-4.

Leake, S.L., Pagni, M., Falquet, L., Taroni, F. and Greub, G. 2016. The salivary microbiome for differentiating individuals: proof of principle. *Microbes and Infection* 18(6), pp. 399–405. doi: 10.1016/j.micinf.2016.03.011.

Lee, H.S., Lee, J.H., Kim, S.O., Song, J.S., Kim, B.I., Kim, Y.J. and Lee, J.H. 2016. Comparison of the oral microbiome of siblings using next-generation sequencing: a pilot study. *Oral Diseases* 22(6), pp. 549–556. doi: 10.1111/odi.12491.

Lee, K.K., MacCallum, D.M., Jacobsen, M.D., Walker, L.A., Odds, F.C., Gow, N.A.R. and Munro, C.A. 2012. Elevated cell wall chitin in *Candida albicans* confers echinocandin resistance in vivo. *Antimicrobial Agents and Chemotherapy* 56(1), pp. 208–217. doi: 10.1128/AAC.00683-11.

Lewis, M. a. O. and Williams, D.W. 2017. Diagnosis and management of oral candidosis. *Bdj* 223(9), pp. 675–681. doi: 10.1038/sj.bdj.2017.886.

Li, J. et al. 2014. Comparative analysis of the human saliva microbiome from different climate zones: Alaska, Germany, and Africa. *BMC Microbiology* 14(1), pp. 1–13. doi: 10.1186/s12866-014-0316-1.

Li, X. et al. 2021. Saliva-derived microcosm biofilms grown on different oral surfaces in vitro. *npj Biofilms and Microbiomes* 7(1). doi: 10.1038/s41522-021-00246-z.

Lindsay, D., Killington, A., Fouhy, K., Loh, M. and Malakar, P. 2022. The CDC biofilm bioreactor is a suitable method to grow biofilms, and test their sanitiser susceptibilities, in the dairy context. *International Dairy Journal* 126, p. 105264. doi: 10.1016/j.idairyj.2021.105264.

Liu, Y. and Filler, S.G. 2011. *Candida albicans* Als3, a multifunctional adhesin and invasin. *Eukaryotic Cell* 10(2), pp. 168–173. doi: 10.1128/EC.00279-10.

Liu, Y. kun, Chen, V., He, J. zhi, Zheng, X., Xu, X. and Zhou, X. dong. 2021. A salivary microbiome-based auxiliary diagnostic model for type 2 diabetes mellitus. *Archives of Oral Biology* 126(April), p. 105118. doi: 10.1016/j.archoralbio.2021.105118.

Loesche, W.J. 1976. Chemotherapy of dental plaque infections. *Oral sciences reviews* 9, pp. 65–107.

Loesche, W.J. 1986. Role of *Streptococcus mutans* in human dental decay. *Microbiological Reviews* 50(4), pp. 353–380. doi: 10.1128/mmbr.50.4.353-380.1986.

Loesche, W.J., Rowan, J., Straffon, L.H. and Loos, P.J. 1975. Association of *Streptococcus mutans* with human dental decay. *Infection and Immunity* 11(6), pp. 1252–1260. doi: 10.1128/iai.11.6.1252-1260.1975.

Lohse, M.B., Gulati, M., Johnson, A.D. and Nobile, C.J. 2018. Development and regulation of single-and multi-species *Candida albicans* biofilms. *Nature Reviews Microbiology* 16(1), pp. 19–31. doi: 10.1038/nrmicro.2017.107.

Lu, H., Shrivastava, M., Whiteway, M. and Jiang, Y. 2021. *Candida albicans* targets that potentially synergize with fluconazole. *Critical Reviews in Microbiology* 47(3), pp. 323–337. doi: 10.1080/1040841X.2021.1884641.

Lynch, M.D.J. and Neufeld, J.D. 2015. Ecology and exploration of the rare biosphere. *Nature Reviews Microbiology* 13(4), pp. 217–229. doi: 10.1038/nrmicro3400.

Lynge Pedersen, A.M. and Belstrøm, D. 2019. The role of natural salivary defences in maintaining a healthy oral microbiota. *Journal of Dentistry* 80(August 2018), pp. S3–S12. doi: 10.1016/j.jdent.2018.08.010.

MacHado, A.L., Giampaolo, E.T., Vergani, C.E., Pavarina, A.C., Da Silva Lopes Salles, D. and Jorge, J.H. 2012. Weight loss and changes in surface roughness of denture base and reline materials after simulated toothbrushing in vitro. *Gerodontology* 29(2), pp. 121–127. doi: 10.1111/j.1741-2358.2010.00422.x.

Mahross, H.Z., Mohamed, M.D., Hassan, A.M. and Baroudi, K. 2015. Effect of Cigarette Smoke on Surface Roughness of Different Denture Base Materials. doi: 10.7860/JCDR/2015/14580.6488.

Malic, S., Hill, K.., Ralphs, J., Hayes, A., Thomas, D.., Potts, A.. and Williams, D.W. 2007. Characterization of *Candida albicans* infection of an *in vitro* oral epithelial model using confocal laser scanning microscopy. *Oral Microbiology and Immunology* (27), pp. 188–194.

Malla, M.A., Dubey, A., Kumar, A., Yadav, S., Hashem, A. and Allah, E.F.A. 2019. Exploring the human microbiome: The potential future role of next-generation sequencing in disease diagnosis and treatment. *Frontiers in Immunology* 10(JAN), pp. 1–23. doi: 10.3389/fimmu.2018.02868.

Marsh, P., Lewis, M., Rogers, H., Williams, D. and Wilson, M. 2016a. *Oral Microbiology*. 6th Editio.

Marsh, P.D. 1994. Microbial ecology of dental plaque and its significance in health and disease. *Advances in dental research* 8(2), pp. 263–271. doi: 10.1177/08959374940080022001.

Marsh, P.D. and Bradshaw, D.J. 1995. Dental plaque as a biofilm. *Journal of Industrial Microbiology* 15(3), pp. 169–175. doi: 10.1007/BF01569822.

Marsh, P.D., Thuy, D., David, B. and Devine, D.A. 2016b. Influence of saliva on the oral microbiota. *Periodontology 2000* 70(97), pp. 80–92.

Mason, M.R., Chambers, S., Dabdoub, S.M., Thikkurissy, S. and Kumar, P.S. 2018. Characterizing oral microbial communities across dentition states and colonization niches. *Microbiome* 6(1), p. 67. doi: 10.1186/s40168-018-0443-2.

De Matteis, V., Cascione, M., Toma, C.C., Albanese, G., De Giorgi, M.L., Corsalini, M.

and Rinaldi, R. 2019. Silver nanoparticles addition in poly(methyl methacrylate) dental matrix: Topographic and antimycotic studies. *International Journal of Molecular Sciences* 20(19). doi: 10.3390/ijms20194691.

Mayer, F.L., Wilson, D. and Hube, B. 2013. *Candida albicans* pathogenicity mechanisms. *Virulence* 4(2), pp. 119–128. doi: 10.4161/viru.22913.

Medilanski, E., Kaufmann, K., Wick, L.Y., Wanner, O. and Harms, H. 2002. Influence of the surface topography of stainless steel on bacterial adhesion. *Biofouling* 18(3), pp. 193–203. doi: 10.1080/08927010290011370.

Mehta, H., Nazzal, K. and Sadikot, R.T. 2008. Cigarette smoking and innate immunity. *Inflammation Research* 57, pp. 497–503. doi: 10.1007/s00011-008-8078-6.

Miles, A.A., Misra, S.S. and Irwin, J.O. 1938. The estimation of the bactericidal power of the blood. *Journal of Hygiene* 38(6), pp. 732–749. doi: 10.1017/S002217240001158X.

Minagi, S., Miyake, Y., Inagaki, K., Tsuru, H. and Suginaka, H. 1985. Hydrophobic interaction in *Candida albicans* and *Candida tropicalis* adherence to various denture base resin materials. *Infection and Immunity* 47(1), pp. 11–14. doi: 10.1128/iai.47.1.11-14.1985.

Mio, T., Yabe, T., Sudoh, M., Satoh, Y., Nakajima, T., Arisawa, M. and Yamada-Okabe, H. 1996. Role of three chitin synthase genes in the growth of *Candida albicans*. *Journal of Bacteriology* 178(8), pp. 2416–2419. doi: 10.1128/jb.178.8.2416-2419.1996.

Mokhtar, M., Rismayuddin, N.A.R., Mat Yassim, A.S., Ahmad, H., Abdul Wahab, R., Dashper, S. and Arzmi, M.H. 2021. Streptococcus salivarius K12 inhibits *Candida albicans* aggregation, biofilm formation and dimorphism. *Biofouling* 37(7), pp. 767–776. doi: 10.1080/08927014.2021.1967334.

Monroe, D. 2007. Looking for chinks in the armor of bacterial biofilms. *PLoS Biology* 5(11), pp. 2458–2461. doi: 10.1371/journal.pbio.0050307.

Monsenego, P. 2000. Presence of microorganisms on the fitting denture complete surface: Study “in vivo.” *Journal of Oral Rehabilitation* 27(8), pp. 708–713. doi: 10.1046/j.1365-2842.2000.00564.x.

Moran, G.P., Coleman, D.C. and Sullivan, D.J. 2012. Candida albicans versus Candida dubliniensis: Why Is *C. albicans* more pathogenic? *International Journal of Microbiology*. doi: 10.1155/2012/205921.

Morse, D.J. 2017. Denture acrylic biofilms: microbial composition, interactions and infection.

Morse, D.J., Wilson, M.J., Wei, X., Bradshaw, D.J., Lewis, M.A.O. and Williams, D.W. 2019. Modulation of *Candida albicans* virulence in *in vitro* biofilms by oral bacteria . *Letters in Applied Microbiology*, pp. 337–343. doi: 10.1111/lam.13145.

Morse, D.J., Wilson, M.J., Wei, X., Lewis, M. a. O., Bradshaw, D.J., Murdoch, C. and Williams, D.W. 2018. Denture-associated biofilm infection in three-dimensional oral mucosal tissue models. *Journal of Medical Microbiology* 67(3), pp. 364–375. doi: 10.1099/jmm.0.000677.

Mouhat, M., Moorehead, R. and Murdoch, C. 2020. *In vitro Candida albicans* biofilm formation on different titanium surface topographies . *Biomaterial Investigations in Dentistry* 7(1), pp. 146–157. doi: 10.1080/26415275.2020.1829489.

Mukai, Y. et al. 2020. Analysis of plaque microbiota and salivary proteins adhering to dental materials. *Journal of Oral Biosciences* 62(2), pp. 182–188. doi: 10.1016/j.job.2020.02.003.

Mukaremera, L., Lee, K.K., Mora-Montes, H.M. and Gow, N.A.R. 2017. *Candida albicans* yeast, pseudohyphal, and hyphal morphogenesis differentially affects immune recognition. *Frontiers in Immunology* 8(JUN), pp. 1–12. doi: 10.3389/fimmu.2017.00629.

Munro, C.A. et al. 2007. The PKC, HOG and Ca2+ signalling pathways co-ordinately regulate chitin synthesis in *Candida albicans*. *Molecular Microbiology* 63(5), pp. 1399–1413. doi: 10.1111/j.1365-2958.2007.05588.x.

Murat, S., Alp, G., Alatalı, C. and Uzun, M. 2019. *In Vitro* Evaluation of Adhesion of *Candida albicans* on CAD/CAM PMMA-Based Polymers. *Journal of Prosthodontics* 28(2), pp. e873–e879. doi: 10.1111/jopr.12942.

Naglik, J.R., Challacombe, S.J. and Hube, B. 2003. *Candida albicans* Secreted Aspartyl Proteinases in Virulence and Pathogenesis . *Microbiology and Molecular Biology Reviews* 67(3), pp. 400–428. doi: 10.1128/mmbr.67.3.400-428.2003.

Nasidze, I., Li, J., Quinque, D., Tang, K. and Stoneking, M. 2009. Global diversity in the human salivary microbiome. *Genome Research* 19(4), pp. 636–643. doi: 10.1101/gr.084616.108.

Nasution, O., Srinivasa, K., Kim, M., Kim, Y.J., Kim, W., Jeong, W. and Choi, W. 2008. Hydrogen peroxide induces hyphal differentiation in *Candida albicans*. *Eukaryotic Cell* 7(11), pp. 2008–2011. doi: 10.1128/EC.00105-08.

Nelson-Filho, P., Borba, I.G., de Mesquita, K.S.F., Silva, R.A.B., de Queiroz, A.M. and Silva, L.A.B. 2013. Dynamics of microbial colonization of the oral cavity in newborns. *Brazilian Dental Journal* 24(4), pp. 415–419. doi: 10.1590/0103-6440201302266.

Neppelenbroek, K.H., Pavarina, A.C., Vergani, C.E. and Giampaolo, E.T. 2005. Hardness of heat-polymerized acrylic resins after disinfection and long-term water immersion. *Journal of Prosthetic Dentistry* 93(2), pp. 171–176. doi: 10.1016/j.prosdent.2004.10.020.

Netea, M.G., Joosten, L.A.B., Van Der Meer, J.W.M., Kullberg, B.J. and Van De Veerdonk, F.L. 2015. Immune defence against *Candida* fungal infections. *Nature Reviews Immunology* 15(10), pp. 630–642. doi: 10.1038/nri3897.

Nevzatoğlu, E.U., Özcan, M., Kulak-Ozkan, Y. and Kadir, T. 2007. Adherence of *Candida albicans* to denture base acrylics and silicone-based resilient liner materials with different surface finishes. *Clinical Oral Investigations* 11(3), pp. 231–236. doi: 10.1007/s00784-007-0106-3.

Niedermeier, W. et al. 2000. Significance of saliva for the denture-wearing population. *Gerodontology* 17(2), pp. 104–118. doi: 10.1111/j.1741-2358.2000.00104.x.

Nikawa, H., Hamada, T. and Yamamoto, T. 1998. Denture plaque - Past and recent concerns. *Journal of Dentistry* 26(4), pp. 299–304. doi: 10.1016/S0300-

5712(97)00026-2.

Nikawa, H., Jin, C., Makihira, S., Egusa, H., Hamada, T. and Kumagai, H. 2003. Biofilm formation of *Candida albicans* on the surfaces of deteriorated soft denture lining materials caused by denture cleansers in vitro. *Journal of Oral Rehabilitation* 30(3), pp. 243–250. doi: 10.1046/j.1365-2842.2003.01024.x.

Nikawa, H., Nishimura, H., Makihira, S., Hamada, T., Sadamori, S. and Samaranayake, L.P. 2000. Effect of serum concentration on *Candida* biofilm formation on acrylic surfaces. *Mycoses* 43, pp. 139–143.

Nobbs, A.H., Vickerman, M.M. and Jenkinson, H.F. 2010. Heterologous Expression of *Candida albicans* Cell Wall-Associated Adhesins in *Saccharomyces cerevisiae* Reveals Differential Specificities in Adherence and Biofilm Formation and in Binding Oral *Streptococcus gordonii*. 9(10), pp. 1622–1634. doi: 10.1128/EC.00103-10.

Nobile, C.J. and Johnson, A.D. 2015. *Candida albicans* Biofilm and Human Disease. *Annual review of microbiology* 69, pp. 71–92. doi: 10.1146/annurev-micro-091014-104330.Candida.

O'Donnell, L.E. et al. 2017. *Candida albicans* biofilm heterogeneity does not influence denture stomatitis but strongly influences denture cleansing capacity. *Journal of Medical Microbiology* 66(1), pp. 54–60. doi: 10.1099/jmm.0.000419.

Ohshima, T., Ikawa, S., Kitano, K. and Maeda, N. 2018. A proposal of remedies for oral diseases caused by *Candida*: A mini review. *Frontiers in Microbiology*. doi: 10.3389/fmicb.2018.01522.

Oncul, B., Karakis, D. and Al, F.D. 2015. The effect of two artificial salivas on the adhesion of *Candida albicans* to heatpolymerized acrylic resin. *Journal of Advanced Prosthodontics* 7(2), pp. 93–97. doi: 10.4047/jap.2015.7.2.93.

Ondov, B.D., Bergman, N.H. and Phillippy, A.M. 2011. Interactive metagenomic visualization in a Web browser Interactive metagenomic visualization in a Web browser. 385(September).

Onwubu, S.C. and Mdluli, P.S. 2021. Comparative Analysis of Abrasive Materials and Polishing System on the Surface Roughness of Heat-Polymerized Acrylic Resins. *European Journal of Dentistry*. doi: 10.1055/s-0041-1736293.

Panagoda, G.J., Ellepola, A.N.B. and Samaranayake, L.P. 1998. Adhesion to denture acrylic surfaces and relative cell-surface hydrophobicity of *Candida parapsilosis* and *Candida albicans*. *Apmis* 106(7), pp. 736–742. doi: 10.1111/j.1699-0463.1998.tb00220.x.

Panagoda, G.J. and Samaranayake, L.P. 1998. The relationship between the cell length, adhesion to acrylic and relative cell surface hydrophobicity of *Candida parapsilosis*. *Medical Mycology* 36(6), pp. 373–378. doi: 10.1080/02681219880000591.

Pappas, P.G. et al. 2015. Clinical Practice Guideline for the Management of Candidiasis: 2016 Update by the Infectious Diseases Society of America. *Clinical Infectious Diseases* 62(4), pp. e1–e50. doi: 10.1093/cid/civ933.

Parks, D.H., Tyson, G.W., Hugenholtz, P. and Beiko, R.G. 2014. STAMP: Statistical analysis of taxonomic and functional profiles. *Bioinformatics* 30(21), pp. 3123–3124.

doi: 10.1093/bioinformatics/btu494.

Paropkari, A.D., Leblebicioglu, B., Christian, L.M. and Kumar, P.S. 2016. Smoking, pregnancy and the subgingival microbiome. *Scientific Reports* 6(July), pp. 1–9. doi: 10.1038/srep30388.

Passariello, C., Di Nardo, F., Polimeni, A., Di Nardo, D. and Testarelli, L. 2020. Probiotic streptococcus salivarius reduces symptoms of denture stomatitis and oral colonization by *Candida albicans*. *Applied Sciences (Switzerland)* 10(9). doi: 10.3390/app10093002.

Pereira-cenci, T. et al. 2008. The effect of *Streptococcus mutans* and *Candida glabrata* on *Candida albicans* biofilms formed on different surfaces. 53, pp. 755–764. doi: 10.1016/j.archoralbio.2008.02.015.

Perry-O'Keefe, H., Rigby, S., Oliveira, K., Sørensen, D., Stender, H., Coull, J. and Hyldig-Nielsen, J.J. 2001. Identification of indicator microorganisms using a standardized PNA FISH method. *Journal of Microbiological Methods* 47(3), pp. 281–292. doi: 10.1016/S0167-7012(01)00303-7.

Petersen, P.E. and Ogawa, H. 2012. The global burden of periodontal disease: Towards integration with chronic disease prevention and control. *Periodontology 2000* 60(1), pp. 15–39. doi: 10.1111/j.1600-0757.2011.00425.x.

Petrova, O.E., Gupta, K., Liao, J., Goodwine, J.S. and Sauer, K. 2017. Divide and conquer: the *Pseudomonas aeruginosa* two-component hybrid SagS enables biofilm formation and recalcitrance of biofilm cells to antimicrobial agents via distinct regulatory circuits. *Environmental Microbiology* 19(5), pp. 2005–2024. doi: 10.1111/1462-2920.13719.

Pfaller, M.A. and Diekema, D.J. 2010. *Epidemiology of invasive mycoses in North America*. doi: 10.3109/10408410903241444.

Philip, N., Suneja, B. and Walsh, L. 2018. Beyond *streptococcus mutans*: Clinical implications of the evolving dental caries aetiological paradigms and its associated microbiome. *British Dental Journal* 224(4), pp. 219–225. doi: 10.1038/sj.bdj.2018.81.

Pidwill, G.R., Rego, S., Jenkinson, H.F., Lamont, R.J. and Nobbs, H. 2018. Coassociation between Group B *Streptococcus* and *Candida albicans* Promotes Interactions with Vaginal Epithelium. *Infection and Immunity* 86(4), pp. 1–18.

Pier-Francesco, A., Adams, R.J., Waters, M.G.J. and Williams, D.W. 2006. Titanium surface modification and its effect on the adherence of *Porphyromonas gingivalis*: An *in vitro* study. *Clinical Oral Implants Research* 17(6), pp. 633–637. doi: 10.1111/j.1600-0501.2006.01274.x.

Ponde, N.O., Lortal, L., Ramage, G., Naglik, J.R. and Richardson, J.P. 2021. *Candida albicans* biofilms and polymicrobial interactions. *Critical Reviews in Microbiology* 47(1), pp. 91–111. doi: 10.1080/1040841X.2020.1843400.

Purevdorj-Gage, B., Costerton, W.J. and Stoodley, P. 2005. Phenotypic differentiation and seeding dispersal in non-mucoid and mucoid *Pseudomonas aeruginosa* biofilms. *Microbiology* 151(5), pp. 1569–1576. doi: 10.1099/mic.0.27536-0.

Quirynen, M. and Bollen, C.M.. 1995. The influence of surface roughness and surface-free energy on supra- and subgingival plaque formation in man. *Journal of Clinical*

Periodontology 22, pp. 1–14.

Radford, D.R., Challacombe, S.J. and Walter, J.D. 1999. Denture plaque and adherence of *Candida albicans* to denture-base materials in vivo and in vitro. *Critical Reviews in Oral Biology and Medicine* 10(1), pp. 99–116. doi: 10.1177/10454411990100010501.

Radford, D.R., Sweet, S.P., Challacombe, S.J. and Walter, J.D. 1998. Adherence of *Candida albicans* to denture-base materials with different surface finishes. *Journal of Dentistry* 26(7), pp. 577–583. doi: 10.1016/S0300-5712(97)00034-1.

Rai, A.K. et al. 2021. Dysbiosis of salivary microbiome and cytokines influence oral squamous cell carcinoma through inflammation. *Archives of Microbiology* 203(1), pp. 137–152. doi: 10.1007/s00203-020-02011-w.

Ramage, G., Martínez, J.P. and López-Ribot, J.L. 2006. *Candida* biofilms on implanted biomaterials: A clinically significant problem. *FEMS Yeast Research* 6(7), pp. 979–986. doi: 10.1111/j.1567-1364.2006.00117.x.

Ramage, G., Tomsett, K., Wickes, B.L., Lo, L., Redding, S.W. and Antionio, S. 2004. Denture stomatitis : A role for *Candida* biofilms. *Oral Surg Oral Med Oral Pathol Oral Radiol Endod* 98, pp. 53–59. doi: 10.1016/j.tripleo.2003.04.002.

Redfern, J., Tosheva, L., Malic, S., Butcher, M., Ramage, G. and Verran, J. 2022. The denture microbiome in health and disease: an exploration of a unique community. *Letters in Applied Microbiology* 75(2), pp. 195–209. doi: 10.1111/lam.13751.

Rickard, A.H., Gilbert, P., High, N.J., Kolenbrander, P.E. and Handley, P.S. 2003. Bacterial coaggregation: An integral process in the development of multi-species biofilms. *Trends in Microbiology* 11(2), pp. 94–100. doi: 10.1016/S0966-842X(02)00034-3.

Rodriguez Fereira, V., Sukumaran, J., Ando, M. and De Baets, P. 2011. Roughness measurement problems in tribological testing. *International Journal Sustainable Construction & Design* 2(1), pp. 115–121. doi: 10.21825/scad.v2i1.20469.

Rollet, C., Gal, L. and Guzzo, J. 2009. Biofilm-detached cells, a transition from a sessile to a planktonic phenotype: A comparative study of adhesion and physiological characteristics in pseudomonas aeruginosa. *FEMS Microbiology Letters* 290(2), pp. 135–142. doi: 10.1111/j.1574-6968.2008.01415.x.

do Rosário Palma, A.L., Domingues, N., de Barros, P.P., Brito, G.N.B. and Jorge, A.O.C. 2019. Influence of *Streptococcus mitis* and *Streptococcus sanguinis* on virulence of *Candida albicans*: *in vitro* and *in vivo* studies. *Folia Microbiologica* 64(2), pp. 215–222. doi: 10.1007/s12223-018-0645-9.

Rosier, B.T., De Jager, M., Zaura, E. and Krom, B.P. 2014. Historical and contemporary hypotheses on the development of oral diseases: Are we there yet? *Frontiers in Cellular and Infection Microbiology* 4(JUL), pp. 1–11. doi: 10.3389/fcimb.2014.00092.

Rosier, B.T., Marsh, P.D. and Mira, A. 2018. Resilience of the Oral Microbiota in Health: Mechanisms That Prevent Dysbiosis. *Journal of Dental Research* 97(4), pp. 371–380. doi: 10.1177/0022034517742139.

Rumbaugh, K.P. and Sauer, K. 2020. Biofilm dispersion. *Nature Reviews*

Microbiology. doi: 10.1038/s41579-020-0385-0.

Salvatori, O., Puri, S., Tati, S. and Edgerton, M. 2016. Innate immunity and saliva in *Candida albicans* -mediated oral diseases. *Journal of Dental Research* 95(4), pp. 365–371. doi: 10.1177/0022034515625222.

Sands, K.M. et al. 2017. Respiratory pathogen colonization of dental plaque, the lower airways, and endotracheal tube biofilms during mechanical ventilation. *Journal of Critical Care* 37, pp. 30–37. doi: 10.1016/j.jcrc.2016.07.019.

Sang, T., Ye, Z., Fischer, N.G., Skoe, E.P., Echeverría, C., Wu, J. and Aparicio, C. 2020. Physical-chemical interactions between dental materials surface, salivary pellicle and *Streptococcus gordonii*. *Colloids and Surfaces B: Biointerfaces* 190, pp. 1–22. doi: 10.1016/j.colsurfb.2020.110938.

Santos, G.C. d. O. et al. 2018. *Candida* infections and therapeutic strategies: Mechanisms of action for traditional and alternative agents. *Frontiers in Microbiology* 9(JUL), pp. 1–23. doi: 10.3389/fmicb.2018.01351.

Sauer, K. et al. 2002. *Pseudomonas aeruginosa* Displays Multiple Phenotypes during Development as a Biofilm. *Society* 184(4), pp. 1140–1154. doi: 10.1128/JB.184.4.1140.

Sauer, K., Cullen, M.C., Rickard, A.H., Zeef, L.A.H., Davies, D.G. and Gilbert, P. 2004. Characterization of Nutrient-Induced Dispersion in. *Journal of Bacteriology* 186(21), pp. 7312–7326. doi: 10.1128/JB.186.21.7312.

Schwartz, J.L. et al. 2021. Old age and other factors associated with salivary microbiome variation. *BMC Oral Health* 21(1), pp. 1–9. doi: 10.1186/s12903-021-01828-1.

Sedghi, L., DiMassa, V., Harrington, A., Lynch, S. V. and Kapila, Y.L. 2021. The oral microbiome: Role of key organisms and complex networks in oral health and disease. *Periodontology 2000* 87(1), pp. 107–131. doi: 10.1111/prd.12393.

Segata, N., Waldron, L., Ballarini, A., Narasimhan, V., Jousson, O. and Huttenhower, C. 2012. Metagenomic microbial community profiling using unique clade-specific marker genes. *Nature Methods* 9(8), pp. 811–814. doi: 10.1038/nmeth.2066.

Semlali, A., Killer, K., Alanazi, H., Chmielewski, W. and Rouabhia, M. 2014. Cigarette smoke condensate increases *C. albicans* adhesion, growth, biofilm formation, and EAP1, HWP1 and SAP2 gene expression. *BMC Microbiology*. doi: 10.1186/1471-2180-14-61.

Şenel, S. 2021. An overview of physical, microbiological and immune barriers of oral mucosa. *International Journal of Molecular Sciences* 22(15). doi: 10.3390/ijms22157821.

de Senna, A.M., Vieira, M.M.F., Machado-de-Sena, R.M., Bertolin, A.O., Núñez, S.C. and Ribeiro, M.S. 2018. Photodynamic inactivation of *Candida* ssp. on denture stomatitis. A clinical trial involving palatal mucosa and prosthesis disinfection. *Photodiagnosis and Photodynamic Therapy* 22(March), pp. 212–216. doi: 10.1016/j.pdpdt.2018.04.008.

Serra, D.O. and Hengge, R. 2014. Stress responses go three dimensional - The spatial order of physiological differentiation in bacterial macrocolony biofilms. *Environmental*

Microbiology 16(6), pp. 1455–1471. doi: 10.1111/1462-2920.12483.

Shade, A., Jones, S.E., Gregory Caporaso, J., Handelsman, J., Knight, R., Fierer, N. and Gilbert, J.A. 2014. Conditionally rare taxa disproportionately contribute to temporal changes in microbial diversity. *mBio* 5(4). doi: 10.1128/mBio.01371-14.

Shaw, L. et al. 2017. The human salivary microbiome is shaped by shared environment rather than genetics: Evidence from a large family of closely related individuals. *mBio* 8(5). doi: 10.1128/mBio.01237-17.

Shchepin, R., Hornby, J.M., Burger, E., Niessen, T., Dussault, P. and Nickerson, K.W. 2003. Quorum Sensing in *Candida albicans*. *Chemistry & Biology* 10(8), pp. 743–750. doi: 10.1016/S1074-5521(03)00158-3.

Shibata, N., Suzuki, A., Kobayashi, H. and Okawa, Y. 2007. Chemical structure of the cell-wall mannan of *Candida albicans* serotype A and its difference in yeast and hyphal forms. *Biochemical Journal* 404(3), pp. 365–372. doi: 10.1042/BJ20070081.

Shulman, J.D., Rivera-Hidalgo, F. and Beach, M.M. 2005. Risk factors associated with denture stomatitis in the United States. *Journal of Oral Pathology and Medicine*. doi: 10.1111/j.1600-0714.2005.00287.x.

da Silva, W.., Leal, C.M.., Viu, F.., Gonc alves, M., Barbosa, C.M.., Del, A.A. and Cury, B. 2015. Influence of surface free energy of denture base and liner materials on *Candida albicans* biofilms. *Journal of Investigative and Clinical Dentistry* 6, pp. 141–146. doi: 10.1111/jicd.12079.

Silverman, R.J., Nobbs, A.H., Vickerman, M.M., Barbour, M.E. and Jenkinson, H.F. 2010. Interaction of *Candida albicans* cell wall Als3 Protein with *Streptococcus gordonii* SspB adhesin promotes development of mixed-species communities. *Infection and Immunity* 78(11), pp. 4644–4652. doi: 10.1128/IAI.00685-10.

Simon-Soro, A. et al. 2022. Polymicrobial Aggregates in Human Saliva Build the Oral Biofilm. *mBio* 13(1), pp. 1–15. doi: 10.1128/MBIO.00131-22.

Simon-Soro, A., Tomás, I., Cabrera-Rubio, R., Catalan, M.D., Nyvad, B. and Mira, A. 2013. Microbial geography of the oral cavity. *Journal of Dental Research* 92(7), pp. 616–621. doi: 10.1177/0022034513488119.

Singh, G., Agarwal, A. and Lahori, M. 2019. Effect of cigarette smoke on the surface roughness of two different denture base materials: An in vitro study. *The Journal of Indian Prosthodontic Society* 19(1), p. 42. doi: 10.4103/jips.jips_82_18.

Sipahi, C., Anil, N. and Bayramli, E. 2001. The effect of acquired salivary pellicle on the surface free energy and wettability of different denture base materials. *Journal of Dentistry* 29(3), pp. 197–204. doi: 10.1016/S0300-5712(01)00011-2.

Skillman, L.C., Sutherland, I.W. and Jones, M. V. 1999. The role of exopolysaccharides in dual species biofilm development. *Joumal of Applied Microbiology Symposium Supplement* 21, pp. 13–18.

Sorgini, D.B., da Silva-Lovato, C.H., Muglia, V.A., de Souza, R.F., de Arruda, C.N.F. and Paranhos, H. de F.O. 2015. Adverse effects on PMMA caused by mechanical and combined methods of denture cleansing. *Brazilian Dental Journal* 26(3), pp. 292–296. doi: 10.1590/0103-6440201300028.

Souza, J.G.S., Bertolini, M., Thompson, A., Barãoa, V.A.R. and Dongari-Bagtzoglou, A. 2020. Biofilm Interactions of *Candida albicans* and Mitis Group. *American Society For Microbiology* 86(9), pp. 1–12.

Soysa, N.S. and Ellepola, A.N.B. 2005. The impact of cigarette/tobacco smoking on oral candidosis: An overview. *Oral Diseases*. doi: 10.1111/j.1601-0825.2005.01115.x.

Stegen, J.C., Lin, X., Konopka, A.E. and Fredrickson, J.K. 2012. Stochastic and deterministic assembly processes in subsurface microbial communities. *ISME Journal* 6(9), pp. 1653–1664. doi: 10.1038/ismej.2012.22.

Stoodley, P., Sauer, K., Davies, D.G. and Costerton, J.W. 2002. Biofilms as complex differentiated communities. *Annual Review of Microbiology* 56, pp. 187–209. doi: 10.1146/annurev.micro.56.012302.160705.

Su, C., Yu, J. and Lu, Y. 2018. Hyphal development in *Candida albicans* from different cell states. *Current Genetics* 64(6), pp. 1239–1243. doi: 10.1007/s00294-018-0845-5.

Sudbery, P.E. 2011. Growth of *Candida albicans* hyphae. *Nature Reviews Microbiology* 9(10), pp. 737–748. doi: 10.1038/nrmicro2636.

Sumi, Y., Miura, H., Michiwaki, Y., Nagaosa, S. and Nagaya, M. 2007. Colonization of dental plaque by respiratory pathogens in dependent elderly. *Archives of Gerontology and Geriatrics* 44(2), pp. 119–124. doi: 10.1016/j.archger.2006.04.004.

Survey2009, A.D.H. 2011. *Adult Dental Health Survey for England, Wales and Northern Ireland 2009,*. Available at: www.ic.nhs.uk/statistics-and-data-collections/primary- care/dentistry/adult-dental-healthsurvey-2009--summary-report-and-thematic-series.

Sutherland, I.W. 2001. Biofilm exopolysaccharides: A strong and sticky framework. *Microbiology* 147(1), pp. 3–9. doi: 10.1099/00221287-147-1-3.

Suzuki, N., Nakano, Y., Yoneda, M., Hirofuji, T. and Hanioka, T. 2022. The effects of cigarette smoking on the salivary and tongue microbiome. *Clinical and Experimental Dental Research* 8(1), pp. 449–456. doi: 10.1002/cre2.489.

Svendsen, I.E. and Lindh, L. 2009. The composition of enamel salivary films is different from the ones formed on dental materials. *Biofouling* 25(3), pp. 255–261. doi: 10.1080/08927010802712861.

Sztajer, H. et al. 2008. Autoinducer-2-regulated genes in *Streptococcus mutans* UA159 and global metabolic effect of the luxS mutation. *Journal of Bacteriology* 190(1), pp. 401–415. doi: 10.1128/JB.01086-07.

Sztajer, H., Szafranski, S.P., Tomasch, J., Reck, M., Nimtz, M., Rohde, M. and Wagner-Döbler, I. 2014. Cross-feeding and interkingdom communication in dual-species biofilms of *Streptococcus mutans* and *Candida albicans. ISME Journal* 8(11), pp. 2256–2271. doi: 10.1038/ismej.2014.73.

Sztukowska, M.N. et al. 2018. Community Development between *Porphyromonas gingivalis* and *Candida albicans* Mediated by InlJ and Als3. Biswas, I. ed. *mBio* 9(2), pp. 1–16. doi: 10.1128/mBio.00202-18.

Taylor, R., Maryan, C. and Verran, J. 1998. Retention of oral microorganisms on cobalt-chromium alloy and dental acrylic resin with different surface finishes. *The*

Journal of prosthetic dentistry 80(5), pp. 592–597. doi: 10.1016/S0022-3913(98)70037-X.

Teughels, W., Van Assche, N., Sliepen, I. and Quirynen, M. 2006. Effect of material characteristics and/or surface topography on biofilm development. *Clinical Oral Implants Research* 17(SUPPL. 2), pp. 68–81. doi: 10.1111/j.1600-0501.2006.01353.x.

Theilade, E., Budtz-Jørgensen, E. and Theilade, J. 1983. Predominant cultivable microflora of plaque on removable dentures in patients with healthy oral mucosa. *Archives of Oral Biology* 28(8), pp. 675–680. doi: 10.1016/0003-9969(83)90101-2.

Thieme, L., Hartung, A., Tramm, K., Graf, J., Spott, R., Makarewicz, O. and Pletz, M.W. 2021. Adaptation of the Start-Growth-Time Method for High-Throughput Biofilm Quantification. *Frontiers in Microbiology* 12(August), pp. 1–8. doi: 10.3389/fmicb.2021.631248.

Thomas, T., Gilbert, J. and Meyer, F. 2012. Metagenomics - a guide from sampling to data analysis. *Microbial Informatics and Experimentation* 2(1), p. 3. doi: 10.1186/2042-5783-2-3.

Tsui, C., Kong, E.F. and Jabra-Rizk, M.A. 2016. Pathogenesis of *Candida albicans* biofilm. *Pathogens and disease* 74(4). doi: 10.1093/femspd/ftw018.

Turnbaugh, P.J., Ley, R.E., Hamady, M., Fraser-Liggett, C.M., Knight, R. and Gordon, J.I. 2007. The Human Microbiome Project. *Nature* 449(7164), pp. 804–810. doi: 10.1038/nature06244.

Unniachan, A.S., Jayakumari, N.K. and Sethuraman, S. 2020. Association between *Candida* species and periodontal disease: A systematic review. *Current Medical Mycology* 6(2), pp. 63–68. doi: 10.18502/CMM.6.2.3420.

Ursell, L.K., Clemente, J.C., Rideout, J.R., Gevers, D., Caporaso, J.G. and Knight, R. 2012. The interpersonal and intrapersonal diversity of human-associated microbiota in key body sites. *Journal of Allergy and Clinical Immunology* 129(5), pp. 1204–1208. doi: 10.1016/j.jaci.2012.03.010.

Vaysse, P.J., Sivadon, P., Goulas, P. and Grimaud, R. 2011. Cells dispersed from Marinobacter hydrocarbonoclasticus SP17 biofilm exhibit a specific protein profile associated with a higher ability to reinitiate biofilm development at the hexadecane-water interface. *Environmental Microbiology* 13(3), pp. 737–746. doi: 10.1111/j.1462-2920.2010.02377.x.

Velsko, I.M. et al. 2019. Microbial differences between dental plaque and historic dental calculus are related to oral biofilm maturation stage. *Microbiome* 7(1), pp. 1–20. doi: 10.1186/s40168-019-0717-3.

Verran, J., Jackson, S., Coulthwaite, L., Scallan, A., Loewy, Z. and Whitehead, K. 2014. The effect of dentifrice abrasion on denture topography and the subsequent retention of microorganisms on abraded surfaces. *Journal of Prosthetic Dentistry* 112(6), pp. 1513–1522. doi: 10.1016/j.prosdent.2014.05.009.

Verran, J., Maryan and J., C. 1997. Retention of *Candida albicans* on acrylic resin and silicone of different surface topography. *The Journal of prosthetic dentistry* 77(5), pp. 535–539.

Verran, J., Packer, A., Kelly, P. and Whitehead, K.A. 2010. The retention of bacteria

on hygienic surfaces presenting scratches of microbial dimensions. *Letters in Applied Microbiology* 50(3), pp. 258–263. doi: 10.1111/j.1472-765X.2009.02784.x.

Verran, J., Rowe, D.L. and Boyd, R.D. 2001. The effect of nanometer dimension topographical features on the hygienic status of stainless steel. *Journal of Food Protection* 64(8), pp. 1183–1187. doi: 10.4315/0362-028X-64.8.1183.

Vila, T., Rizk, A.M., Sultan, A.S. and Jabra-Rizk, M.A. 2019. The power of saliva: Antimicrobial and beyond. *PLoS Pathogens* 15(11), pp. 10–16. doi: 10.1371/journal.ppat.1008058.

Vila, T., Sultan, A.S., Montelongo-Jauregui, D. and Jabra-Rizk, M.A. 2020. Oral candidiasis: A disease of opportunity. *Journal of Fungi* 6(1), pp. 1–28. doi: 10.3390/jof6010015.

Vílchez, R. et al. 2010. *Streptococcus mutans* inhibits *Candida albicans* hyphal formation by the fatty acid signaling molecule trans-2-decenoic acid (SDSF). *ChemBioChem* 11(11), pp. 1552–1562. doi: 10.1002/cbic.201000086.

De Waal, Y.C.M., Winkel, E.G., Raangs, G.C., Van Der Vusse, M.L., Rossen, J.W.A. and Van Winkelhoff, A.J. 2014. Changes in oral microflora after full-mouth tooth extraction: A prospective cohort study. *Journal of Clinical Periodontology* 41(10), pp. 981–989. doi: 10.1111/jcpe.12297.

Watts, H.J., Véry, A.-A., Perera, T.H.S., Davies, J.M. and Gow, N.A.R. 1998. *Candida albicans. Microbiology* 144, pp. 689–695.

Webb, B.C., Thomas, C.J., Willcox, M.D.P., Harty, D.W.S. and Knox, K.W. 1998. *Candida*-associated denture stoma titis. Aetiology and management: A review. Part 2. Oral diseases caused by *candida* species. *Australian Dental Journal*. doi: 10.1111/j.1834-7819.1998.tb00157.x.

Whitehead, K.A., Colligon, J. and Verran, J. 2005. Retention of microbial cells in substratum surface features of micrometer and sub-micrometer dimensions. *Colloids and Surfaces B: Biointerfaces* 41(2–3), pp. 129–138. doi: 10.1016/j.colsurfb.2004.11.010.

Whitehead, K.A., Colligon, J.S. and Verran, J. 2004. The production of surfaces of defined topography and chemistry for microbial retention studies, using ion beam sputtering technology. *International Biodeterioration and Biodegradation* 54(2–3), pp. 143–151. doi: 10.1016/j.ibiod.2004.03.010.

Whitehead, K.A. and Verran, J. 2006. The effect of surface topography on the retention of microorganisms. *Food and Bioproducts Processing* 84(4 C), pp. 253–259. doi: 10.1205/fbp06035.

Williams, D. and Lewis, M. 2011. Pathogenesis and treatment of oral candidosis. *Journal of Oral Microbiology* 3(2011). doi: 10.3402/jom.v3i0.5771.

Williams, D.W., Kuriyama, T., Silva, S., Malic, S. and Lewis, M.A.O. 2011. *Candida* biofilms and oral candidosis: Treatment and prevention. *Periodontology 2000* 55(1), pp. 250–265. doi: 10.1111/j.1600-0757.2009.00338.x.

Wolf, A., Moissl-Eichinger, C., Perras, A., Koskinen, K., Tomazic, P. V. and Thurnher, D. 2017. The salivary microbiome as an indicator of carcinogenesis in patients with oropharyngeal squamous cell carcinoma: A pilot study. *Scientific Reports* 7(1), pp. 1–

10. doi: 10.1038/s41598-017-06361-2.

Wood, D.E. and Salzberg, S.L. 2014. Kraken : ultrafast metagenomic sequence classification using exact alignments.

World Health Organization. 2022. *WHO fungal priority pathogens list to guide research, development and public health action*.

Wright, C.J. et al. 2013. Microbial interactions in building of communities. *Molecular Oral Microbiology* 28(2), pp. 83–101. doi: 10.1111/omi.12012.

Wu, Y., Chi, X., Zhang, Q., Chen, F. and Deng, X. 2018. Characterization of the salivary microbiome in people with obesity. *PeerJ* 2018(3), pp. 1–21. doi: 10.7717/peerj.4458.

Xiao, J. et al. 2012. The exopolysaccharide matrix modulates the interaction between 3D architecture and virulence of a mixed-species oral biofilm. *PLoS Pathogens* 8(4), pp. 7–9. doi: 10.1371/journal.ppat.1002623.

Xu, H., Sobue, T., Bertolini, M., Thompson, A. and Dongari-Bagtzoglou, A. 2016. *Streptococcus oralis* and *Candida albicans* Synergistically Activate μ-Calpain to Degrade E-cadherin from Oral Epithelial Junctions. *Journal of Infectious Diseases* 214(6). doi: 10.1093/infdis/jiw201.

Xu, X. et al. 2015. Oral cavity contains distinct niches with dynamic microbial communities. *Environmental Microbiology* 17(3), pp. 699–710. doi: 10.1111/1462-2920.12502.

Yamashita, Y. and Takeshita, T. 2017. The oral microbiome and human health. *Journal of Oral Science* 59(2), pp. 201–206. doi: 10.2334/josnusd.16-0856.

Yang, C., Scoffield, J., Wu, R., Deivanayagam, C., Zou, J. and Wu, H. 2018. Antigen I/II mediates interactions between *Streptococcus mutans* and *Candida albicans*. *Molecular Oral Microbiology* 33(4), pp. 283–291. doi: 10.1111/omi.12223.

Yitzhaki, S., Reshef, L., Gophna, U., Rosenberg, M. and Sterer, N. 2018. Microbiome associated with denture malodour. *Journal of Breath Research* 12(2). doi: 10.1088/1752-7163/aa95e0.

Zakaria, W., Almunajem, Y. and Alnowaiser, H. 2018. Denture Hygiene: The Sharing Responsibility. *International Journal of Dental Research* 6(1), p. 41. doi: 10.14419/ijdr.v6i1.12191.

Zamperini, C.A., MacHado, A.L., Vergani, C.E., Pavarina, A.C., Giampaolo, E.T. and Da Cruz, N.C. 2010. Adherence in vitro of *Candida albicans* to plasma treated acrylic resin. Effect of plasma parameters, surface roughness and salivary pellicle. *Archives of Oral Biology* 55(10), pp. 763–770. doi: 10.1016/j.archoralbio.2010.06.015.

Zarco, M.F., Vess, T.J. and Ginsburg, G.S. 2012. The oral microbiome in health and disease and the potential impact on personalized dental medicine. *Oral Diseases* 18(2), pp. 109–120. doi: 10.1111/j.1601-0825.2011.01851.x.

Zaura, E. et al. 2017. On the ecosystemic network of saliva in healthy young adults. *ISME Journal* 11(5), pp. 1218–1231. doi: 10.1038/ismej.2016.199.

Zaura, E., Keijser, B.J., Huse, S.M. and Crielaard, W. 2009. Defining the healthy “core

microbiome" of oral microbial communities. *BMC Microbiology* 9, pp. 1–12. doi: 10.1186/1471-2180-9-259.

Zaura, E., Nicu, E.A., Krom, B.P. and Keijser, B.J.F. 2014. Acquiring and maintaining a normal oral microbiome: Current perspective. *Frontiers in Cellular and Infection Microbiology* 4(JUN), pp. 1–8. doi: 10.3389/fcimb.2014.00085.

Zengler, K. and Zaramela, L.S. 2018. The social network of microorganisms - How auxotrophies shape complex communities. *Nature Reviews Microbiology* 16(6), pp. 383–390. doi: 10.1038/s41579-018-0004-5.

Zhang, N. et al. 2019. Elevation of O-GlcNAc and GFAT expression by nicotine exposure promotes epithelial-mesenchymal transition and invasion in breast cancer cells. *Cell Death and Disease* 10(5). doi: 10.1038/s41419-019-1577-2.

Zhao, X. et al. 2004. ALS3 and ALS8 represent a single locus that encodes a *Candida albicans* adhesin; functional comparisons between Als3p and Als1p. *Microbiology* 150(7), pp. 2415–2428. doi: 10.1099/mic.0.26943-0.

Zhao, X., Daniels, K.J., Oh, S.H., Green, C.B., Yeater, K.M., Soll, D.R. and Hoyer, L.L. 2006. *Candida albicans* Als3p is required for wild-type biofilm formation on silicone elastomer surfaces. *Microbiology* 152(8), pp. 2287–2299. doi: 10.1099/mic.0.28959-0.

Zheng, S., Bawazir, M., Dhall, A., Kim, H.E., He, L., Heo, J. and Hwang, G. 2021. Implication of Surface Properties, Bacterial Motility, and Hydrodynamic Conditions on Bacterial Surface Sensing and Their Initial Adhesion. *Frontiers in Bioengineering and Biotechnology* 9(February), pp. 1–22. doi: 10.3389/fbioe.2021.643722.

Zhu, J. et al. 2022. Over 50,000 Metagenomically Assembled Draft Genomes for the Human Oral Microbiome Reveal New Taxa. *Genomics, Proteomics and Bioinformatics* 20(2), pp. 246–259. doi: 10.1016/j.gpb.2021.05.001.

Zissis, A.J., Polyzois, G.L., Yannikakis, S.A. and Harrison, A. 2000. Roughness of Denture Materials: A Comparative Study. *The International Journal of Prosthodontics* 13(2), pp. 136–140.

Zomorodian, K. et al. 2011. Assessment of *Candida* species colonization and denture-related stomatitis in complete denture wearers. *Medical Mycology* 49(2), pp. 208–211. doi: 10.3109/13693786.2010.507605.